# Material Evaluation of an Elastomer, Epoxy and Lightweight Concrete Rail Attachment System for Direct Fixation Light Rail Applications

Benjamin R Swarner

A thesis
submitted in partial fulfillment of the
requirements for the degree of

Master of Science in Civil Engineering

University of Washington

2016

Committee:

Donald Janssen, Chair

John Stanton

Laura Lowes

Program Authorized to Offer Degree:
Civil and Environmental Engineering

University of Washington

## Abstract

Material Evaluation of an Elastomer, Epoxy and Lightweight Concrete Rail Attachment System for Direct Fixation Light Rail Applications

Benjamin R Swarner

Chair of the Supervisory Committee:
Associate Professor Emeritus Donald Janssen
Civil and Environmental Engineering

Sound Transit plans to extend its current light rail system, which runs along the I-5 corridor in Seattle, Washington, across the I-90 Homer Hadley floating bridge as part of a project to connect the major city centers in the region. But, no light rail has ever crossed a floating bridge due to several unique engineering challenges. One of these challenges is attaching the rails to the existing bridge deck without drilling into the bridge pontoons. This research program was developed to test and analyze a direct fixation method that uses lightweight concrete plinths and an elastomer-epoxy system to attach the rails to the bridge deck. The elastomer used was a two-part, pourable elastomer with cork particles intermixed to alter the mechanical properties of the material. A lightweight concrete mixture was analyzed for use in the plinths, and system tests investigated the system response under tensile, compressive and shear loading. The shear response of the system was examined further under varying loading conditions including different surface preparations, elastomer thicknesses, strain-rates and after freeze-thaw conditioning. Experimental data was examined for trends based on these parameters to best characterize the system, and the elastomer was evaluated in the context of modern elastomer research.

# Acknowledgments

There are several people I would like to specifically thank for their support and contribution to this project. First, I want to thank Don Janssen, John Stanton and Laura Lowes for serving on my defense committee. Each of these professors have encouraged, mentored and advised me throughout my graduate studies, and it has been an honor and a pleasure to work with each of them. A special note of thanks goes to Don Janssen for his excellent advising throughout this research. Despite retiring in September 2014, he continued to work closely with me on this project. Don, thank you for trusting me with the opportunity and responsibility of leading this project.

Second, thank you to my beautiful wife, Megan, who has stood by my side during this whole project. She shared in my successes, supported me in my failures and urged me forward when I was tired and wanted to quit. Thanks for all the times you came to the concrete lab to help and keep me company even before we were married! I could not have done it without you.

Third, to my parents, in-laws and extended family: your motivation and support were crucial—thank you. Mom and Dad, thanks for keeping me accountable and caring about my work (and progress), and thanks for letting me invade your space and take over your computer so often during the writing process. Aunt Linda and Uncle Steve, thanks for helping me hurdle the intimidation and feelings of inadequacy over completing a project of

this magnitude. Your support helped me past the most difficult part of this process; sharing your experiences with me helped me to believe that I could (and wanted to) finish this thesis.

Finally, thank you to all of my friends who worked with me on the project and kept me sane over the last two years. Among them, a few deserve special thanks. Jeff McClintock, Carson Baker and Sam Dougherty: thanks for your hours of help in the lab mixing concrete and assembling test specimens. Todd Maki, Lisa Berg, Bryan Kennedy and Matt Sisley: thanks for keeping our office an enjoyable place to work and being diligent on your own projects. Thank you Bill Elkey, Eric Herzstein, Agatha Kotsonis and the rest of the Parsons team for giving me a great place to practice structural engineering outside of school while completing this project.

Many others also provided encouragement, support and motivation throughout this project, and I am extremely thankful for you. The vast support of so many humbles me and reminds me how blessed I am. Thanks!

*This paper is dedicated to:*

*my many former and current mentors—thank you for investing in me,*

*to my wife, her parents and mine—for your unconditional love and support,*

*and to the Lord Jesus Christ, in whom are hidden all the treasures of wisdom and knowledge—thank you for giving me an understanding of this small part of your creation.*

# Table of Contents

# List of Figures

# List of Tables

# 1 Introduction

## 1.1 Research Motivation

Two floating bridges span Lake Washington in Seattle, Washington, connecting the east and west corridors of the metropolitan area. Bellevue and Redmond are well established as major urban centers on the east side of the lake, but ever-increasing roadway congestion threatens the connectivity of the city centers, highlighting the need for alternate modes of transportation between the city centers. Sound Transit plans to extend its current light rail system, which runs along the I-5 corridor, across the I-90 Homer Hadley floating bridge as part of the East Link Extension project (Figure 1-1). However, no light rail train has ever crossed a floating bridge because of several unique engineering challenges.

One challenge in adding a rail system to a floating bridge is the differential movement between the stationary approach and the floating bridge caused by environmental conditions such as wind and waves, vehicular movement across the bridge and water-level changes. A unique, ground-breaking track bridge system was designed and tested to accommodate these critical locations.

This paper focuses on a second challenge: the challenge of attaching the rails to the bridge deck. Typically, in direct fixation rail systems constructed today, each rail sits atop a continuous reinforced concrete pedestal called a plinth, secured by embedded fasteners. The plinth is attached to the concrete deck by standard reinforced concrete methods.

However, due to the limited thickness of the I-90 bridge deck, this type of connection is not


**Figure 1-1.** Map of Sound Transit's East Link Extension Project to Connect the East and West Corridors of the Metropolitan Area (Sound Transit 2015)

possible without drilling into the heavily post-tensioned pontoons that keep the bridge afloat, a dangerous and impractical option. Additionally, adding continuous plinths significantly increases the weight of the structure.

Therefore, a hybrid, direct fixation system was developed using precast, lightweight concrete (LWC) blocks in lieu of continuous plinths and an elastomer-epoxy system to attach the blocks to the bridge deck. Based on their function, the LWC blocks are still considered plinths.

Using lightweight concrete reduces the weight of the plinths by up to 33 percent over roughly 300 cubic yards of concrete used for the plinths on the bridge. The elastomer-epoxy system not only provides a method of attaching the plinths to the concrete deck, but also aids in damping vibrations from and to the trains. Furthermore, an elastomer layer reduces the dynamic impact load of the train on the rails, reducing necessary maintenance and extending the lifespan of the system. Figure 1-2 highlights the elastomer-epoxy system connecting the

plinth to the bridge deck.

## 1.2 Research Objective

While manufacturers provide material properties for their elastomers, the shape, thickness and construction-related variability significantly affect the effective design properties. Additionally, the proprietary elastomer chosen for use in this attachment system is a pourable elastomer that uses a cork filler to alter the material properties. Both the pourable nature and the material filler are atypical of common elastomers used in structural applications today. Therefore, material testing of the complete system must be performed to understand the design properties. This research program investigated the system response under tensile, compressive and shear loadings to achieve three primary objectives and assessed the impact of certain variables on the system response.

The primary objectives of this research are:

- to design and evaluate a lightweight concrete mixture suitable for use in the plinths,
- to evaluate the material properties used to design the attachment system and determine influencing factors, and
- to compare the test results with the manufacturer's published values and previous research on elastomeric bearings.

## 1.3 Overview of Report

This thesis describes the background, process, results and analysis of over 200 tests conducted at the University of Washington's Structural Research and Concrete Materials Laboratories between January 2014 and April 2015.

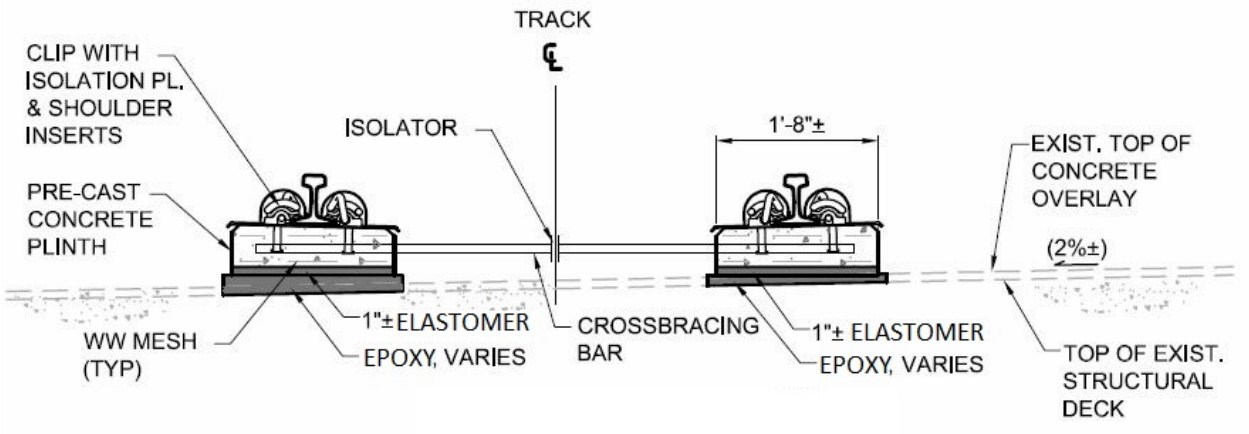


**Figure 1-2.** Conceptual Detail of a Plinth Attached to Concrete Deck by Elastomer-Epoxy System (Sound Transit 2013)

Chapter 2 discusses considerations for working with lightweight aggregate concrete and general material behavior of elastomer to provide a background understanding of the material. It also introduces previous research for comparison. Chapter 3 describes the the physical properties of the materials, highlighting the proportions and properties of the suitable LWC mixture. Next, Chapter 4 details the general procedure of assembling each specimen, and Chapter 5 describes the setup, instrumentation and specific procedure for each test. Results for each set of tests are presented in Chapter 6, and Chapter 7 analyzes the data by comparing it with modern elastomeric theory. Finally, Chapter 8 summarizes and draws conclusions from the research and provides direction for future work.

# 2 Background

The materials comprising the rail-attachment system were lightweight concrete (LWC), elastomer, epoxy and normal concrete. A general understanding of these materials is necessary to frame the research included in this thesis. Chapter 3 discusses the specific properties of the materials used, but this chapter provides the background of lightweight aggregate and typical behavior of elastomer. It also addresses the expected loads on the attachment system.

## 2.1 Lightweight Aggregate

The process of expanding rock in a kiln to make lightweight aggregate creates voids in the aggregate that decrease the density of the rock. This decreases overall concrete strength compared to normal concrete and leads to a higher, more variable rate of water absorption. The American Concrete Institute's educational bulletin, E1 (ACI 2007), and the Portland Cement Association's (PCA) Design and Control of Concrete Mixtures (Kosmatka and Panarese 1994) are helpful resources for understanding of the effect of normal and lightweight aggregates on concrete mixtures. This section cites those documents often as it describes typical characteristics and practical considerations for working with lightweight aggregates.

### 2.1.1 Typical Characteristics of Lightweight Aggregate

Various characteristics of lightweight aggregate greatly affect the strength, weight and workability of the resultant concrete. The effects of shape, bulk density, gradation and absorption

on the workability of plastic concrete and the strength, durability and density of hardened concrete are discussed in this section. These effects are often compensated for by minor changes in $w/c$ ratio and paste content and by the addition of admixtures. The relationship between the various properties is complex, and a simple observation of the aggregate qualities is not enough to discern specific concrete properties. Therefore, only general trends will be presented.

**Shape and Surface Texture** Aggregate shape is usually described by its compactness and angularity. Compactness is the ratio of a particle's surface area to its volume, and angularity is the relative sharpness of a particle's edges and corners. For example, a spherical or cubical particle has a higher compactness ratio than a flat or elongated particle. Increased coarse aggregate compactness reduces the water and fine aggregate required for workability as flatter or more elongated particles tend to lock together and resist movement (ACI 2007). An increase in angularity also increases aggregate interlock and requires more cement paste to maintain workability (Kosmatka and Panarese 1994). The shape of lightweight aggregate varies considerably with different types of rock and different production methods, but expansion of aggregate in the rotary kiln tends to produce fairly compact but angular particles (ACI 2007).

The surface texture of lightweight aggregate is often rough, especially aggregate that has been crushed to meet size and gradation requirements (discussed below). A rough surface with exposed pores means increased surface area that aids in the bond strength between cement paste and aggregate but also requires an increase in the $w/c$ ratio or paste content to maintain the same workability that is experienced with smooth aggregate. The surface texture of the fine aggregate primarily affects the workability of plastic concrete due to a higher surface area to volume ratio, while the surface texture of the coarse aggregate primarily affects the paste-aggregate bond strength (ACI 2007).

**Bulk Specific Gravity (BSG)** Bulk density, or unit weight, is the measure of the mass of the aggregate in relation to its volume including the voids. This is normalized by the density of water to form the bulk specific gravity (BSG). BSG measured in oven-dry conditions is the most consistent measurement when comparing aggregates because water inside pores add weight to the rock. However, aggregates with different void concentrations could appear to have similar bulk densities in oven dry conditions and very different bulk densities under other moisture conditions.[1] Additionally, for dry applications like interior building structure or construction in dry climates, the aggregate will dry out (at least partially). In this case, a higher aggregate void content leads to lighter aggregate, but in wet applications, the opposite is true: a higher void content leads to heavier aggregate due to the weight of the water in its pores. Therefore, it is most useful to measure the bulk density under the closest repeatable condition to the ultimate concrete exposure. Equation 2-1 expresses the BSG for saturated surface dry conditions:

$$\left\{ BSG = \frac{W}{V \times \gamma_w} \right\}_{SSD} \tag{2-1}$$

where $W$ is the weight of the aggregate, $V$ is the volume of the aggregate and $\gamma_w$ is the density of water. The subscript $SSD$ indicates that $BSG$, $W$ and $V$ are measured in the saturated, surface-dry condition.

For lightweight aggregates, the saturated surface-dry BSG is mainly affected by aggregate void content and particle size. Increased volume of saturated voids increases the specific gravity of the aggregate. Additionally, the rotary kiln increases the voids in the aggregate during the expansion process, but crushing removes many of the larger voids. Therefore, lightweight fine aggregate tends to be denser than lightweight coarse aggregate that did not go through as extensive a crushing process (ACI 2007).

BSG is typically inversely proportional to hardened concrete strength, although not linearly. In general, an increase in density results from fewer voids, and a reduction in voids

[1] Pores that are connected to the exterior aggregate surface will fill with water when saturated. Isolated, interior pores remain dry.

can be expected to lead to higher aggregate strength.

**Gradation** Aggregate gradation also plays an important role in mixture design since it affects the workability, strength and density of the resultant concrete. Gradation refers to the distribution of particle sizes and is measured by pouring an aggregate sample through a series of sieves with decreasing opening size. A pan underneath the stack of sieves catches the finest particles. A well-graded mixture contains similar amounts of aggregate of all sizes from the maximum aggregate size to particles passing the smallest sieve (typically a sieve with 200 openings per square inch). This leads to the optimal arrangement of aggregate particles in a mixture with the smaller particles filling in the gaps between the larger particles.

A well-graded mixture reduces the paste that is necessary in the mixture and results in "the maximum strength with minimum volume change due to shrinkage" (ACI 211.2). Conversely, a poorly-graded mixture has many aggregate particles of the same size leaving large gaps between particles that have to be filled with paste. Since paste is usually the most expensive component of concrete, a well-graded mixture reduces the cost of the batch (ACI 2007). For lightweight aggregate, it also reduces the specific gravity of the resultant concrete since the paste ($SG_{paste} = 1.95$) is heavier than the lightweight aggregate ($SG_{SSD} \approx 1.5$).

Additionally, it is important to note that while the gradation is generally measured by mass, it is the volume of each particle size that is important. Consider Figure 2-1; the benefits of a well graded mixture are derived from the smaller particles filling the gaps between the larger particles. For lightweight aggregate, a larger percentage of finer particles (by mass) is required to maintain the correct volume distribution of particle size because the aggregate specific gravity increases with decreasing particle size (ACI 2007). This increases the resultant concrete unit weight since the smaller particles are heavier.

However, the crushing process used to grade the lightweight aggregate often produces a more uniform size distribution than naturally graded aggregate. Figure 2-2 compares the gradation of the lightweight fines used in this project to that of standard building sand from the UW concrete laboratory. It can be seen that the lightweight fines are coarser through the

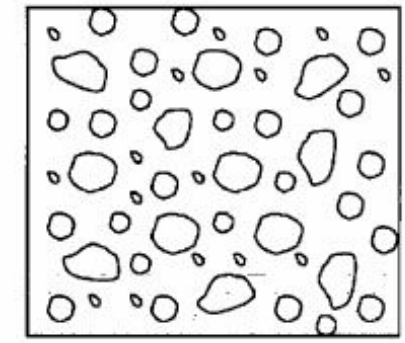

**Figure 2-1.** An Illustration of a Well-Graded Mixture (ACI 2007).

critical mid-size range resulting in a more uniform gradation. Because of this, water drains more quickly through the lightweight fine aggregate, making it more difficult to control the moisture content in the aggregate stockpile. The uniform gradation also increases the paste content required to fill the gaps between particles and to maintain workability of the concrete (ACI 2007).

**Absorption** Absorption is a measure of the total pore volume accessible by water. It is computed as the difference of the saturated surface-dry (SSD) and oven-dry (OD) masses of the aggregate relative to the oven-dry mass and reported as a percentage of the oven-dry mass as shown in Equation 2-2:

$$Absorption, \%, = \frac{W_{SSD} - W_{OD}}{W_{OD}} \times 100 \tag{2-2}$$

where $W_{SSD}$ is the weight of the aggregate in saturated surface-dry conditions and $W_{OD}$ is the weight of the aggregate in oven-dry conditions.

Knowing the absorption value of the aggregate is crucial to accurately proportioning the water in a mixture. Wet aggregate with a moisture content higher than its absorption will add water to the mixture, raising the $w/c$ ratio, and lead to a weaker mixture that is prone to segregation unless properly accounted for. Alternatively, if a moisture content less than

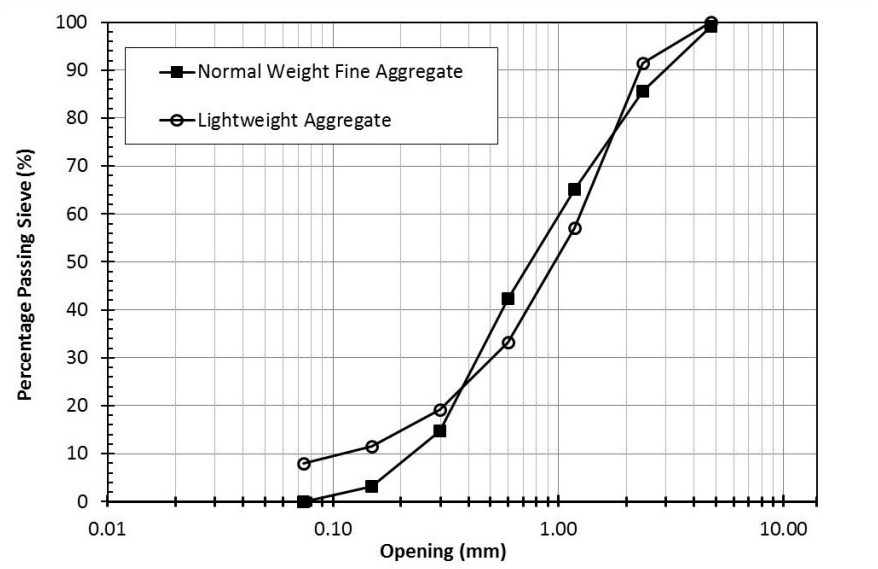


**Figure 2-2.** Normal Weight vs. Lightweight Fine Aggregate Gradation.

its absorption is unaccounted for, the aggregate will absorb mixing water out of the mixture, leading to a stronger, but less workable mixture.

Lightweight aggregate absorbs far more moisture than normal aggregate due to its porous structure. Typical absorption values for lightweight aggregate range from 5%–20%. Because the absorption values are so high, the lightweight aggregate will typically only absorb two-thirds of its absorption when stored outdoor in a stockpile (ACI 2007). This means more water will be need to be added to the mixture and the rate of absorption becomes significant with regard to mixing time.

In addition to increased absorption, lightweight aggregates typically show an increased rate of absorption. But, because of more extensive pore and capillary veins in lightweight aggregate, visual water on the surface of the aggregate does not necessarily indicate the saturated condition (ACI 211.2). Aggregates that look wet but are not fully saturated at the time of mixing will continue to absorb water during mixing, removing water from the concrete mixture and causing workability concerns. Extended soaking of the aggregate tends to reduce this effect.

**Air Content Control** Entrained air is an important part of lightweight concrete mixtures, especially when the resultant concrete will have high exposure to freezing and thawing. Air entraining admixtures lower the surface tension of the mixing water to create more bubbles and prevent air bubbles from coalescing. This leads to a uniform dispersion of small air bubbles throughout the cement paste. Difficulty controlling the water in a mixture leads to a difficulty controlling the air content, and negative admixture interaction between water-reducing admixtures can lead to a loss of air. This is made worse when uniformly graded fine aggregate does not have small particles to help trap air bubbles in paste, allowing the air to "float out" (ATS 5).

With this in mind, certain practical considerations should be noted when working with lightweight aggregate.

### 2.1.2 Practical Considerations for Working with Lightweight Aggregates

In light of the aforementioned characteristics, practical considerations for working with lightweight aggregates are presented in this section regarding aggregate moisture conditioning.

**Aggregate Moisture Conditioning** The greater absorption and the higher rate of absorption that are characteristic of lightweight concrete aggregates necessitate an extra measure of moisture control for best results when mixing. Aggregates are most cost-effectively shipped in a dry condition, but the aggregates must be thoroughly soaked prior to mixing. Outside storage is convenient but can allow for an unpredictable level of moisture absorption in wet environments. Drainage and evaporation can severely affect the moisture content of the aggregate stockpile. Since mixture proportions are primarily given in terms of SSD or OD moisture conditions, care must be taken to ensure that aggregates have adequate time to absorb available moisture so that measured aggregate water content represents the degree

of saturation of the aggregate stockpile (ACI 211.2).

Additionally, damp aggregates are preferred in mixtures because they absorb less mixing water and are not as likely to segregate in storage (ACI 211.2). Pre-wetting the aggregate is advantageous to ensure the internal voids are filled and to maintain a uniform moisture content. The most common methods of pre-wetting aggregate are atmospheric methods including sprinkling, using a soaker hose and water submersion, but thermal and vacuum methods are also practiced (ACI 213R). Care should be taken when freezing and thawing occurs frequently because concrete mixed with fully saturated aggregates is more susceptible to freeze-thaw degradation than concrete made with air-dry or damp aggregates (ACI 211.2).

Practically, multiple moisture content tests may be necessary prior to batching to account for drainage caused by gravity, and stockpiles should be constantly sprinkled or covered after soaking to avoid evaporation.

## 2.2 Typical Elastomer Behavior

Elastomers behave much differently than standard materials used by structural engineers such as concrete, timber and steel. Extremely large strain capacities and non-linear stress-strain relationships characterize most elastomers. Temperature and loading rate also contribute significantly to the observed physical properties of the viscoelastic material. In spite of these sources of nonlinearity, almost all analysis of elastomeric bearings assume linear elastic material behavior to approximate the actual response (Stanton and Roeder 1982). Additionally, elastomers are virtually incompressible, so they undergo large deformations with very little change in volume (Gent and Lindley 1959, Gent and Meinecke 1970). Furthermore, due to largely proprietary makeup, the physical properties affecting structural performance can vary significantly by manufacturer and even within a manufacturer by product line.

Initially, these properties made structural designers hesitant to specify their use in structural applications. But since the early 1980's, their use has become much more widespread as engineers have become more comfortable with their properties and confident in the per-

formance of existing bearings. Today, elastomeric bearings are widely used for a variety of structural applications including bridge bearings, seismic isolation and mechanical vibration damping.

### 2.2.1 Material Composition

Traditional elastomers are made from natural rubber or synthetic compounds. Vulcanization, the process of adding sulfur and heat to natural rubber, increases its strength, stiffness and durability by creating molecular bridges between individual polymer strands linking the strands together (Treloar 2009, pp. 8-10). Classical elastomer theory is based on these types of materials. However, some newer elastomers incorporate solid filler components[2] (similar to the aggregate in concrete) to reduce the amount of rubber material used. Additionally, other chemical cross-linking methods besides vulcanization are occasionally employed for specialized applications. While there is a lot of research on classical elastomers, the effects of these filler components and alternate cross-linking methods are not widely known, and assumptions used in classical elastomer theory, such as complete incompressibility, may insufficiently describe behavior of multi-component elastomers.

#### 2.2.1.1 Reinforcement and The Geometric Effect

Before discussing the material response, the effects of reinforcement and specimen geometry must be addressed. Civil engineering applications of elastomers in compression or shear typically involve horizontal layers of elastomer separated by—and bonded to—thin, steel plates called shims to resist the lateral spreading of the elastomer when it is compressed. The reinforcement stiffens the compression response without affecting the direct shear response (Derham 1986). Reinforced bearings are particularly useful as seismic isolators and seating pads where stiff compression response and controlled shear deformation are required. In

[2]The filler components referred to in this paper are distinct from those materials commonly used in the vulcanization process, which are also called fillers, that alter the chemical properties of the rubber, such as carbon black.

unreinforced bearings, lateral spreading is restrained by friction on the loading surface. As surface properties of loading heads vary, the extent of the restraint changes and causes the apparent stiffness to change as well. This makes unreinforced bearings difficult to characterize or generalize without knowledge of the loading surfaces.

The elastomer in this project was technically unreinforced (i.e. there were no laminated steel plates), but the layer thickness and boundary conditions of the test specimens (bonded ends) were such that the single elastomer layer resembled a layer of a reinforced bearing.

It has been observed since the earliest studies of elastomer that the geometry of the elastomer layers plays an important role in the bearing's behavior. Keys (1937) is credited as the first to define the shape factor, $S$, and nearly all research on elastomer layers since has confirmed its usefulness in describing apparent elastomeric material properties (e.g. Gent and Lindley 1959, Stanton and Roeder 1982, Pinarbasi and Akyuz 2004, etc.). As shown in Equation 2-3, the shape factor relates the plan area of a bearing, $A$, with $A_B$, the traction-free area around the perimeter of an elastomer layer that is free to bulge out when compressed.

$$S = \frac{A}{A_B} = \frac{A}{Pt} \tag{2-3}$$

where $P$ is the perimeter and $t$ is the thickness of the elastomer layer.

For a constant area, decreasing thickness leads to a higher shape factor. Increasing $S$ is known to increase restraint on the layer's ability to bulge thereby increasing the axial stiffness of the layer because "the vertical deflection is accommodated [increasingly] by volumetric strain in the elastomer" (Van Engelen and Kelly 2014). On the other hand, increasing the layer thickness (reducing $S$) gradually reduces the contribution of end effects on the stress distribution within the block (Holownia 1972).

It has been noted that the plan aspect ratio of rectangular bearings (i.e. length-to-width) also affects the elastomer's response (Gent and Meinecke 1970); bearings with the same $S$ but different aspect ratios respond slightly differently, but the variation in compression response due to aspect ratio was found to be negligible compared to the variation and error

in other areas of the calculation (Stanton and Lund 2015). Yura et al. (2001) found that the shear stiffness depends on the length-to-thickness ratio as much or more than the shape factor. As computational power increases, accuracy and precision improve to the point that a parameter that accounts for both aspect ratio and layer slenderness would be useful for all types of loading (Stanton and Lund 2015).

The following sections describe the general behavior exhibited by traditional elastomer under tension, shear and compression loading, and special considerations for laboratory testing are presented. Specific variations in properties caused by proprietary filler additives are not discussed but can have a significant effect on observed material properties, and the results from tests on an elastomer with a cork filler will be compared to the traditional properties described in this section.

### 2.2.2 Tensile Behavior

Many have experienced the tension properties of rubber through the use of the rubber band. It stretches easily at first but becomes very stiff right before it breaks. In structural terms, the first, "stretchy" phase can be described as a large deformation with respectively little tension force (pulling)—having a low stiffness. The second, stiff phase is characterized by a significant increase in the force required just to obtain even a small increase in deformation. This is opposite of most structural materials, which exhibit their stiffest behavior at low strains[3] followed by plastic ("stretchy") behavior after yielding.

The tension stress-strain relationship of rubber is complex. Figure 2-3 shows a typical stress-strain curve for a vulcanized, natural rubber that exhibits a fairly stiff initial response followed by a period of softening between about 30-250 percent strain and dramatic stiffening after about 300 percent strain where it continues until failure beyond 600 percent strain. The shape of this curve is typical, but the location and size of each region of the curve differ for different elastomer materials based on chemical make-up, conditioning process and shape

[3]Strain is a dimensionless measure of deformation found by taking the ratio of deformation to the original length, $\Delta L/L$.

factor. Gent et al. (2001) shows that the maximum strain of vulcanized rubber normally falls within the range 300–600 percent, and Treloar (2009) documents rubber tensile break as high as 1,000 percent elongation.

ASTM D412 governs tension testing of thermoplastic rubber and defines a yield strain as "the point where the rate of change of stress with respect to strain, goes through a zero value," but it does not specify a method to quantify stiffness or modulus. Figure 2-3 shows that a simple, linear model, such as Young's modulus, cannot effectively describe the tensile response over a large strain range, so a multi-linear or non-linear model is needed to effectively describe its behavior.

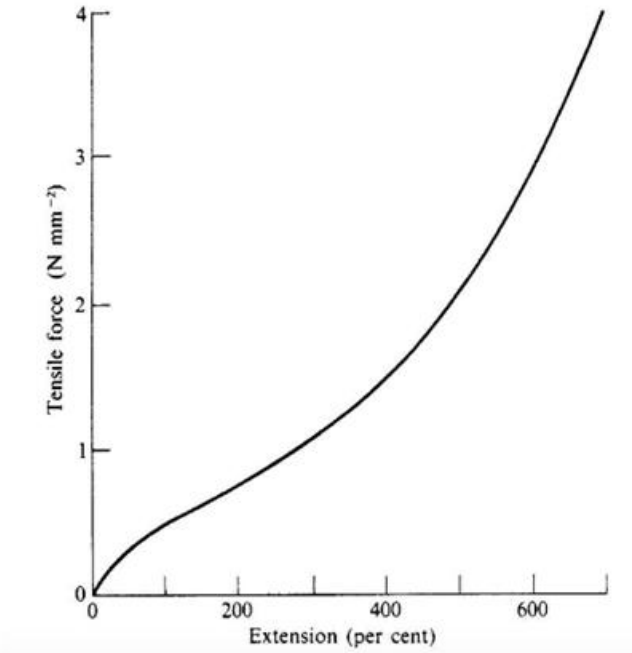


**Figure 2-3.** Typical force-extension curve for vulcanized rubber (Treloar 2009, p. 2)

### 2.2.3 Shear Behavior

The 'simple' shear response (Figure 2-4b) is a complex combination of flexure and shear (Gent and Meinecke 1970), but it is usually approximated by the linear-elastic equation:

$$\tau = G\gamma \tag{2-4}$$

where $G$ is the shear modulus of the elastomer. This reflects an inaccurate assumption that the shear stress is uniform throughout the specimen. Rather, the shear stress must be zero at the corners to satisfy equilibrium (Stanton and Roeder 1982). In practice, the mathematical singularity at the corners is typically ignored since practice informs that the highest debonding stresses occur at the corners, and the linear-elastic approximation is used.

Figure 2-5 shows a typical stress-strain response of natural rubber under shear loading. It can be seen that the slope of the curve is approximately constant initially but significantly increases beyond 150 percent strain. According to a list of practical design considerations by Sheriden et al. (2001), the shear stress-strain relationship can be practically taken as linear through 75 percent strain, and Yura et al. (2001) found that a secant between zero and 50 percent strain "gives the correct value of the maximum shear force when [a bridge bearing] is strained to the maximum design level." $G$ is usually about three times less than $E$, between 100 and 300 psi (Stanton and Roeder 1982, Yura et al. 2001).

### 2.2.4 Compression of Unrestrained Elastomer

As expressed previously, elastomer is characterized in part by its near-incompressibility—the bulk modulus, $K$, approaches infinity, and Poisson's ratio, $\nu$, approaches 0.5. This means the elastomer has a strong resistance to volume change when loaded ($K$ is discussed below in more detail). Therefore, when an elastomer layer is compressed in the vertical direction, the sides want to spread out laterally. Figure 2-6a shows how the sides react when the boundaries of an elastomer layer are unbonded and frictionless. Tests examining this configuration often

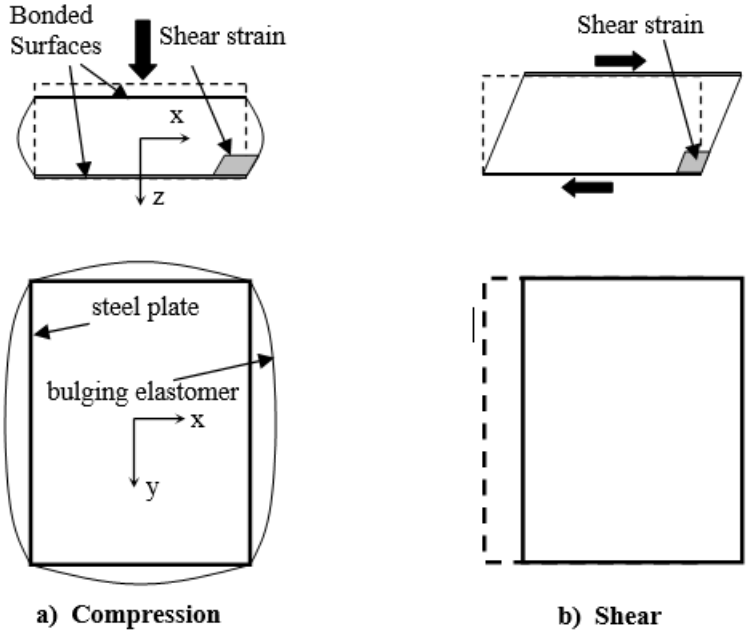


**Figure 2-4.** Diagrams illustrating elastomer deformation when loaded in Compression and Shear (Stanton and Lund 2015)

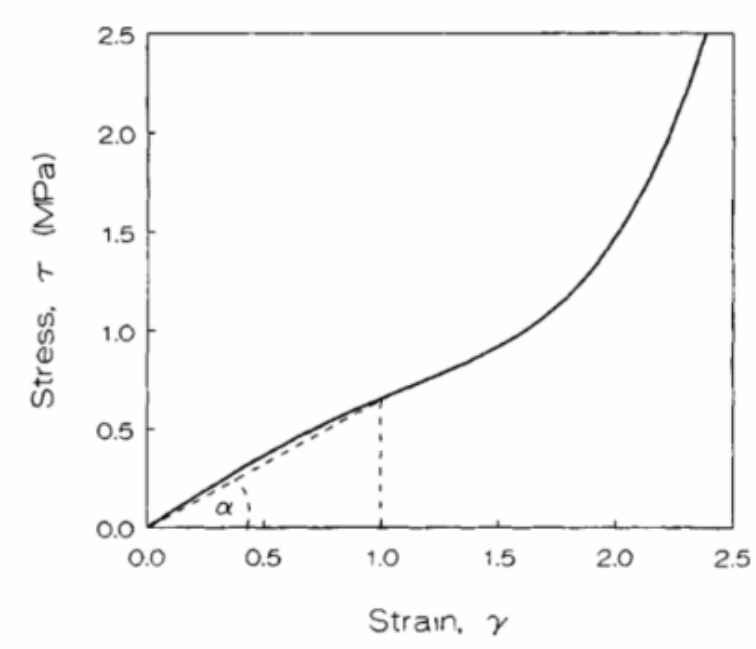


**Figure 2-5.** Typical shear stress-strain response of vulcanized natural rubber containing carbon black (Gent 2001, p. 315).

use lubricants to reduce friction between the loading head and the elastomer layer. In the case of an elastomer loaded in this configuration, the stress in the vertical ($z$) direction is uniform and the vertical stress, $\sigma_z$, is defined by the common equation (Gent and Meinecke 1970):

$$\sigma_z = E\epsilon_z. \tag{2-5}$$

For a completely incompressible elastomer, there is no volume change when loaded, so the area outside of the original perimeter due to lateral spreading has exactly the same volume as the volume displaced by the loading head. For compressible elastomers ($K < \infty$) the volume outside the original perimeter is less than the volume displaced by the loading head because there is volumetric strain.

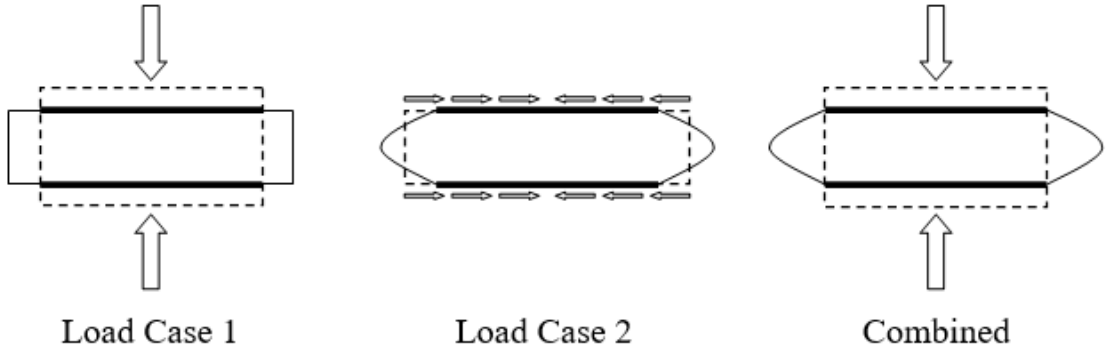


**Figure 2-6.** Response of a bonded elastomer layer in compression by superimposing two load cases (Stanton and Lund 2015)

#### 2.2.4.1 Bulk Compressibility

Bulk compressibility, measured by the bulk modulus, $K$, is defined as the rate of change of an applied, hydrostatic stress, $\sigma$, with respect to the volumetric strain, $\Delta V/V$:

$$\sigma = K \times \frac{\Delta V}{V}. \tag{2-6}$$

Classical analysis of elastomers (e.g. Gent and Lindley 1959, Gent and Meinecke 1970) assumes complete incompressibility, which corresponds to an infinite $K$ and a Poisson's ratio, $\nu$, equal to 0.5. This approximation significantly simplifies their derivations of theoretical compressive behavior but is only sufficiently accurate when "the elastomer layers are no thinner than about seven percent of their smaller plan dimension" (Stanton and Lund 2015). Holownia (1972) indicates that the value of $\nu$ should fall between 0.4985 to 0.4999 instead of 0.5 (completely incompressible). Though the difference may seem trivial, it is actually quite large since $K$ changes from infinity to below 1,000 ksi in this range. Holownia (1980) notes that accurate knowledge of $\nu$ is extremely important for elastomers because small changes in $\nu$ lead to large differences in the stress distribution.

For elastomer layers with higher shape factors, the assumption of incompressibility leads to the overestimation of compressive stiffness, buckling load and resonant frequency (Koh and Lim 2001, Pinarbasi and Akyuz 2004). Additionally, adding material fillers with lower bulk moduli during the manufacturing process (like cork) may invalidate the incompressibility assumption entirely. For this reason, Holownia (1972) states that "it is very important to know exactly the value of [Poisson's ratio] for the material employed."

### 2.2.5 Compression of Restrained Elastomer

When bonded surfaces (i.e. layers of reinforcement) restrain lateral spreading, the sides bulge out in a parabolic shape and cause shear strains at the bonded interfaces (Gent and Meinecke 1970, Holownia 1972). Figure 2-6 illustrates the superposition of the unrestrained case with

the restraining forces that achieve the correct bulge shape. Figure 2-4a highlights the bulge that forms as a result of the compression loading and depicts the shear strain caused by the bulge (Stanton and Lund 2015).

For restrained elastomer layers, the compression response changes from that reflected in Equation 2-5 to (Stanton and Roeder 1982):

$$\sigma_z = E_a \epsilon_z \tag{2-7}$$

where $E_a$ is the apparent elastic modulus that takes into account the pure elastic modulus of the material ($E$) and any lateral restraint. When bonded elastomer layers are tested in compression, $E_a$ is the observed slope of the stress-strain response and is proportional to $E$ by the equation:

$$E_a = f_c E \tag{2-8}$$

where $f_c$ is a constant that depends on bulk compressibility and shape factor. Traditionally, equations relating $E_a$ to $E$ give $f_c$ the form:

$$f_c = A + BS^2 \tag{2-9}$$

where $A$ and $B$ relate to the specimen geometry, bulk compressibility and shear modulus, which are all intimately connected to the compression response.

Gent and Lindley (1959) derived the solution for the $E_a$ for an infinite strip and a circular shape assuming complete incompressibility:

$$E_{a,inf.strip} = E\left(\frac{4}{3} + \frac{4}{3}S^2\right) \tag{2-10}$$

and

$$E_{a,circ} = E\left(1 + 2S^2\right). \tag{2-11}$$

Others expanded on that solution to include other shapes including rectangular layers (Gent

and Meinecke 1970) and to include the compressible case (Kelly 1997, Holownia 1972).

The inclusion of bulk compressibility was vital to elastomer theory. For incompressible elastomers the area of the bulge is equal to the volume displaced by the loading head—that is, the volume that would have spread out laterally in the unrestrained case. As $K$ decreases from infinity, the bulge becomes smaller but retains its parabolic shape (Holownia 1972). This leads to lower shear strains in the elastomer and a lower $E_a$ (Stanton and Roeder 1982).

Stanton and Lund (2015) used the same model for $f_c$ as used in classical elastomer theory (Equation 2-9) but refined the coefficients $A$ and $B$. They determined both theoretically and experimentally that $A$ was based on the shape of the elastomer layer:

$$A = \begin{cases} \frac{4}{3}, & \text{for cases of plain strain;} \\ 1, & \text{for rectangular bearings,} \end{cases} \tag{2-12}$$

and $B$ was based on the compressibility index, $\lambda$:

$$B = \frac{4}{3}\left\{\frac{3}{2\lambda^2}\left(1 - \tanh\frac{2\lambda}{2\lambda}\right)\right\} \tag{2-13}$$

where

$$\lambda = S\sqrt{\frac{E}{K}}. \tag{2-14}$$

This closed-form derivation of $B$ is exact for the special case of an infinite strip, but it serves as an approximation for rectangular bearings, for which $B$ cannot be derived directly. Stanton and Lund (2015) present a finite difference method that allows $B$ to be solved for other cases, but the approximation is sufficient for this work.

For small bearings, the $A$ term controls the stiffness expression, but for large bearings ($S \geq 6$), the $BS^2$ term dominates the expression (Stanton and Lund 2015).

#### 2.2.5.1 Shear Strain from Compressive Loading

Shear strain resulting from compressive loading depends on the shape factor and bulk compressibility. For circular bearings and infinite strips of incompressible elastomer, the relationship of compression strain to shear strain is found by the common equation:

$$\gamma = 6S\epsilon_z, \tag{2-15}$$

but this underestimates the shear strain for other shapes (Stanton and Roeder 1982).

The relationship between compressive loading, $\sigma_z$ and the shear stress induced by bulging, $\tau$ is more accurately shown by Stanton and Roeder (1982) to be:

$$\tau = g_c f_c E \epsilon_z \tag{2-16}$$

where $g_c$ is a constant that relates the shear stress to the apparent compressive stress. Additionally, Stanton et al. (2008) states that:

$$\gamma = \frac{\sigma}{GS} \tag{2-17}$$

for small displacements. When a parabolic bulge shape is assumed, Equation 2-17 can be simplified to:

$$\gamma = 4h/t \tag{2-18}$$

where $h$ is the maximum parabolic bulge height of the layer. The shear modulus, $G$, converts that shear strain into the shear stress felt by the elastomer.

These properties—the compressive, bulk and shear moduli—are all related by the elasticity equation:

$$E = \frac{9KG}{3K + G}. \tag{2-19}$$

Maintaining a constant bulk modulus, an increase in $G$ would lead to a similar increase

in $E$, but an increase in $K$ while maintaining a constant $G$ would have minimal effect on $E$. For normal, incompressible rubber material, $K$ is three orders of magnitude greater than $E$ and $G$. Similarly, Poisson's ratio, $\nu$, can be related to these properties as well by the equations:

$$\nu = \frac{3K - 2G}{2\left(3K + G\right)} \tag{2-20}$$

and

$$\nu = 0.5\left(1 - \frac{E}{3K}\right). \tag{2-21}$$

#### 2.2.5.2 Compression and Shear Strength

In all types of loading except isotropic tension, failure is caused by tearing and crack propagation. In each case, a form of the fracture mechanics equation (Equation 2-22) can be used to characterize the tearing energy (Lake and Thomas 2001, Stanton et al. 2008).

$$G = Ut \tag{2-22}$$

where $U$ is the elastic energy density.

Lake and Thomas (2001) completed a detailed investigation of crack growth for various loading configurations. Their work shows that the failure mode does not change based on strength, temperature or loading direction for typical rubber materials. Failure in compression or shear is caused by tension stresses along the traction-free perimeter that develop near the bonded edges.

In design, AASHTO requires a stability check for bridge bearings. The average compressive stress is limited to half the predicted buckling stress according to the buckling theory developed and verified experimentally by Gent (1964) and Stanton et al. (1990) respectively (AASHTO 2010: (C)14.7.5.3.4). In AASHTO's bearing design 'Method A,' compression stress at the service limit state is limited to no more than 800 psi (AASHTO 2010: 14.7.6.3.2), though this is generally thought of as highly conservative. Laminated, elastomeric bearings

are used in other applications and outside the United States at much higher stresses (Stanton and Roeder 1982, Sommer 2013, p. 185). Design for direct shear is usually controlled by displacement restraints of the structure.

### 2.2.6 Other Considerations for Laboratory Tests

Varying test conditions such as specimen geometry, extension rate, temperature, humidity and pretest conditioning can greatly affect the observed material properties. Therefore, the researcher must take care to maintain these variables by changing only one in each test sequence, holding the rest constant. Material property tests should report the values of each variable along with the result for repeatability and comparison of the test data. In addition to specimen geometry (discussed in Section 2.2.1.1), a brief discussion of loading/extension rate and temperature are discussed here.

**Loading Rate** The stress-strain properties of elastomers are inherently rate-dependent, meaning the material properties vary when measured at different loading rates. Occasionally, rate-independent tests are desired—tests that are either excessively fast or slow to capture upper and lower bounds of the desired material properties. Other rates create properties that fall in between the boundaries of the rate-independent tests. Faster rates typically lead to the material appearing stiffer and stronger, while slower rates often lead to a reduction in observed strength and stiffness. ASTM D4014 prescribes a rate-independent compression stiffness test for bridge bearings that finds the lower bound of the compression stiffness by loading to the design load by increments of one-fifth the design load. At each increment, the load is held constant for 30 seconds, then the load and deflection is measured. The stiffness is then determined as the slope of the best fit line through the points.

**Temperature** Elastomers are sensitive to heat, and the temperature during testing should be controlled. ASTM D412 dictates the standard testing temperature range to be 69.8–77.0 degrees Fahrenheit, and ASTM D4014 gives a slightly wider range for testing elastomeric

bearings for bridges (62.7–84.2 degrees Fahrenheit). Testing temperatures outside the ASTM specifications may be agreed upon by customer and supplier according to their project needs (ASTM D1349). Other standardizing bodies suggest maintaining the same temperature for testing that was used to store the material to ensure a uniform temperature gradient through the volume of the elastomer because a non-constant temperature throughout the material can cause uneven and irreproducible material properties. At low temperatures, crystallization of the elastomer can occur, increasing the modulus of natural rubber 100-fold (Sommer 2013)

### 2.2.7 Pourable Elastomers

Very little research has been performed on pourable elastomers for structural uses. Pourable elastomers are most commonly used in bridge joint and crack sealing applications and are also common in the automotive, sanitary and electronics industries, but they are rarely used in load-bearing applications. Most research is performed by manufacturers in their research and development departments, and information learned from this research is then considered proprietary.

Some of the most commonly advertised features of pourable elastomer are its self-leveling nature, simple mixing procedure and long-lasting, low-maintenance final product. Pourable elastomers are usually two- or multi-component products that cure when mixed together. They typically have short working times (under 10 minutes) and take several hours to fully cure, many up to 24 hours. The maximum elongation is usually between 300–500 percent, and the reported strengths vary significantly.

## 2.3 Expected Demands on the Track Fixation System

Before exploring the test materials, procedures and results, it is important to address the expected demands on the system. The “design train” prescribed by Sound Transit’s Design Criteria (Sound Transit 2013) is a fully loaded, four-car train weighing a total of 158.8 kips per car with an unfactored maximum axle load of 28 kips. For the purpose of this research,

14 kips (58.3 psi) is considered to be the maximum compressive service load experienced by a single plinth, and in an extreme event (i.e. a fully-loaded, tipping train) the design train exerts a 28 kip compressive force (116.6 psi) on a single plinth.

The primary force on the plinths acting transversely to track is the dynamic hunting force. The hunting force occurs as the train "hunts" for the rails. It is analogous to the train bouncing from side to side against the rails as it travels down the track. The hunting force is estimated to be 10 percent of the axle weight of the design train under service loading (2.8 kips), and it is prescribed to be applied 3.5 ft above the low rail simultaneously with vertical load (Sound Transit 2013). This leads to a complicated combination of vertical and horizontal load and moment applied to the plinth.

A conservative assumption for shear analysis of the elastomer is to apply the full hunting force to each plinth rather than dividing the load between the two parallel plinths.[4] Figure 2-7 illustrates the assumed loading. The unfactored hunting force amounts to approximately 12 psi of shear stress on the elastomer.

Another expected lateral force is the component of the weight of the light rail vehicle that is parallel to the bridge deck as the bridge rolls and rocks over the waves. Sound Transit (2010) provides the expected roll of the bridge in an extreme event to be two degrees, not including the effect of the light rail vehicle. To account for the vehicle without an intensive study of its effect on the movement of the bridge, a five degree rotation is used to calculate the induced shear stress in the plinth. A 14 kip wheel load would place a five psi shear stress on the elastomer with a five degree roll of the bridge:

$$\frac{14,000 \text{ lb} \times \sin(5^\circ)}{240 \text{ in}^2} \simeq 5 \text{ psi}. \tag{2-23}$$

The greatest shear stress felt by the elastomer as a train moves along the rails will be caused by the restraint of the bonded elastomer layer as the weight of the train loads the elastomer in compression. This was discussed in Section 2.2.5 and is completely dependent on the

[4]It is conservative provided the cross-bracing bar is installed in the LWC as shown in Figure 2-7.

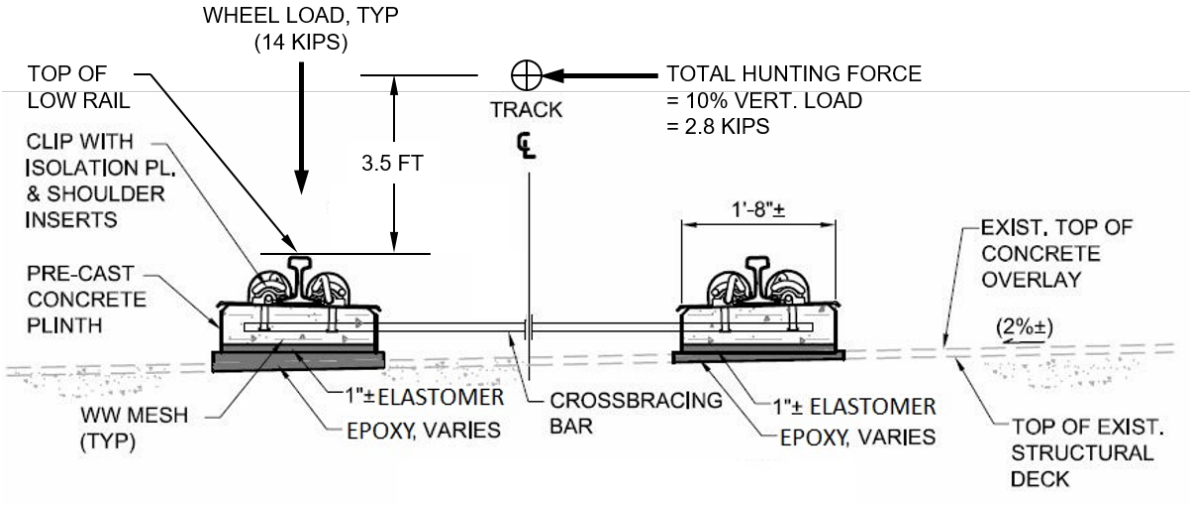


**Figure 2-7.** A sketch of the hunting force as applied to the track attachment system. (Original figure from Sound Transit (2013))

shear modulus of the elastomer and the geometry of the layer. According to Equation 2-17, the shear stress caused by the compressive load of the design train is approximately 31 psi.

Generally, shear stresses or strains resulting from all types of loadings (compression, rotation and direct shear) are superimposed. This is known to be incorrect and has been called a "major unanswered question" in the behavior of elastomeric bearings, but no better alternatives are available (Stanton and Roeder 1982). Superimposing the shear forces due to train weight, hunting force and rocking of the bridge, the total expected shear stress is 46 psi. The expected loads for this system are summarized in Table 2-1.

**Table 2-1.** Expected Load Summary

| **Load Type** | **Expected Load (Extreme Condition)** | **Compression Stress** | **Shear Stress** |
|---|---|---|---|
| Train Weight | 28 kips | 117 psi | 31 psi |
| Hunting Force | 2.8 kips | 0 psi | 12 psi |
| Bridge Rocking (5 degrees) | 1.2 kips | 0 psi | 5 psi |
| **Sum** | | **117 psi** | **48 psi** |

# 3 Materials

Specimens were created to model the complete system used in Sound Transit's plinth design in order to characterize the system response in tension, compression and shear loading. They generally consisted of lightweight and normal weight concrete produced in the concrete laboratory at the University of Washington as well as elastomer, epoxy adhesive and their respective bonding primers provided by EdilonSedra. Figure 3-1 is a schematic of the individual materials comprising each specimen.

This chapter describes each material used throughout the project. Because of the proprietary nature of the elastomer, epoxy and primers, their make-up will not be discussed beyond what is publicly available. Physical properties for the lightweight and normal weight concrete mixtures, two elastomers: Corkelast VA-60 and Editaan 70U, and an epoxy, DexG, are discussed below.

## 3.1 Lightweight Concrete

Lightweight concrete was chosen for the plinth concrete in order to reduce the superimposed dead load on the floating bridge. Therefore, all test specimens representing plinths and/or interactions with the plinths contained lightweight concrete.

Lightweight aggregates from Stalite Corporation in North Carolina (Stalite) were used with Type III Portland Cement to achieve a mixture with a six- to nine-inch slump and six percent air while maintaining a minimum initial concrete strength (at 18 hours) of 2,500 psi and a 28-day strength of 4,000 psi. Stalite aggregate was chosen for the low saturated

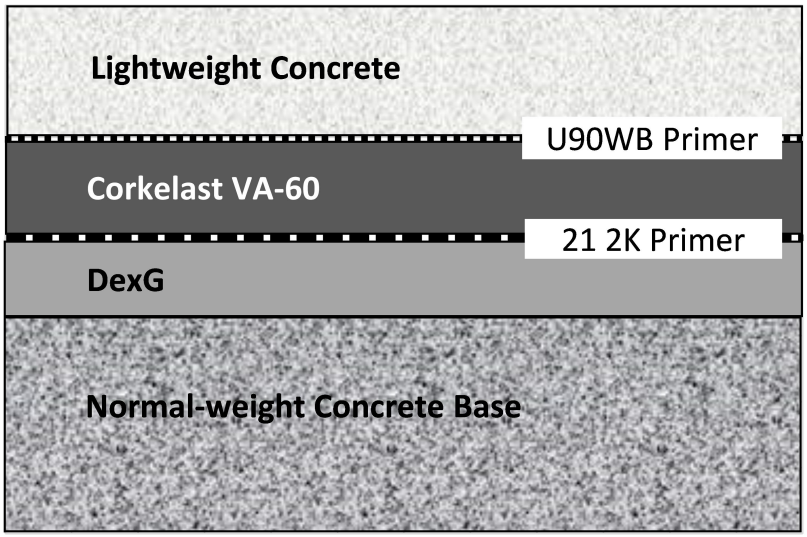


**Figure 3-1.** Schematic Showing Test Specimen Layers.

surface dry (SSD) unit weight of the resulting concrete after comparing aggregates from several suppliers.

Slump, fresh unit weight and volumetric air content were measured from fresh mixtures, and compression strength, tensile strength (split tension), elastic modulus and hardened unit weight tests were performed on cured cylinders at standard intervals. The mixture proportions and resultant concrete properties are described below.

### 3.1.1 Mixture Proportions

As mentioned above, each mixture was proportioned for the target fresh mixture results of a six- to nine-inch slump with six percent air. The water-cement ratio, paste content, aggregate gradation and the addition of admixtures were used to achieve these results.

First, mixtures were proportioned with a water to cement ratio of 0.4 to increase the cohesiveness of the paste and aid in early strength gain while allowing easy mixing. Due to the difficulty of controlling the moisture content of the lightweight fine aggregate, the actual water-cement ratio varied and significantly affected workability in many of the trial mixtures.

Next, the paste content was targeted at 27.7 percent (by volume) based on previous experience with conventional mixtures. Paste comprises cementitious materials combined with water and admixtures. It is heavier than most lightweight aggregate, so reducing the paste content in a mixture reduces the unit weight of the concrete, a target objective when developing lightweight concrete mixtures.

In addition, an imbalance between viscosity of the plastic mixture and paste content tends to cause mixture segregation: the coarse aggregate floats to the surface of the mix (or sinks to the bottom in the case of normal aggregate). It was discovered through trial and error that mixtures containing lightweight fine aggregate met workability requirements more reliably when the paste content was increased to 32 percent due to the increased paste requirements of angular (crushed) aggregate (Kosmatka and Panarese 1994, p. 80).

Aggregate gradation is another important part of mixture proportioning. Different aggregate sizes are blended together to form a well-graded mixture; one that maintains a smooth transition between coarse and fine aggregates and minimizes the paste required. Figure 3-2 shows the individual gradations of coarse, medium and fine aggregate and how they combine to achieve a target gradation curve. A coarse to fine ratio of 52:48 by volume seemed to provide the smoothest combined gradation curve and was used for all mixtures.

Finally, air-entraining, water-reducing and high-range water-reducing admixtures were used to fine-tune the mixture. These admixtures were selected because they were frequently used at a local precast plant. Since water expands about nine percent through its freezing process (IAPWS 2013), entrained air voids in the paste are necessary for freeze-thaw durability to reduce hydraulic pressure by providing room for the displaced water (Kosmatka and Panarese 1994, p. 12). An air-entraining agent, Daravair 1000, was used to achieve a six percent air content of the mixture, creating a Class A(AE) mixture as defined by AASHTO for use where freezing and thawing cycles are expected (AASHTO 2010: 5.4.2.1). A standard dose (150 mL/100 lb cement) of the normal range water reducer, WRDA 64, was held constant throughout all mixtures for increased time to initial set, and ADVA 575, a high-range water reducer, was added to improve workability.

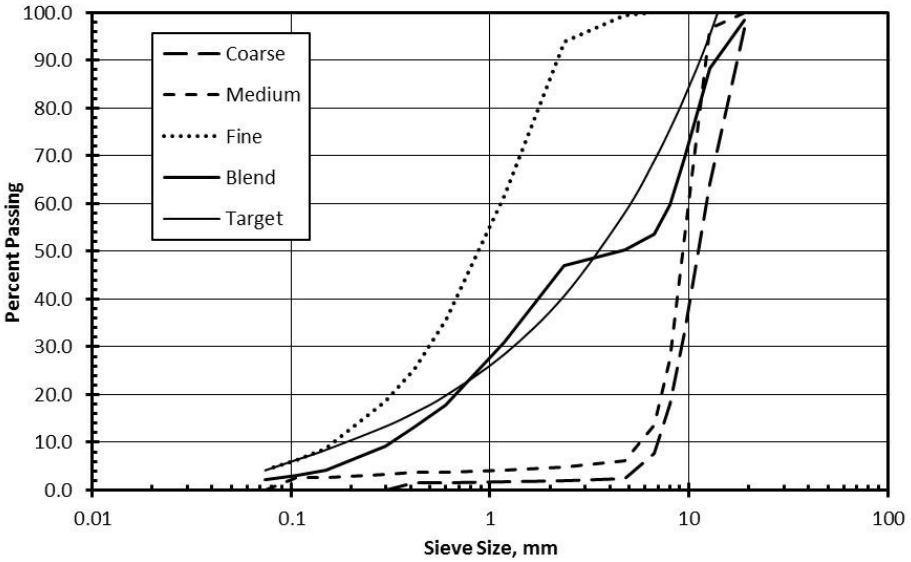


**Figure 3-2.** Lightweight Aggregate Smoothed Gradation Curve.

A side effect of the high-range water reducer was a reduction in entrained air, so the two admixtures had to be well-balanced. However, the variability in moisture content of the aggregate (Section 2.1.1) made the relationship between admixtures difficult to quantify. Therefore, the admixture ratios were determined by trial and error on numerous test batches.

Once proportioned, mixtures were mixed and cast in a specific and precise manner to minimize error. This procedure is described in detail in Appendix A.

### 3.1.2 Resultant Concrete Properties

Prior to producing the concrete used in the elastomer testing, a preliminary batch that adhered closely to the fresh mix criteria was mixed and subjected to a series of materials tests to evaluate compressive strength (ASTM C39), splitting tensile strength (ASTM C496) and elastic modulus (ASTM C469). The hardened unit weight was also measured in saturated surface-dry (SSD) conditions, a modification of ASTM C567, to approximate the expected, unfactored dead load on the bridge. The results are presented in Table 3-1 and are considered representative for all LWC batches.

**Table 3-1.** Resultant Properties of a Representative Lightweight Concrete Mixture

| **Test** | **ASTM Standard** | **Value** |
|---|---|---|
| Compressive Strength[a] | ASTM C39 | 5,475 psi |
| Slump | ASTM C143 | 9 in |
| Air Content | ASTM C173 | 7.1 % |
| Splitting Tensile Strength[a] | ASTM C496 | 482 psi |
| Elastic Modulus[a] | ASTM C469 | 2,416 ksi |
| Hardened Unit Weight | ASTM C567 mod. | 105.6 pcf |

[a]28-day Value

## 3.2 Normal Weight Concrete

The primary goal in designing the normal weight concrete used to represent the deck surface was to create a suitable base for elastomer compression tests (Section 5.2.2). The normal weight concrete strength was capacity controlled by the strength of the other system elements and had a minimum strength of 5,000 psi. Normal concrete was also used in lower stress conditions as a base for tension pull-off testing (Section 5.1.2) and as a loading block for shear testing (Section 5.3.1).

Concrete was mixed in the UW concrete laboratory using Type I-II Portland Cement from LaFarge Corporation in Seattle, Washington and aggregates from glacial pits in Dupont, Washington provided by Salmon Bay Sand and Gravel (Ballard, Washington). Excess concrete from other experiments in the University of Washington structures lab with more stringent (higher) strength requirements was used whenever possible to responsibly reduce lab waste and increase time efficiency in the lab.

## 3.3 EdilonSedra Elastomers

Two pourable, polyurethane elastomers were provided by EdilonSedra for use in this testing: Corkelast VA-60 (Corkelast) and Editaan 70U (Editaan). Both elastomers were developed for use in rail fastening systems to elastically absorb dynamic loads and provide damping that reduces noise and vibration. They also aid in the electrical insulation of rail systems. Both are two-component, pourable products that chemically react when mixed.

EdilonSedra publishes certain mechanical properties of their elastomers for use in design of their materials. Unfortunately, they do not report the dimensions of their test specimens alongside the published properties, making it difficult to interpret the provided results. The one exception is for the elastic modulus in compression; they report the specimen dimensions to be 50 mm by 50 mm by 25 mm (approximately 2 inches by 2 inches by 1 inch). Table 3-2 provides a summary of the reported mechanical properties for Corkelast and Editaan, which will be compared with the test results of this project in Chapter 6. Refer to the Product Data Sheets and Safety Data Sheets for the two elastomers in Appendix E for other material properties. The following sections discuss Corkelast and Editaan in more detail.

**Table 3-2.** Mechanical Properties of EdilonSedra Elastomers.

| **Property** | **Standard** | **Corkelast Value** | **Editaan Value** |
|---|---|---|---|
| Tensile Strength | ISO 527 | 145 psi | 290 psi |
| Modulus of Elasticity | ISO 527 | 508 psi | 1160 psi |
| Tensile Strain at Break | ISO 527 | $> 140$ % | $> 100$% |
| Static Compressive Modulus | ISO 604 | 856 psi | 2,030 psi |
| Tear Strength | ISO 34 | $> 62.8$ lb/in | $> 69$ lb/in |
| Adhesive Strength on Concrete[a] | Based on ISO 4624 | $> 116$ psi | $> 217$ psi |
| Cured Density | ISO 1183-1-A | 65.5 pcf[2] | 56.81 pcf |

[a]Cohesive Elastomer failure

### 3.3.1 Corkelast VA-60

Corkelast was the main elastomer used throughout the project. It uses small pieces of cork filler throughout the material to alter the material properties. Presumably, because of the cork in the material, the elastomer is more compressible and has a lower stiffness and unit weight than common rubber materials.

Corkelast must be applied quickly after mixing the two components in a clean, dry environment. At room temperature the working window for placing the material is 1–18 minutes. Its minimum curing time, the earliest time the material can carry dynamic load, varies between 1.5–5 hours depending on the surface temperature. The product data sheet (Appendix E) states that Corkelast can be fully loaded after 24 hours, but an EdilonSedra representative noted in private correspondence that material testing should take place after seven days when the material properties stabilize.

### 3.3.2 Editaan 70U

Editaan was also used in this research to compare results and verify test procedures. Editaan is stronger than Corkelast, but without the cork additive, it is also much stiffer than Corkelast and is presumed to have a higher Poisson's ratio. The higher stiffness is undesirable for light rail applications when considering vibration damping. In the product information, Editaan is reported as being lighter weight than Corkelast, but this does not reflect the author's personal experience.

The working time for Editaan is also short, ranging from 7–17 minutes depending on product temperature. The typical pot life experienced was 9 minutes. After mixing, the minimum cure time is four to seven hours depending on surface temperature, and the elastomer can be fully loaded after 24 hours.

Table 3-2 gives the mechanical properties of Editaan, and the complete product and safety data sheets can be found in Appendix E. Again, the specimen dimensions are not reported but for the elastic modulus. As with Corkelast, $E$ was tested on a 50 mm by 50 mm

by 25 mm cube.

## 3.4 DexG Epoxy

DexG is a self-leveling, high performance structural grout produced by EdilonSedra. The product data sheet (Appendix E) also states that the epoxy is solvent-free, utilizing "special epoxy resins and high quality mineral filler materials." The material was developed for under-grouting structures with heavy, dynamic loads such as railway track structures and is often used in conjunction with the elastomers described in Section 3.3. The epoxy is shipped in two components that are mixed together at use, creating the chemical reaction that initiates curing. The material has a 20-minute placing window at room temperature after mixing and is fully cured and load-ready in 24 hours.

Table 3-3 provides a summary of the mechanical properties of DexG reported by EdilonSedra. Refer to the Product Data Sheet and Safety Data Sheet in Appendix E for other material properties.

**Table 3-3.** Mechanical Properties of DexG as Provided by EdilonSedra

| **Property** | **Standard** | **Value** |
|---|---|---|
| Flexural-Tensile Strength | EN 196-1 | 8,224 psi |
| Compression Strength | Based on EN 196-1 | 13,054 psi |
| Modulus of Elasticity | ISO 179 | 652,680 psi |
| Shear Strength | ASTM D1002 | 2,176 psi |
| Cured Density | ISO 1183-1-A | 100 pcf |

## 3.5 Primers

Two EdilonSedra primers, U90WB and 21-2K, were used to maximize bond between the elastomer and adjacent concrete and DexG, respectively. Both are two-component primers that are mixed together at time of use.

### 3.5.1 Primer U90WB

Primer U90WB is a water-based primer that is applied by brush or roller to pretreated steel or concrete surfaces to increase the bond strength with EdilonSedra elastomers. It has a 60-minute working window after mixing, and elastomer may be placed on the primed concrete after 24–72 hours of curing time according to the product data sheet. The adhesive strength of primer U90WB to a prepared concrete surface is reported as greater than 218 psi based on cohesive concrete failure when tested according to ISO 4624. Refer to Appendix E for the complete product and safety data sheets.

### 3.5.2 Primer 21-2K

Primer 21-2K is an solvent-based bonding primer used to aid the bond between EdilonSedra elastomers and epoxy. It has a 45-minute working window after mixing the two components and cures fully in one hour. The epoxy must be mixed and applied between 1–8 hours after primer application. The adhesive strength varies depending on the type of elastomer it bonds to, but the primer is designed so that any structural failure will occur cohesively in the elastomer and not at the bond layer. Appendix E contains the complete product and safety data sheets for Primer 21-2K.

### 3.5.3 Materials Summary

In summary, six materials were used to create each specimen: lightweight concrete, normal concrete, Corkelast or Editaan elastomer, DexG epoxy and bonding primers U90WB and

21-2K. The lightweight concrete strength was at least 4,000 psi as specified by Sound Transit engineers, while the normal concrete was capacity designed to provide an adequate base for all tests and did not fail during testing. The mechanical properties of EdilonSedra materials were presented as provided by EdilonSedra, but EdilonSedra did not provide specimen dimensions with the results of their testing. Previous work discussed in Chapter 2 shows (and the current study confirms) that specimen dimensions greatly affect the apparent material properties of elastomer, so EdilonSedra's results cannot be usefully interpreted without further information.

# 4 | General Specimen Assembly

The elastomer, epoxy adhesive and associated primers were manufactured by EdilonSedra. This chapter describes the process in which the EdilonSedra products were mixed and applied to create the specimens used in the various tests performed as part of this research.

Prior to any material application, lightweight concrete blocks were moist-cured for a minimum of 14 days. They were then pressure washed to remove all laitance and contaminants from the concrete surface. Normally, the blocks were either dried with pressurized air or allowed to air-dry for at least 24 hours immediately following the pressure-washing. But due to personnel and laboratory availability, some of the lightweight concrete blocks to be used in the tension testing were returned to the moist curing environment after pressure-washing before drying and material application. There was no maximum time given between surface cleaning and material application before the surface was deemed unclean and in need of re-washing, but the material application directions provided by EdilonSedra stated to apply the product "as quickly as possible after preparation of the surface to prevent further contamination and corrosion of the surface" (Appendix E).

Application of EdilonSedra products followed their guidelines for mixing, application and timing after thorough pre-treatment of the concrete blocks. All specimen assembly and mixture of EdilonSedra products occurred in the University of Washington concrete laboratory at temperatures between 65–75 degrees Fahrenheit and relative humidity levels between 45–65 percent (Refer to Appendix E for temperature and humidity guidelines for all materials provided by EdilonSedra). Additionally, a schematic of the various material layers

is provided in Figure 3-1 for reference.

## 4.1 Primer U90WB

Primer U90WB (used to adhere the elastomer to the lightweight concrete) was mixed by hand for 60 seconds and then applied per material specification either by roller or brush, depending upon specimen size. Though the manufacturer's guidelines suggest machine mixing, the small quantity of primer needed for the laboratory specimens made machine mixing impractical. The primer was cured for a minimum of 24 hours (and not longer than 72 hours) as required by the product data sheet for controlled temperature applications[1] (Appendix E). After curing, the primer-lightweight concrete bond was confirmed by a pull-off (P.A.T.) test conducted by engineers from KPFF in accordance with ISO 4624. The minimum required P.A.T. pull-off strength was 1.5 MPa (220 psi), and the P.A.T. tested area was re-primed if the disturbed area was more than 10 percent of the bond surface.

## 4.2 Elastomer

The elastomer was prepared by mixing the two components together for at least 60 seconds using a spiral mixing paddle mounted in a drill press. Small batches used a 3-inch diameter by 4-inch long paddle while larger batches used a 4-inch diameter by 5-inch long paddle. The paddle size varied by batch size, allowing the paddle to remain covered by the elastomer components to avoid introducing excess air during the mixing process. Additionally, the energy forced into the system by the paddle during mixing affected the rate of chemical reaction of the combined components; excessive mixing accelerated the reaction, leading to hotter temperatures, faster curing and shortening the already small window of applicability (typically 17 minutes, Appendix E). This was mitigated by using the smaller paddle for

[1]Note: After the testing program was completed, EdilonSedra reduced the curing window for Primer U90WB to 24–48 hours.

smaller batches and limiting the mixing time to the 60 second minimum. For both paddles the drill press was operated at 470 rpm.

Oil-based mold-release agents were specifically avoided, per EdilonSedra's instruction, so molds were prepared using plastic wrap against steel and wood forms, and small plastic forms (tension pull-off testing) were briefly immersed in molten paraffin to facilitate mold-release. The freshly mixed elastomer was then poured onto the primed, lightweight concrete specimens to the desired thickness. Figure 4-1 shows elastomer being poured onto a primed compression specimen. After allowing the elastomer to cure for at least 24 hours at room temperature, the surface was sanded with an orbital sander using coarse sandpaper (40-grit) to remove the shiny surface and expose some of the cork particles in the elastomer.

## 4.3 Primer 21-2K and DexG

Sanded elastomer was then primed using Primer 21-2K. The primer components were hand-mixed for 60 seconds and then applied to the elastomer by brush or roller. After a minimum of one hour (maximum 12 hours), the primer-coated specimens were inverted and supported 0.25 inches above previously prepared base concrete pieces. Formwork attached to the base concrete surrounded the assembly and extended above the bottom edge of the elastomer to form a confining dam for the epoxy application. Figure 4-2 shows a plinth (compression specimen) inverted over a concrete slab awaiting DexG application.

The epoxy (DexG) was mixed using the 3-inch diameter spiral mixing paddle in a drill press running at 470 rpm for at least 50 seconds and poured into the quarter-inch gap in such a way to avoid trapped air, maximizing the bond strength. For the shear and tension specimens, this was accomplished by pouring the DexG from one end of the form onto the base concrete surface (Figure 4-3).

The formwork dam allowed the epoxy to flow on the base concrete block, underneath the lightweight concrete-elastomer block, to the other end of the specimen, completely filling the 0.25-inch void between the base concrete and the primed elastomer. Occasionally, DexG


**Figure 4-1.** Liquid elastomer is poured onto a primed lightweight concrete block that will be used for compression testing.


**Figure 4-2.** A plinth inverted over a concrete slab awaiting DexG application. A wood-reinforced duct tape barrier creates a dam for the DexG to flow into. The wooden reinforcing is not shown.

**Figure 4-3.** Four shear specimen awaiting DexG Application.


**Figure 4-4.** Two shear specimen during DexG Application. The DexG flows from the large dam on the left underneath the lightweight concrete block to the right.

would leak out of the form during casting, and the specimen would require patching. A shear specimen requiring patching is shown in Figure 4-5. Figure 4-6 shows a close-up image of a shear specimen after all material application was completed, before the testing apparatus was assembled.

For the larger compression specimen, the DexG was poured through a central hole cast into the specimen and allowed to flow radially outward under the block (Figure 4-7). While this method ensured that no air bubbles would be captured between the plinth and the base, the dam, made of duct tape, proved ineffective to withstand the dense liquid DexG, and in many cases the DexG pushed the tape free and flowed down the base. This left unfilled areas between the plinth and the base that had to be patched once the initial DexG pour had cured. Various dam-reinforcement tactics were attempted, but leaking occurred on many specimens.

An unfortunate outcome of this procedure was that the final test specimens varied significantly. Some specimens had the DexG rise too high along the side of the specimen, adding confinement to the elastomer that would prevent the lateral bulge and increase the measured stiffness. Therefore, the confining DexG was removed to the extent possible, but the degree to which this affected the test results is unknown. Due to the larger size of the specimen, the effect was thought to be minimal.

Minimum curing times prior to load testing were 24 hours for the DexG epoxy (including patched specimens) and seven days for the elastomer (Appendix E).


**Figure 4-5.** This double shear specimen required patching when the DexG did not flow all the way through the quarter-inch gap.

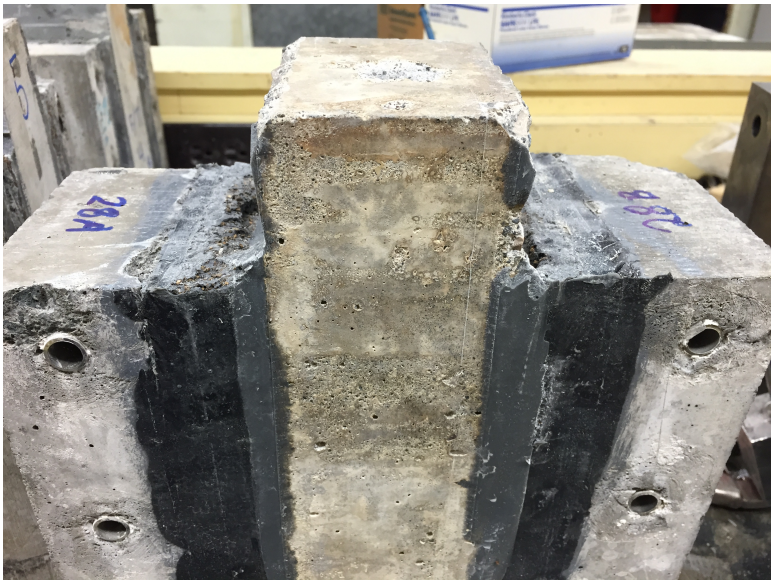

**Figure 4-6.** A Complete Shear Specimen.


**Figure 4-7.** For the full-size plinths used in compression testing, the DexG was poured through a central blockout, flowing radially outward under the block.

# 5 | Setup and Procedure

## 5.1 Tension

Pull-off testing was conducted to determine the strength of the LWC-elastomer system in direct tension. The tests were performed in accordance with ASTM C1583—a test primarily used to evaluate the bond strength of bridge deck overlays. This test required a steel disk to be glued to the top of the concrete test specimen. The pull-off apparatus, which was then attached to the steel disc, applied tension to the top surface of the concrete. The base concrete was used as the reaction surface for the testing. A photograph of the tension pull-off apparatus is shown in Figure 5-1. The photograph shows multiple specimens attached to a concrete base as well as the test apparatus set up to test one of the specimens.

### 5.1.1 Specimen Preparation

The tension pull-off testing was conducted on 2.25-inch diameter lightweight concrete cores that were attached to a normal concrete base using the elastomer-epoxy process described in Chapter 4. Three batches of tension specimens (A, B and C) were produced for testing, each characterized by unique material and procedural elements. The varying characteristics are described below.

An original set of ten specimens (Batch A) was prepared using a Stalite coarse, normal-weight fine concrete mixture. Editaan 70U, the stiffer of the two elastomers, was applied to these specimens. Half of the specimens were air-dried overnight prior to the original priming

**Figure 5-1.** Tension Pull-off Test Apparatus.

while the other half were removed from moist curing, and air pressure was used to blow off any moisture on the surface in order to evaluate the extent of drying necessary to achieve bonding. Section 6.1 discusses this effect.

A second set of six specimens (Batch B) was prepared using a Stalite coarse, Stalite fine concrete mixture. Corkelast VA60, a more flexible elastomer, was applied to these specimens. Unlike Batch A, however, the specimens were returned to the curing room after pressure washing for approximately one week. Four of the specimens were air-dried overnight prior to priming while the remaining two specimens were dried using compressed air immediately prior to priming.

Finally, Batch C was a set of ten lightweight concrete specimens prepared using a Stalite coarse, normal-weight fine concrete mixture. Priming with U90WB primer began immediately after pressure-washing and air-drying the concrete cores, but the elastomer was not applied to Batch C specimens until approximately 70 hours after applying the U90WB primer, just two hours before the end of the manufacturer's application range (72 hours). See Appendix E for more information on the suggested curing time of Primer U90WB. In

addition to the difference in the time of material application, five Batch C specimens were prepared using a 0.5-inch-thick Corkelast layer, and the other five maintained the standard 1.0-inch thick Corkelast layer.

Aside from the aforementioned differences between the batches, all other elements of setup and procedure were held constant for all specimens to limit the independent variables in the test.

### 5.1.2 Test Set-up

Up to five lightweight concrete cylinders were attached by the elastomer-epoxy system to a 16-inch by 16-inch normal weight concrete base (Figure 5-2). A 2-inch diameter metal disk was glued to the top of each tension-test specimen using glue provided by the test equipment supplier (German Instruments). The apparatus was then connected to the metal disk (shown in Figure 5-1). Steel spacers were placed around the specimen as necessary to achieve the proper height for the loading apparatus to transfer the reaction loading of the test apparatus to the base concrete. Washers were used as spacers where necessary to ensure a level reaction base.

### 5.1.3 Test Procedure

The loading was accomplished by hand-cranking the test apparatus at a rate of four revolutions per minute. The test apparatus had a total extension range of approximately 0.26 inches and a digital readout to indicate the maximum load applied, accurate to 0.1 MPa. In cases for which the maximum extension range was reached without total tension failure of the specimen, the maximum load reached was recorded as the failure load. The maximum load and failure mode were recorded and are discussed in Section 6.1. Unfortunately, the apparatus setup prevented observation of the elastomer during testing.

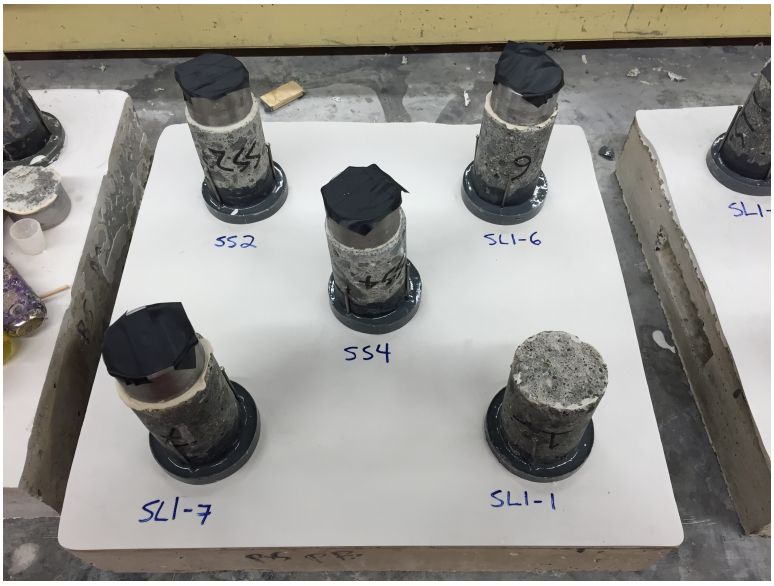


**Figure 5-2.** Tension Pull-off Specimen Attached to 16"x 16" Concrete Base

## 5.2 Compression

Models of the block-elastomer-deck system were tested in direct compression to verify the compressive stiffness of the elastomer. Lateral bulging was also measured to understand the bulging ratio of the material compared to the vertical deflection.

### 5.2.1 Specimen Preparation

Each specimen consisted of a 12-inch by 20-inch by 6-inch lightweight concrete block cast with minimal reinforcement that represented the lightweight concrete plinth (full-scale), a layer of Corkelast and DexG (with their respective primers) applied according to the general procedure described in Chapter 4, and a 14-inch by 22-inch by 4-inch normal weight concrete block that represented the concrete deck. Out of the 12 specimens created, four different elastomer thicknesses were used: 0.5 inch, 1.0 inch, 1.5 inches and 2.0 inches, with three specimens tested at each thickness. Table 5-1 relates each specimen to its elastomer thickness, and a schematic of the specimen arrangement on the loading table is shown in Figure 5-3.

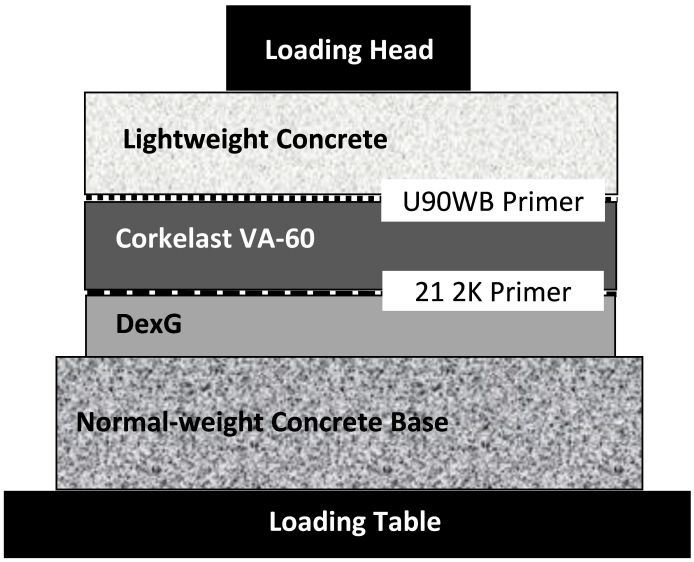


**Figure 5-3.** Compression Test Schematic

**Table 5-1.** Compression Specimen Matrix

| Specimen | Elastomer Thickness |
|---|---|
| C-1 | 0.5 in. |
| C-2 | 0.5 in. |
| C-3 | 0.5 in. |
| C-4 | 1.0 in. |
| C-5 | 1.0 in. |
| C-6 | 1.0 in. |
| C-7 | 1.5 in. |
| C-8 | 1.5 in. |
| C-9 | 1.5 in. |
| C-10 | 2.0 in. |
| C-11 | 2.0 in. |
| C-12 | 2.0 in. |

### 5.2.2 Test Setup

Each compression specimen was setup in a Baldwin universal testing machine with a 300,000-pound capacity. The specimen was centered under the 10-inch loading head, and pieces of plywood were placed under the loading head and between the base and the loading table to even out the load as it was applied and prevent local crushing of the concrete at locations of minor obtrusions. A diagram of the complete setup is shown in Figure 5-3.

Duncan potentiometers (POTs) centered on each 20-inch side (front and back of the specimen shown in Figure 5-4) measured vertical displacement. Lateral bulging at mid-height of the exposed elastomer was measured in the center of all four sides of the test specimen using horizontal Duncan POTs that were fixed to the test machine's loading base. Figure 5-4 shows a picture of a specimen in the testing machine that is ready for loading.

### 5.2.3 Test Procedure

Each specimen underwent two loading runs at a target loading rate of 6,000 pounds per minute to about 30,000 pounds, more than double the maximum expected service load on each block (Section 2.3). Since the purpose of the testing was to characterize compression behavior under expected and extreme loading conditions, double the maximum service load was considered adequate. To preserve the specimens, the blocks were not tested to failure.

Load, deformation and lateral bulge were recorded eleven times per second throughout each test by the internal load cell and six potentiometers. A discussion of the results is presented in Section 6.2.

## 5.3 Shear

Shear testing of the elastomer-concrete system was accomplished through a procedure developed for this investigation. The procedure is referred to as a double shear test because two separate lightweight concrete-elastomer-epoxy assemblies were loaded in shear simultane-

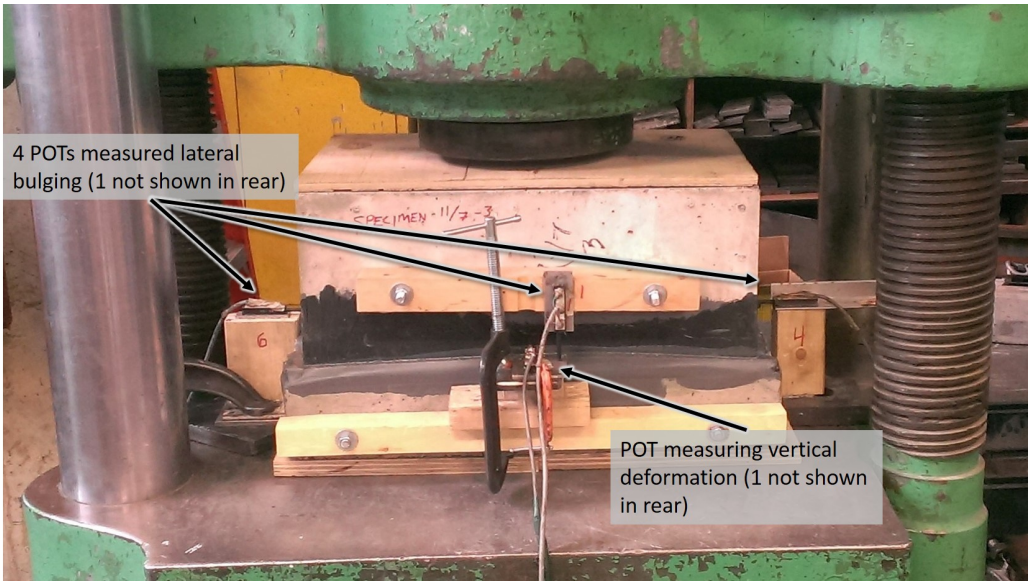


**Figure 5-4.** Compression Test Set-up

ously in the procedure. The testing program investigated the effects of surface preparation prior to material application, shear rate, elastomer thickness, tension/compression stress during shear loading (combined loading) and freeze-thaw exposure on shear behavior of the system. In addition, the shear behavior of the DexG epoxy was individually investigated using the same setup and procedure to prove its minimal effect on the system response.

### 5.3.1 Test Specimens

A double shear specimen consisted of a 3-inch by 4-inch by 10-inch normal weight concrete block as the centerpiece of the double shear setup representing the normal-weight concrete deck. Two 4-inch by 8-inch by 2-inch-thick lightweight concrete blocks were attached on either side of the centerpiece by the method described in Chapter 4. A drawing of a typical double shear specimen is shown in Figure 5-5.

The typical thickness of the elastomer for shear testing was one-inch but was varied for specific tests in the procedure. When investigating the effects of elastomer thickness on overall shear response, the elastomer thickness was varied between 0.5-inches and 2-inches.

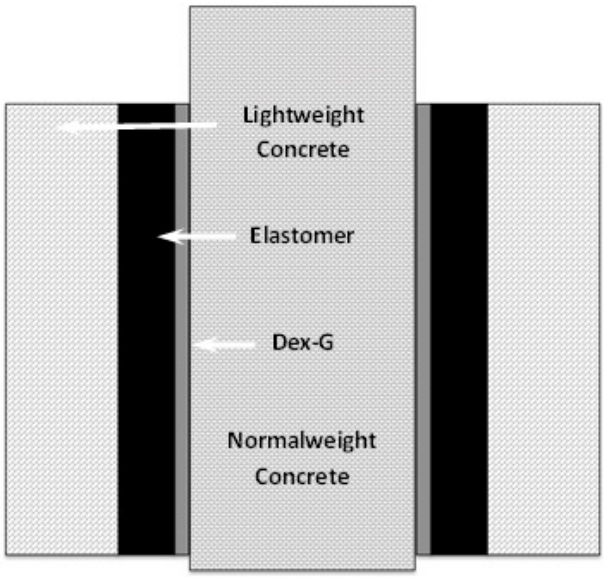


**Figure 5-5.** Shear Specimen Schematic

Tests investigating the effects of shear rate used 0.5-inch elastomer thickness for the highest rate due to equipment limitations and 1.0-inch elastomer for the remaining shear rates. The epoxy layer was maintained at a quarter-inch thickness for all shear tests.

### 5.3.2 Test Set-up

In order to keep the two lightweight concrete pieces from rotating during loading, four steel "legs" were attached by threaded rods through tubes cast into the lightweight concrete blocks (Figure 5-6). Approximately 6,500 pounds of force was maintained through the use of precision springs to clamp the steel legs to the lightweight concrete. This was designed so that static friction would prevent the legs from sliding against the specimen during loading.

Nuts on threaded rods spanning the distance between the lightweight concrete blocks fixed the lateral position of the specimen relative to the centerpiece. For the testing requiring lateral loading perpendicular to the direction of the shear loading, precision springs were used with the rods and compressed as necessary to provide the desired tension or compression stress. For the remaining tests the threaded rods spanning the space between the lightweight

concrete sidepieces were locked in place with nuts to keep the spacing between these concrete pieces constant and parallel.

The specimen, complete with steel legs attached, was then placed in an Instron universal testing machine with digital loading control. Pin and roller bearings on the Instron loading base supported the lightweight sidepieces, and an aluminum block with the same area as the centerpiece was placed on top of the centerpiece as an extension so that the larger-diameter loading head would not contact the lightweight sidepieces during testing. Figure 5-7 shows a picture of a shear specimen ready for testing in the Instron test machine.

The test equipment measured force and machine head displacement automatically, but to correct for system-related deformation (i.e. seating, machine deformation, etc.), an extensometer was attached to the concrete centerpiece and the steel frame, measuring the average shear displacement of the lightweight concrete blocks to the centerpiece at low deformations. Since the maximum range of the extensometer was less than one inch, the extensometer measured displacement from the beginning of the test through 0.5-inches of displacement and was removed. The loading head position was used to determine strain for the remainder of each test. During data analysis, machine-head displacement values were adjusted using the extensometer measurements. The tests were not stopped when the extensometer was removed, eliminating the possibility of creep or stress redistribution in the elastomer due to a change in loading rate during the tests.

### 5.3.3 Test Procedure

The test procedures for shear testing were based on ASTM D4014 but varied according to the purpose of the test. Most of the specimens were loaded at constant shear-strain rates, but in a few cases a constant loading rate was used instead. This is indicated for each specific test where applicable. Extensometer deformation, loading head position and load were recorded continuously throughout each test. Six different series of tests were conducted to evaluate shear behavior of the system. The distinct procedures are discussed below.

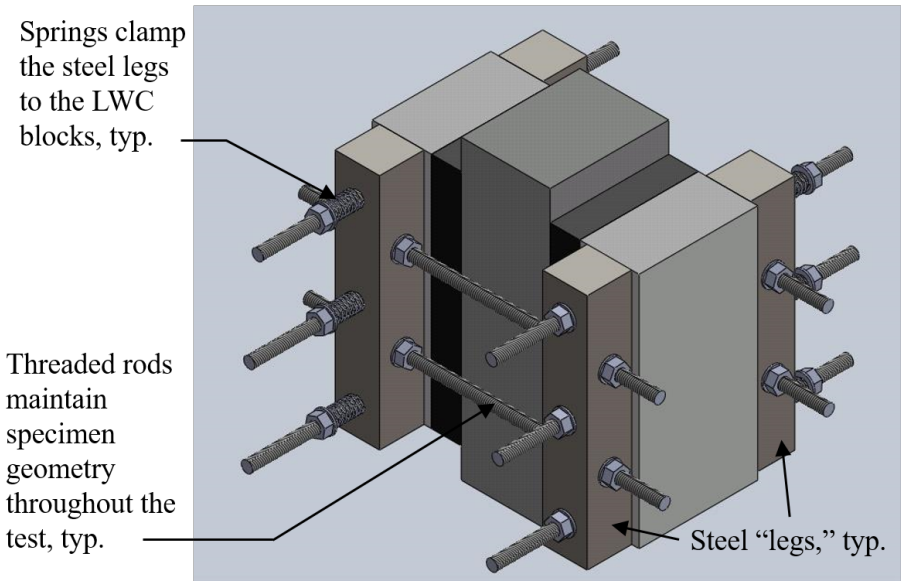


**Figure 5-6.** Rendering of Shear Setup Showing Steel Legs for Lateral Control.

#### 5.3.3.1 Bond Strength in Shear with Various Surface Finishes

Shear testing was conducted to evaluate the effect of concrete surface finish/texture on the behavior of the elastomer under shear loading. Four different surface treatments were used on the lightweight concrete blocks prior to applying the U90WB primer (described in Chapter 4). Three specimens were prepared for each surface finish: pressure-washed, sandblasted, exposed aggregate and tined (Figure 5-8).

The testing was conducted with constant load rate. For the first two tests, the load rate was 5,000 lb/min, but this was reduced to 4,000 lb/min for the remaining tests to facilitate easier removal of the strain gage used to monitor shear deformation up to 0.4 inches. The elastomer thickness was 1 inch, which resulted in a strain rate (at 20 percent strain) of about 40 percent/minute for the first two tests and 29 percent/minute for the remaining tests. This test sequence did not involve a preconditioning run; rather, the first loading for each specimen was to failure since the effect of surface preparation was the primary purpose of this series of tests.

**Figure 5-7.** Shear Set-up in Instron

**Figure 5-8.** The four surface finishes tested were (from left to right) tined, sand-blasted, exposed aggregate and pressure-washed. They are shown primed, awaiting elastomer.

#### 5.3.3.2 Shear Stiffness with Different Elastomer Thicknesses

Specimens were prepared with elastomer thicknesses of 0.5, 1.0, 1.5 and 2.0 inches. Three specimens were prepared at each elastomer thickness. Testing was conducted at a shear strain rate of approximately 120 percent/minute. Each specimen was loaded 4 times to about 50 percent strain followed immediately by loading to failure (similar to ASTM D4014-03). The shear performance was observed in the final loading to failure.

#### 5.3.3.3 Shear Strength and Stiffness under Combined Loading

In order to determine whether tension and compression stresses perpendicular to the direction of shear loading affected the shear stiffness, precision springs were added to the lateral-spacing bars between the two sides of the double shear specimen. A specimen set up for combined compression and shear stress is shown in Figure 5-9. Springs applying uniform a compression force to the elastomer can be seen on the left and right sides of the specimen. All of the combined loading specimens had 1-inch thick elastomer layers, and the tests were

conducted at a constant strain rate of approximately 125 percent/minute. Each specimen was preconditioned by loading to 30 percent strain and unloading before loading to failure.

Six shear tests were completed with different perpendicular stresses applied: 55 psi, 83 psi, 97 psi and 115 psi compression, and 5 psi and 20 psi tension. A test with 40 psi in tension was attempted; however, the specimen failed during assembly when one of the lightweight concrete blocks split. The friction-clamping to the sides of the lightweight concrete pieces effectively produced a tensile effect in the concrete due to the Poisson effect. The applied tension force plus the tension field induced by clamping exceeded the maximum tension

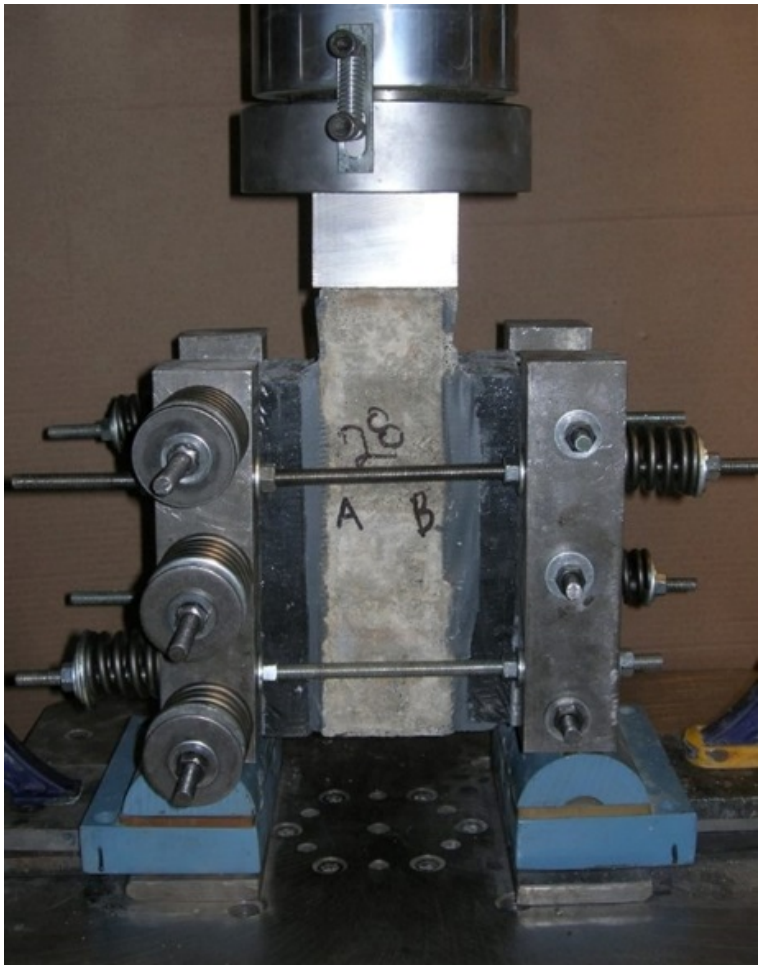


**Figure 5-9.** Double Shear Specimen with Springs to Apply Compression Stress

strength of the lightweight concrete, causing the block to fracture.

#### 5.3.3.4 Shear Strength and Stiffness with Different Strain Rates

Specimens with elastomer thicknesses of one inch were tested at four different strain rates: 30 percent, 55 percent, 140 percent and 300 percent/minute plus or minus three percent strain. In addition, a specimen with a 0.5-inch-thick elastomer was tested at just under 600 percent strain per minute (machine limitations prevented shear strain rates greater than 300 percent/minute for 1.0-inch-thick elastomer thicknesses). Each specimen was preconditioned by loading to 30 percent strain and unloading before loading to failure.

#### 5.3.3.5 Shear Strength and Stiffness under Freeze-Thaw Conditioning

Four double shear specimens were subjected to repeated cycles of freezing and thawing prior to testing. The primary purpose of this testing was to determine whether there would be excessive deterioration in the shear behavior at the lightweight concrete-elastomer interface.

Prior to freeze-thaw exposure the elastomer (Corkelast, 1.0-inch thickness) was applied to the lightweight concrete, and the lightweight concrete-elastomer pieces were returned to the curing room the next day where they remained for an additional six days. The pieces were removed from the curing room and kept at 50 percent relative humidity for 24 hours (at room temperature).

The concrete-elastomer units were then submerged in water and cycled from 40°F to 0°F and back to 40°F at a rate of five cycles per day in accordance with ASTM C666. After 300 cycles the pieces were warmed to room temperature and the assembly of double shear specimens was completed following the general application procedure (The elastomer was sanded and primed, and DexG epoxy was used to bond the full double shear specimen together). For conventional concrete, the 300-cycle freeze-thaw exposure would be considered to represent worst-case exposure conditions. Each freeze-thaw specimen was preloaded once to about 30 percent strain, unloaded and subsequently loaded to failure.

#### 5.3.3.6 Shear Behavior of Epoxy

In order to isolate the behavior of the DexG adhesive from the Corkelast-DexG system, four shear specimens were prepared with only the 0.25-inch layer of DexG between the lightweight concrete and the normal-weight center section of the double shear specimens. Because the DexG is significantly stiffer than the elastomer, the loading was load-controlled rather than deflection-controlled. A loading rate of 4,000 lb/min (62.5 psi, shear stress per minute) was used for the testing to approximate the load rate felt by the DexG layer in an elastomer double shear test in which a 1-inch thick layer of elastomer was loaded at 125 percent shear strain per minute. Each specimen was loaded once to failure.

#### 5.3.3.7 Summary of Shear Procedures

Table 5-2 presents the six types of double shear tests and a short description of each for quick reference.

**Table 5-2.** Summary of Shear Test Procedures

| **Shear Test** | **No. Tests** | **Elastomer Thick-ness** | **X Preload Runs to Y strain** | **Test Description/Objective** |
|---|---|---|---|---|
| Surface Finish | 12 | 1.0 in | 1 / 30% | Comparison of bond strength in shear. Four surface finishes: Pressure Washed, Exposed Aggregate, Sand-Blasted, Tined. |
| Elastomer Thickness | 12 | Varies | 4 / 50% | Influence of elastomer thickness on shear response; 0.5, 1.0, 1.5 and 2.0 inches. |
| Combined Loading | 6 | 1.0 in | 1 / 30% | Influence of axial load on shear response; 20 psi tension – 115 psi compression. |
| Strain Rate | 7 | 1.0 in[a] | 1 / 30% | Influence of shear rate on shear response; 30 – 600 % strain/min. |
| Freeze-Thaw | 4 | 1.0 in | 1 / 30% | Influence of freeze-thaw conditioning on shear response. |
| Epoxy Behavior | 4 | 1.0 in | 0 / N/A | Stiffness and bond strength of DexG. |

[a]SR-7 was 0.5-in

# 6 Results

This chapter presents the results from the tension, compression and shear tests performed at the University of Washington, and observations and trends are noted and discussed.

## 6.1 Tension Pull-off

Results of the tension pull-off tests are presented below for each elastomer batch: A (Editaan), B (Corkelast) and C (Corkelast). The results from the test apparatus were displayed in total force and have been converted to average tensile stress. They are summarized in Table 6-1. Results for each individual specimen are provided for reference in Table B-1.

### 6.1.1 Editaan 70U

**Batch A** The average maximum tensile stress for the lightweight concrete specimens that were air-dried overnight before priming was 252 psi. Specimens that were blown dry with pressurized air immediately prior to priming (free water was blown from the surface until the surface looked lighter in color) achieved an average maximum tensile stress of 230 psi. However, the standard deviation for the overnight-dried specimens was 29 psi, and the standard deviation for the air-pressure-dried specimens was 21 psi. Therefore, there is not a statistically significant difference between the two drying methods, and the average tensile strength for the Editaan samples (Batch A) was 239 psi.

In all but one of the tests, failure was characterized by tearing of the Editaan elastomer

**Table 6-1.** Summary of Tension Pull-off Results

| Batch | Specimen Count | Test Conditions | Cracking Location | Strength | Std. Dev. |
|---|---|---|---|---|---|
| A | 4 | Air-Dried Overnight | Editaan/ LWC | 252 psi | 29 psi |
| A | 5 | Pressure-Dried | Editaan/ LWC | 230 psi | 21 psi |
| A | 9 | All (Combination of Drying Methods) | Editaan/ LWC | 239 psi | 26 psi |
| B | 4 | Returned to Fog Room, Air-Dried Overnight | U90WB[a] | 81 psi | 27 psi |
| B | 2 | Returned to Fog Room, Pressure-Dried | Corkelast | 119 psi[b] | 16 psi |
| C | 4 | 1-inch Corkelast, Early Failure | Corkelast-U90WB Bond[c] | 74 psi | 8 psi |
| C | 3 | 1-inch Corkelast, Load Flattened Before DFL[b] | No Visible Cracking[d] | 113 psi[b] | 6 psi |
| C | 2 | 0.5-inch Corkelast, Early Failure | Corkelast-U90WB Bond[e] | 74 psi | 8 psi |
| C | 3 | 0.5-inch Corkelast, Achieved Published Strength | Corkelast-U90WB Bond[f] | 147 psi[b] | 0 psi |

[a]Except: Specimen SS-1 failed in the Corkelast near the bond with DexG.

[b]DFL = Deflection Limit Reached.

[c]Except: No visible failure occurred for Specimen SL1-8, but the max stress was low (84.8 psi).

[d]Except: Specimen SS-4b showed signs of a crack beginning to form at the Corkelast/U90WB bond.

[e]Except: Specimen SL1-1 had no apparent cracking, and the load continued to rise throughout the test.

[f]Except: Specimen SL1-2 had no apparent cracking, but the load leveled off prior to the deflection limit.

and a significant drop in load after a peak load was reached. Figure 6-1 shows a typical tension failure in the Editaan layer. The exception was a air-dried specimen that failed entirely in the lightweight concrete (SLF-4), though there was not a significant difference in strength between that specimen and the other Editaan specimens.

EdilonSedra reports the Editaan tensile strength by ISO 527 as 290 psi (Appendix E), 17.6 percent higher than than the average tensile strength of the Batch A specimens. It is probable that the Batch A results are less than the reported tensile strength because of local stress concentrations around the circumference of the small-diameter specimens due to the inverse bulging (pulling inward) of the elastomer under tension. Recalling Equation 2-17, an increased shape factor leads to a reduction in shear strain in the elastomer that results from axial loading. And though it is well known that specimen geometry has a large impact on the apparent stiffness and strength of the elastomer, it is impossible to quantify the effect of shape factor on the different strength results without further information because EdilonSedra does not provide the shape factor used in their tests.[1]

EdilonSedra also reports the adhesive strength on concrete as 217.6 psi when used with primers U90WB and 21-2K[2]—almost 10 percent lower than the average Batch A results. Oddly, the failure reported in the EdilonSedra adhesion test is cohesive Editaan failure, not bond failure, and it is unclear why the Editaan would fail at a stress lower than its tensile strength unless the specimen geometry was different or other test variables differed between tests. Uncovering the reason for the difference between EdilonSedra's published tensile and adhesion strength values as well as learning the specimen geometry of their tests would shed significant light on the Batch A results.

---

[1]Several attempts at contacting EdilonSedra representatives yielded no further information on specimen dimensions. In addition, the researchers did not have access to the ISO standards and could not verify any requirements for specimen dimensions specified in the test documentation.

[2]EdilonSedra's value is based on ISO 4624, but again, they did not include specimen dimensions.

**Figure 6-1.** Typical Editaan Tensile Failure. The dark area is Editaan and the lighter patches are lightweight concrete.

### 6.1.2 Corkelast VA-60

Two groups of tension specimens were tested with Corkelast as the elastomer: Batch B and Batch C.

**Batch B** Failure strengths for Batch B were significantly lower than the Editaan specimens (Batch A) as expected from the difference in the mechanical properties of the elastomers (discussed in Section 3.3). Interestingly, the modes of failure were different as well. Three of the overnight-dried Corkelast specimens (SS-2, SS-3 and SS-4) failed at the bond between the primed lightweight concrete and the Corkelast at an average stress of 83 psi, while the fourth specimen (SS-1) reached the maximum deflection limit of the test apparatus at a stress of 74 psi. Examination of specimen SS-1 showed the initiation of cracking in the Corkelast near the DexG interface. Overall, the average strength for the air-dried specimens was 81 psi.

An example of the premature failure at the bond between the UW90B primer and the lightweight concrete is shown in Figure 6-2. Light flecks of concrete observed on the otherwise

bare primer surface indicate efflorescence or laitance accumulation on the concrete surfaces that likely occurred when the lightweight concrete was returned to the curing room between pressure-washing and primer application. This would weaken the bond between the U90WB primer and the lightweight concrete and could explain the lower failure strength at the bond.

For the two pressure-dried specimens (SS-5 and SS-6), however, cracking occurred between the DexG and the primed Corkelast with the load leveling-off but not decreasing. Testing was halted when the maximum deformation limit of the test equipment was reached. In contrast to the overnight-dried specimens, no failure was observed between the primed lightweight concrete and the Corkelast for either specimen. It is likely that the pressurized air used to dry the concrete surface also removed some of the laitance or contaminant build-up on the surface, leading to a better bond at that interface. The average tensile stress achieved was 119 psi.

The mechanical properties of Corkelast are published in the Corkelast Product Data Sheet provided by EdilonSedra (Appendix E). However, as with Editaan, the specimen dimensions are not reported in the product literature. The reported tensile strength by ISO 527 is 145 psi, and the reported strength of adhesion to concrete using primers U90WB and 21-2K is 20 percent less at 116 psi. The failure mode is again reported as cohesive Corkelast failure, and further information about this load reduction would be helpful in interpreting the impact of shape factor on the tension results. The 119 psi tensile strength recorded by Batch B specimens that did not fail prematurely achieved the lower published adhesion strength, but fell 17.9 percent short of the published tensile strength. Notably, the shortfall is roughly the same as that of the Batch A specimens to Editaan's published strength. This supports the theory that the difference between EdilonSedra's testing and this research was the shape factor of the specimens, increasing the concentrated stresses around the perimeter of the tension specimens and thus reducing the apparent strength of the materials.

**Batch C** Batch C was designed to investigate the influence of shape factor and specimen preparation on the apparent tensile strength of the system. Results from Batch C specimens

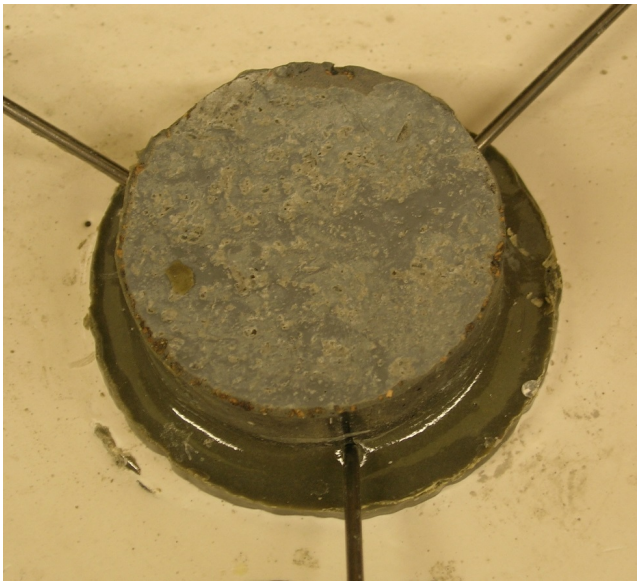

**Figure 6-2.** Tension Failure Surface Showing U90WB Primer with no Concrete Adhering.

fall into four groups separated by shape factor and failure type. The results from these four groups are presented in Table 6-1 and are discussed below. Table 6-2 highlights the results from Batch C apart from the other two batches to analyze the effect of shape factor on the tension test results.

Multiple specimens of both elastomer thicknesses failed at the Corkelast-U90WB primer interface after reaching an average stress of 74 psi. Each specimen that was P.A.T. tested and re-primed showed interface failure for most of the cross-section, but the bond held true at the P.A.T. test location. After the test it was forced apart for examination, whereupon

**Table 6-2.** Batch C: Shape Factor Effect

| **Shape Factor, S**[a] | 0.5625 | | 1.125 | |
|---|---|---|---|---|
| **Failure Type** | Primer Interface | Defl. Limit | Primer Interface | Defl. Limit |
| **Tensile Strength** | 74 psi | 113 psi | 74 psi | 147 psi |
| **Percent of Published** | 51% | 78% | 51% | 101% |

[a]Defined in Equation 2-3

it tore through the Corkelast layer, not the bond (Figure 6-3). In other words, the integrity of the bond at the P.A.T. test location was maintained even when the rest of the bond was compromised.

These P.A.T. test locations were re-primed the day after the initial primer application, resulting in the elastomer being applied approximately 44 hours after the re-priming as opposed to 72 hours for all other locations. The lower failure strength of the bond suggests that the window of time after priming for Corkelast application should be reduced significantly from the manufacturer's suggested maximum of 72 hours for temperatures between 60°F and 84°F (Appendix E)[3].

Where the bond strength between the various layers was sufficient, failure occurred at a much higher tensile strength. One-inch specimens ($S = 0.5625$, the same as Batches A and B) that did not experience early bond failure reached an average of 113 psi before the load leveled off. This was similar to the 119 psi tensile strength of the Batch B specimens that did not fail prematurely (same material and shape factor). Testing was halted when the deflection limit was reached, but examination of the specimens after the apparatus was removed revealed that there was no visible cracking in two of the three specimens in this group (SS-2b and SL1-6). The third (SS-4b) showed signs of a crack beginning to form at the Corkelast-U90WB bond.

Three of the five specimens with half-inch elastomer layers ($S = 1.125$) reached the manufacturer's published strength of 145 psi prior to reaching the deflection limit (SL1-2) or experiencing bond failure (SL1-3, SL1-4). These three specimens were the only specimens of either elastomer to reach the full tensile strength published by EdilonSedra. Those specimens characterized by $S = 1.125$ that did not fail at the bond layer experienced a 30 percent increase in tension strength compared to specimens with $S = 0.5625$. This was primarily because in the same deformation distance, the test apparatus was able to apply twice as much strain on the thinner elastomer before reaching its deflection limit.

---

[3]Prior to the submission of this thesis, the results were provided to EdilonSedra, and they reduced the window from 72 to 48 hours.

**Figure 6-3.** Tension Failure Surface Showing Failure in Corkelast at P.A.T. Test.

Additionally, consistent with Equation 2-17, the larger shape factor of the Corkelast layer reduced the shear strain caused by inverse bulging, thereby reducing the shear stress around the perimeter and allowing the elastomer to achieve the manufacturer's reported strength. Ultimately, the increased tensile strength observed for the specimens with half-inch elastomer layers was the only tension result that achieved the manufacturer's reported tension strength of 145 psi.

For all Batch C specimen, the deflection limit of the test apparatus was reached before total loss of tension capacity. While it is unlikely that the load would have risen much higher for any specimen, the reported tension values mark a lower bound for each specimen's tensile strength.

### 6.1.3 Tension Testing Summary

The results of the tensile test specimens for which no obvious early-failure was observed are summarized in Table 6-3. They are compared in the table with the manufacturer's stated tensile strength for each material as listed in Appendix E.

Specimens with Editaan had considerably higher tensile-strength results than those with Corkelast. However, specimens with $S = 0.5625$ only achieved 74–82 percent of the full tensile strength published by EdilonSedra, regardless of the elastomer type, suggesting the influence of shape factor reducing the apparent tensile strength of the elastomer. Furthermore, the Corkelast specimens with $S = 1.125$ that were designed to reduce perimeter stress concentrations by increasing $S$ had significantly higher tensile strength results than the specimens with $S = 0.5625$, achieving the full published tensile strength of the Corkelast. This further indicates that the small deformation range of the test apparatus and the undesired local stresses caused by the small shape factor limited the apparent strength of the material. Further investigation of the specimen dimensions and adhesion strength referred to in the product literature for each elastomer would shed additional light on the subject.

The tension testing also identified two areas of concern in the fabrication process. First, specimens should be thoroughly cleaned before each material application. Priming the concrete as soon as possible after pressure-washing and removing particulate buildup on the surface with pressurized air before each subsequent material application ensures a clean bonding surface for all layers. Second, allowing the UW90B primer to cure for up to 72 hours (laboratory conditions) may be too long, as unexpected failures at the primer-elastomer interface occurred in some cases.

**Table 6-3.** Tension Testing Summary

| **Elastomer Type / S** | Editaan/0.5625 | Corkelast/0.5625[a] | Corkelast/1.125 |
|---|---|---|---|
| **Observed Tension Strength** | 239 psi | 108 psi | 147 psi |
| **Published Tension Strength** | 290 psi | 145 psi | 145 psi |
| **Percent of Published** | 82% | 74% | 101% |

[a]Includes specimens from both Batch B and Batch C.

## 6.2 Compression

Full-scale models of the block-elastomer-deck system were tested in direct compression at four different elastomer thicknesses to identify the compressive stiffness of the system. In addition to vertical deformation and load, lateral bulging of the Corkelast was measured during compression to understand the compressibility of the material and correlate the compression and the shear results. The results were then analyzed for trends and patterns in relation to the previous work cited in Chapter 2.

### 6.2.1 Compressive Stiffness

Load and deformation were recorded continuously throughout each compression test, and the second loading of each specimen was processed for analysis.[4] From the stress-strain curve generated for each specimen, a secant modulus and two chord moduli (hereby called the working and overload moduli) were drawn between 0–58 psi (0–14 kips), 19–50 psi (4.5–12 kips) and 58–117 psi (14–28 kips), respectively, to characterize system stiffness under different loading conditions. The secant modulus (0–58 psi) approximates the compressive stiffness over the full expected stress range of the system under service conditions. Similarly, the working modulus (19–50 psi) seeks to refine the characterization of the central part of the response curve, and the overload modulus (58–117 psi) represents the stress-strain response under extreme conditions (e.g. a fully-loaded, tipping train).

Figure 6-4 shows a typical stress-strain curve generated from a compression test with the secant, working and overload moduli superimposed. From this figure, it is apparent that the elastic modulus of the material is approximately constant, decreasing only slightly between one and three percent strain. This was typical of specimens of all thicknesses.

---

[4]The first loading of each specimen was thought of as a preconditioning cycle and is not compared in this section. A graph comparing the first and second loading runs of a typical specimen is presented in Appendix C.

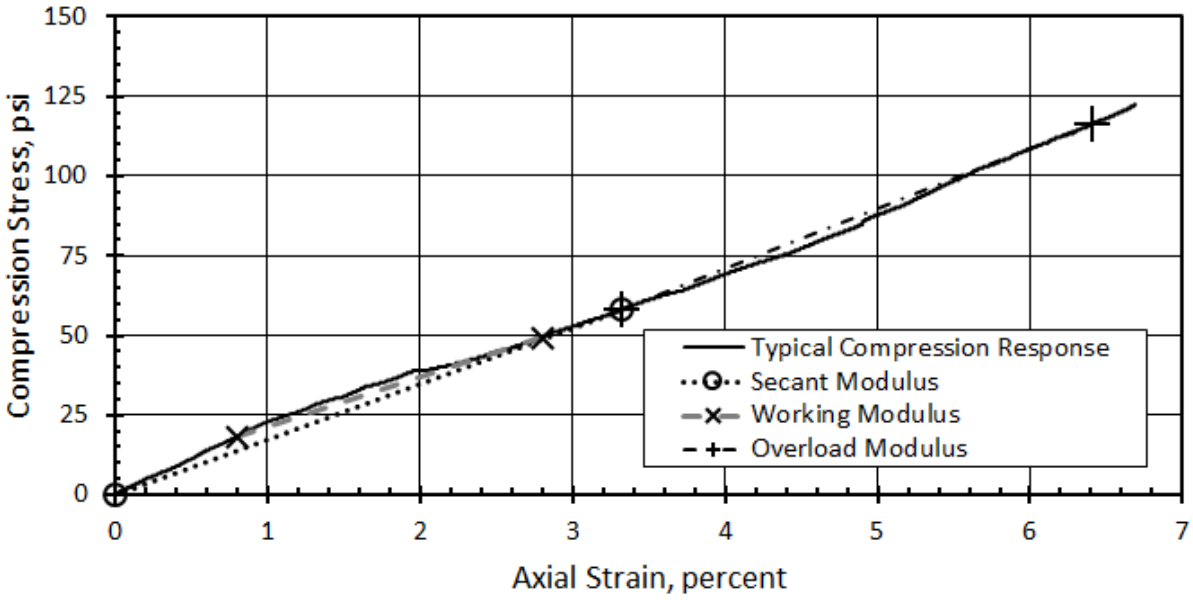


**Figure 6-4.** Typical Compression Stress-Strain Plot Showing the Secant, Working and Overload Moduli (1-inch Elastomer Thickness).

#### 6.2.1.1 0.5-inch Elastomer

As expected, the plinths tested with half-inch elastomer made up the stiffest group. The three specimens that were tested produced an average secant modulus of 3,722 psi, a working modulus of 3,568 psi and an overload modulus of 2,342 psi, but the standard deviation was very high in the lower stress range. Table 6-4 shows each specimen's resultant moduli and the group statistics. For all three specimens in this group, after a high initial stiffness from 0 to about 0.5 percent strain, the stress-strain curve increased at a lower, but constant rate through the range of the overload modulus.

Notably, the standard deviation was much higher for the secant and working moduli than for the overload modulus, signifying greater modulus variability at lower loads. Figure 6-5 illustrates this variability by showing a plot of stress-strain curves for each specimen with a half-inch elastomer layer.

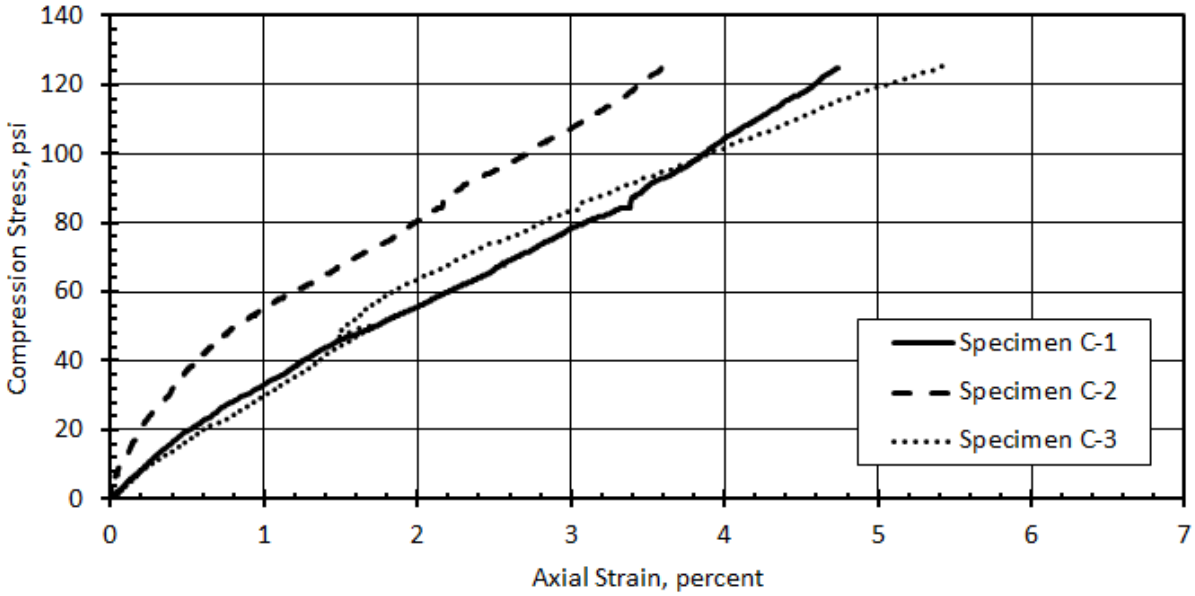


**Figure 6-5.** Stress-strain curves for specimens with 0.5-inch elastomer.

**Table 6-4.** Compression Stiffness of 0.5-inch Elastomer Group

| **Specimen** | **Elastomer Thickness** | **Secant Modulus** | **Working Modulus** | **Overload Modulus** |
|---|---|---|---|---|
| C-1 | 0.5 in | 2,748 psi | 2,489 psi | 2,491 psi |
| C-2 | 0.5 in | 5,145 psi | 4,983 psi | 2,618 psi |
| C-3 | 0.5 in | 3,272 psi | 3,233 psi | 1,917 psi |
| Average: | | 3,722 psi | 3,568 psi | 2,342 psi |
| Standard Deviation: | | 1,260 psi | 1,280 psi | 373 psi |

#### 6.2.1.2 1.0-inch Elastomer

Table 6-5 shows the results and statistics of the 1.0-inch elastomer group. The average stiffness of the three specimens tested with a 1.0-inch Corkelast layer was less than that of the 0.5-inch group throughout the entire load range; the secant modulus was 2,111 psi. However, in this group the three moduli were much closer together, ranging only 148 psi between the average secant modulus (highest) and the working modulus (lowest). This is illustrated by comparing Figure 6-5 with Figure 6-6, a plot of the stress-strain curves of each specimen with a 1-inch elastomer thickness. The stress-strain curves of the one-inch specimens are much straighter than the curves from the half-inch specimens.

The variation in the data was reasonably low compared to the specimens with 0.5-inch elastomer thickness (Table 6-4 and Table 6-5). Standard deviations for each 1-inch modulus were one-third the size of those describing the half-inch elastomer group. Because the total difference in average moduli is less than even the smallest standard deviation of one modulus, it can be said that the moduli are approximately the same and that the material response in compression is completely linear over the entire loading range.

**Table 6-5.** Compression Stiffness of 1.0-inch Elastomer Group

| **Specimen** | **Elastomer Thickness** | **Secant Modulus** | **Working Modulus** | **Overload Modulus** |
|---|---|---|---|---|
| C-4 | 1.0 | 1,746 psi | 1,562 psi | 1,899 psi |
| C-5 | 1.0 | 2,120 psi | 2,003 psi | 1,924 psi |
| C-6 | 1.0 | 2,467 psi | 2,323 psi | 2,188 psi |
| Average: | | 2,111 psi | 1,963 psi | 2,004 psi |
| Standard Deviation: | | 361 psi | 382 psi | 160 psi |

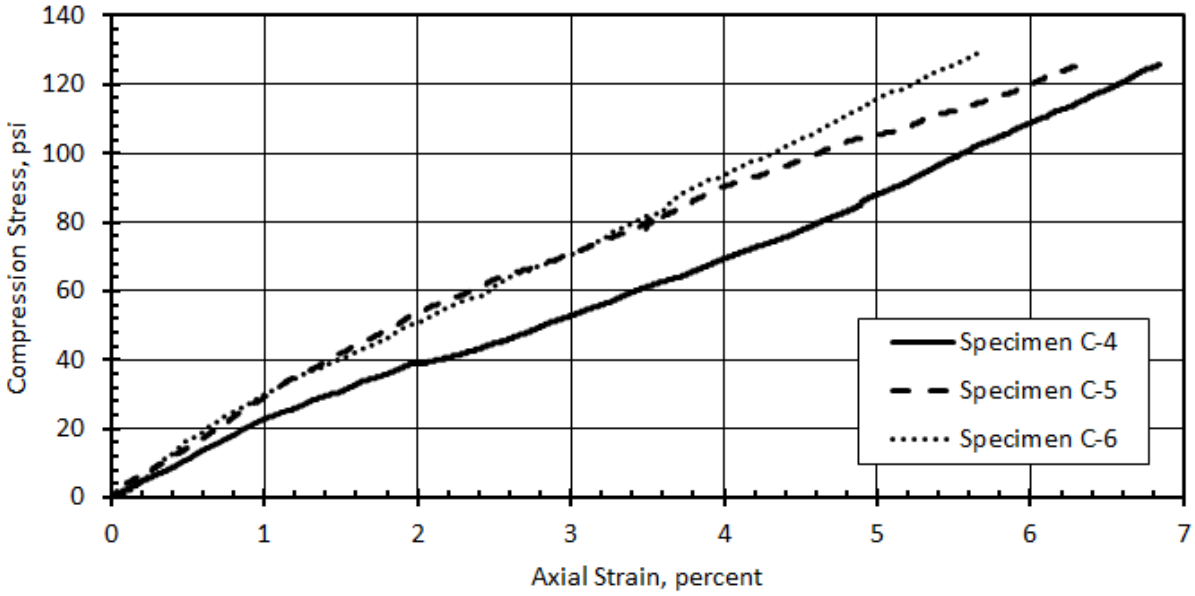


**Figure 6-6.** Stress-strain curves for specimens with 1-inch elastomer.

#### 6.2.1.3 1.5-inch Elastomer

Figure 6-7 presents compression stiffness curves for each of the 1.5-inch specimens, and Table 6-6 shows the results and statistics of the 1.5-inch elastomer group. With an average secant modulus of 1,843 psi, two of the specimens in the 1.5-inch elastomer group (C-7, C-8) were consistent with expected results, showing a decrease in stiffness when compared to groups with thinner elastomer layers. Results from the third specimen (C-9) were significantly different from the group on all loading runs. The instrumentation appeared to be functioning properly, and there was no visual difference between C-9 and the other 1.5-inch specimens. Therefore, C-9 was considered an outlier and left out of statistical analysis.

For this group, the standard deviation of the data was low (about 200 psi for each modulus); but, the difference between the three moduli was even smaller: 97 psi between the highest and lowest moduli. Therefore the difference was considered negligible, and the elastic modulus was taken to be constant throughout the entire loading range.

**Table 6-6.** Compression Stiffness of 1.5-inch Elastomer Group

| Specimen | Elastomer Thickness | Secant Modulus | Working Modulus | Overload Modulus |
|---|---|---|---|---|
| C-7 | 1.5 | 1,964 psi | 1,913 psi | 1,978 psi |
| C-8 | 1.5 | 1,722 psi | 1,581 psi | 1,789 psi |
| C-9[a] | 1.5 | 4,170 psi | 3,648 psi | 3,598 psi |
| Average: | | 1,843 psi | 1,747 psi | 1,884 psi |
| Standard Deviation: | | 171 psi | 235 psi | 134 psi |

[a]Specimen C-9 was removed from the statistical analysis as it was found to be incongruent with the rest of the data.

#### 6.2.1.4 2.0-inch Elastomer

Table 6-7 contains the results and statistics of the 2.0-inch elastomer group, and Figure 6-8 shows the stress-strain curves for the three corresponding specimens. The 2.0-inch elastomer

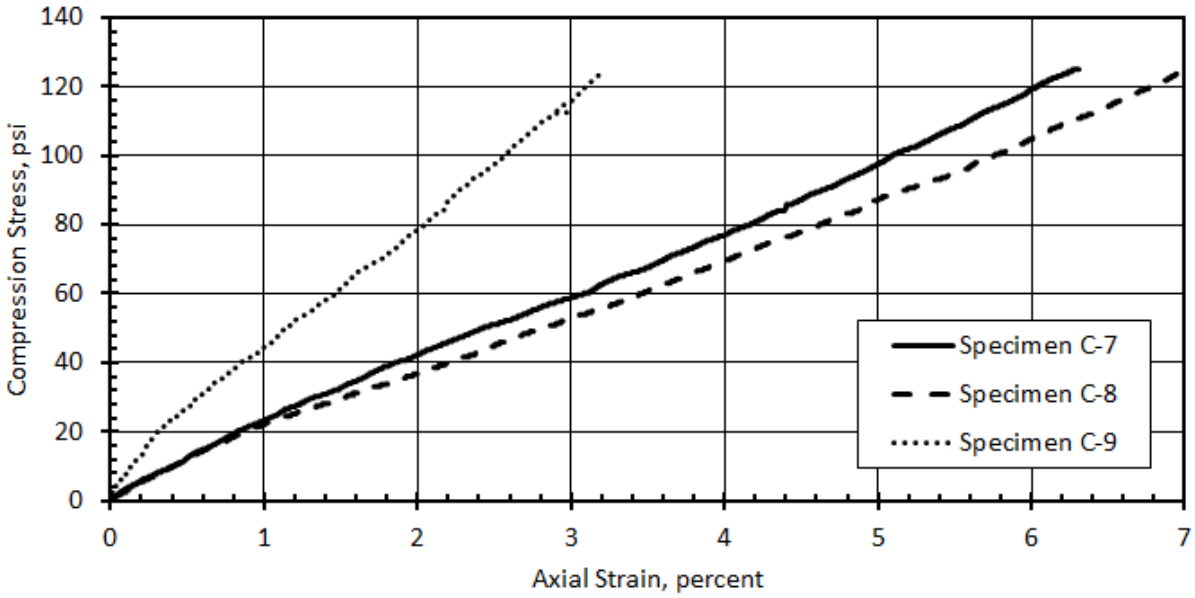


**Figure 6-7.** Stress-strain curves for specimens with 1.5-inch elastomer. Specimen C-9 was removed from the statistical analysis as it was found to be incongruent with the rest of the data.

group had an average secant modulus of 2,171 psi. Although this result appears higher than that of the 1.5-inch elastomer group, this increase is not statistically significant given the measured variability.

Additionally, the difference between the highest and lowest moduli was 157 psi, and the average overload and working moduli were only 35 psi apart. With a reasonably large scatter at lower loads, marked by a standard deviation of 489 psi for the working modulus, and a minimal difference in moduli, the stiffness can be considered constant throughout the entire loading range.

Despite the increased variability of measured stiffness in the lower load range, the overload modulus was very precise as indicated by the standard deviation of 78 psi. In fact, the low standard deviation of the overload modulus was the lowest of any group of three specimen of the same thickness.

**Table 6-7.** Compression Stiffness of 2.0-inch Elastomer Group

| Specimen | Elastomer Thickness | Secant Modulus | Working Modulus | Overload Modulus |
|---|---|---|---|---|
| C-10 | 2.0 | 1,910 psi | 1,748 psi | 1,935 psi |
| C-11 | 2.0 | 1,980 psi | 1,786 psi | 2,017 psi |
| C-12 | 2.0 | 2,622 psi | 2,613 psi | 2,090 psi |
| Average: | | 2,171 psi | 2,049 psi | 2,014 psi |
| Standard Deviation: | | 392 psi | 489 psi | 78 psi |

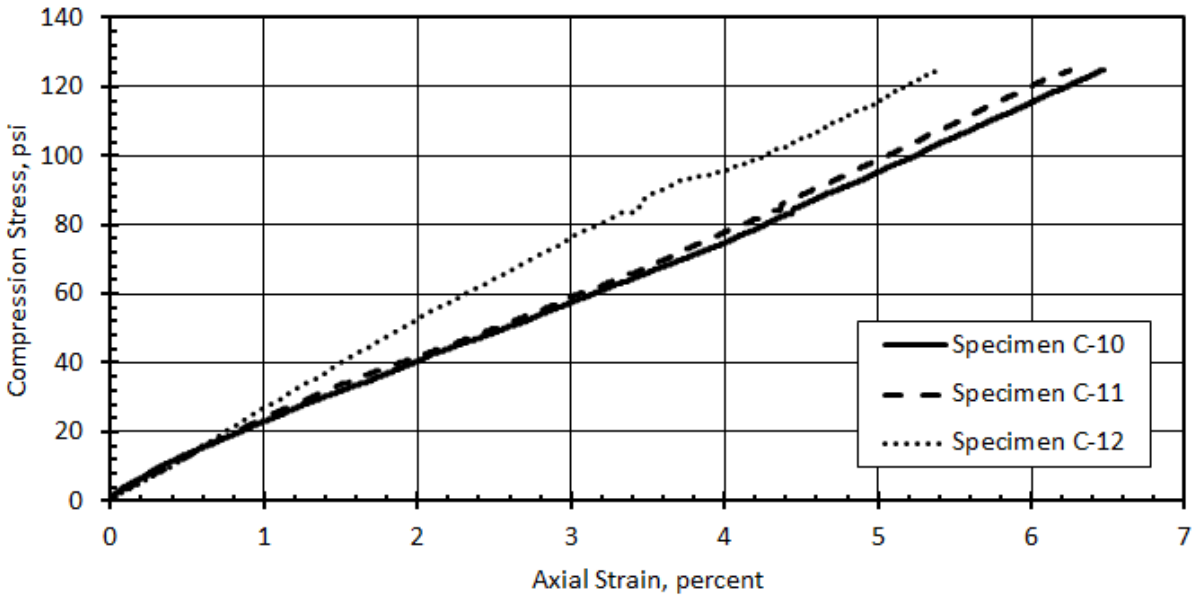


**Figure 6-8.** Specimen stress-strain curves for specimens with 2-inch elastomer.

### 6.2.2 Variability

A closer look at the variation of the moduli also sheds light on the compression behavior. Figures 6-9, 6-10 and 6-11 show the average moduli with error bars denoting the standard deviation for each thickness. The plots are kept separate from each other for clarity in viewing the error bars.

Two observations can be made from the comparison of the variation for each thickness and modulus. First, the variation of test data was much higher for the 0.5-inch thickness group than for the other thickness groups across all three moduli. This variation was likely a result of the combination of small variations in shape factor due to construction tolerance and increased variability in confinement of the elastomer. Confinement effectively increases the shape factor of the elastomer layer since it restricts the area free to bulge. For a thin layer of elastomer (compared to the plan area), any confinement produced by surrounding DexG would have a greater impact on the results as compared to specimens with greater elastomer thicknesses. For example, DexG that rose to 0.25 inches around a specimen with a 1-inch elastomer layer would cover 25 percent of the thickness, but the same quarter-inch rise around a specimen with a half-inch elastomer layer would cover 50 percent of the exposed elastomer. While confinement from excess DexG was reduced by chipping away overly thick DexG layers, the actual DexG overlap at the time of testing was not measured. The variation attests to the increased effect of construction tolerance on thinner elastomer layers.

The second observation that can be made from the comparison of average variation by elastomer thickness is the lower variability in the overload modulus for all thicknesses. The average variation of the overload modulus in every thickness group and overall was over 30 percent less than the average variation of the other two moduli. This seems to indicate that there are factors affecting the compression stiffness in the lower stress range that do not affect the stiffness under higher load—factors that make the compression stiffness more variable at low stress such as edge restraint (DexG overlap), material crystallization (not discussed in this paper) or an effect of the cork filler.

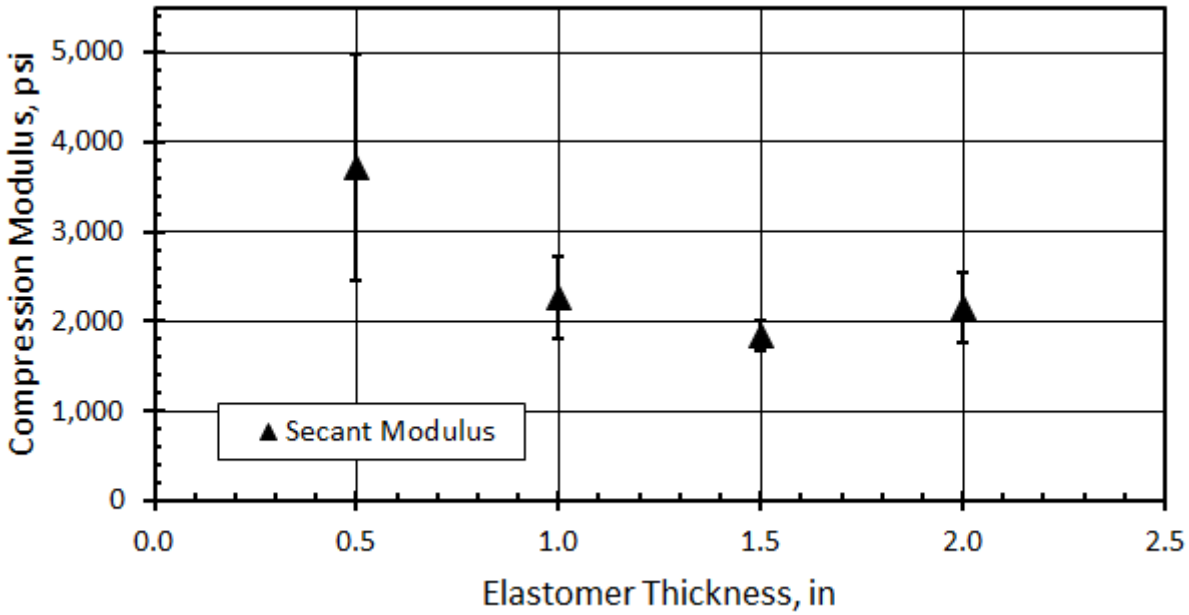


**Figure 6-9.** Average Secant Moduli by Elastomer Thickness with Error Bars Showing the Standard Deviation of the Results at Each Thickness.

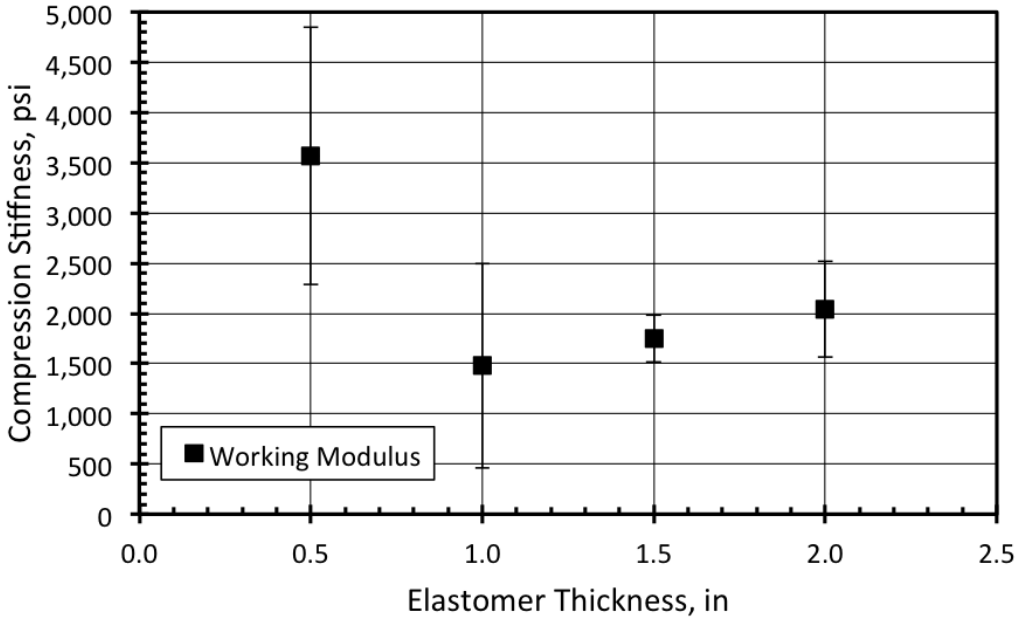


**Figure 6-10.** Average Working Moduli by Elastomer Thickness with Error Bars Showing the Standard Deviation of the Results at Each Thickness.

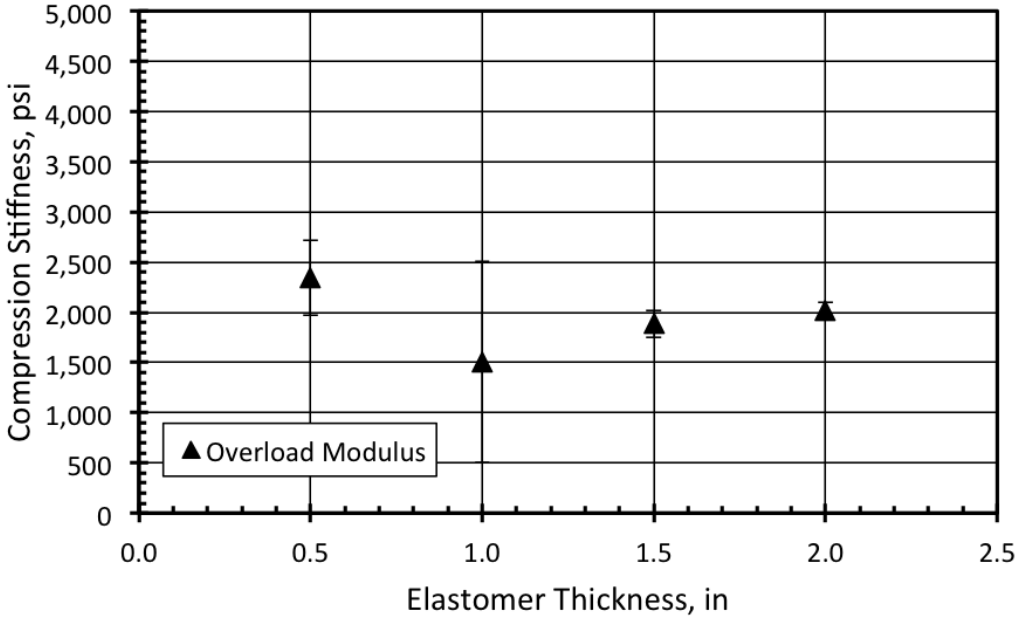


**Figure 6-11.** Average Overload Moduli by Elastomer Thickness with Error Bars Showing the Standard Deviation of the Results at Each Thickness.

In statistics, when the variation of a sample is high, the confidence in the distribution of the data is low, and all moduli generated from the half-inch specimens have a much higher variation than specimens at other elastomer thicknesses. While a trend of decreasing stiffness with increasing elastomer thickness can be observed over the secant and working moduli for the first three thickness groups, a closer look at thicknesses greater than or equal to one inch is more insightful to the characterization of the compression stiffness.

Based on the variation of the data, the compression moduli for specimens with one-inch elastomer thickness or greater did not vary significantly with elastomer thickness. Figure 6-12 highlights this by substituting a decreasing exponential regression for a linear regression through all the data. This captures the similarity in stiffness of the thicker specimens while separating out the higher stiffness observed for those with 0.5-inch layers at low levels of stress. This is insightful as it leads to the discussion of the influence of shape factor rather than thickness alone being the defining geometric characteristic for the response of bonded

elastomer layers in compression (Chapter 7).

Increased stiffness of the 0.5-inch specimens is due to the fixity of the boundary conditions—the elastomer is fixed to both the lightweight concrete on one end and the DexG on the other. As the layer is compressed, the elastomer tries to spread out, but because it is restrained from lateral spreading at the boundaries. Shear stresses develop near the boundaries, and the unrestrained area for spreading is reduced, becoming a bulge shape along the perimeter of the specimen. This means the area able to bulge is extremely important, and as layer thickness decreases, the apparent compression modulus increases significantly. This is explored further in Chapter 7, and the results are compared with current elastomer theory.

### 6.2.3 Compression Testing Summary

The stress-strain behavior of the Corkelast in compression was fairly linear throughout the entire loading range with the exception of the thinnest, most highly-restrained specimens, which experienced increased stiffness at low strains. Additionally, while a steady decrease in apparent modulus occurred as the layer thickness increased, the half-inch specimens exhibited much higher stiffness than the other thicknesses, out of line with a linear trend by thickness. The variability in the data points to the influence of shape factor (which is based on the inverse of the thickness) rather than thickness itself being the more influential geometric quantity for bonded elastomer layers.

Also, the high variability in modulus for the half-inch specimens likely resulted from small changes in thickness and lateral confinement of the elastomer by DexG that rose up the sides of the elastomer. It should be considered that confinement provided by the DexG extending above the bottom of the elastomer layer raises the stiffness of the Corkelast.

These results are analyzed in Chapter 7, comparing the results with previous work using shape factor and other material properties. The analysis finds that this result is consistent with the previous research and the theoretical prediction of the material modulus, but it also indicates that the classical elastomer theory may need to be adjusted slightly for elastomers

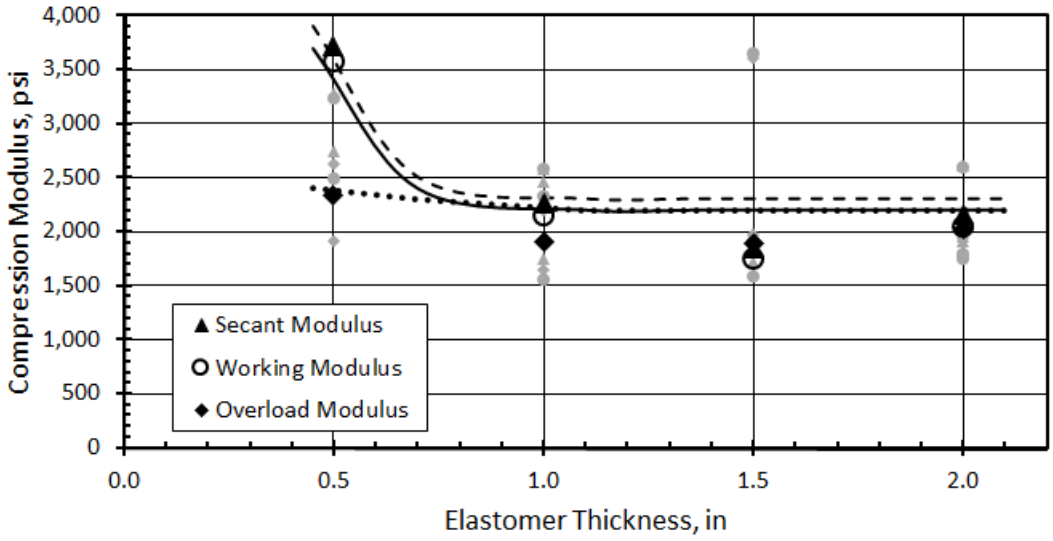


**Figure 6-12.** Effect of Elastomer Thickness on Average Compression Moduli. Light gray markers represent the moduli of each individual specimen, while black markers are the average for each modulus at each thickness.

with solid filler compounds.

## 6.3 Shear

This section presents the results of the double shear tests. As described in Section 5.3, the testing program investigated the effects of surface preparation, elastomer thickness, combined stress, shear rate and freeze-thaw conditioning on the shear strength and stiffness of the elastomer. It also included a procedure that measured the shear behavior of the DexG epoxy.

For all tests, the shear stiffness was approximated by two moduli: a secant modulus from 0–20 percent shear strain characterizing the shear behavior under normal operation and a chord modulus from 20–30 percent shear strain to characterize the shear behavior under extreme load cases (Refer to Sections 2.3 and 7.1.2 for information on expected loading.). These moduli were chosen to help identify the decreasing shear stiffness with increasing levels

of shear strain. In addition, the maximum shear stress was determined for each test. Failure was defined as a 10 percent reduction in strength from the maximum to prevent unnecessary damage to the double shear test apparatus.

Figure 6-13 shows the secant and chord moduli on a typical shear stress versus shear strain curve from a specimen with a one-inch thick elastomer layer. The chord modulus was always less than the secant modulus due to the nonlinearity of the stress-strain response. This response was consistent for all the shear specimen, but stands in stark contrast to the typical shear stress-strain response of vulcanized elastomer (Figure 2-5) that is marked by a linear response past 150 percent strain where it increases rather than decreases. It is likely that debonding of the elastomer layer contributed to the appearance of nonlinearity in the response curve. The debonding was observed during testing, but unfortunately, was not measured. The observations of this debonding are described below before the following sections detail the results and trends observed during the six shear tasks.

**Debonding Failure Mode** The predominant failure mode of the shear tests was the slow peeling away of the elastomer from the DexG and LWC surfaces as shown in Figure 6-14. For lack of a better term, this failure mode is henceforth called debonding. But, though the failure occurred close to the bonds, it usually occurred entirely in the elastomer, and the integrity of the bond itself was maintained. This is clear by the particles of cork still attached to the DexG and LWC surfaces in Figure 6-15.

Debonding always occurred in two locations per elastomer layer: the elastomer tore away from the top of the LWC block closest to the loading head and from the DexG on the bottom of the centerpiece. Tearing began at these locations because of the high peeling stresses induced by the deformed shape. Figure 6-16 depicts the s-shape of the top and bottom surfaces of the deformed elastomer. The figure illustrates two observations that reveal the high peeling stresses at these critical locations.

First, the deformed thickness (the s-shaped curve) is longer then the unloaded thickness of the elastomer. So the surface must be under tension.

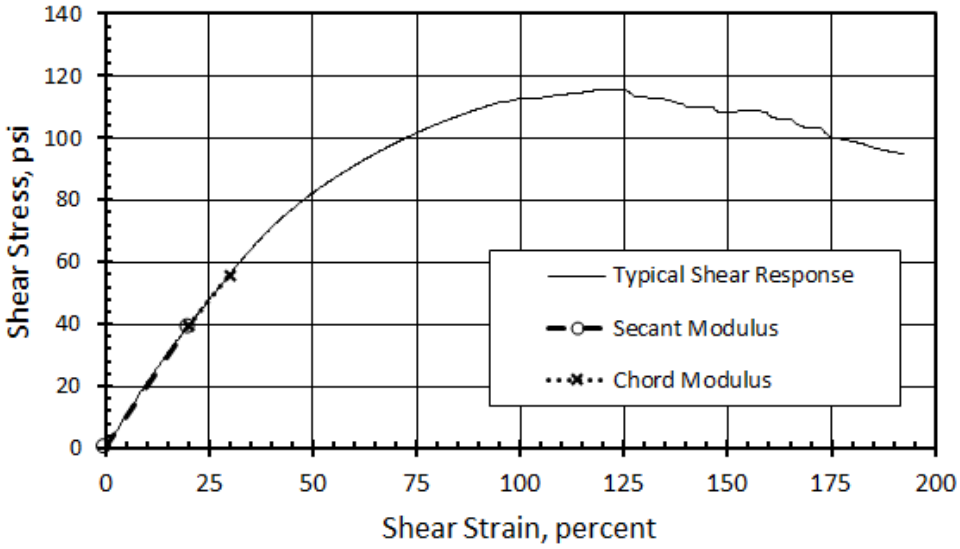


**Figure 6-13.** Typical Shear Results.

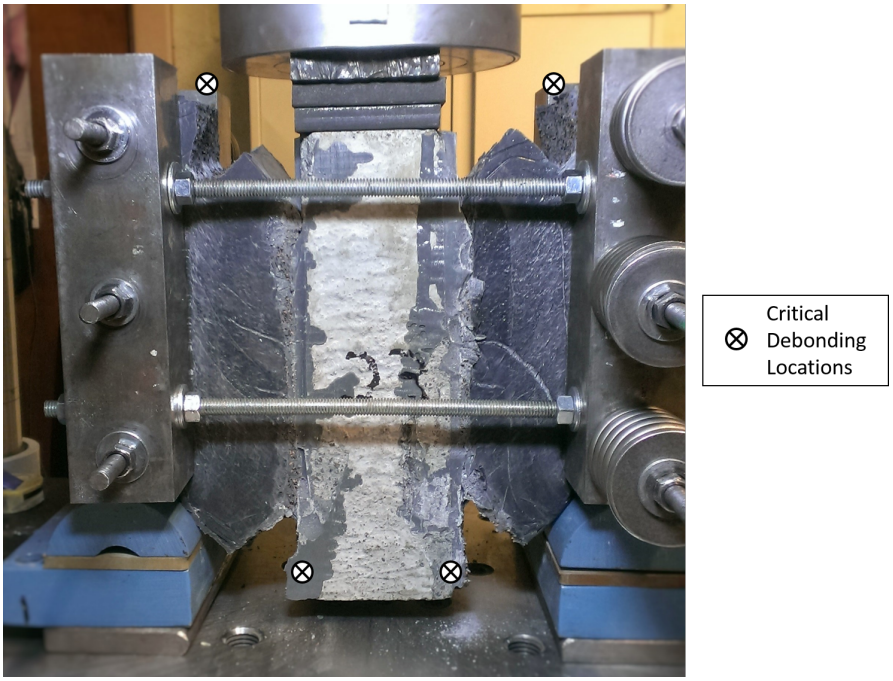


**Figure 6-14.** Photo of a double shear test at maximum deformation showing the tearing of the elastomer away from the DexG and LWC blocks (debonding) due to peeling stresses at two critical locations per elastomer layer.

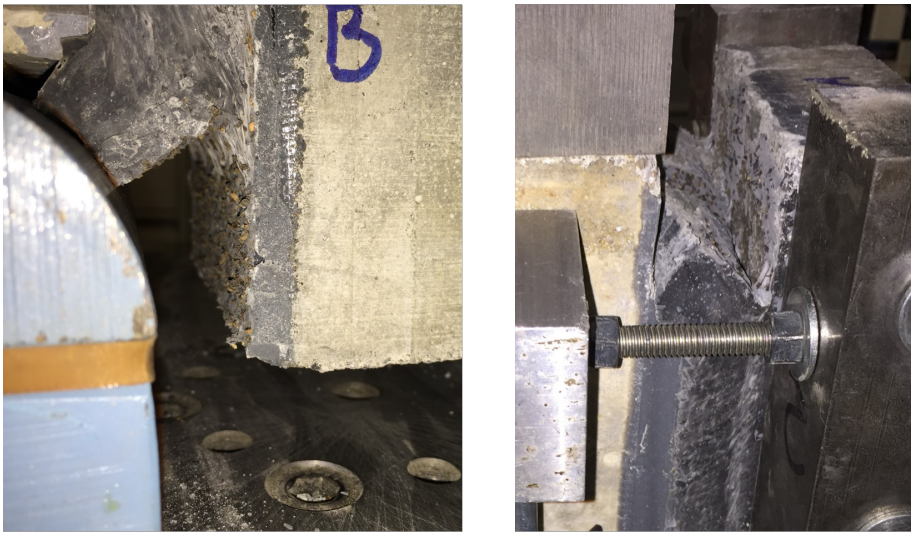


**Figure 6-15.** A close look at the debonded regions of the shear specimen shows cork pieces still attached to the DexG (left) and LWC block (right), indicating failure occurred in the elastomer near the bond, not at the bond itself.

Second, at the end of the deformed thickness that remained bonded, the elastomer overlaps the interface line, inducing a compression field in that region that strengthens the bond. Since there is no compressive field at the other end of the s-curve, the elastomer is "peeled off" of the concrete by the tension mentioned above. When thinner elastomer layers undergo this deformation, the curvature of the deformed thickness (the s-shape) is higher, leading to a greater tension strain. It stands to reason, then, that the debonding force is higher for—and thus has a greater effect on—thinner elastomer layers due to the tighter curvature of the deformed thickness.

Additionally, the debonding is local, and its extent is likely to be related to the thickness-to-length ratio. If the thickness is higher with respect to the length, then the debonding will have a greater effect on shear stiffness.

A close examination of test videos could prove helpful in determining *when* debonding began to occur in relation to the shear response to understand if there is a correlation between the apparent nonlinearity of the curve and the onset of debonding, but that is beyond the

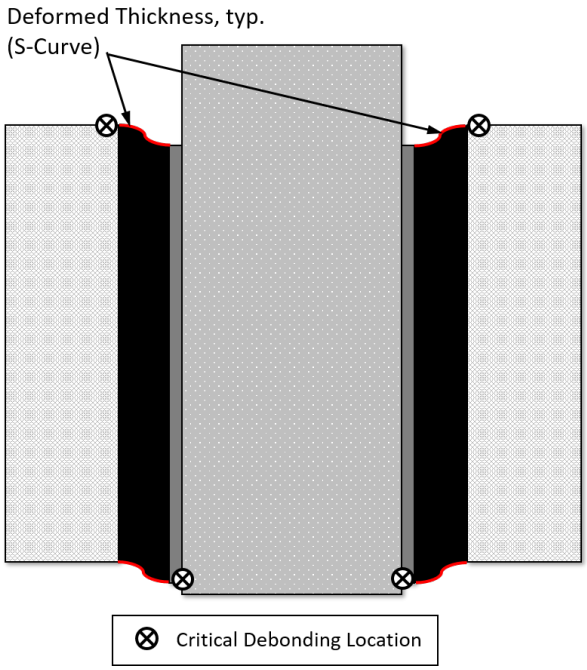


**Figure 6-16.** Schematic of a Deformed Shear Specimen

scope of this thesis. Once debonding begins, the actual area resisting the shear force is less than the original $A$. Without adjusting for the changing area, the curve would appear to lose stiffness, when in reality, the shear modulus may be constant as described in Figure 2-5.

### 6.3.1 Bond Strength in Shear with Various Surface Finishes

Shear testing was conducted to evaluate the effect of concrete surface finish/texture on the behavior of Corkelast in order to determine the desired surface finish for the plinths. The sand-blasted specimen results shown in Figure 6-17 represent typical shear stress versus shear strain results for each of the surface finishes (Other shear response curves are included in Appendix D). Table 6-8 summarizes the shear strength and stiffness for each of the tests. The results are quite similar for low levels of strain and diverge somewhat at higher strains.

Figures 6-18 and 6-19 compare the shear moduli and shear strength with the surface treatment. The difference in shear stiffness between the different surface finishes does not

appear to be significant, attested to by the low overall standard deviation (Table 6-8). All specimens tested at 4,000 lb/min achieved over 140 percent shear strain prior to failure. Failure was generally a combination of peeling of the elastomer to lightweight concrete bond, failure of the DexG to base concrete bond and fracture of the lightweight concrete. Specimens SF-2 and SF-6, which were tested at a higher loading rate, failed in the lightweight concrete—not at the bond interfaces—at shear strain values of 98 percent and 126 percent strain respectively. These specimens are considered anomalies, but they prompt further analysis of the effect of load rate on shear behavior (Section 6.3.4). Because of the high strain capacity demonstrated by all surface finishes, it was determined that each tested surface finish facilitated sufficient bond.

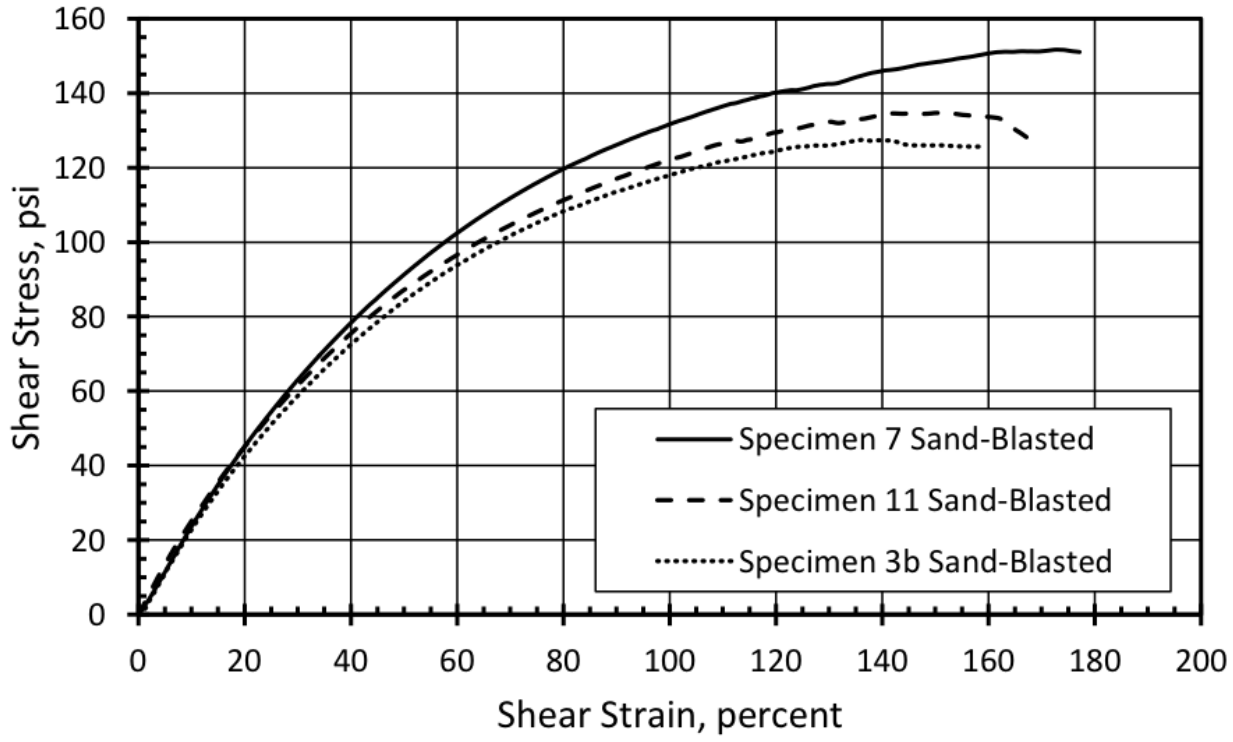


**Figure 6-17.** Typical Shear Results for Surface Finish Assessment (Sand Blasted Surface Finish)

**Table 6-8.** Summary of Surface Finish Results

| Specimen | Surface Finish | Secant Modulus | Chord Modulus | Maximum Shear Strength |
|---|---|---|---|---|
| SF-2[a] | Exposed Aggregate | 209 psi | 117 psi | 118 psi |
| SF-6[a] | Exposed Aggregate | 197 psi | 133 psi | 132 psi |
| SF-10 | Exposed Aggregate | 233 psi | 122 psi | 144 psi |
| **Exposed Aggregate Average:** | | 213 psi | 124 psi | 131 psi |
| **Exposed Aggregate Std. Dev.:** | | 18 psi | 8 psi | 13 psi |
| SF-1 | Pressure Washed | 215 psi | 107 psi | 140 psi |
| SF-5 | Pressure Washed | 202 psi | 127 psi | 127 psi |
| SF-9 | Pressure Washed | 236 psi | 156 psi | 142 psi |
| **Pressure Washed Average:** | | 218 psi | 130 psi | 136 psi |
| **Pressure Washed Std. Dev.:** | | 17 psi | 25 psi | 8 psi |
| SF-3B | Sand Blasted | 220 psi | 124 psi | 129 psi |
| SF-7 | Sand Blasted | 233 psi | 144 psi | 153 psi |
| SF-11 | Sand Blasted | 232 psi | 151 psi | 136 psi |
| **Sand-Blasted Average:** | | 228 psi | 140 psi | 140 psi |
| **Sand-Blasted Std. Dev.:** | | 7 psi | 14 psi | 12 psi |
| SF-4 | Tined | 216 psi | 131 psi | 146 psi |
| SF-8 | Tined | 211 psi | 137 psi | 136 psi |
| SF-12 | Tined | 240 psi | 152 psi | 142 psi |
| **Tined Average:** | | 222 psi | 140 psi | 142 psi |
| **Tined Std. Dev.:** | | 15 psi | 11 psi | 5 psi |
| **Overall Average:** | | 220 psi | 133 psi | 137 psi |
| **Overall Std. Dev.:** | | 14 psi | 15 psi | 10 psi |

[a] Higher loading rate used.

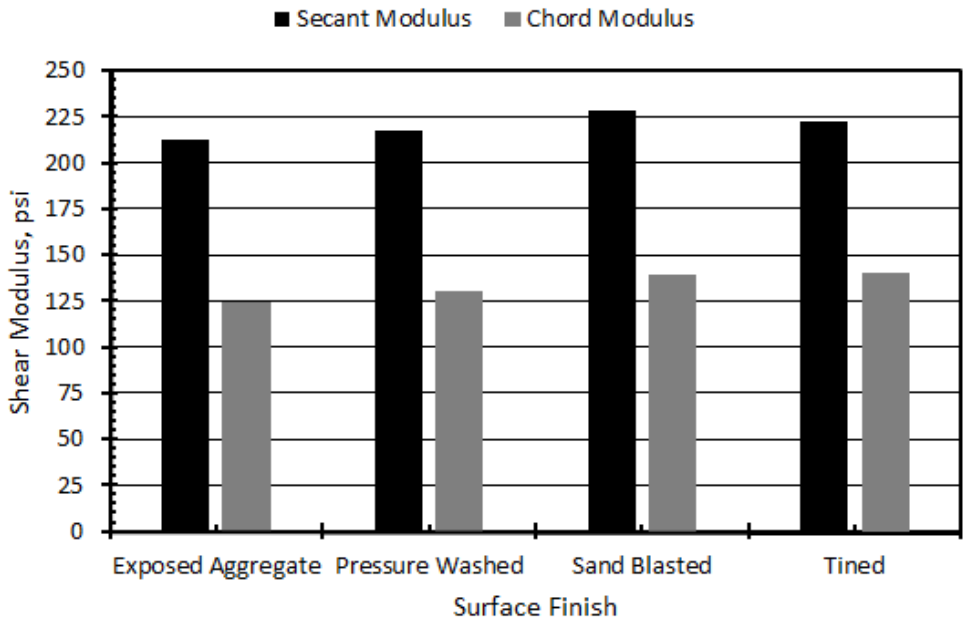


**Figure 6-18.** The Effect of Surface Finish on Shear Stiffness.

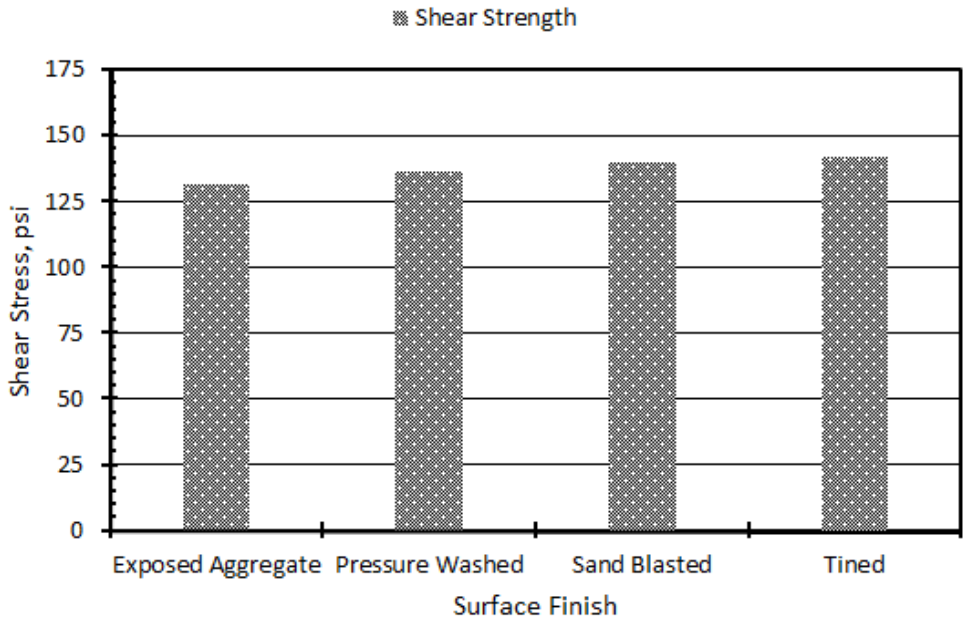


**Figure 6-19.** The Effect of Surface Finish on Shear Strength.

### 6.3.2 Shear Response with Different Elastomer Thicknesses

Average secant and chord modulus values are presented in Table 6-9 along with variability characteristics for the four layer thickness tested: 0.5 inch, 1.0 inch, 1.5 inches and 2.0 inches. At first glance, a flat or generally upward trend is noticed for both moduli (Figure 6-20). Neglecting the half-inch results, however, a distinct downward trend exists for both moduli between one and two inches, and the low variability of the data suggests that this observation is significant beyond the normal scatter of test data. Therefore, it is the half-inch thick specimens that break the downward trend, being significantly lower in both moduli. This is contrary to both the common understanding of elastomer behavior (as described in Section 2.2.3) and the experience of the compression results where the thinnest elastomer layers appeared the stiffest (Section 6.2.1).

The likely explanation for this discrepancy is that the debonding failure began at a lower strain for the half-inch specimens, causing the shear modulus to appear to decrease sooner than the other thicknesses. If this is the case, the shear modulus does not actually decrease, but the unaccounted decrease in area causes that appearance. It is reasonable, as discussed above, for the debonding force to be greater in the half-inch specimens due to the tighter curvature of the deformed thickness (s-shape) and the lower length-to-thickness ratio.

**Table 6-9.** Shear Response with Different Elastomer Thickness

| | **Elastomer Thickness, in.** | | | |
|---|---|---|---|---|
| | **0.5** | **1.0** | **1.5** | **2.0** |
| **Secant Modulus** | 142 psi | 195 psi | 179 psi | 170 psi |
| **Standard Deviation** | 16 psi | 1 psi | 19 psi | 14 psi |
| **Chord Modulus** | 104 psi | 143 psi | 134 psi | 125 psi |
| **Standard Deviation** | 9 psi | 3 psi | 11 psi | 4 psi |
| **Shear Strength** | 132 psi | 127 psi | 103 psi | 92 psi |
| **Standard Deviation** | 10 psi | 16 psi | 1 psi | 2 psi |

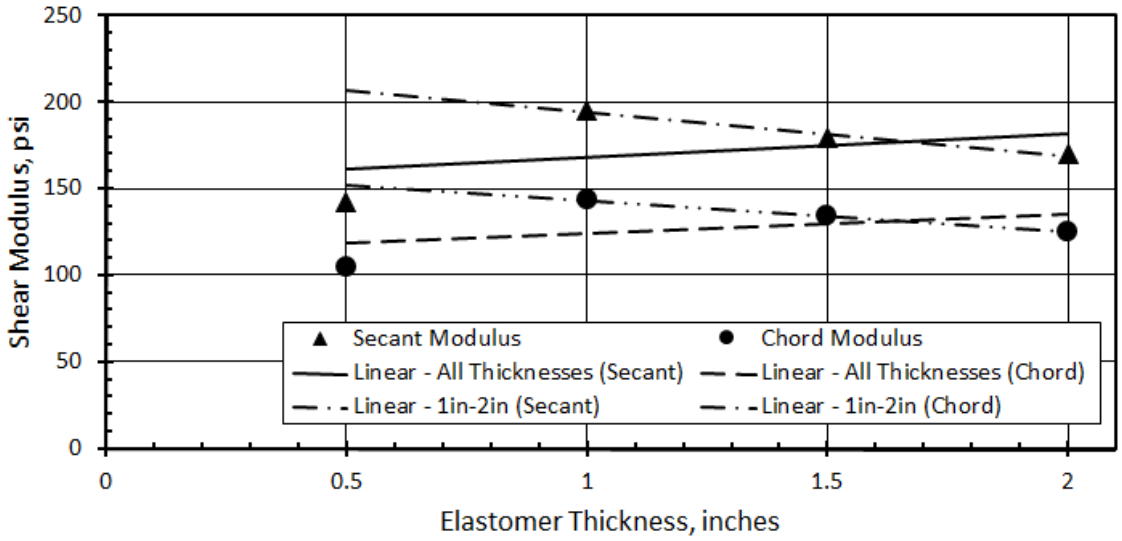


**Figure 6-20.** The Effect of Elastomer Thickness on Shear Stiffness.

The strength behavior does not reflect the same inconsistency with the half-inch specimens (Figure 6-21). Instead, as expected, the half-inch specimens are the strongest, and there is a steady downward trend in strength with increasing elastomer thickness.

### 6.3.3 Shear Response under Combined (Axial) Loading

Uniform axial stresses applied prior to loading in shear ranged from 20 psi in tension to 115 psi in compression. Secant and chord modulus values measured from the stress-strain data are presented in Table 6-10 and shown in Figure 6-22. There appears to be a slight increase in secant modulus with increasing compression stress, though the effect is very minor. The chord modulus is essentially flat despite changes in axial load. Axial stress also minimally affected the shear strength (Figure 6-23). The addition of 115 psi compressive stress only increased the shear strength by about 10 percent, while applying 20 psi in tension reduced the shear strength by less than five percent on average.

According to Equation 2-17, the 115 psi compressive stress introduces a 40 percent shear strain by the bulging of the elastomer. The negative effect this would have on the capacity,

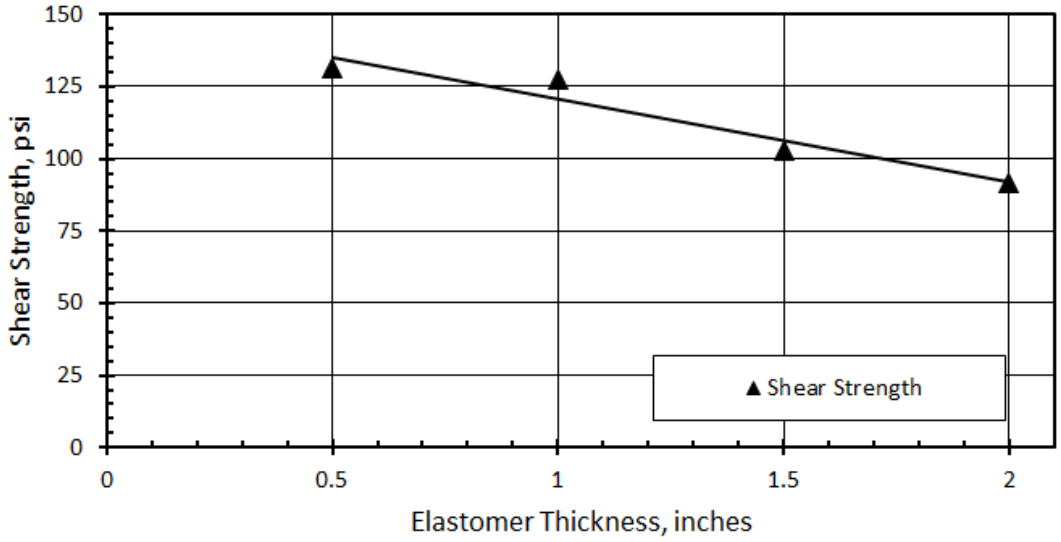


**Figure 6-21.** The Effect of Elastomer Thickness on Shear Strength.

**Table 6-10.** Shear Response with Combined (Axial) Loading (Compression Positive).

| Specimen | Axial Loading | Secant Modulus | Chord Modulus | Shear Strength |
|---|---|---|---|---|
| CL-1 | 97 | 209 psi | 145 psi | 127 psi |
| CL-2 | 83 | 194 psi | 137 psi | 121 psi |
| CL-3 | -5 | 172 psi | 144 psi | 103 psi |
| CL-4 | -20 | 192 psi | 156 psi | 118 psi |
| CL-5 | 55 | 207 psi | 167 psi | 113 psi |
| CL-6 | 115 | 220 psi | 165 psi | 130 psi |

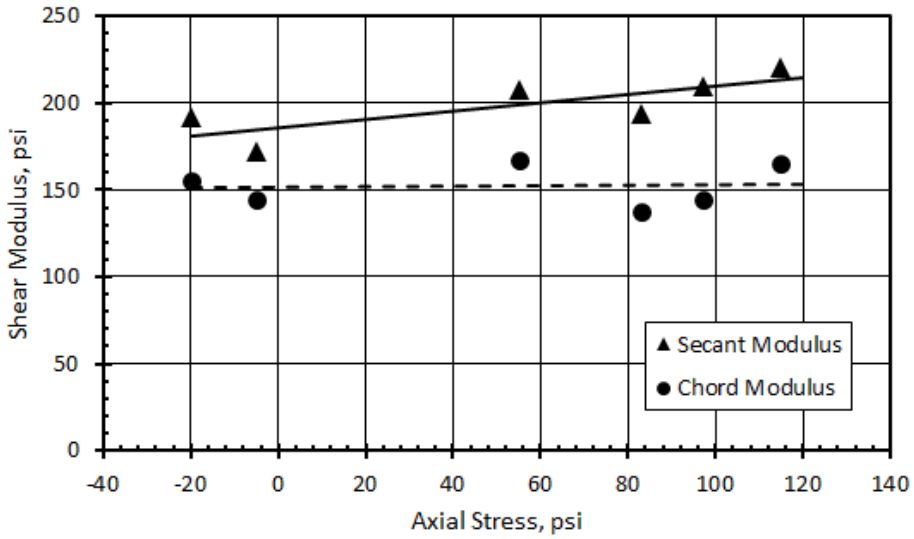


**Figure 6-22.** Effect of Combined Loading on Secant and Chord Shear Moduli (Compression Positive).

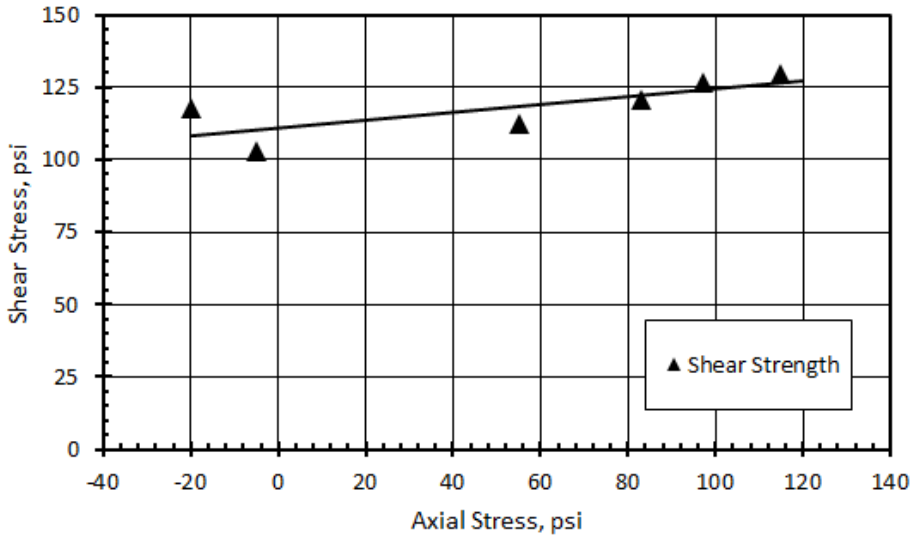


**Figure 6-23.** Effect of Combined Loading on Shear Strength.

however, is combated by the resistance the compressive force provides against debonding, allowing for a stiffer, stronger system as achieved by all the specimen with added compressive stress. On the other hand, the 20 psi tension stress correlates to an 8 percent shear strain, but the tension stress accelerates the onset of debonding, leading to a weaker, softer system. Ultimately, the shear response to axial load is small compared to the overall stiffness and strength of the elastomer.

### 6.3.4 Shear Response with Different Loading Rates

Shear rates were varied from about 30 to 300 percent shear strain per minute for specimens with a 1.0-inch-thick elastomer layer. Later, a specimen with a 0.5-inch-thick elastomer was tested at just under 600 percent shear-strain per minute.[5] Table 6-11 presents the strain rate of each specimen and the corresponding stiffness and strength results.

It is reasonable to adjust SR-7 for its different thickness from the other strain rate specimens according to the results described in Section 6.3.2. Since the half-inch results in the thickness tests significantly deviated from the trend of the other three thicknesses (Figure 6-20), it was difficult to define an expected shear modulus. However, it is likely that whatever caused the decrease in stiffness in the thickness testing also occurred for SR-7. This assumption is supported by the fact that though shear stiffness generally increased with an increasing strain rate, SR-7 was only as stiff as SR-6 in the low strain region and less stiff than both SR-5 and SR-6 in the range of the chord modulus (even though SR-5 and SR-6 were tested at much slower loading rates).

Therefore, an estimation of the secant and chord moduli of a one-inch specimen tested at 600 percent-strain/minute was made by multiplying the SR-7 result by a thickness conversion factor, $c_{MOD}$, derived from the thickness results. The factor simply relates the shear moduli of the one-inch thick specimens to the half-inch thick specimens for both the secant and

[5]Machine limitations prevented shear strain rates greater than 300 percent shear strain per minute for 1.0-inch-thick elastomer thicknesses

chord moduli:

$$c_{MOD} = \frac{195}{142} \simeq \frac{143}{104} = 1.37. \tag{6-1}$$

Using the same method for shear strength, the strength of SR-7 is reduced by about 3 percent ($c_{STR} = 0.969$). The reduction is due to the fact that the average strength of the half-inch specimens was greater than that of the one-inch specimens. The adjusted SR-7 result is included in Table 6-11 as SR-7 MOD.

Figure 6-24 shows stress-strain curves for the seven specimens tested at different strain rates along with a curve for SR-7 MOD that was estimated by dividing each SR-7 strain value by 1.37, reflecting the increase in modulus without affecting the shear strength. It can be seen that increasing the strain rate led to both increased stiffness and increased strength. Plotting the secant and shear moduli against the strain rate accentuates this (Figure 6-25), showing that the increase in modulus is linear over the range of strain rates tested. The gap in Figure 6-24 between 55 percent/minute and 137 percent/minute (gray and black lines in the figure) simply reflects a lack of data for strain rates in that range.

Shear rate had a different effect on the strength of the elastomer (as shown in Figure 6-26).

**Table 6-11.** Shear Modulus and Strength for Different Strain Rates.

| **Specimen** | **Thickness** | **Strain Rate** | **Secant Modulus** | **Chord Modulus** | **Maximum Shear Strength** |
|---|---|---|---|---|---|
| SR-1 | 1.0 in | 31 %/min | 173 psi | 140 psi | 119 psi |
| SR-2 | 1.0 in | 53 %/min | 195 psi | 151 psi | 105 psi |
| SR-3 | 1.0 in | 55 %/min | 181 psi | 138 psi | 87 psi |
| SR-4 | 1.0 in | 137 %/min | 215 psi | 166 psi | 116 psi |
| SR-5 | 1.0 in | 197 %/min | 224 psi | 173 psi | 119 psi |
| SR-6 | 1.0 in | 296 %/min | 231 psi | 180 psi | 154 psi |
| SR-7 | 0.5 in | 595 %/min | 231 psi | 167 psi | 152 psi |
| SR-7 MOD. | 1.0 in | 595 %/min | 317 psi | 229 psi | 148 psi |

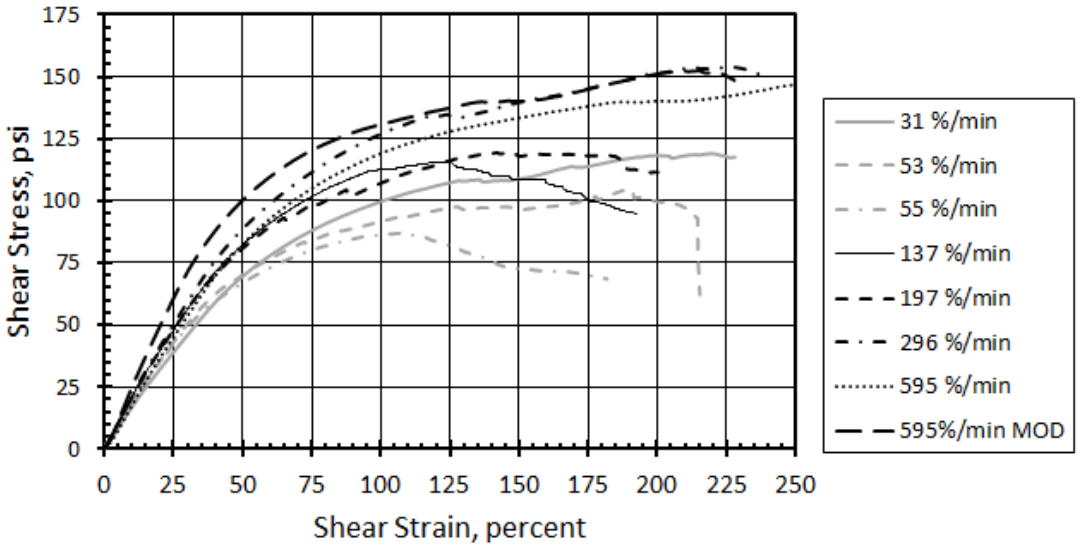


**Figure 6-24.** Typical stress-strain curves for specimens tested at different strain rates.

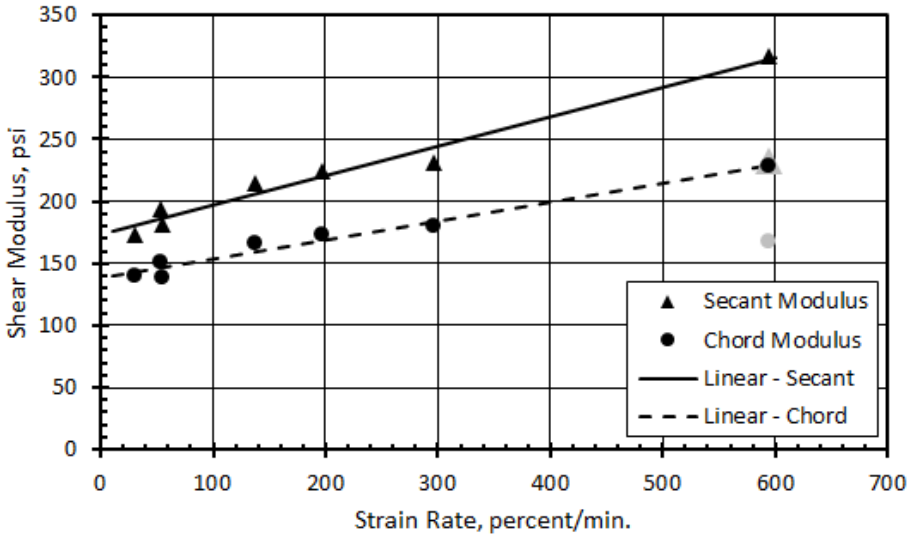


**Figure 6-25.** Shear Modulus versus Shear Strain Rate using modified SR-7 modulus values to account for its different thickness. The gray markers are the unmodified SR-7 values and are not included in the linear regressions.

The maximum shear strength increased about 30 percent by increasing the strain rate from 50–300 percent/minute but plateaued and did not continue to increase when the shear rate was increased to 600 percent/minute. The adjustment for the different thickness of SR-7 magnifies the asymptotic relationship between strain rate and shear strength because it reduces the strength of the specimen tested at the highest strain rate.

After 50 percent strain all the results diverge with no apparent groupings (Figure 6-24). This may be caused by varied timing of the onset of debonding failure. If this is the case, then a possible interpretation of these results is that a higher rate of strain preserves the integrity of the bond up to a higher strain. It is also possible that the debonding process is a slow tear such that the faster strain rates exceed the speed of the tear, causing the tear to 'lag' behind the strain it would tear at when loaded at a slower rate. Regardless, it is promising that this type of failure is a slow failure that does not result in immediate loss of capacity.

### 6.3.5 Shear Response after Freeze-Thaw Conditioning

The primary purpose of the freeze-thaw testing was to determine whether there would be excessive deterioration in the shear behavior at the LWC-Corkelast interface.

A comparison of non-freeze-thaw and freeze-thaw results is shown in Table 6-12. The post-freeze-thaw shear modulus values were 15 percent lower than the average values for 1.0-inch elastomer specimens reported in Section 6.3.2 (Table 6-9). Similarly, the average shear stress at 100 percent shear strain dropped 37 percent for the freeze-thaw specimens. This seems like a large decline, but the designer should note that the material still possesses 63 percent of its shear integrity after a lifespan in harsh environmental conditions without significant change in stiffness. Notably, the precision of the results was very high, leading to a high confidence in these results.

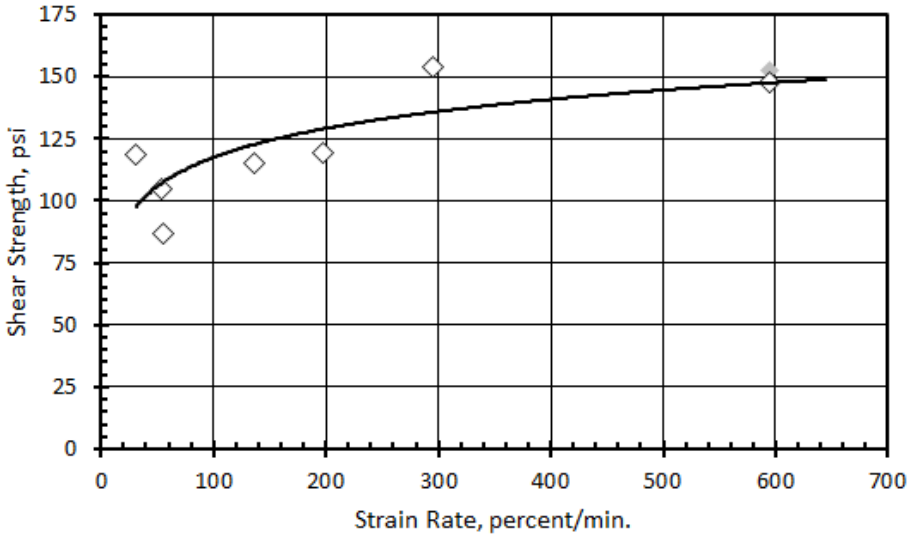


**Figure 6-26.** Effect of Shear Strain Rate on Shear Strength using the modified strength for SR-7 (SR-7 MOD) to account for its different thickness. The gray marker is the unmodified SR-7 strength and is not included in the logarithmic regression.

**Table 6-12.** Freeze-Thaw Specimen Comparison (1-inch thick elastomer)

| | **No Freeze-Thaw Exposure** | | | **Freeze-Thaw Exposure** | | |
|---|---|---|---|---|---|---|
| | **Secant Modulus** | **Chord Modulus** | **Stress at 100% Strain** | **Secant Modulus** | **Chord Modulus** | **Stress at 100% Strain** |
| **Value** | 195 psi | 160 psi | 157 psi | 171 psi | 134 psi | 99 psi |
| **Standard Deviation** | 14 psi | 13 psi | 14 psi | 6 psi | 2 psi | 8 psi |

### 6.3.6 Shear Response of DexG Epoxy

Four shear specimens were prepared without elastomer to test the bond strength of the DexG in shear. A 0.25-inch layer of DexG bonded the lightweight concrete to the normal-weight center section of the double shear specimens. The average shear modulus and strength are summarized in Table 6-13 along with the strain at the maximum stress. For the DexG specimens, a single value for the shear modulus was taken as the secant from 0-100 psi shear stress (well beyond the expected shear loading for the track attachment system).

A typical shear-stress, shear-strain curve for the specimens is shown in Figure 6-27. The DexG shows much higher strength and lower ductility than the elastomer results presented previously. This was marked by a very high initial stiffness and a small region of yielding before a very brittle failure. The extreme stiffness and strength compared to Corkelast indicates that the DexG has very little effect on the system shear response as long as the bonds are sufficient as they were in these cases.

**Table 6-13.** Shear Modulus and Strength of DexG

| **Parameter** | **Average Value** |
|---|---|
| Shear Modulus (0-100 psi shear stress) | 1,130 psi |
| Maximum Shear Stress | 325 psi |
| Percent Shear Strain at Maximum Stress | 2.2 % |

### 6.3.7 Shear Testing Summary

Shear testing was conducted to evaluate the effect of concrete surface, elastomer thickness, combined loading, strain rate and freeze-thaw exposure on the behavior of the attachment system. Shear strength was recorded for each test; a secant modulus (0-20 percent shear strain) and a chord modulus (20 to 30 percent shear strain) were calculated to measure the shear modulus at different levels of load. The shear modulus was always higher at low shear

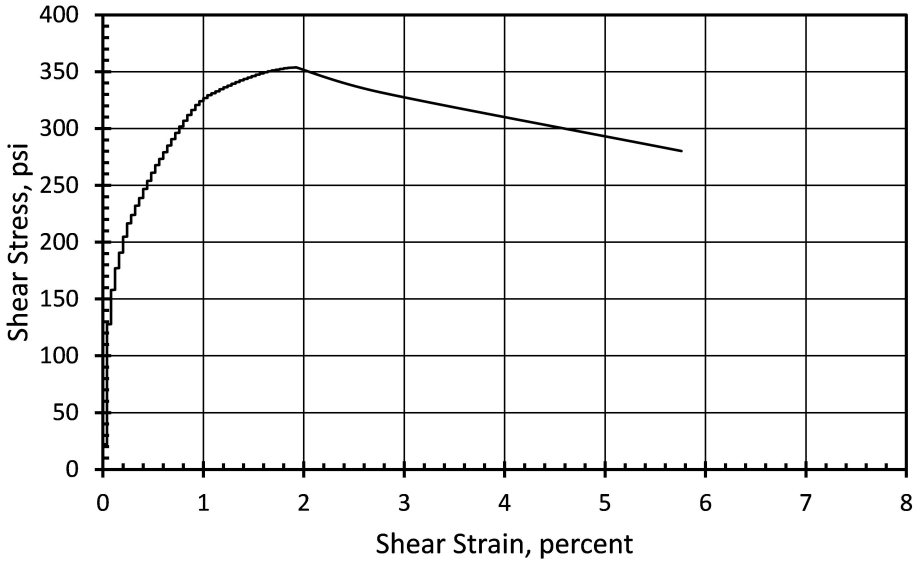


**Figure 6-27.** Typical Shear Response of DexG Specimens.

strains than at higher levels, and it is probable that the extreme nonlinearity of the stress-strain response was due to debonding action, the tearing of the elastomer close to its bonds with the LWC and DexG.

There was little difference between the results of the surface finish specimens beyond the normal scatter of the data. The four finishes (exposed aggregate, pressure-washed, sand-blasted and tined) were all sufficient to maintain the bond with the elastomer in shear loading.

In the thickness testing, the average secant modulus for the standard 1.0-inch Corkelast thickness was 195 psi and the chord modulus was 143 psi. Shear strength declined linearly with increasing layer thickness. Above one inch, the shear modulus also declined with increasing thickness, but contrary to the general elastomer theory discussed in Chapter 2, the half-inch specimens broke that trend. The most plausible reason for this discrepancy is premature debonding due to increased edge-peeling stresses.

Axial stress had a very minor effect of increasing the secant modulus as the axial stress increased in compression, and there did not appear to be any effect of axial stress on the

chord modulus. However, tension stress did reduce the apparent shear strength, probably as a result of accelerating the debonding action.

Shear strain rates lower than about 125 percent/minute resulted in lower shear modulus values, but once the shear rate increased above 140 percent/minute, the shear modulus was essentially constant, nearly unaffected by rate change. Shear strength also increased rapidly when the strain rate was increased at low strains but plateaued as the strain rate passed 300 percent/minute. Additionally, the results indicated that the debonding failure of the elastomer in shear is a slow process that lags behind when the strain rate is fast enough. It is promising that the shear failure type of Corkelast is slow and does not result in immediate loss of strength capacity.

Finally, artificial aging in the form of freezing and thawing exposure reduced the shear modulus values to approximately 85 percent of the normal values. Impressively, the bearing maintained 63 percent of its strength after a 'lifespan' of harsh environmental conditions.

Finally, the DexG was extremely strong and stiff compared to Corkelast. Its strength and stiffness has little influence on the shear response of the complete track attachment system as long as it is well bonded to both the normal concrete and the elastomer.

# 7 | Analysis

The results must be analyzed to ensure their usefulness to the structural design engineer. This section does so by calculating common elastic constants from the test data and using them to compare the results with modern elastomer theory. The lateral bulging of the elastomer during monotonic compressive loading is closely connected to these elastic constants, and analysis of the bulge allows for the translation of the results from individual plinths to the world of elastomeric bearings. Stanton and Lund (2015) require $K$ and $E$ in addition to $S$ to calculate the compressibility index, $\lambda$ (Equation 7-9). Additionally, the calculation of $E$ is dependent on $K$ and $G$; therefore, $G$ is also required. Poisson's ratio, $\nu$, is also helpful in characterizing the material.

In this section the volume of the bulge is calculated and compared with the volume displaced by the loading head to formulate a volumetric strain that is used in turn to estimate $K$ for each specimen. Then, $K$ is combined with $G$, calculated from the shear test results, to calculate $E$ and $\nu$. These values, which are standard across the structural engineering field can be used to compare this elastomer with other elastomers and research contexts. This chapter analyzes the compression and shear results by calculating these properties and comparing the results with the theoretical and numerical solutions for standard elastomeric bearings presented in Stanton and Lund (2015).

## 7.1 Material Constants

The structural designer typically understands material properties in terms of $E$, $K$, $G$ and $\nu$. Any two of these four properties are independent, while the other two are dependent. In this research, $K$ and $G$ are the independent variables that are measured through the compression and shear testing. $E$ and $\nu$ are then calculated from $K$ and $G$.

It is important to note that these constants are defined only for small displacements. Since elastomers undergo large displacements, the constants are not strictly valid but are used anyway, faute de mieux.

### 7.1.1 Bulk Modulus

The bulk modulus was approximated for all 12 compression specimen by taking the slope of the best fit line on a axial stress versus volumetric strain plot created by utilizing the lateral bulging data.[1] The calculation is only ball-park because the exact bulk modulus is found by dividing the volumetric strain by the hydrostatic stress (i.e. average of all three directions) rather than the vertical stress. However, since all three stresses vary across the surface, from about zero at the edges to a peak in the middle of the plan area, an approximation using the average vertical stress is considered sufficient for this analysis.

#### 7.1.1.1 Volumetric Strain

The bulge height, $h$, was measured at the center of the elastomer thickness on each side of the plinth and averaged on sides with equal length, taking into account different bulge values for the long, $h_L$, and short, $h_W$, sides of the plinth. A typical plot of the average horizontal deformation of the elastomer (bulge height) versus average vertical deformation is shown in Figure 7-1.

---

[1] Note that $\sigma = K\frac{\Delta V}{V}$

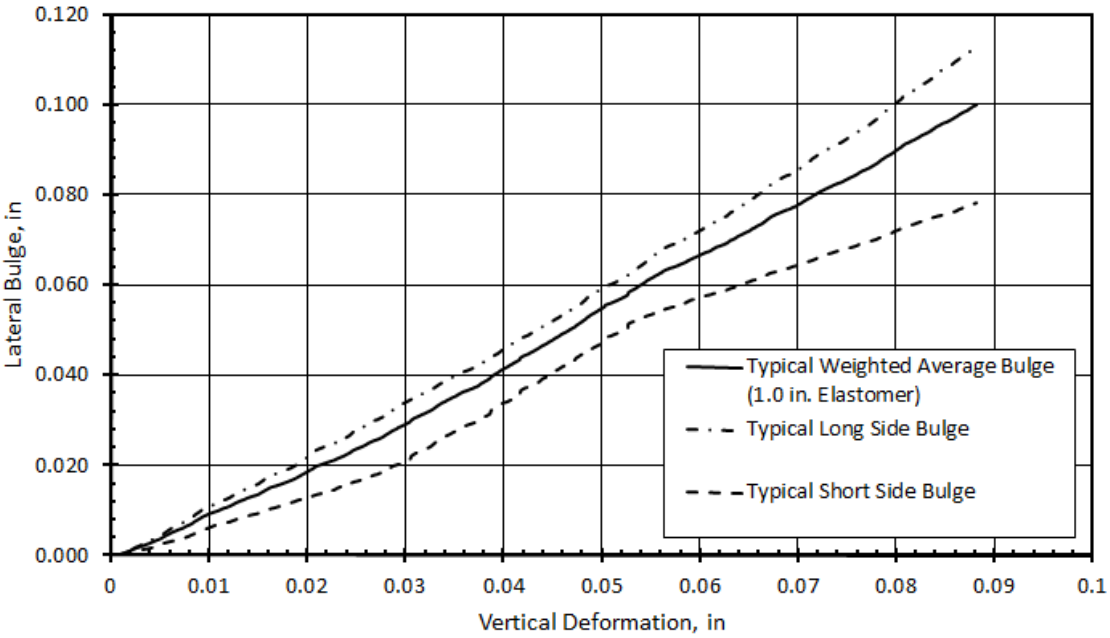


**Figure 7-1.** Typical Bulging Results, 1.0-inch Elastomer Thickness.

Holownia (1971), Stanton and Roeder (1982) and others show that the shape of the bulge for a layer in a reinforced elastomeric bearing is parabolic, with zero horizontal deflection at the top and bottom of the layer. This is similar to the layer of elastomer in this plinth attachment system: the bonds with the LWC and DexG prevent lateral deformation at the bonds. It can be shown that the area inside a parabola is exactly two-thirds its circumscribing rectangle (Figure 7-2). Thus, the cross-sectional area of the bulge can be taken as:

$$A_{Bi} = \frac{2}{3} h_i t_z \tag{7-1}$$

where $i$ is $L$ or $W$, designating the location of bulge on the length or width of the plinth, $t_z$ is the deformed thickness of the elastomer $(t_0 - w)$, $t_0$ is the initial thickness of the elastomer, and $w$ is the measured deformation of the elastomer in the $z$ (vertical) direction.

The volume of the bulge, $V_B$, was then calculated assuming that the bulge was uniform along each side of the plinth (an overestimation), and the corners were neglected

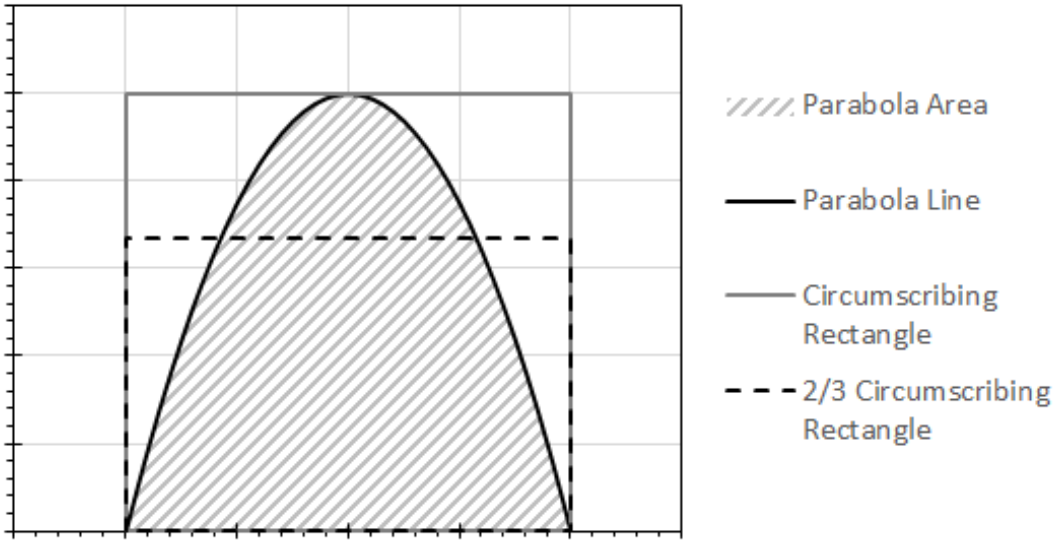


**Figure 7-2.** The area under a negative parabola is exactly 2/3 the area of the circumscribing rectangle.

(Equation 7-2):

$$\begin{aligned} V_B &= \alpha\ P\ A_{Bulge} \\ &= \alpha\ P \left[\frac{2}{3}\ t\ h_{weighted}\right] \\ &= \alpha\ \frac{2}{3}\ P\,(1-\epsilon_z)\,t_0\ h_{weighted} \\ &= \alpha\ \frac{2\ A}{3\ S}\,(1-\epsilon_z)\ \ h_{weighted} \end{aligned} \tag{7-2}$$

where $P$ is the perimeter of the specimen, $\epsilon_z$ marks the vertical strain of the elastomer and $h_{weighted}$ is the the weighted average of the long and short bulge lengths to the full perimeter:

$$h_{weighted} = \left[\frac{L}{L+W} * h_L + \frac{W}{L+W} * h_W\right]. \tag{7-3}$$

Assuming a uniform bulge height along each side of the plinth simplifies the mathematics but leads to the overestimation of the bulge volume by an unknown amount, thereby leading

to an underestimation of the volumetric strain. Therefore, equation 7-2 includes a bulge reduction factor, $\alpha$, that ranges from 0 to 1 to account for this effect. This project did not have sufficient measurement of the bulge to calibrate this factor but only measured the bulge in the center of each side of the plinth, so $\alpha$ was taken to be 1.0 (no reduction), and further research with sophisticated measurement of the bulge shape at several points along each side of the bearing is needed to calibrate this factor.

The volume displaced by the loading head, $V_z$, was taken to be:

$$V_z = wA = \epsilon_z t_0 A, \tag{7-4}$$

and the net volumetric strain was calculated in terms of the shape factor and a weighted bulge height by Equation 7-5:

$$\frac{\Delta V}{V_0} = \frac{V_z - V_B}{V_0} = \epsilon_z - \alpha \frac{2h_{weighted}}{3tS} \tag{7-5}$$

#### 7.1.1.2 Bulk Modulus Results

After calculating the volumetric strain, the bulk modulus of each specimen was approximated. $K$ was consistently greater at low strains than at high strains but could be closely approximated by a bilinear regression because it was nearly constant for each specimen after about 10–20 percent volumetric strain. Figure 7-3 shows a typical $\sigma_z$ versus $\Delta V/V$ plot with regression lines that approximate the bulk modulus at low and high strains.

A plot of bulk modulus versus shape factor (Figure 7-4) illustrates a slight decrease in $K$ with increasing $S$ when omitting the outlying data points (C-9 and 'C-2 Low Strain') and also indicates that a linear regression over the whole load range provides a sufficient approximation of $K$ for calculating $E$ and $\nu$. It can also be seen that the difference between the low and high strain ranges is more pronounced in the thinner layers (higher $S$).

The resultant $K$ is only an estimate because the vertical stress is used in the calculation instead of the hydrostatic stress. To reflect the approximate nature of the calculation, the

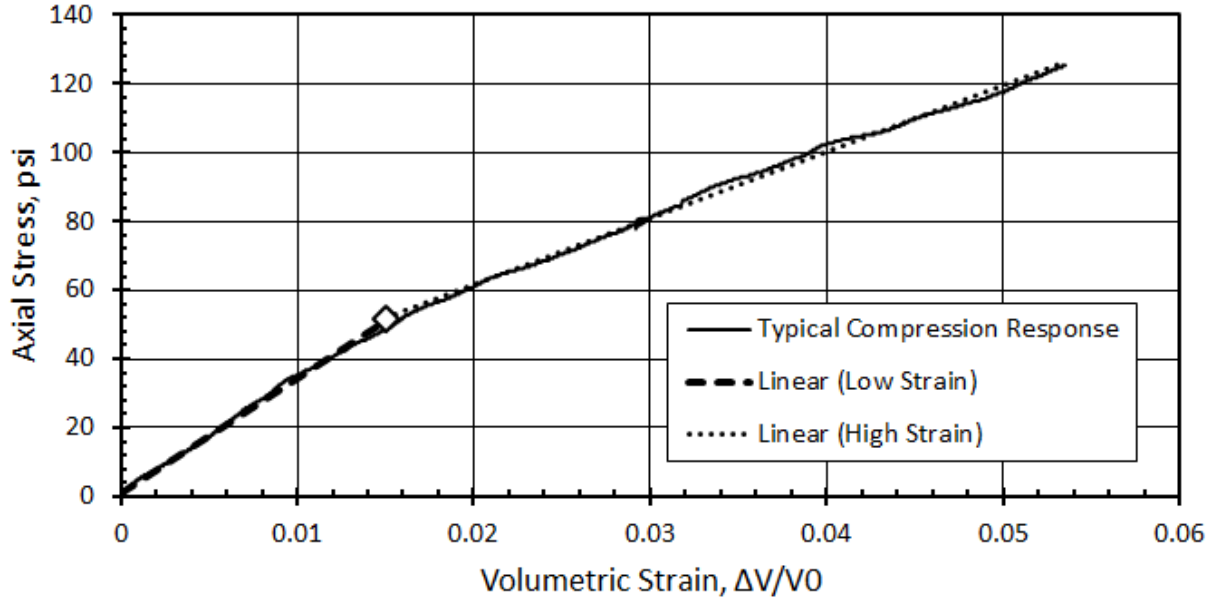


**Figure 7-3.** Typical Load vs. Volumetric Strain Plot with a Bilinear Regression to Approximate the Bulk Modulus

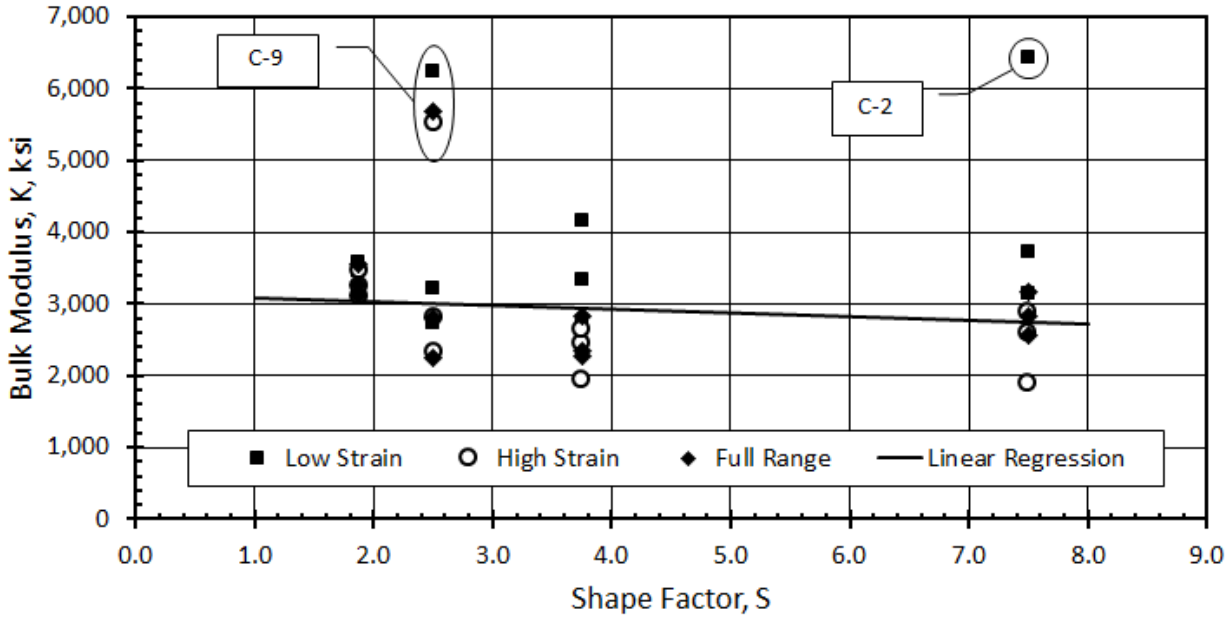


**Figure 7-4.** Bulk Modulus vs. Shape Factor

results were rounded to the nearest 100 psi. Excluding the outliers, the calculated $K$ averaged 2,800 psi with a standard deviation of 430 psi across the full load range with $\alpha$ equal to 1.0.

### 7.1.2 Shear Modulus

The shear modulus is the second independent elastic property needed for calculating $E$ and $\nu$. It was calculated reliably with the double shear method described previously. But, due to the nonlinearity of the stress-strain response, the magnitude of $G$ depends on where the slope is measured along the curve. Figure 7-5 shows the shear modulus for each specimen measured by drawing secants from 0 to various strain levels ($A\%$) to illustrate the large dependence of $G$ on where the measurement is taken along the stress-strain curve. The shear modulus is greater in all cases when measured along the initial part of the curve than when measured from 0 to 20–25 percent.

Therefore, the shear strain experienced by the elastomer under monotonic compression must be approximated to correctly characterize the shear modulus during expected loading. Based on Figure 2-6 and Equation 2-18, the maximum shear strain experienced by the compression specimens at $\sigma_z$ equal to 117 psi (unfactored extreme event) was calculated to be about 40 percent. Since shear stress varies along the $z$-axis and is maximum at the top and bottom of the elastomer layer where it is restrained by the bonds with the concrete and DexG, the average shear strain can be roughly approximated as half of the maximum: 20 percent. This is equivalent to the secant modulus described in Section 6.3. While the assumption is imperfect, the curve shown in Figure 7-5 indicates that the difference in $G$ in the 20–25 percent range is small and decreasing.

Figure 7-6 shows a plot of $G$ versus $t$ for the specimens tested with a constant strain rate of about 130 percent per minute and at constant load rates equivalent to about 30–40 percent strain per minute. $G$, in the figure, is taken as the secant modulus from 0–20 percent strain. While there is a large scatter in the shear modulus results overall, $G$ ranges between 195–240 psi for one-inch thick elastomer layers, and $G$ is taken as the average, 215 psi, for calculations

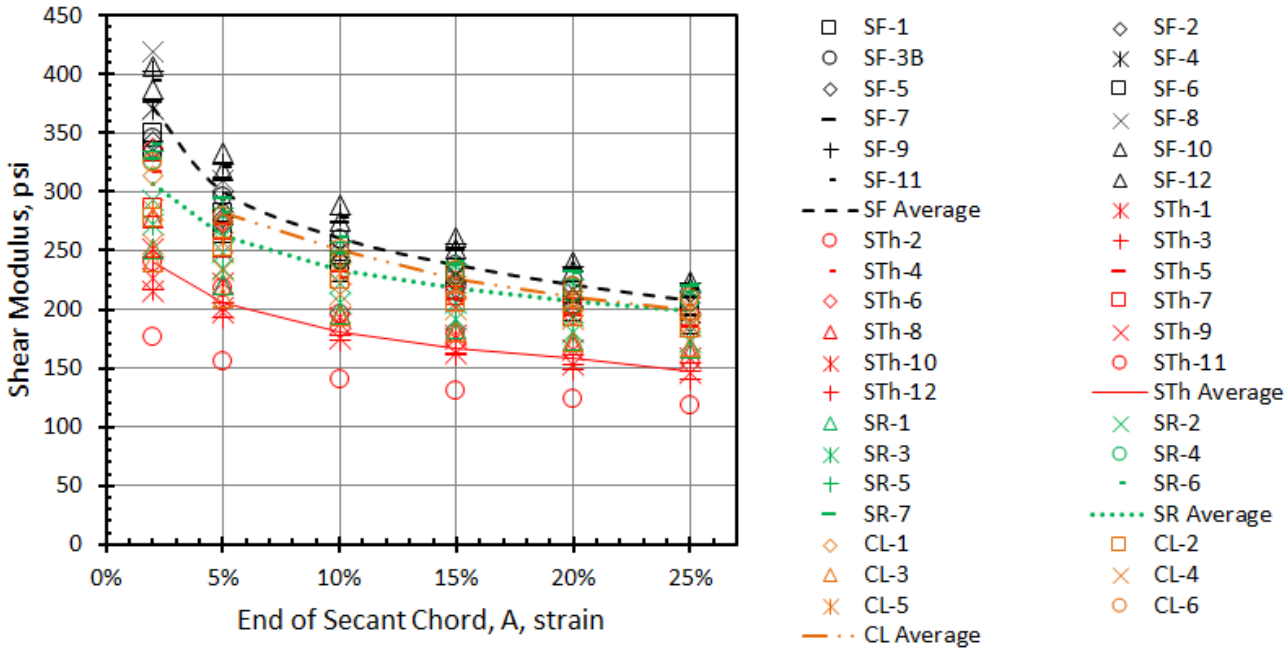


**Figure 7-5.** Variation of Shear Modulus based on Strain Limits

of $E$ and $\nu$. The data from the one-inch specimens was isolated because of Sound Transit's desire to use a layer thickness less than or equal to one inch in the final attachment system.

The shear modulus observed from the shear tests is about 13 times less than the $K$ calculated from the compression tests. This is much different than common, nearly-incompressible elastomers for which $K$ is often three orders of magnitude larger than $G$. This supports the hypothesis that the cork filler increases the bulk compressibility over pure rubber (decreasing the bulk modulus). But the increase in compressibility could also be attributed to the lack of vulcanization and the chemical reaction for curing that gives Corkelast its initial pourability.

### 7.1.3 Poisson's Ratio and Elastic Modulus

From $K$ and $G$, the elastic modulus, $E$, and Poisson's Ratio, $\nu$, were calculated by the elastic equations 7-6 and 7-7:

$$E = \frac{9KG}{3K + G}, \tag{7-6}$$

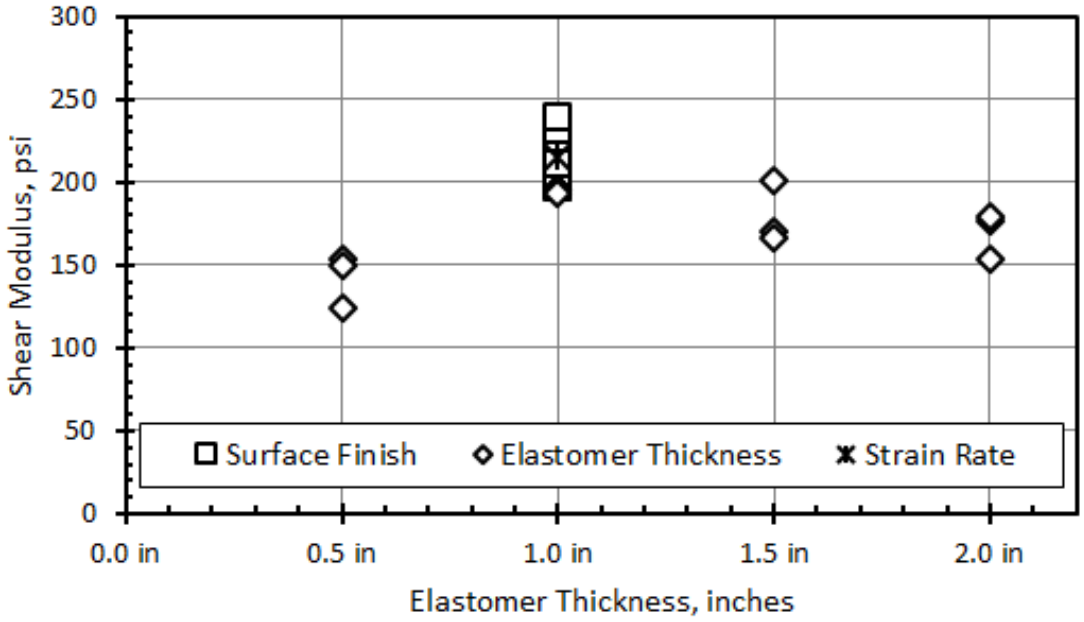


**Figure 7-6.** Shear Modulus vs. Elastomer Thickness with $G$ Measured as the Secant between 0–20% Strain

and

$$\nu = \frac{3K - 2G}{2\,(3K + G)} \tag{7-7}$$

Table 7-1 provides the elastic constants as measured or calculated for each compression specimen. Based on the following observations of $E$ and $\nu$, Corkelast should not be considered incompressible.

Using a range of $G$ between 200–230 psi and a range of $K$ between 2,380–3,240 psi (one standard deviation on either side of the mean), the elastic modulus falls between 584–668 psi. The average for the compression specimens is 629 psi with a remarkably low standard deviation of 0.7 psi. This suggests a break from the traditional incompressibility assumptions since $G$ equals $E/3$ in the completely incompressible state.

Similarly, $\nu$ falls between 0.453–0.470. This is significantly greater than the predicted $\nu = 0.3$ that was based on the extreme compressibility of the cork filler. But it is at the

**Table 7-1.** Elastic constants $E$, $K$ and $\nu$ for each compression specimen. $E$ and $\nu$ were calculated based on the $K$ and $G$ measured from compression and shear test results.

| **Specimen** | ***S*** | ***K*** | ***E*** | $\boldsymbol{\nu}$ | $\boldsymbol{E_a}$ |
|---|---|---|---|---|---|
| C-1 | 7.5 | 2,821 psi | 629 psi | 0.463 | 2,489 psi |
| C-2 | 7.5 | 3,156 psi | 631 psi | 0.467 | 2,618 psi |
| C-3 | 7.5 | 2,552 psi | 627 psi | 0.459 | 3,233 psi |
| C-4 | 3.75 | 2,280 psi | 625 psi | 0.454 | 1,562 psi |
| C-5 | 3.75 | 2,335 psi | 626 psi | 0.455 | 2,575 psi |
| C-6 | 3.75 | 2,833 psi | 629 psi | 0.463 | 2,323 psi |
| C-7 | 2.5 | 2,807 psi | 629 psi | 0.463 | 1,913 psi |
| C-8 | 2.5 | 2,243 psi | 625 psi | 0.454 | 1,581 psi |
| C-10 | 1.875 | 3,108 psi | 630 psi | 0.466 | 1,748 psi |
| C-11 | 1.875 | 3,254 psi | 631 psi | 0.468 | 1,786 psi |
| C-12 | 1.875 | 3,553 psi | 632 psi | 0.470 | 2,590 psi |
| **Average:** | | 2,813 psi | 629 psi | 0.462 | 2,220 psi |
| **Standard Deviation:** | | 430 psi | 2.5 psi | 0.006 | 536 psi |

NOTE 1: C-9 removed from analysis

NOTE 2: $G = 215$ psi was used for the calculation of $E$ and $\nu$

NOTE 3: The working modulus (Chapter 6) is used for the apparent elastic modulus, $E_a$.

very low end of the range Holownia (1980) gives for typical elastomers (0.45000–0.49990). Holownia (1974) believed that the incompressibility assumption was flawed even for materials with $\nu$ equal to 0.4985, so it is safe to say that Corkelast does exhibit compressible properties to the extent that incompressibility is a poor assumption for this material for all shape factors.

## 7.2 Compression Analysis

In this section, the compression modulus results are analyzed by comparing the average moduli together and relating the results to the previous work cited in Chapter 2. Table 7-2 provides the average moduli and standard deviation for each elastomer thickness.

### 7.2.1 Initial Analysis

In Chapter 6, Figure 6-12 presents the measured secant, working and overload compression moduli for each specimen with the corresponding averages in relation to elastomer thickness. It was noted that there is a sharp increase in stiffness for the thinner layer. However, when comparing the moduli with the shape factor instead of the thickness (Figure 7-7), the

**Table 7-2.** Average Moduli and Variation by Elastomer Thickness

| Elastomer Thickness | Shape Factor | | Secant Modulus | Working Modulus | Overload Modulus |
|---|---|---|---|---|---|
| 0.5 | 7.50 | **Average:** | 3,722 psi | 3,568 psi | 2,342 psi |
| | | **St. Dev.:** | 1,260 psi | 1,280 psi | 373 psi |
| 1.0 | 3.75 | **Average:** | 2,111 psi | 1,963 psi | 2,004 psi |
| | | **St. Dev.:** | 361 psi | 382 psi | 160 psi |
| 1.5 | 2.50 | **Average:** | 1,843 psi | 1,747 psi | 1,884 psi |
| | | **St. Dev.:** | 171 psi | 235 psi | 134 psi |
| 2.0 | 1.88 | **Average:** | 2,171 psi | 2,049 psi | 2,014 psi |
| | | **St. Dev.:** | 392 psi | 489 psi | 78 psi |

variation of the moduli is approximately linear. This highlights the importance of the shape factor in elastomeric bearing analysis.

Additionally, comparison of the elastomer stiffness results with values published by EdilonSedra supports the relationship between the effective elastic modulus and shape factor. The reported compressive modulus of Corkelast, measured according to ISO 604 between 29–72.5 psi compressive stress on a 2-inch by 2-inch by 1-inch block ($S = 0.5$), was 856 psi (Appendix E). While the shape of the EdilonSedra curve resembled those of the specimens tested in this research, the modulus reported by EdilonSedra was much lower. But Figure 7-7 shows that EdilonSedra's result, when plotted against $S$, lines up with the rest of the data points. Further investigation by comparison to previous work is needed for a complete understanding of the results.

### 7.2.2 Stanton and Lund (2015)

As discussed in Section 2.2.5, Stanton and Lund (2015) observed a linear relationship between $E_a/E$ and $S^2$ in typical elastomers used in bridge bearings. They determined the coefficients characterizing the line, $A$ and $B$, and defined the compressibility index, $\lambda$. Their equations are repeated here for convenience:

$$\frac{E_a}{E} = A + BS^2, \tag{7-8}$$

$$\lambda = S\sqrt{\frac{E}{K}}, \tag{7-9}$$

$$A = \begin{cases} \frac{4}{3}, & \text{for cases of plain strain;} \\ 1, & \text{for rectangular bearings,} \end{cases} \tag{7-10}$$

and

$$B = \frac{4}{3}\left\{\frac{3}{2\lambda^2}\left(1 - \tanh\frac{2\lambda}{2\lambda}\right)\right\}. \tag{7-11}$$

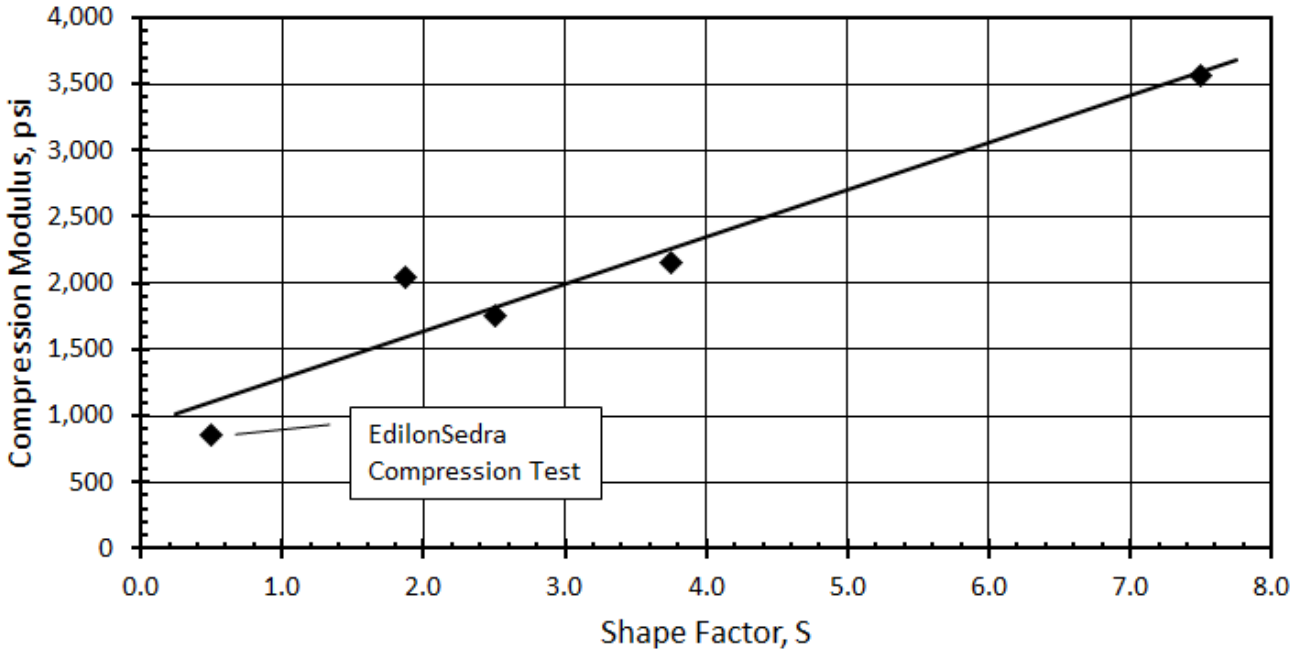


**Figure 7-7.** Compressive Modulus vs. Shape Factor

$A$ and $B$ as proposed by Stanton and Lund[2] were calculated for $K$, $E$ and $S$ of the elastomer layers tested (Sections 7.1). Table 7-3 reports the material constants measured or calculated for each specimen as described previously including $\lambda$ and $B$ for use in Equation 7-8. Figure 7-8 shows a plot of $E_a/E$ versus $S^2$ with a linear regression through the measured data and Stanton and Lund's prediction curve, which drops toward $A$ for low shape factors. The working modulus was used for $E_a$.

The shape of Stanton and Lund's curve reasonably reflects the trend of $E_a/E$, but it overestimates all but the highest results when $G$ is 215 psi and $\alpha$ equals one (See Equation 7-2). Erroneous assumptions of $\alpha$ and $G$ contribute to the discrepancy between the prediction and the results. The bulge reduction factor was acknowledged in the calculation of volumetric strain but was ignored in the analysis up to this point due to the lack of sophisticated bulge measurements. Though an in depth exploration of $\alpha$ is beyond the scope of this thesis, it

[2]As discussed in Section 2.2.5, $B$ is only exact for an infinitely long strip. It is used here as an approximation for the case of a rectangular bearing.

**Table 7-3.** Measured and Calculated Material Constants for Analysis

| Specimen | $S$ | $K$, psi | $E$, psi | $\nu$ | $\lambda$ | $B$ |
|---|---|---|---|---|---|---|
| C-1 | 7.5 | 2,800 | 325 | 0.481 | 2.55 | 0.12 |
| C-2 | 7.5 | 3,200 | 326 | 0.483 | 2.41 | 0.14 |
| C-3 | 7.5 | 2,600 | 325 | 0.479 | 2.68 | 0.11 |
| C-4 | 3.75 | 2,300 | 324 | 0.476 | 1.42 | 0.32 |
| C-5 | 3.75 | 2,300 | 324 | 0.477 | 1.40 | 0.33 |
| C-6 | 3.75 | 2,800 | 325 | 0.481 | 1.27 | 0.38 |
| C-7 | 2.5 | 2,800 | 325 | 0.481 | 0.85 | 0.62 |
| C-8 | 2.5 | 2,200 | 324 | 0.476 | 0.95 | 0.55 |
| C-9 | 2.5 | 5,700 | 327 | 0.490 | 0.60 | 0.85 |
| C-10 | 1.875 | 3,100 | 326 | 0.483 | 0.61 | 0.84 |
| C-11 | 1.875 | 3,300 | 326 | 0.483 | 0.59 | 0.85 |
| C-12 | 1.875 | 3,600 | 326 | 0.485 | 0.57 | 0.88 |

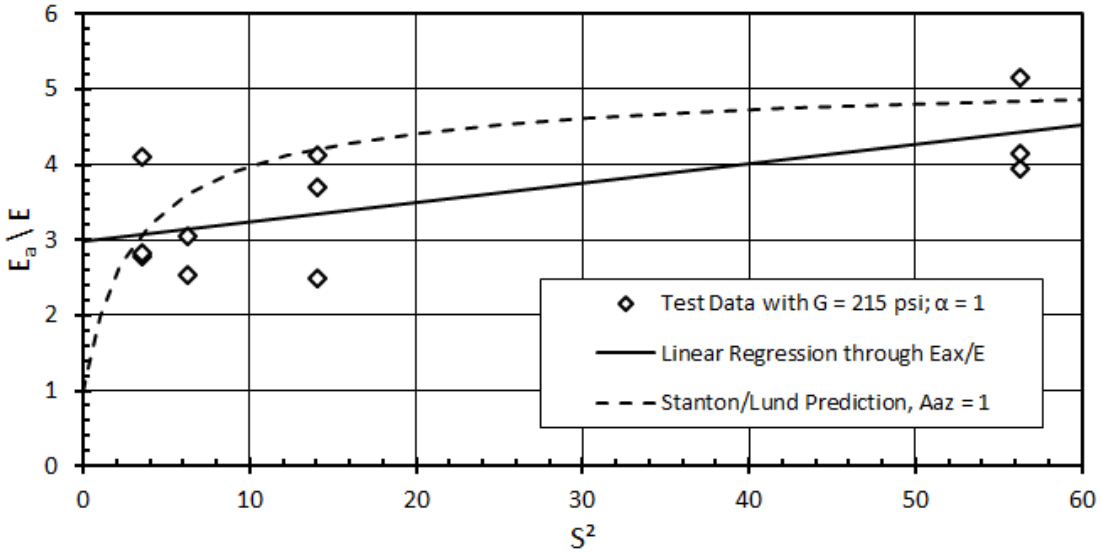


**Figure 7-8.** Comparison with Stanton and Lund's model for the relationship between $E_a/E$ and $S^2$ with $G = 215psi$ and $\alpha = 1.0$

is important to note that reducing $\alpha$ from 1.0 in order to more accurately predict the bulge volume reduces $K$ and brings the prediction closer to the measured results. $G$ affects the data and prediction curve in a similar way. Figure 7-9 illustrates that with $\alpha = 0.6$ and $G = 200$ psi the prediction curve fits the data much more closely.

It is possible that this observation calls for an adjustment of $A$ and/or $B$ to account for the hybrid material (cork and elastomer). However, it is far more likely that the constants persevere for Corkelast as established by Stanton and Lund and that the discrepancy between predicted and calculated values for $E_a/E$ stems from faulty assumptions in the calculation of the compressive properties of the layer. One suspect assumption was used to determine the shear modulus: that the average shear strain in a compressed layer is equal to half the maximum shear strain. If the average shear strain is more than half the maximum, it leads to a lower shear modulus being used to calculate $E$ and $\nu$.

One major discontinuity between the data and the prediction is the drop-off toward $E_a/E = A$ as $S^2$ goes to zero. The data does not seem to reflect the predicted decrease but converges at about 3.2. This may be due to variability in the test data and the lack of low shape factors tested. So while this research partially verifies the Stanton-Lund model for compressible elastomers of $3 < S < 7.5$, more specimens with low shape factors ($S < 2$) need to be evaluated with Corkelast to fully characterize its behavior.

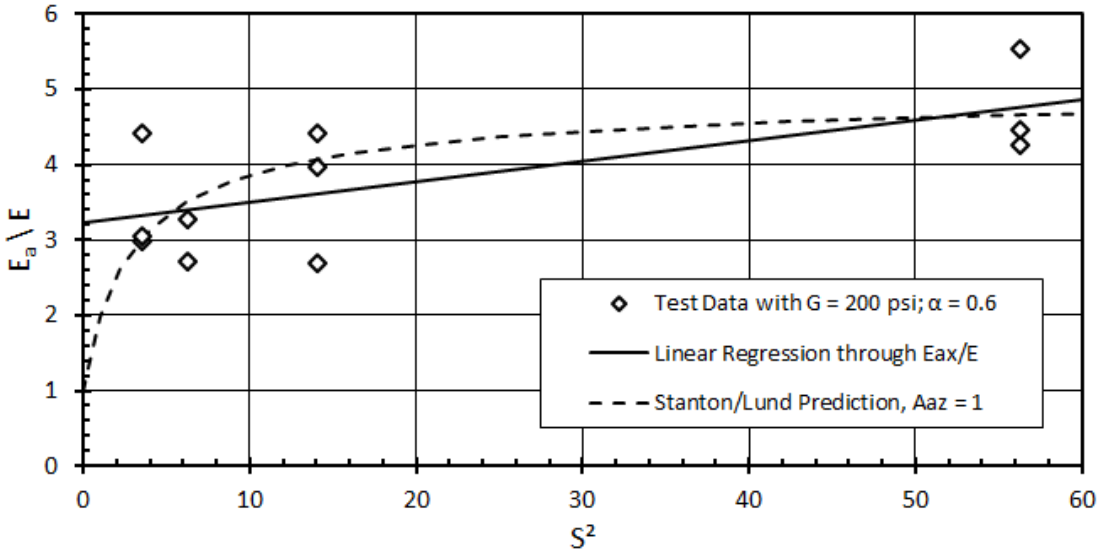


**Figure 7-9.** Comparison with Stanton and Lund's model for the relationship between $E_a/E$ and $S^2$ with $G = 200psi$ and $\alpha = 0.6$

# 8 Conclusions and Recommendations

## 8.1 Summary of Research

A two-component elastomer and a corresponding epoxy from EdilonSedra, in conjunction with bonding primers, were evaluated in their function as part of a direct fixation rail system being considered for the Interstate-90, Homer Hadley floating bridge. Results from system tests in tension, compression and shear were analyzed and used to verify the physical properties of the materials provided by the manufacturer and inform the designers of the system properties. Test data and analysis were also compared with previous research on (single-component) elastomers to understand the influence of filler components like cork on the behavior of the elastomer.

Tensile and shear strength as well as the elastic modulus (compression) and shear modulus of the elastomer are critical to design the rail attachment system. Each of these were investigated in this thesis, and several factors were tested on how they affected shear strength and stiffness. The data was analyzed and the bulk modulus, Poisson's ratio, and a theoretical elastic modulus were calculated for further characterization of the material and comparison with other work. The analysis used a combination of the compression and shear test results and partially validated a theory developed by Stanton and Lund (2015) for compressible elastomers. Since elastomer properties are highly dependent on the shape factor of the material, the effect of shape factor on compression and shear stiffness was also evaluated.

### 8.1.1 Tensile Bond

Tension pull-off tests were performed on 2.25-inch diameter lightweight concrete cores attached by an EdilonSedra elastomer and epoxy to a normal weight concrete deck. The tensile strength was determined using the Pull-off Bond Test according to ASTM C1583. While tensile results for the 0.5-inch-thick Corkelast tension pull-off tests ($S = 1.125$) exceeded the manufacturer's reported tensile strength (145 psi, ISO 527), the 1.0-inch-thick specimens ($S = 0.5625$) did not. The dependence of elastomeric properties on the shape factor is well known and discussed in Chapter 2. It is believed that the small shape factor contributed to the lower strength for the one-inch specimens.

Tension testing also identified two issues related to the elastomer-lightweight concrete bond that should be considered for the actual block-rail production:

1. Lightweight concrete blocks should be protected from additional water exposure following pressure-washing. Laboratory samples that were returned to a moist environment for a week following the pressure-washing appeared to have developed laitance which inhibited the lightweight concrete-U90WB primer bond. The consistent weakness of that bond resulted in premature failures and significantly lower tensile strengths.

2. The maximum 72 hours between initial U90WB primer application and elastomer placement listed in the manufacturer's recommendations for the U90WB primer appears to be too long. Laboratory specimens that experienced 70 hours between U90WB application and Corkelast placement exhibited premature failure between the primer and the Corkelast, while locations that were re-primed 44 hours prior to Corkelast placement showed cohesive failure in the Corkelast itself. This could be a practical concern for blocks that are primed but cannot have the Corkelast applied within two days.

### 8.1.2 Compression

Full-scale plinth specimens were tested in compression over the range of load expected on the attachment system during the design lifespan of the bridge. The compression test results suggest that the manufacturer's compression data (based on tests in accordance with ISO 604) may not be appropriate for all design applications. The compression testing with full-scale specimens indicated that the Corkelast is considerably stiffer than the manufacturer's reported compressive stiffness. Average stiffness measurements for specimens with 1.0-inch, 1.5-inch and 2.0-inch Corkelast layers were between 2,000–2,600 psi, more than double the value provided in the product data sheet (856 psi, Appendix E). This was primarily due to the difference in shape factor. Additional confinement occurred when the Corkelast was only 0.5-inches thick due to DexG surrounding some of the elastomer sides. This effect appeared to increase the compression stiffness by approximately 50 percent.

The lateral bulging of the elastomer during compression testing was also measured on all four sides of the test specimens to further understand the compression stiffness and Poisson's ratio of the material.

### 8.1.3 Shear

Shear testing was conducted using a double shear test configuration on 4-inch by 8-inch blocks. The test setup was developed specifically for this project but would be useful in testing shear properties of elastomers and epoxies for a variety of applications. Setup of the double shear testing configuration is much simpler and faster than the setup of a single shear configuration, and it can be used in any standard compression machine. In addition, the shear properties of the two specimens are inherently averaged in the configuration, leading to a reduction in the number of tests required for reliable conclusions.

Using the double shear configuration, testing was conducted to evaluate the effect of surface preparation, elastomer thickness, combined stress, strain and load rate dependency and freeze-thaw conditioning on the shear stiffness and strength of the elastomer. The shear

response of the DexG epoxy was also measured. Shear results indicated that the Corkelast is less stiff at low rates of shear strain, but once the shear rate is at least 100-120 percent strain per minute the shear modulus is essentially constant. Due to the nonlinearity of the elastomer's stress-strain relationship, the value of the shear modulus depends on where along the stress-strain curve it is measured. In this testing program, the secant modulus (0–20 percent strain) ranged between 200–220 psi, and the overload modulus (20–30 percent strain) lay between 175–200 psi. As expected, the average working modulus (4.5–12 percent strain) fell in between the secant and overload moduli.

The nonlinear nature of the shear response was probably a result of debonding of the elastomer near the ends, and debonding probably reduced the failure strength as well. The contribution of debonding to the overall response was probably related to the length-to-thickness ratio of the elastomer layer. Increasing the length-to-thickness ratio while maintaining the surface area of the material would most likely reduce the contribution of debonding to the overall shear response.

## 8.2 Research Conclusions

The following conclusions were drawn from the testing and analysis described in this thesis:

1. Careful surface preparation of the lightweight and normal concrete is crucial to the integrity of the bonds. Concrete cleaning and primer requirements need to be more stringent than indicated in the product literature. Laitance and efflorescence that degrade the bonds can re-appear on the concrete surfaces after cleaning if the concrete is subject to moisture or if there is an extended period between cleaning and material application, so the concrete should be kept dry and primed as soon as possible after cleaning. Clean surfaces are much more crucial to the bond integrity than the surface finish of the lightweight concrete.

2. Elastomer tensile strength is noticeably dependent on the shape factor. Local stress

concentrations reduce the apparent tensile strength but decrease with increasing shape factor such that the tensile strength published in the product literature is achievable, but only for high shape factors.

3. The compression modulus is approximately linear throughout the load range tested (up to 125 psi) but is noticeably dependent on the shape factor. Stanton and Lund (2015)'s complex relationship between $\frac{E_a}{E}$ and $S^2$ slightly underpredicted $\frac{E_a}{E}$ Corkelast at each thickness. This indicates that the factors $A$ and $B$ need to be adjusted for special elastomers (pourable, non-vulcanized and filled elastomers), but the analysis validated the general relationship, especially at shape factors greater than three.

4. Corkelast retains its shear load capacity well beyond 100 percent shear strain. Its shear failure is ductile, characterized by a slow decrease in shear stiffness with increasing strain. Debonding contributes significantly to shear failure, but increasing the length-to-thickness ratio of the specimen reduces its negative effect.

5. Freeze-thaw exposure reduces the shear modulus slightly and reduces the shear stress at 100 percent shear strain by just over a third, though that level of stress can be maintained for shear deflections considerably higher than 100 percent strain.

6. Shear stiffness increases linearly as the strain rate increases between 30–600 percent per minute.

7. The shear modulus depends minimally on axial (combined) stress up to 120 psi compression stress.

## 8.3 Recommendations for Future Research

The use of elastomer in structural applications is largely limited to bridge bearings and isolation systems since elastomer properties are less familiar to most structural designers than

those of concrete, steel and timber. The scope of this thesis was limited to a few specific materials for a specific application, but the test program revealed areas where continued research would benefit the field of structural engineering by increasing the understanding of elastomer behavior in general. Among these are the following:

- The addition of solid filler components (like cork) to elastomer changes its physical properties, requiring a modification of classical elastomer theory to accurately describe behavior. Further investigation of solid filler components in elastomer using various filler concentrations and different filler components (similar to Holownia (1980)'s work with carbon black) is needed to correctly predict results in design applications and to incorporate usage guidelines into design codes and manuals of standard practice.

- Stanton and Lund (2015)'s $A$ and $B$ factors should be adjusted for these differences.

- Pourable elastomers are not usually used in unconfined environments because they do not undergo vulcanization. However, they are extremely convenient for some structural applications. General research in this area is needed to make it an advantageous, cost-effective alternative for construction that designers are confident to specify.

- The double shear test method is valuable as an alternative to the quadruple shear apparatus described in ASTM D4014-03 because it can be used in any standard compression testing machine and it reduces the time to achieving reliable results. Development of the double shear test method for inclusion in ASTM D4014-03 should continue by standardizing the apparatus and procedure and by calibrating the method using other materials and aspect ratios. Additionally, Corkelast should be subjected to the quadruple shear method and the results compared to uncover deficiencies in either method.

- The tension strength of the Corkelast should be re-evaluated using a test apparatus that

    1. is able to measure the deformation of the elastomer during the test, and

2. has a sufficient deformation capacity to fully break the tension specimens.

The elastic modulus in tension could then be compared with that observed in compression as a way to confirm or further develop the constants, $A$ and $B$, in Stanton and Lund (2015)'s model for highly compressible elastomers.

- Finally, the effect of debonding on the nonlinearity of the shear response should be investigated thoroughly. This research identified debonding as a probable driver of the observed reduction in shear stiffness, but it did not confirm its effect. Understanding when debonding began and how it affected the shear response for the tests discussed in this thesis would be beneficial for fully characterizing the elastomer. The length-to-thickness ratio should also be explored for use by designers to control the effect of debonding and optimize the material for efficient design.

# Bibliography

AASHTO (2010). *LRFD Bridge Design Specifications*. American Association of State Highway and Transportation Officials, Washington, D.C., 5th edition.

ACI 211.2 (2004). "Standard practice for selecting proportions for structural lightweight concrete." *ACI 211.2-98*, American Concrete Institute.

ACI 213R-14 (2014). "Guide for structural lightweight-aggregate concrete." *ACI 213R-14*, American Concrete Institute.

ACI E1 (2007). "Aggregates for concrete." *ACI E1-07*, American Concrete Institute.

ASTM C1583-13 (2013). "Standard test method for tensile strength of concrete surfaces and the bond strength or tensile strength of concrete repair and overlay materials by direct tension (Pull-off method)." *ASTM C1583/C1583M-13*, ASTM International.

ASTM C39-15a (2015). "Standard test method for compressive strength of cylindrical concrete specimens." *ASTM C39-15a*, ASTM International.

ASTM C469-14 (2014). "Standard test method for static modulus of elasticity and poisson's ratio of concrete in compression." *ASTM C469-14*, ASTM International.

ASTM C496-11 (2011). "Standard test method for splitting tensile strength of cylindrical concrete specimens." *ASTM C496/C496M-11*, ASTM International.

ASTM C567-14 (2014). "Standard test method for determining density of structural lightweight concrete." *ASTM C567/C567M-14*, ASTM International.

ASTM D1349-14 (2014). "Standard practice for rubber—standard conditions for testing." *ASTM D1349-14*, ASTM International.

ASTM D4014-03 (2012). "Standard specification for plain and steel-laminated elastomeric bearings for bridges." *ASTM D4014-03*, ASTM International.

ASTM D412-15 (2015). "Standard test methods for vulcanized rubber and thermoplastic elastomers—tension." *ASTM D412-15*, ASTM International.

Carolina Stalite Company (2015), <`http://www.stalite.com/index.php`> (28 Nov. 2015).

Conceptual Engineering Detail (2013). "Track attachment: Light weight pre-cast concrete plinth support system conceptual details." Sound Transit East Link Project, I-90 Floating Bridge (Details are preliminary).

Derham, C. J. (1986). *Elastomerics* (Jan.).

Dransfield, J. (2012). "Air-entraining admixtures." *Report No. ATS 5*, Cement Admixtures Association, Knowle, West Midlands, UK, <`http://www.admixtures.org.uk/downloads/ATS%205%20Air%20Entraining.pdf`>.

EdilonSedra (2015), <`https://www.edilonsedra.com/`> (28 Nov. 2015).

Gent, A. N. (1964). "Elastic stability of rubber compression springs." *Journal of Mechanical Engineering Science*, 86(3), 86.

Gent, A. N. and Lindley, P. B. (1959). "The compression of bonded rubber blocks." *Institution of Mechanical Engineers Proceedings*, 173, 111–122.

Gent, A. N. and Meinecke, E. A. (1970). "Compression, bending and shear of bonded rubber blocks." *Polymer Engineering and Science*, 10(1), 48–53.

Gent, A. N., Sueyasu, T., and Wang, C. (2001). "Tables of physical constants." *Engineering with Rubber - How to Design Rubber Components*, A. N. Gent, ed., Hanser Publishers, 2nd edition, Chapter Appendix, 358.

Holownia, B. P. (1971). "Compression of bonded rubber blocks." *Journal of Strain Analysis*, 6(2), 121–123.

Holownia, B. P. (1972). "Effect of poisson's ratio on bonded rubber blocks." *Journal of Strain Analysis*, 7(3), 236–242.

Holownia, B. P. (1974). "Effect of carbon black on the elastic constants of elastomers." *Journal of the Institution of the Rubber Industry*, 8(4), 157–160.

Holownia, B. P. (1980). "Effect of different types of carbon black on elastic constants of elastomers." *Plastics and Rubber, Materials and Applications*, 5(3), 129–132.

International Association for the Properties of Water (IAPWS) (2013). *Why does water expand when it freezes?*, <`http://www.iapws.org/faq1/freeze.html`> (28 Nov. 2015).

Kelly, J. M. (1997). *Earthquake Resistant Design with Rubber*. Springer-Verlag, New York, London.

Keys, W. C. (1937)." *Mechanical Engineering*, 59, 345.

Koh, C. G. and Lim, H. L. (2001). "Analytical solution for compression stiffness of bonded rectangular layers." *International Journal of Solids and Structures*, 38, 445–455.

Kosmatka, S. and Panarese, W. C. (1994). *Design and Control of Concrete Mixtures*. Portland Cement Association, Skokie, IL, 13th edition.

Lake, G. J. and Thomas, A. G. (2001). "Strength." *Engineering with Rubber - How to Design Rubber Components*, A. N. Gent, ed., Hanser Publishers, 2nd edition, Chapter 5, 100–137.

Pinarbasi, S. and Akyuz, U. (2004). "Investigation of compressive stiffness of elastomeric bearings." *Sixth International Congress on Advances in Civil Engineering*, Istanbul, Turkey, 694–703 (Oct.).

Salmon Bay Sand and Gravel (2015), <http://www.sbsg.com/> (28 Nov. 2015).

Sheriden, P. M., James, F. O., and Miller, T. S. (2001). "Design of components." *Engineering with Rubber - How to Design Rubber Components*, A. N. Gent, ed., Hanser Publishers, 2nd edition, Chapter 8, 226–232, 249.

Sommer, J. (2013). *Troubleshooting Rubber Problems.* Hanser Publishers, <http://app.knovel.com/hotlink/toc/id:kpTRP00007/troubleshooting-rubber/troubleshooting-rubber>.

Sound Transit (2010). *Track Bridge System and Prototype Project: Phase 1 Design Services Technical Requirements*, <http://www.globaltelematics.com/pitf/I-90railBridgeScopeOfWork.9.10.pdf> (Sept.).

Sound Transit (2013). *Design Criteria Manual (Revision 3)* (Aug.).

Sound Transit (2015). *East Link Project Updates*, <http://www.soundtransit.org/Projects-and-Plans/East-Link-Extension/Project-updates> (28 Nov. 2015).

Stanton, J. and Lund, H. (2015). "Effects of Bulk Compressibility on the Response of Elastomeric Bearings." Unpublished manuscript.

Stanton, J., Thonstad, T., and Sisley, M. (2015). "Bulk Modulus Tests of Corkelast." Unpublished manuscript.

Stanton, J. F. and Roeder, C. W. (1982). "Elastomeric bearings design, construction, and materials." *Report No. NCHRP 248*, Transportation Research Board – National Research Council, Washington, D.C.

Stanton, J. F., Roeder, C. W., Mackenzie-Helnwein, P., White, C., Kuester, C., and Craig, B. (2008). "Rotation limits for elastomeric bearings." *Report No. NCHRP 596*, Transportation Research Board – National Research Council, Washington, D.C.

Stanton, J. F., Scroggins, G., Taylor, A. W., and Roeder, C. W. (1990). "Stability of laminated elastomeric bearings." *Journal of Engineering Mechanics*, American Society of Civil Engineers, 116(6), 1351–1371.

Treloar, L. R. G. (2009). *Physics of Rubber Elasticity*. Oxford University Press, 3rd edition, <http://app.knovel.com/hotlink/toc/id:kpPREE0007/physics-rubber-elasticity/physics-rubber-elasticity>.

Van Engelen, N. and Kelly, J. M. (2014). "Correcting for the influence of bulk compressibility on the design properties of elastomeric bearings." *Journal of Engineering Mechanics*, 141(6).

Yura, J., Kumar, A., Yakut, A., Topkaya, C., Becker, E., and Collingwood, J. (2001). "Elastomeric bridge bearings: Recommended test methods." *Report No. NCHRP 449*, Transportation Research Board – National Research Council, Washington, D.C.

# Appendix A | Mixing and Casting Procedure

The concrete mixing procedure was developed based on ASTM C192 and optimized for the tilting drum mixers in the University of Washington's concrete laboratory. The same procedure was used consistently for all batches and is described below.

First, half of the mixing water was added to coat the bottom of the drum to prevent the paste from sticking to the drum. The mixing water also contained the air entraining agent and normal range water reducer as well as a portion of the high range water reducer. Because the high range water reducer counteracted the air-entraining agent, the remainder of the high range water reducer was added later in the mixing cycle to ensure proper functionality. Second, half of the coarse aggregate and all of the fine aggregate were added. Then the full amount of cement was added, and the mixer was turned on.

Immediately upon starting the mixer, the remainder of the water/admixture combination was poured into the mixer. This method of adding the water after starting the mixer proved to be effective in rinsing any cement off the side of the drum. After ninety seconds, the rest of the coarse aggregate was added. The ninety-second delay provided time for the paste to become fully mixed before coating all of the aggregate, allowing the admixtures to fully spread throughout the paste. After another ninety seconds, a three-minute resting period (mixer off) was observed before a final two-minute mixing period.

If the mixture appeared too dry during the final mixing period, additional high range water reducer was added, and the mixture was allowed to mix for a minimum of one additional minute. Finally, the mixture was poured from the drum into a wheelbarrow and briefly hand

mixed to ensure consistency. Slump, air content and fresh unit weight tests were performed, and cylinders were cast in oiled, steel molds.

Two hours after mixing, the cylinders were leveled off and placed (covered) in a heated chamber set to approximately 130 degrees Fahrenheit, modeling curing conditions at a local precast plant. After 18 hours, the specimens were removed from heat, de-molded and stored in a moist (fog) room at 73 degrees Fahrenheit until tested. Before being placed in the fog room, the cylinders intended for compression or elastic modulus testing were capped with a sulfur-based capping compound.

# Appendix B | Tension Specimen Results

Table B-1 contains the results for each tension test as well as a description of the distinguishing characteristics of each specimen (i.e. elastomer type/thickness, drying method, etc.). The maximum load was displayed on the test apparatus in kN and was converted to psi using a core diameter of 2.25 inches ($A = 3.98$ in$^2$) and a metric conversion factor of 224.8089 lb/kN.

SS-2b, SS-3b and SS-4b are marked with an asterisk (*). This is because specimens SS-2, SS-3 and SS-4 experienced such clean breaks after their first tests, exposing the lightweight concrete surface, that they were re-primed and tested again. The letter 'b' is attached to indicate the results of the second test.

As part of a quality control procedure, a precision adhesion test (P.A.T. test) was conducted on a few specimen to test the bond of the U90WB primer. Most specimens were not measured (NM), but the P.A.T. test results for those tested are included in the table, displayed in psi (145.0377 psi/MPa) for easy comparison with tension strength results.

**Table B-1.** Test Results for Individual Tension Specimens

| Specimen | Elastomer Type | Batch | Elastomer Thickness | Drying Method | Max Stress | Break Description | P.A.T. Test Result |
|---|---|---|---|---|---|---|---|
| SLF-1 | Editaan 70U | A | 1.0 in | Air-Dry | 231.8 psi | Editaan and Lightweight Aggregate | NM |
| SLF-2 | Editaan 70U | A | 1.0 in | Air-Dry | 294.0 psi | Editaan (near DexG) | NM |
| SLF-4 | Editaan 70U | A | 1.0 in | Air-Dry | 248.8 psi | LWC (near elastomer) | NM |
| SLF-5 | Editaan 70U | A | 1.0 in | Air-Dry | 231.8 psi | Not Recorded | NM |
| SLF-11 | Editaan 70U | A | 1.0 in | Pressurized Air | 220.5 psi | Not Recorded | NM |
| SLF-13 | Editaan 70U | A | 1.0 in | Pressurized Air | 214.9 psi | Mostly Editaan, some LWC | NM |
| SLF-15 | Editaan 70U | A | 1.0 in | Pressurized Air | 226.2 psi | Editaan, LWC and U90WB/Editaan bond | NM |
| SLF-16 | Editaan 70U | A | 1.0 in | Pressurized Air | 220.5 psi | Editaan, some LWC | NM |
| SLF-17 | Editaan 70U | A | 1.0 in | Pressurized Air | 265.7 psi | Editaan and LWC | NM |
| SS-1 | Corkelast VA60 | B | 1.0 in | Air-Dry | 73.5 psi | Corkelast/Deflection Limit | NM |
| SS-2 | Corkelast VA60 | B | 1.0 in | Air-Dry | 107.4 psi | U90WB/LWC bond | NM |

*Continued on the next page...*

**Table B-1 (continued).** Test Results for Individual Tension Specimens

| Specimen | Elastomer Type | Batch | Elastomer Thickness | Drying Method | Max Stress | Break Description | PAT Test Result |
|---|---|---|---|---|---|---|---|
| SS-3 | Corkelast VA60 | B | 1.0 in | Air-Dry | 96.1 psi | U90WB/LWC bond | NM |
| SS-4 | Corkelast VA60 | B | 1.0 in | Air-Dry | 45.2 psi | U90WB/LWC bond | NM |
| SS-5 | Corkelast VA60 | B | 1.0 in | Pressurized Air | 130.0 psi | Corkelast/Deflection Limit | NM |
| SS-6 | Corkelast VA60 | B | 1.0 in | Pressurized Air | 107.4 psi | Corkelast/Deflection Limit | NM |
| SL1-1 | Corkelast VA60 | C | 0.5 in | Pressurized Air | 67.8 psi | No apparent cracking; load increased until Deflection Limit | 812 psi |
| SL1-2 | Corkelast VA60 | C | 0.5 in | Pressurized Air | 147.0 psi | Deflection Limit | NM |
| SL1-3 | Corkelast VA60 | C | 0.5 in | Pressurized Air | 147.0 psi | Small crack starting to form at Corkelast/U90WB bond | 754 psi |
| SL1-4 | Corkelast VA60 | C | 0.5 in | Pressurized Air | 147.0 psi | Corkelast/LWC bond: (Corkelast/U90WB or LWC/U90WB) | NM |
| SL1-5 | Corkelast VA60 | C | 0.5 in | Pressurized Air | 79.2 psi | Corkelast/U90WB bond | 914 psi |
| SL1-6 | Corkelast VA60 | C | 1.0 in | Pressurized Air | 118.7 psi | Deflection Limit | NM |

*Continued on the next page...*

**Table B-1 (continued).** Test Results for Individual Tension Specimens

| Specimen | Elastomer Type | Batch | Elastomer Thickness | Drying Method | Max Stress | Break Description | PAT Test Result |
|---|---|---|---|---|---|---|---|
| SL1-7 | Corkelast VA60 | C | 1.0 in | Pressurized Air | 73.5 psi | Corkelast/U90WB bond | 928 psi |
| SL1-8 | Corkelast VA60 | C | 1.0 in | Pressurized Air | 84.8 psi | Corkelast | NM |
| SL1-9 | Corkelast VA60 | C | 1.0 in | Pressurized Air | 67.8 psi | Corkelast/U90WB bond | 1,015 psi |
| SS-2b* | Corkelast VA60 | C | 1.0 in | Pressurized Air | 107.4 psi | Deflection Limit | NM |
| SS-3b* | Corkelast VA60 | C | 1.0 in | Pressurized Air | 67.8 psi | Corkelast/U90WB bond | 885 psi |
| SS-4b* | Corkelast VA60 | C | 1.0 in | Pressurized Air | 113.1 psi | Corkelast/U90WB bond | 725 psi |

# Appendix C | Compression Specimen Results

Each compression specimen underwent two loading runs (except for specimen C-3 that was only loaded once). The results discussed in Chapter 6 were from the second loading run, and the analysis in Chapter 7 was also based on that run. The first loading run was performed for preconditioning purposes.

For completeness, Figure C-1 shows the typical comparison between the first and second runs. It can be seen that the stress-strain responses for each run are almost exactly the same. The lack of difference between loading runs suggests there was no re-loading effect. Thus it was reasonable to use the data from the only C-3 run in the absence of the second C-3 loading run.

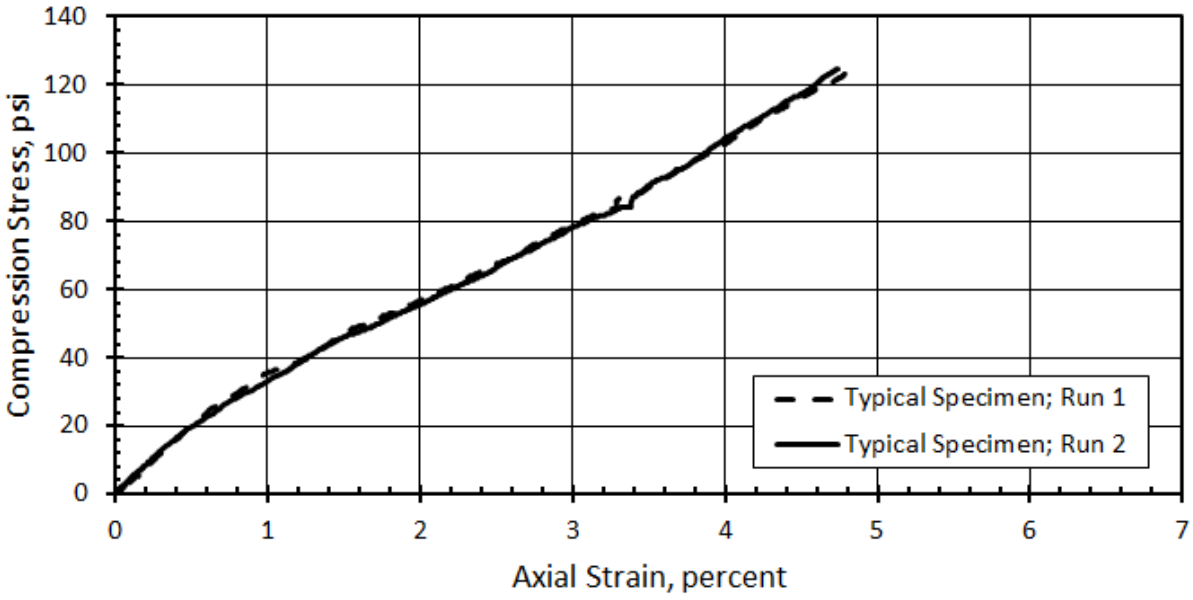


**Figure C-1.** Typical Comparison Between First and Second Compressive Loading Runs

# Appendix D | Shear Specimen Results

The following figures show the stress-strain responses of each individual shear specimen after preconditioning. As discussed in Section 5.3.2, the deformation was measured by two methods. First, an extensometer was placed on the double shear apparatus and specimen centerpiece. This is considered to be an accurate measurement of the average shear deformation of the two elastomer layers. However, the limited deformation capacity of the extensometer required that it was removed before the end of the test to protect the equipment. The shear moduli used for comparison and analysis were calculated from the extensometer data. The second method of measuring deformation was the internal position of the loading head. The precision of this method was just as high as the extensometer, but the position head measurement included mechanical seating and other unwanted deformation. So the position head measurement was used only to capture the picture of the entire stress-strain curve through failure.

In the following figures, the stress-strain curve calculated using the extensometer data is displayed as a dashed line. The curve calculated using the position head measurement is displayed as a solid line.

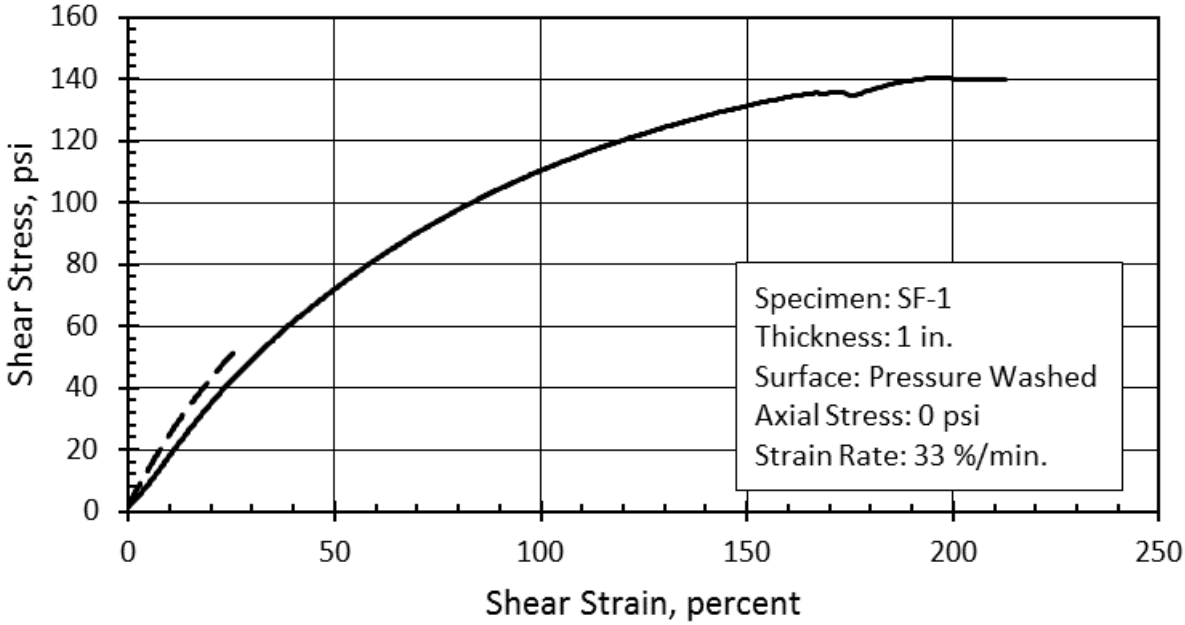


**Figure D-1.** Shear Response of Specimen SF-1

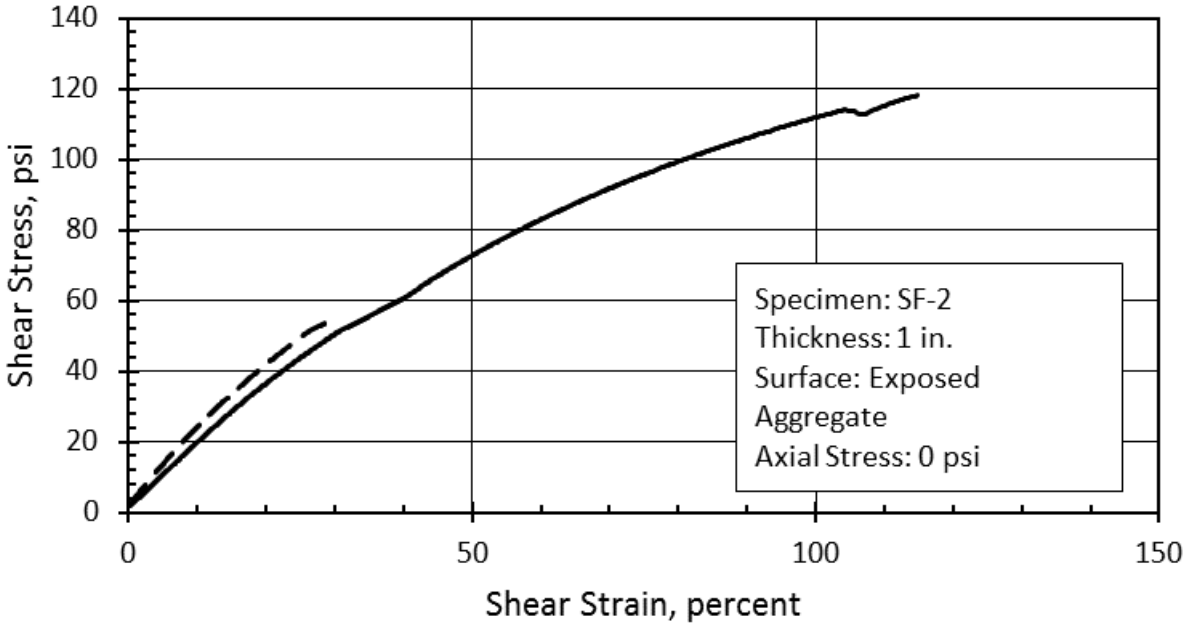


**Figure D-2.** Shear Response of Specimen SF-2

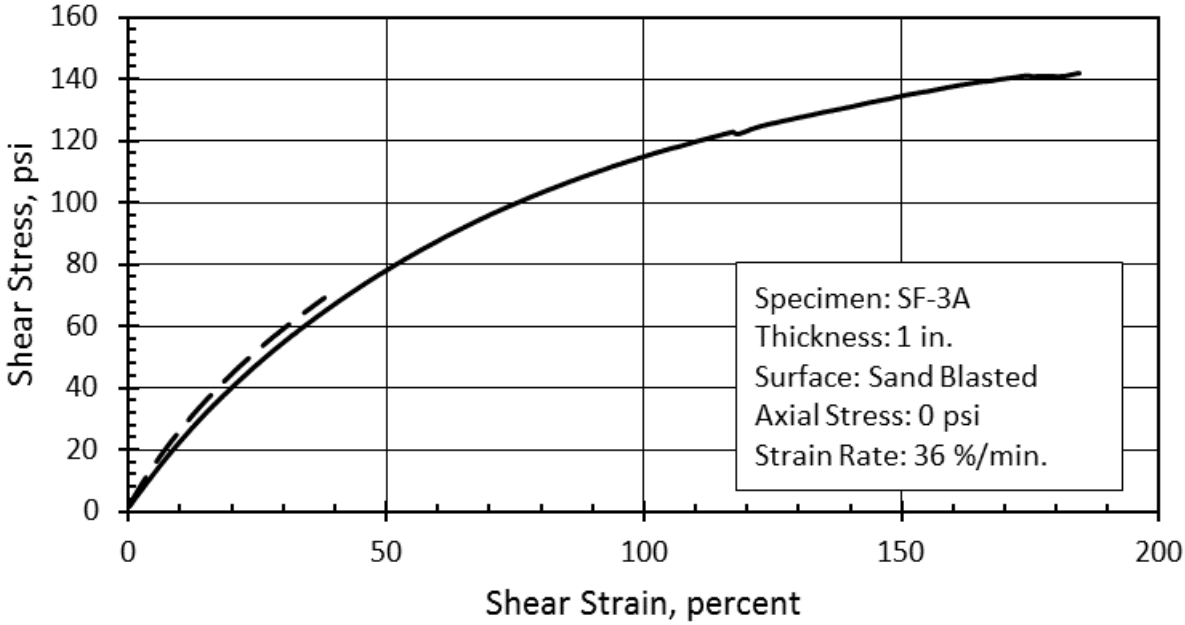


**Figure D-3.** Shear Response of Specimen SF-3

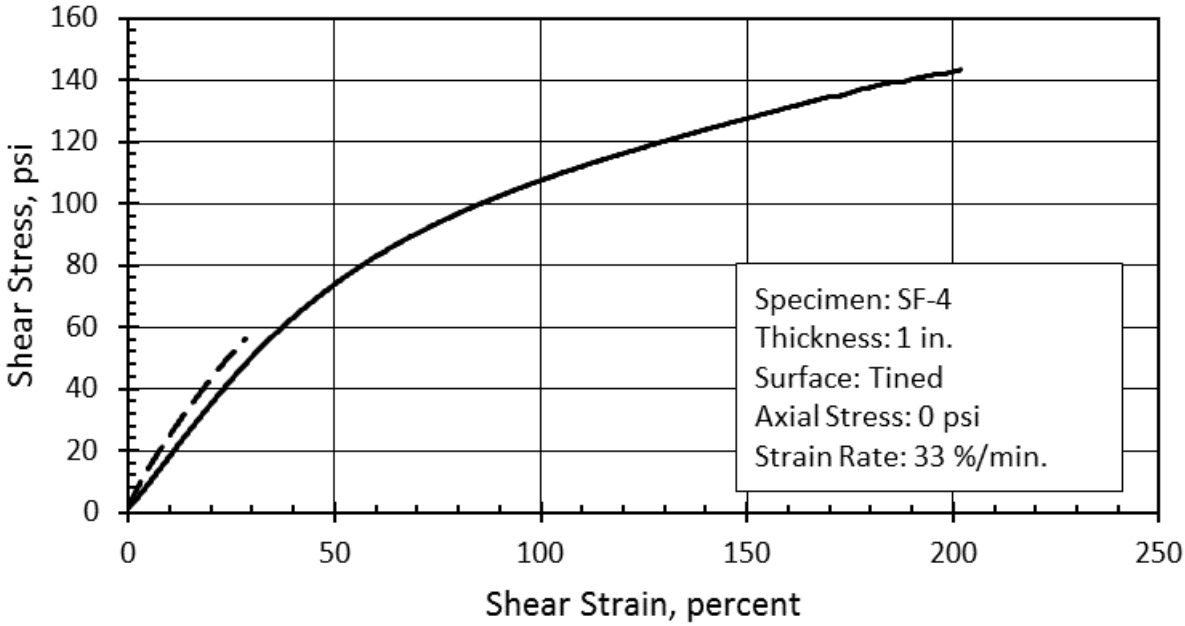


**Figure D-4.** Shear Response of Specimen SF-4

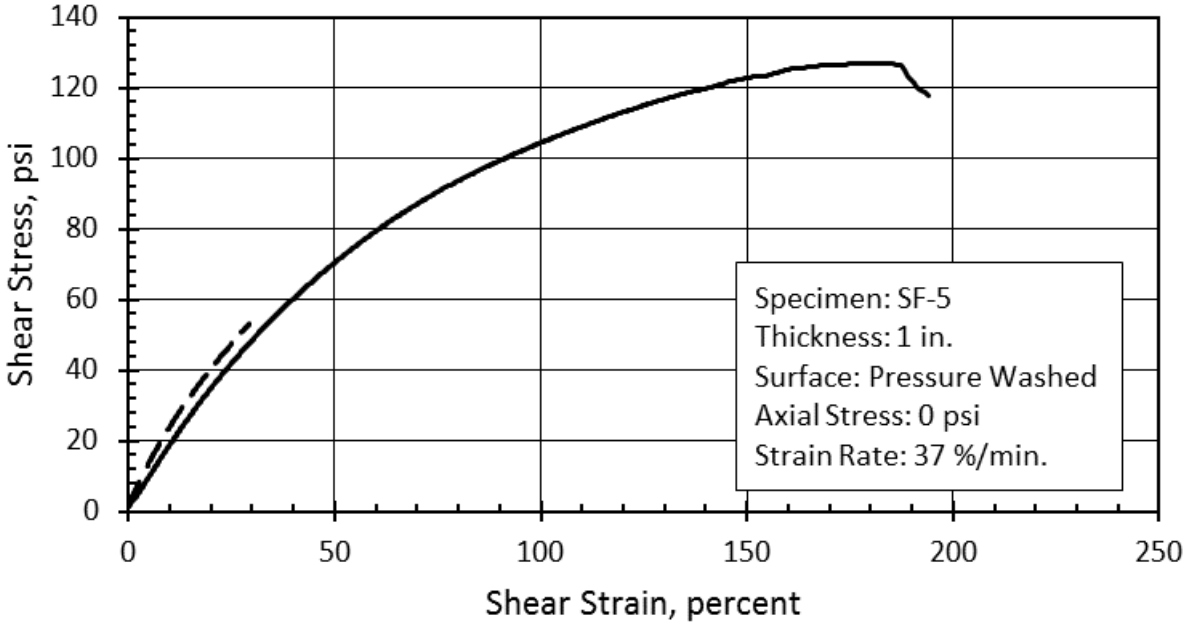


**Figure D-5.** Shear Response of Specimen SF-5

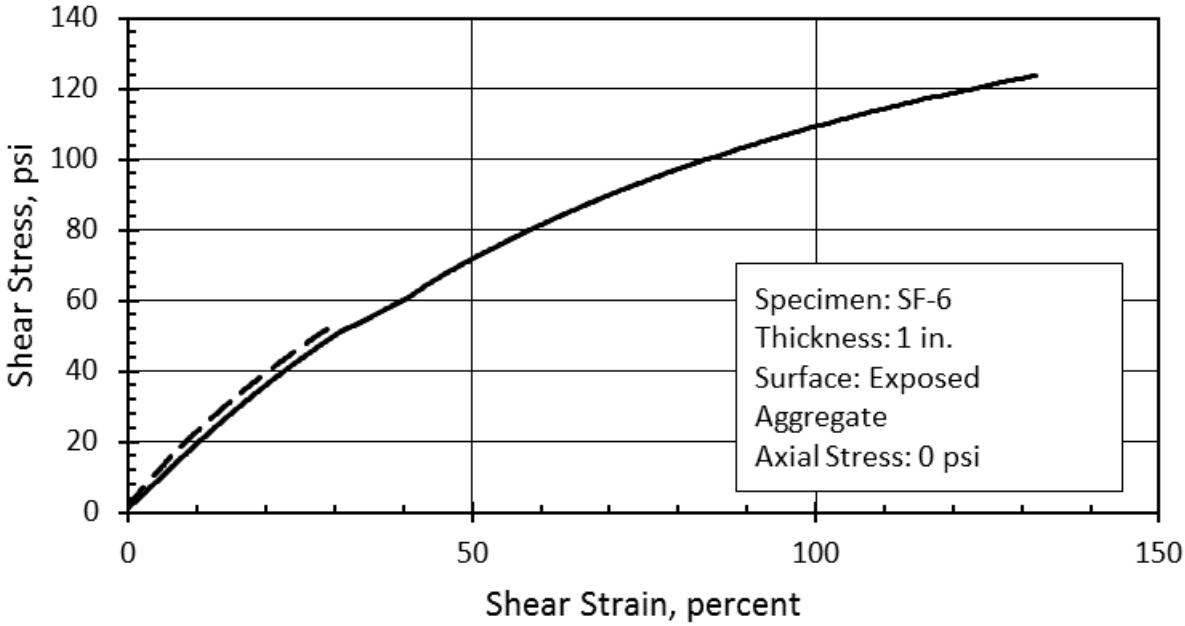


**Figure D-6.** Shear Response of Specimen SF-6

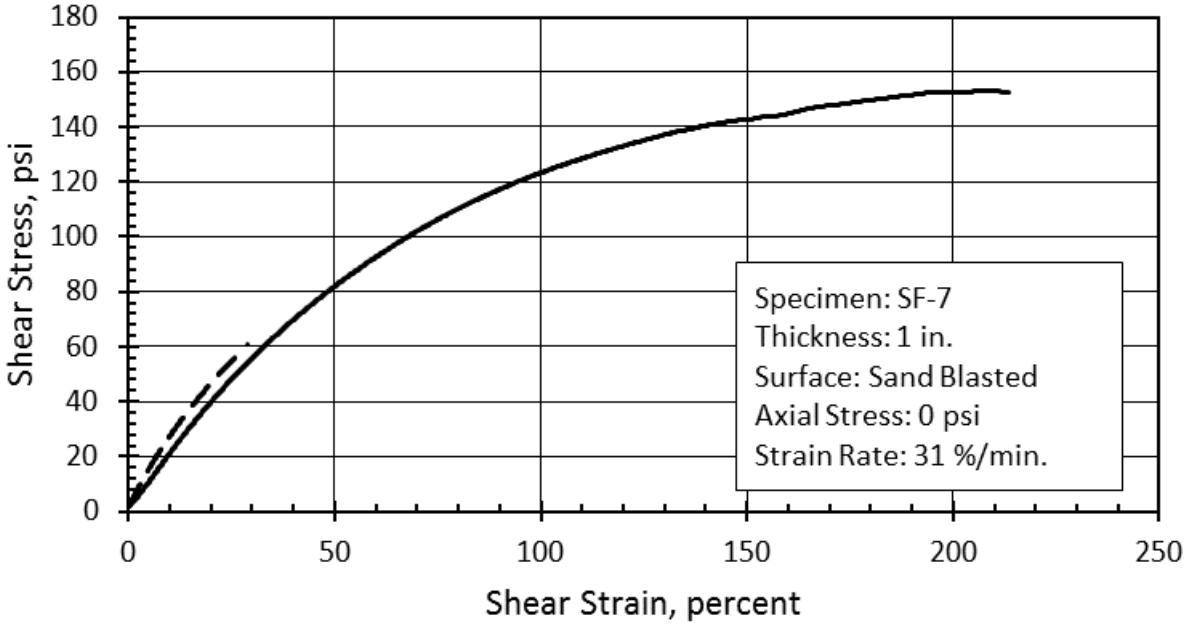


**Figure D-7.** Shear Response of Specimen SF-7

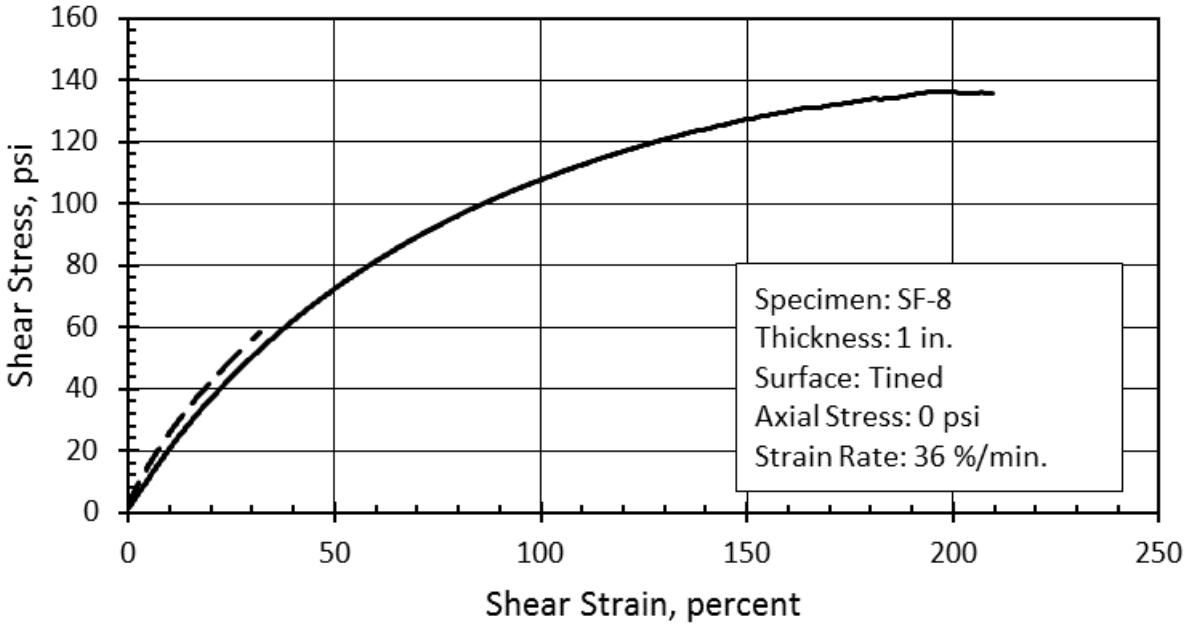


**Figure D-8.** Shear Response of Specimen SF-8

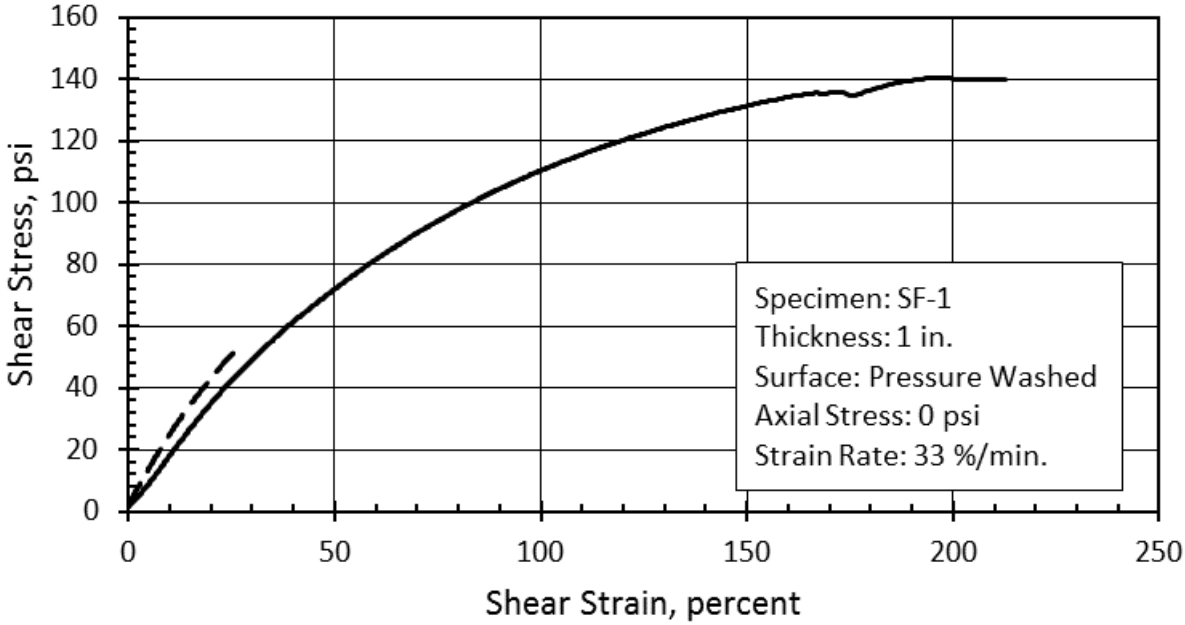


**Figure D-9.** Shear Response of Specimen SF-1

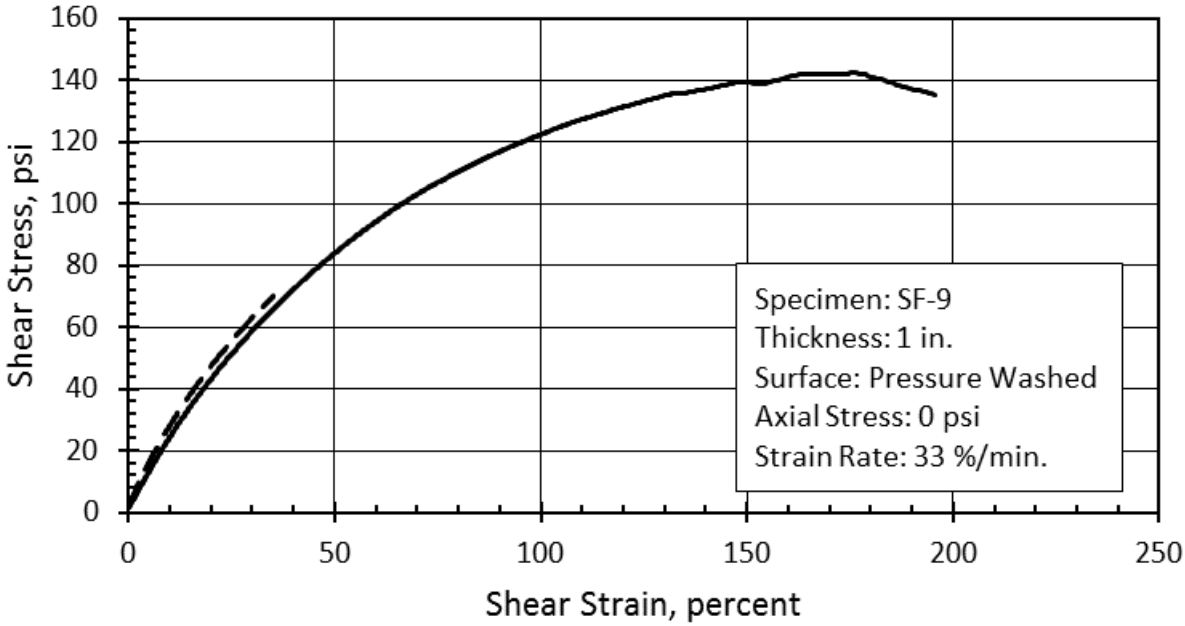


**Figure D-10.** Shear Response of Specimen SF-9

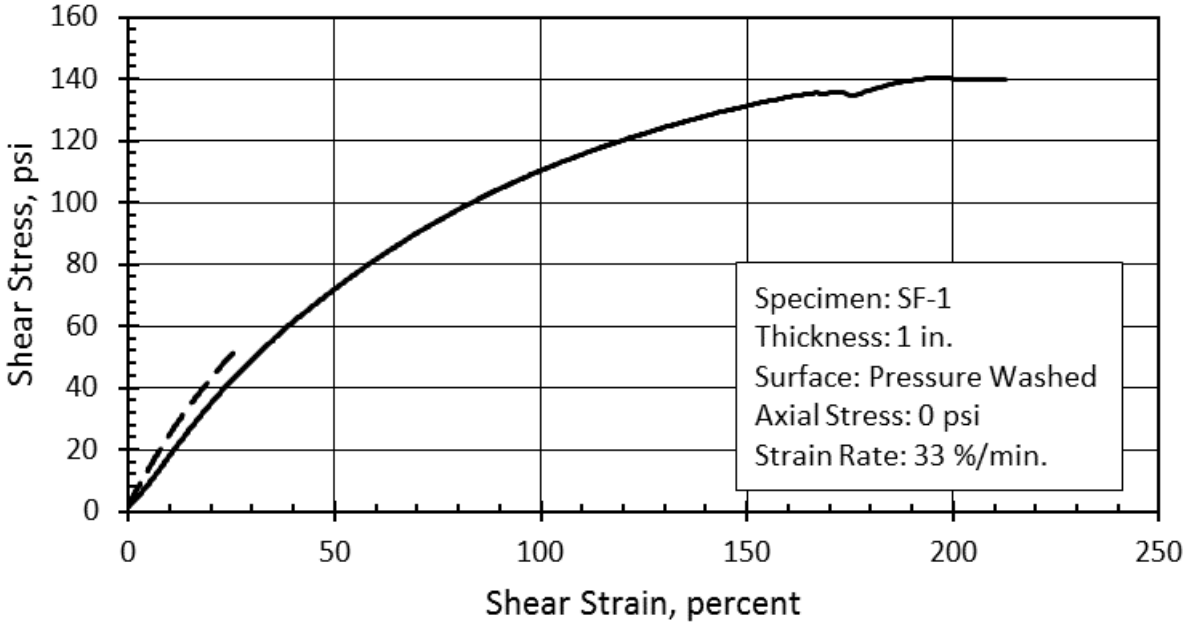


**Figure D-11.** Shear Response of Specimen SF-1

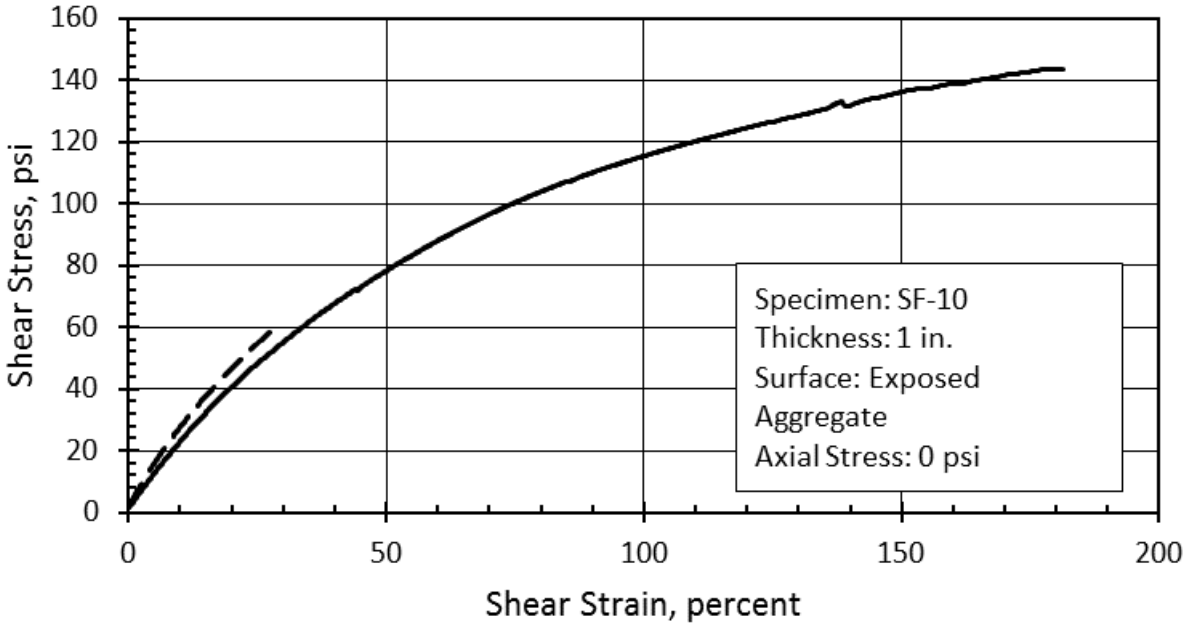


**Figure D-12.** Shear Response of Specimen SF-10

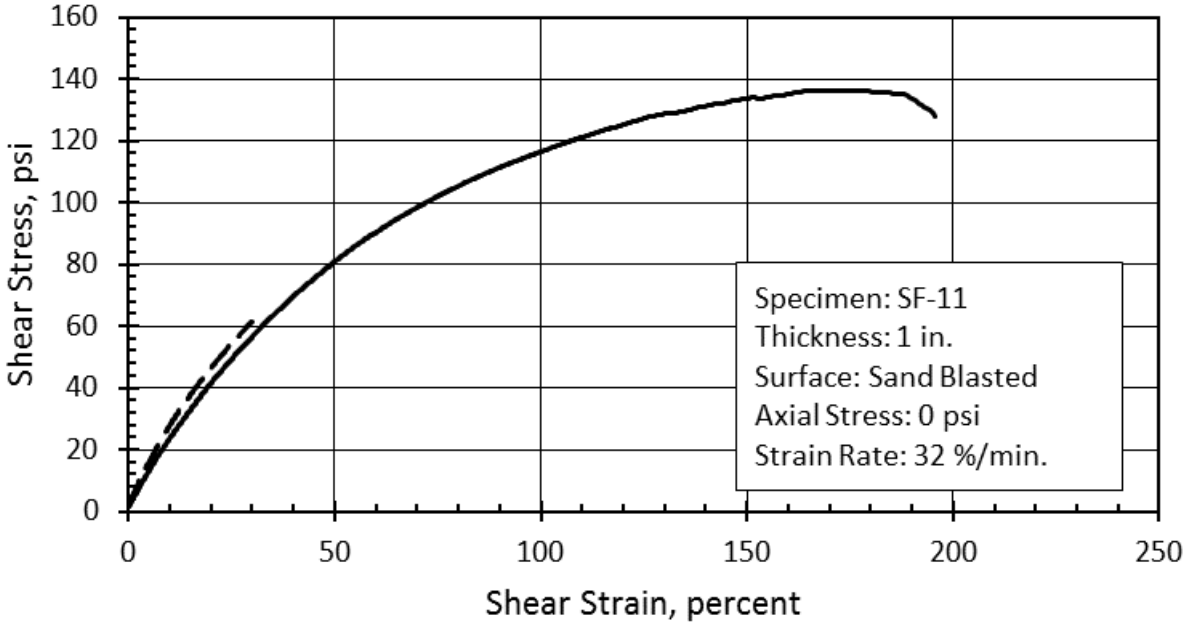


**Figure D-13.** Shear Response of Specimen SF-11

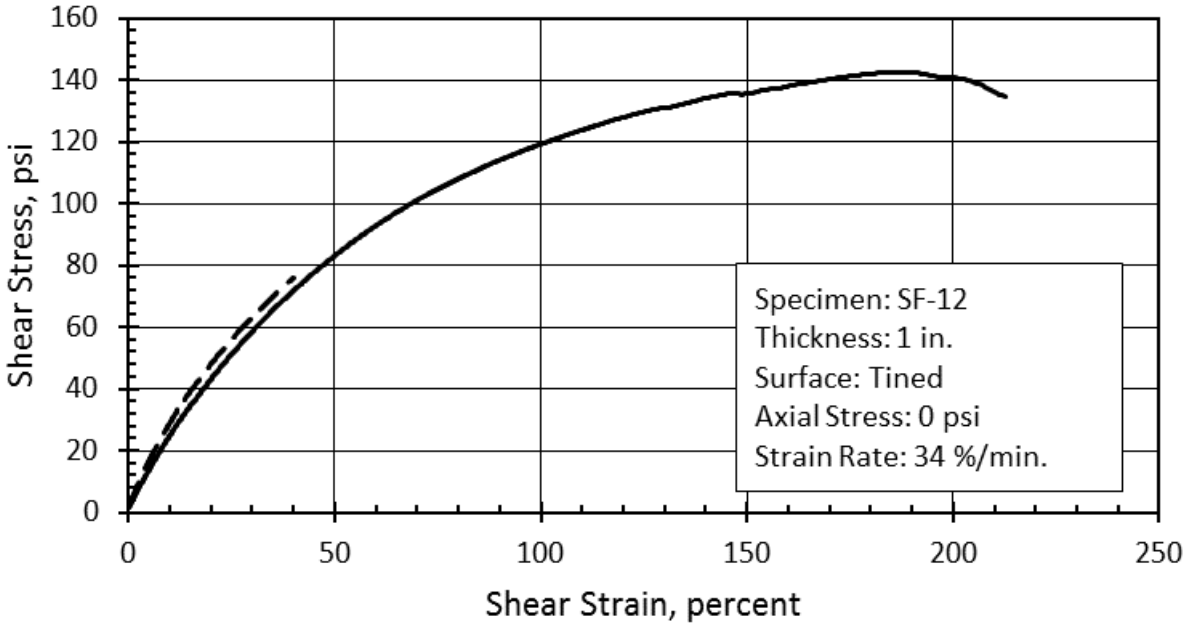


**Figure D-14.** Shear Response of Specimen SF-12

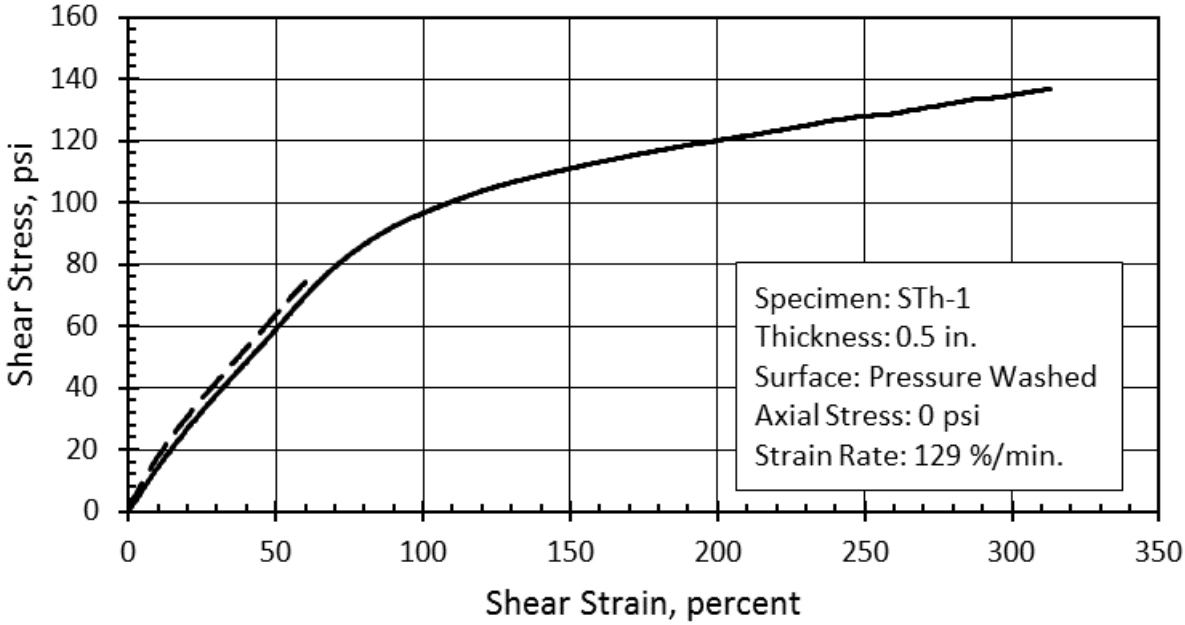


**Figure D-15.** Shear Response of Specimen STh-1

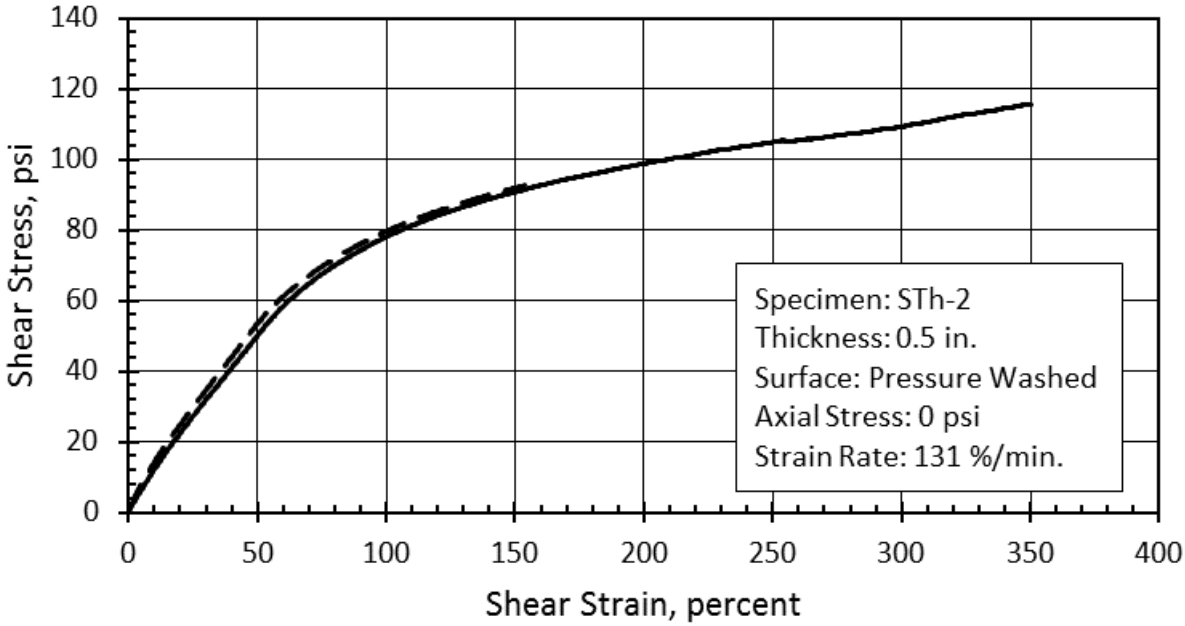


**Figure D-16.** Shear Response of Specimen STh-2

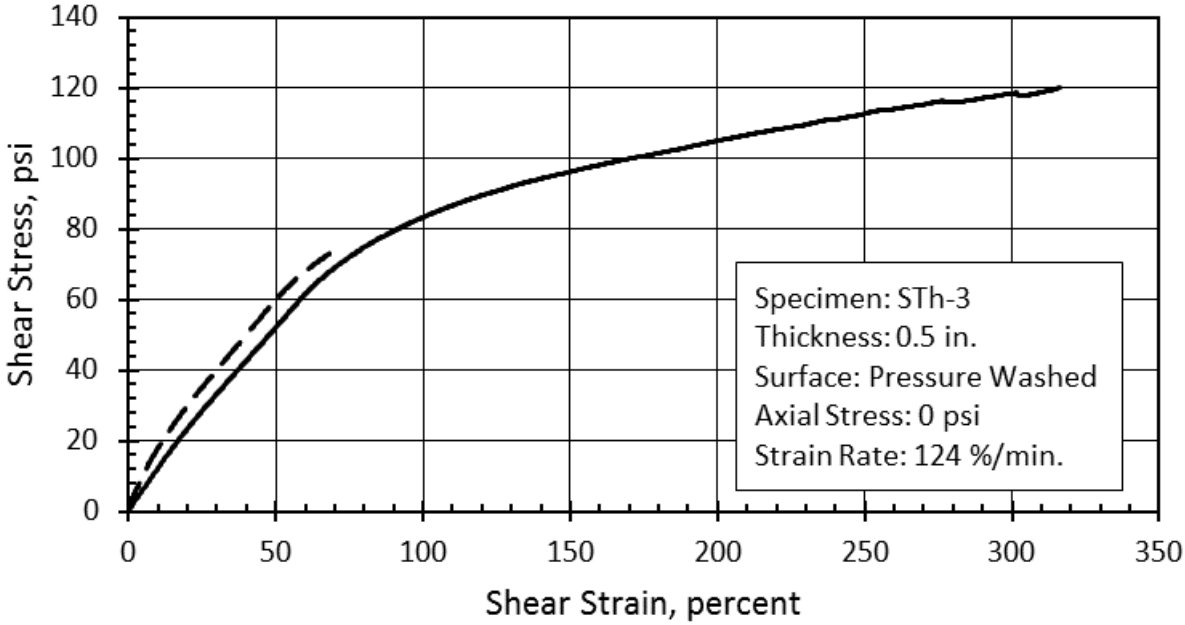


**Figure D-17.** Shear Response of Specimen STh-3

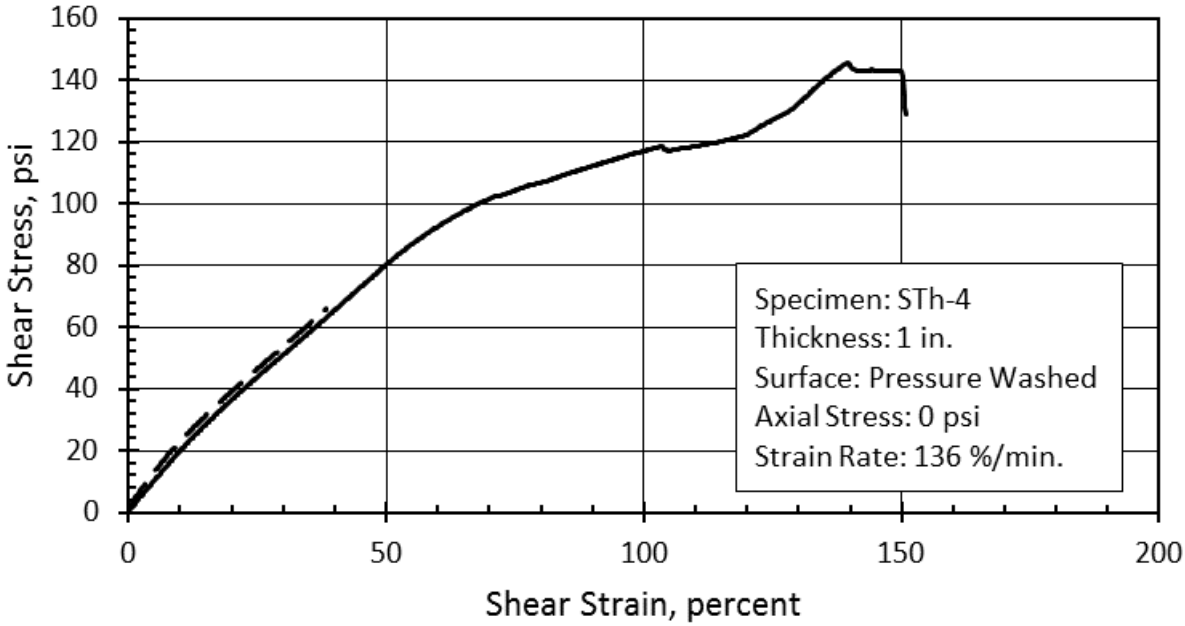


**Figure D-18.** Shear Response of Specimen STh-4

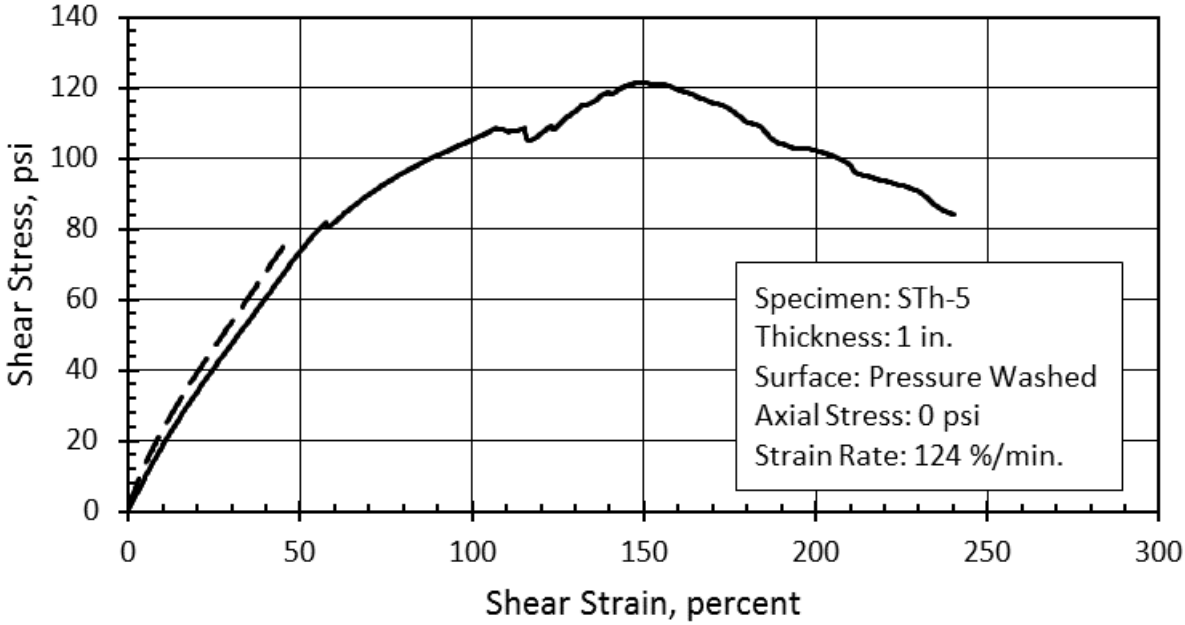


**Figure D-19.** Shear Response of Specimen STh-5

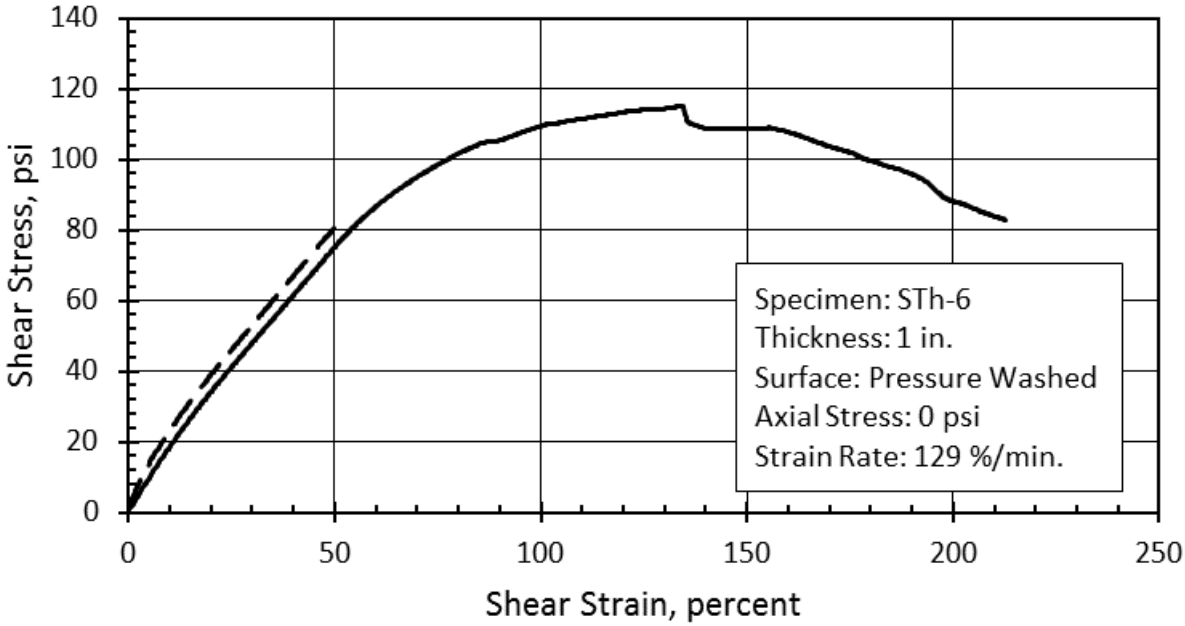


**Figure D-20.** Shear Response of Specimen STh-6

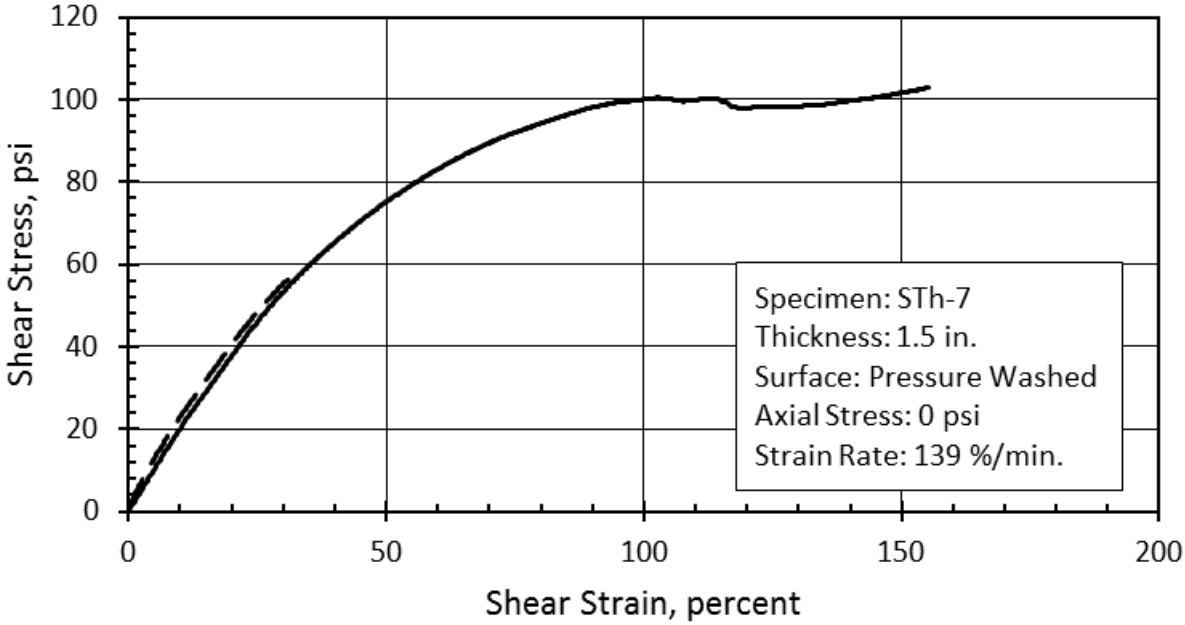


**Figure D-21.** Shear Response of Specimen STh-7

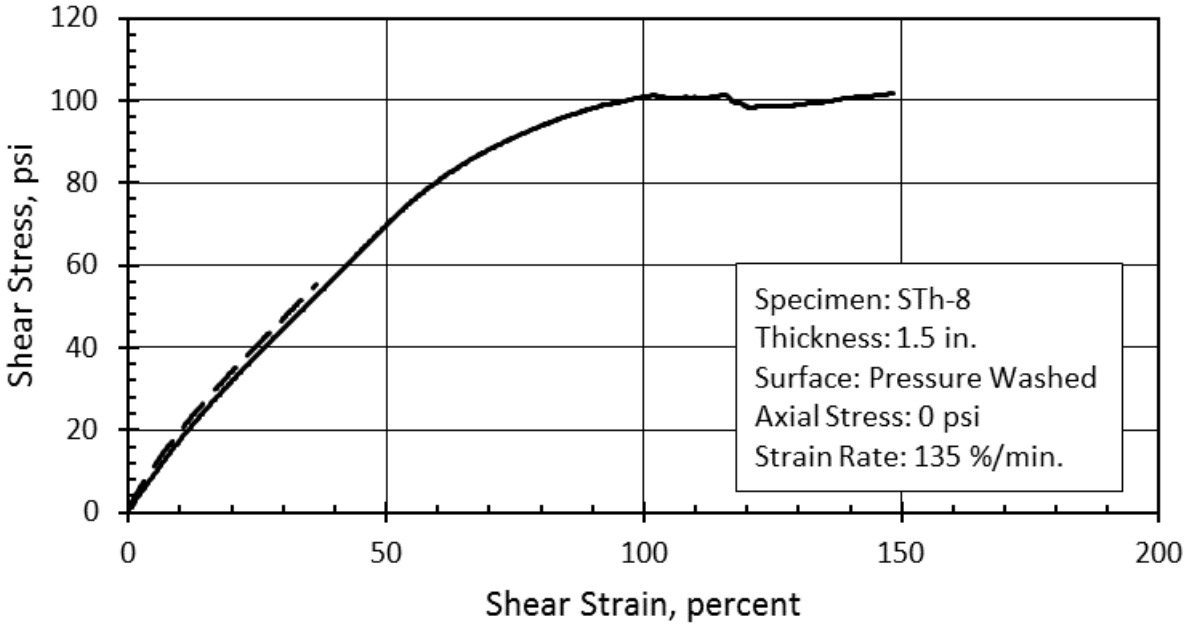


**Figure D-22.** Shear Response of Specimen STh-8

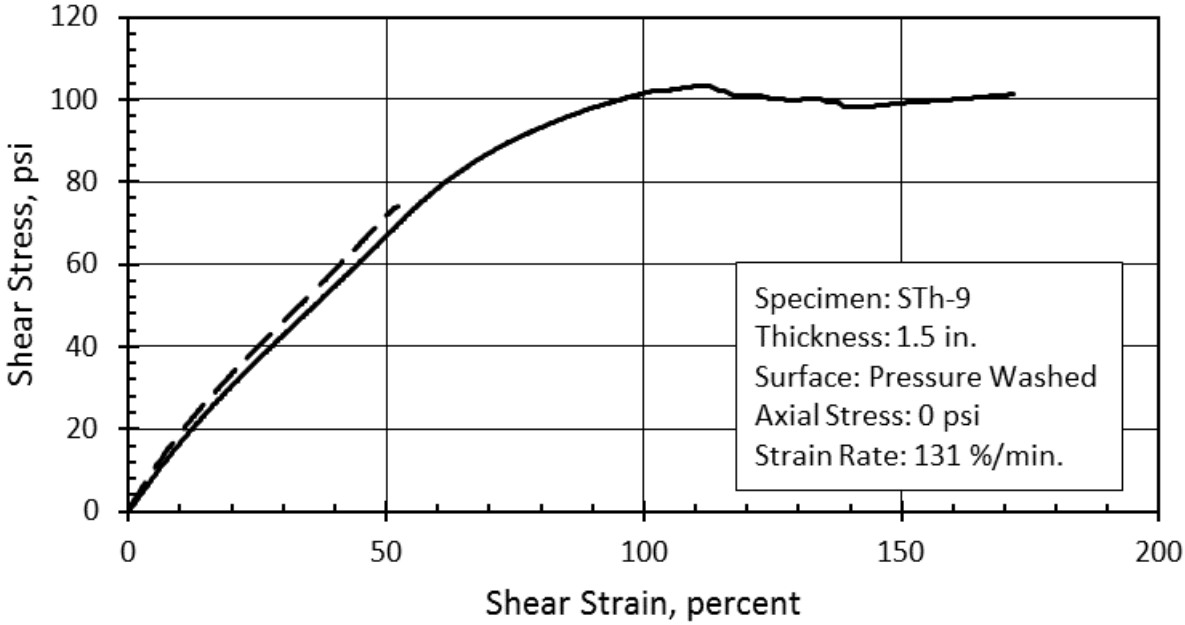


**Figure D-23.** Shear Response of Specimen STh-9

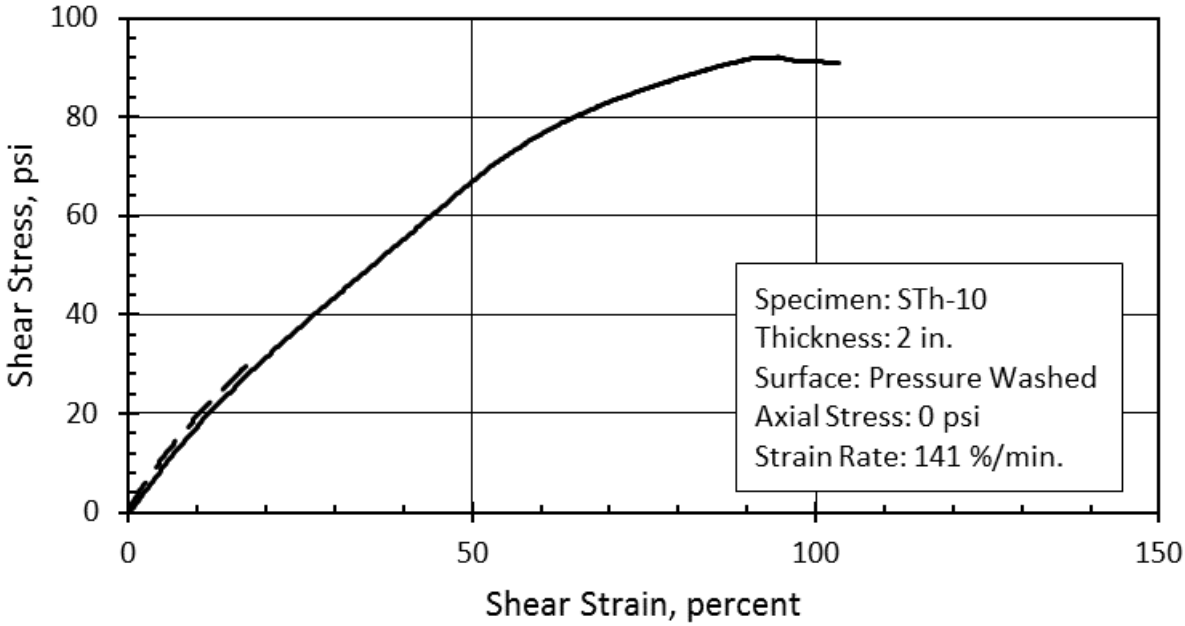


**Figure D-24.** Shear Response of Specimen STh-10

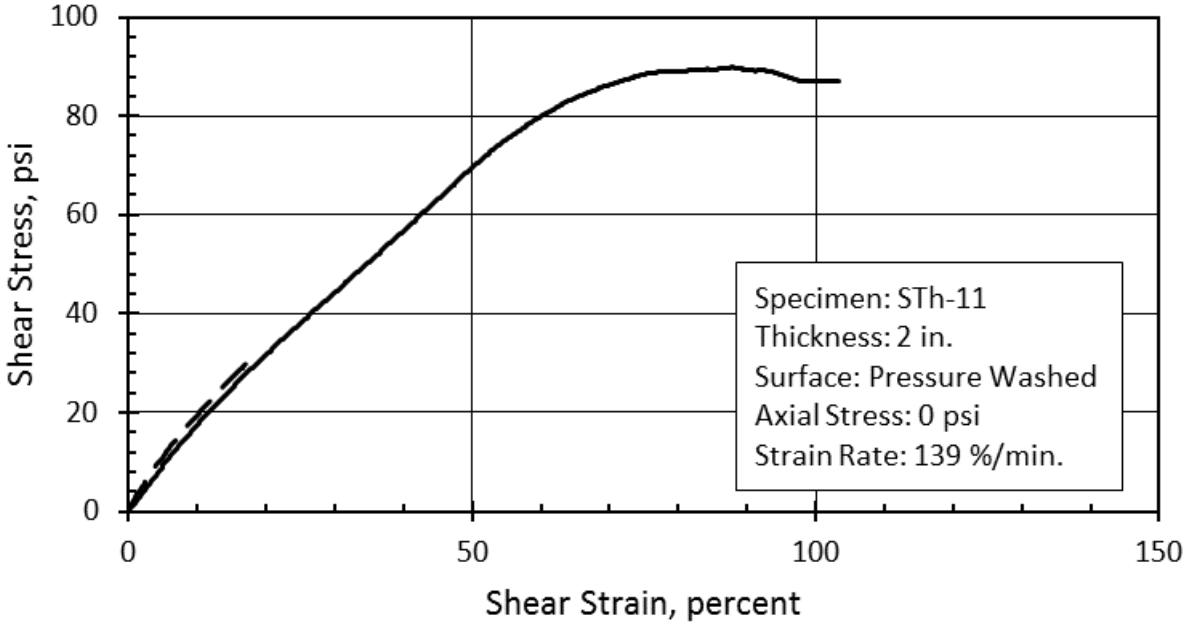


**Figure D-25.** Shear Response of Specimen STh-11

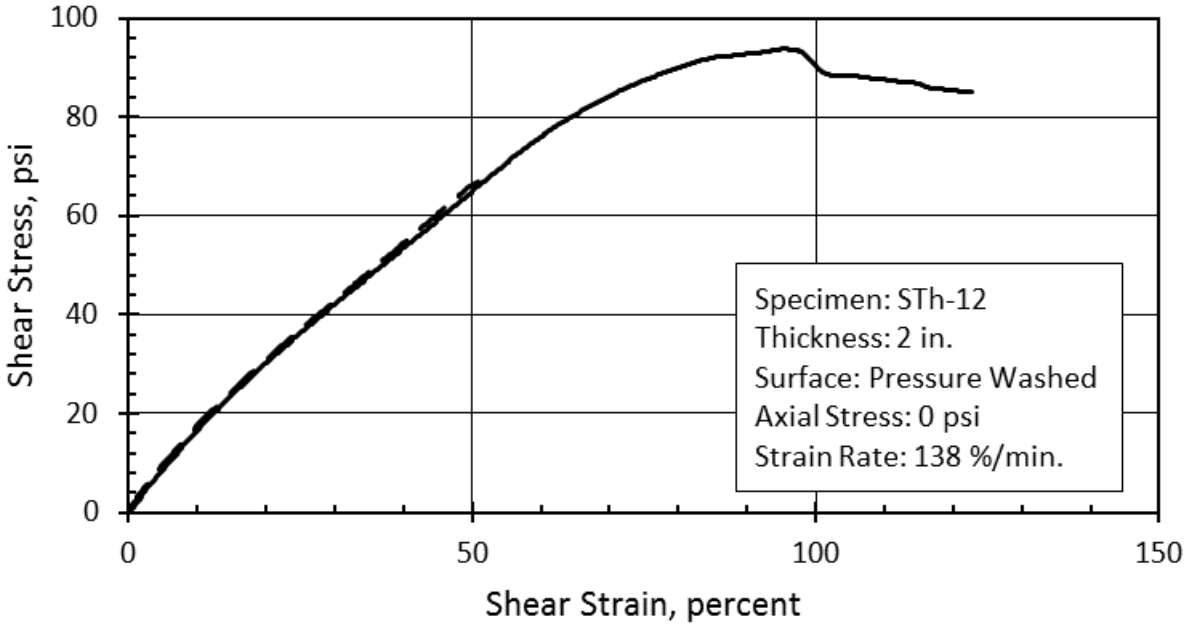


**Figure D-26.** Shear Response of Specimen STh-12

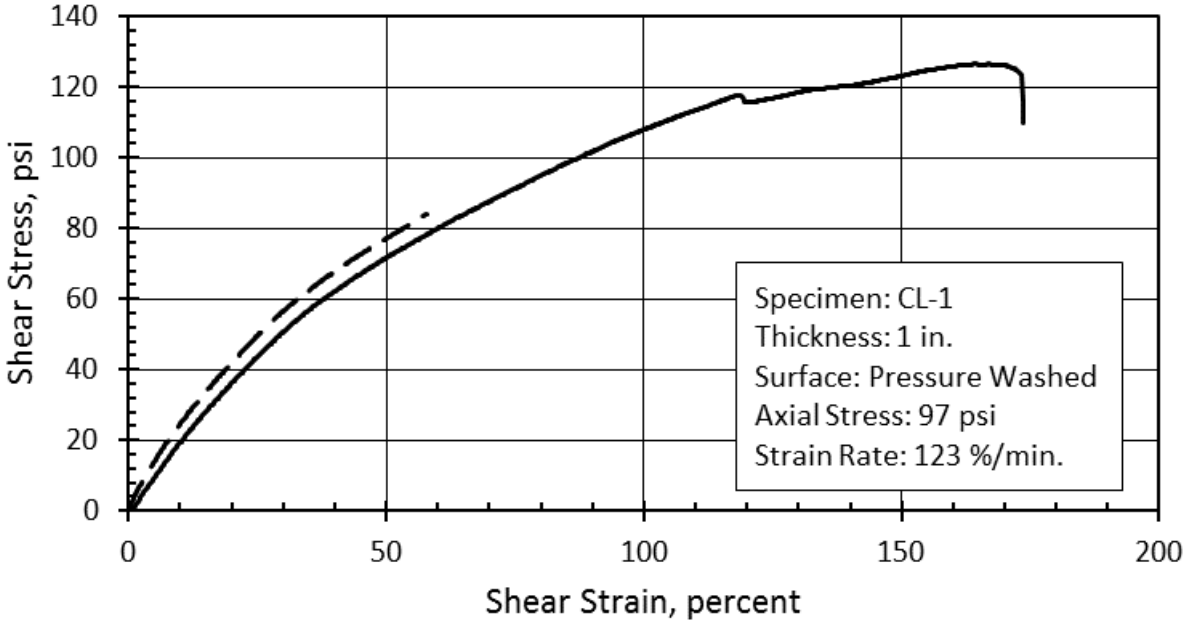


**Figure D-27.** Shear Response of Specimen CL-1

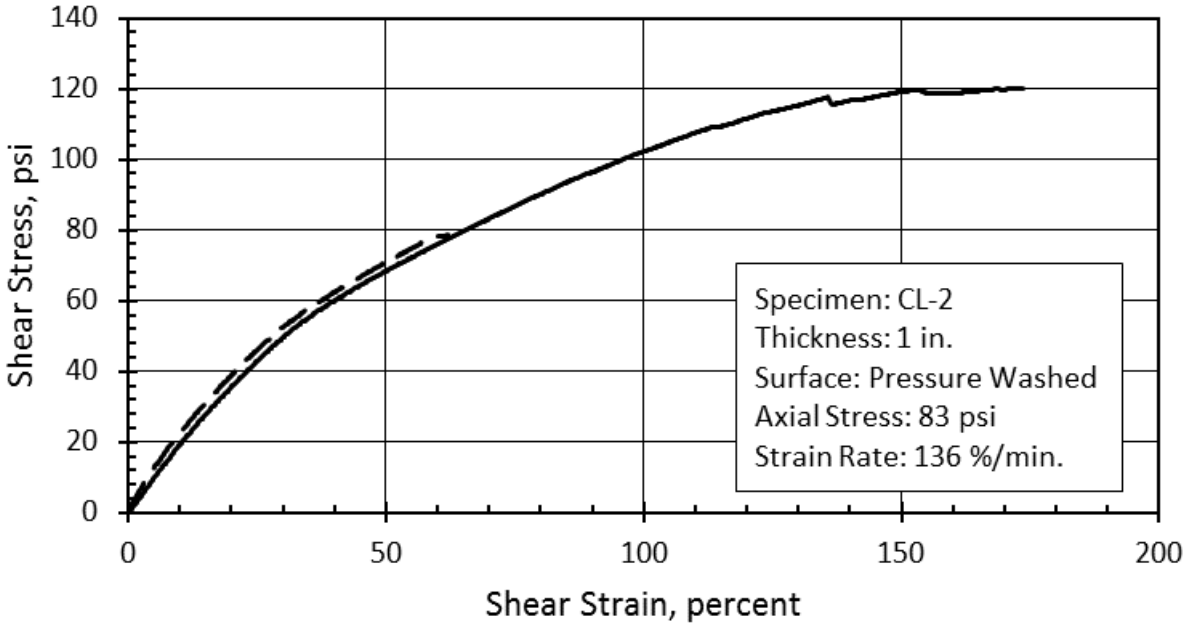


**Figure D-28.** Shear Response of Specimen CL-2

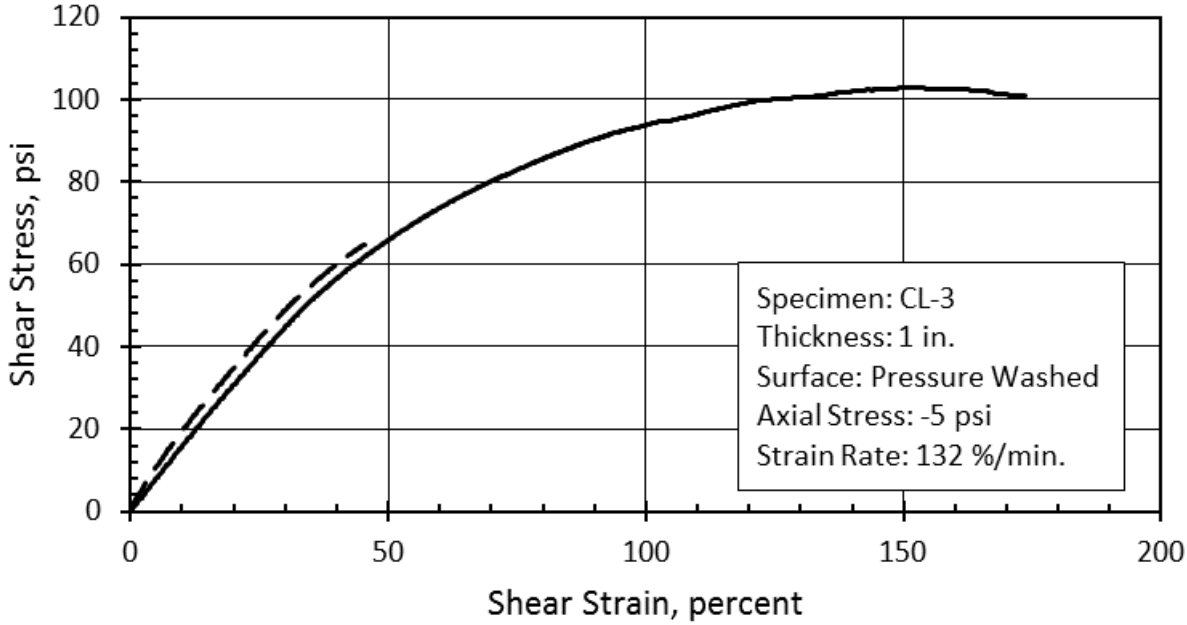


**Figure D-29.** Shear Response of Specimen CL-3

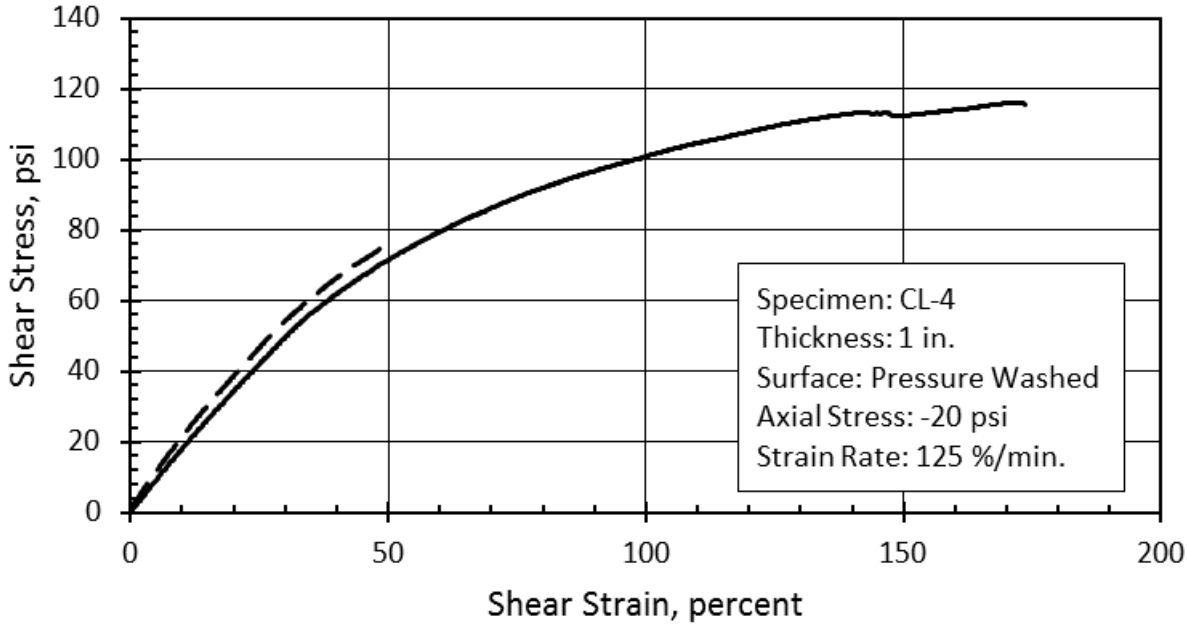


**Figure D-30.** Shear Response of Specimen CL-4

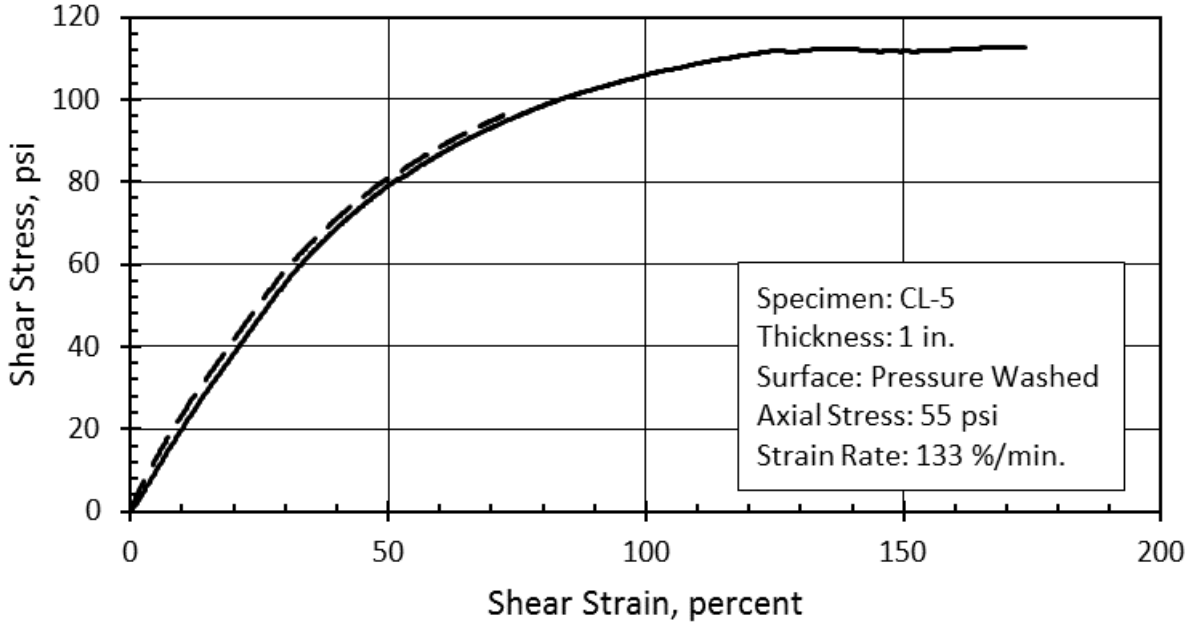


**Figure D-31.** Shear Response of Specimen CL-5

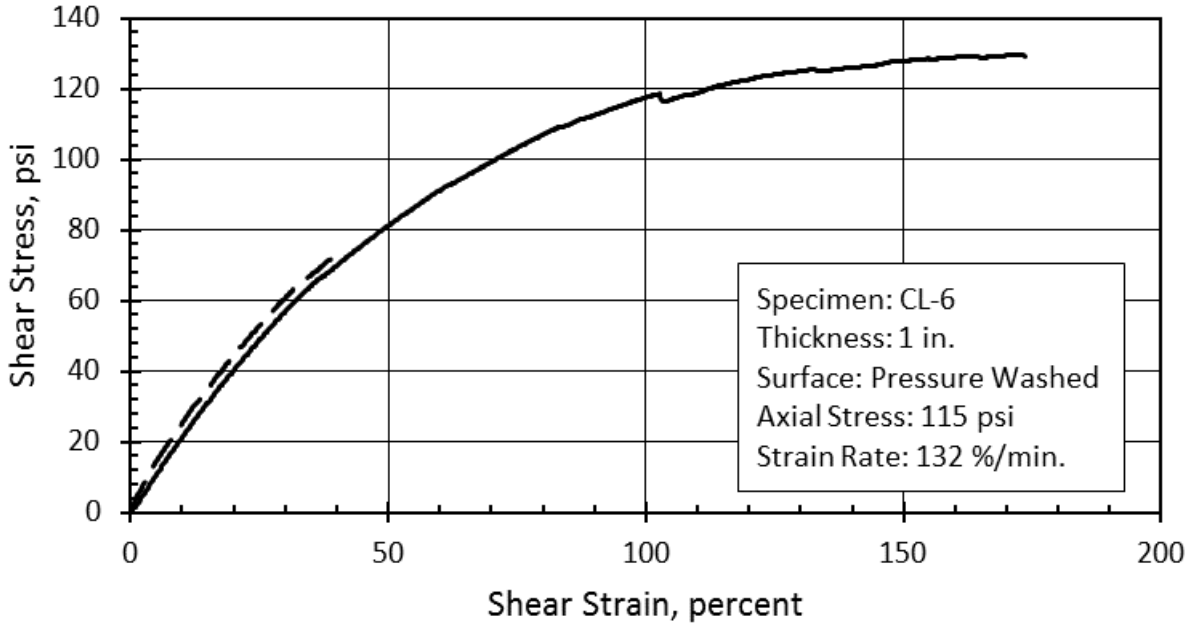


**Figure D-32.** Shear Response of Specimen CL-6

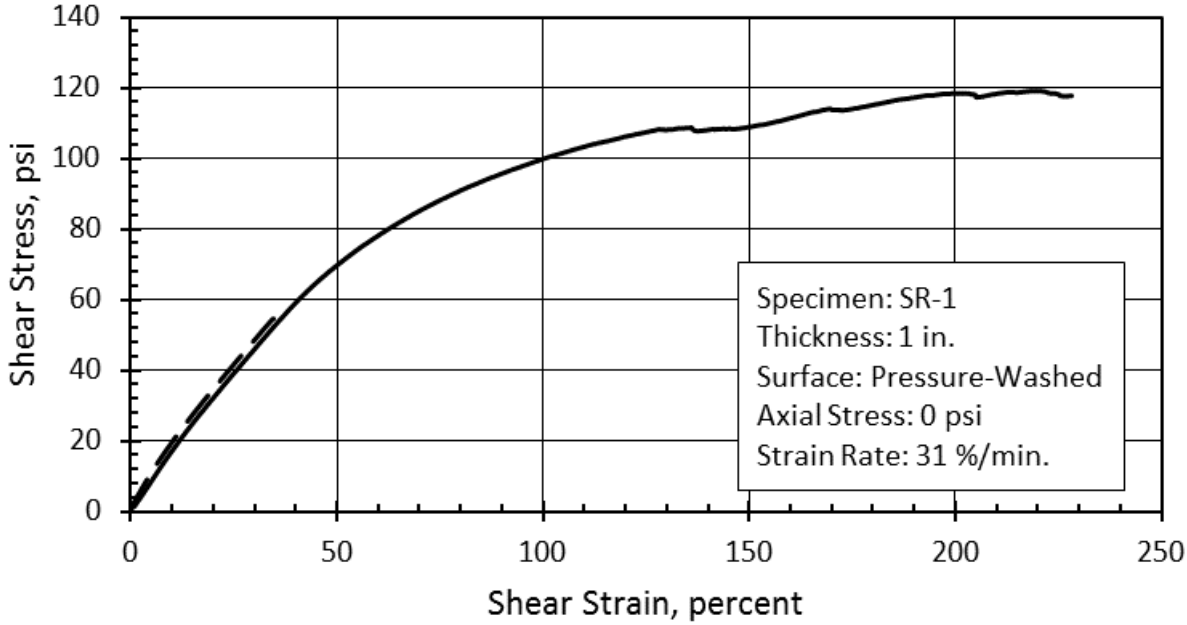


**Figure D-33.** Shear Response of Specimen SR-1

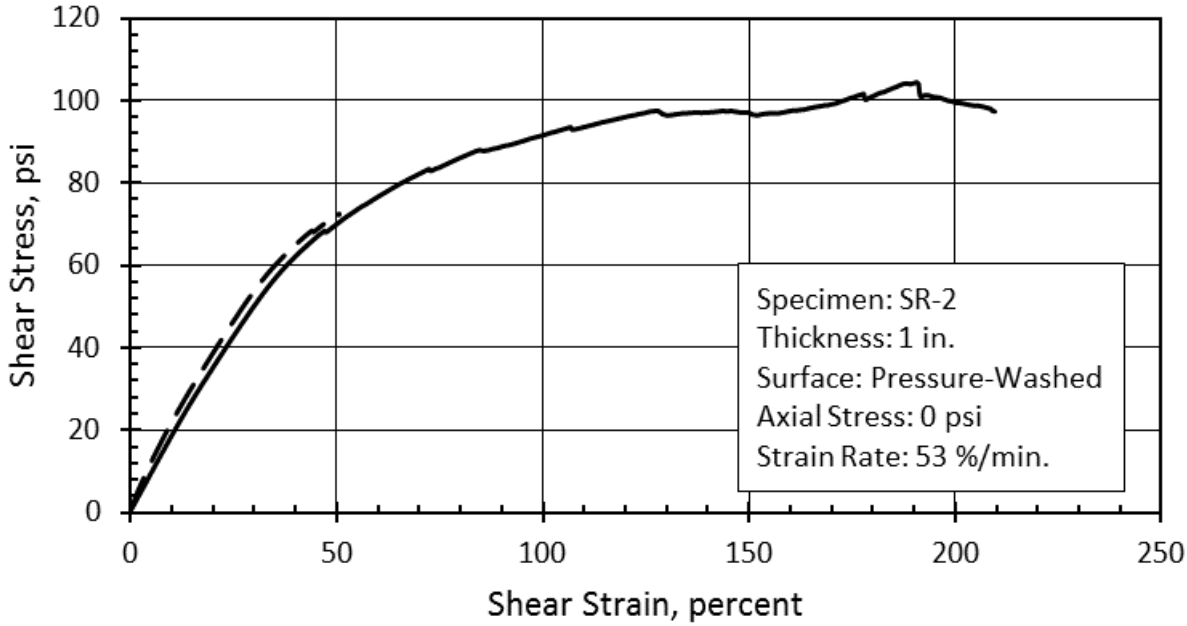


**Figure D-34.** Shear Response of Specimen SR-2

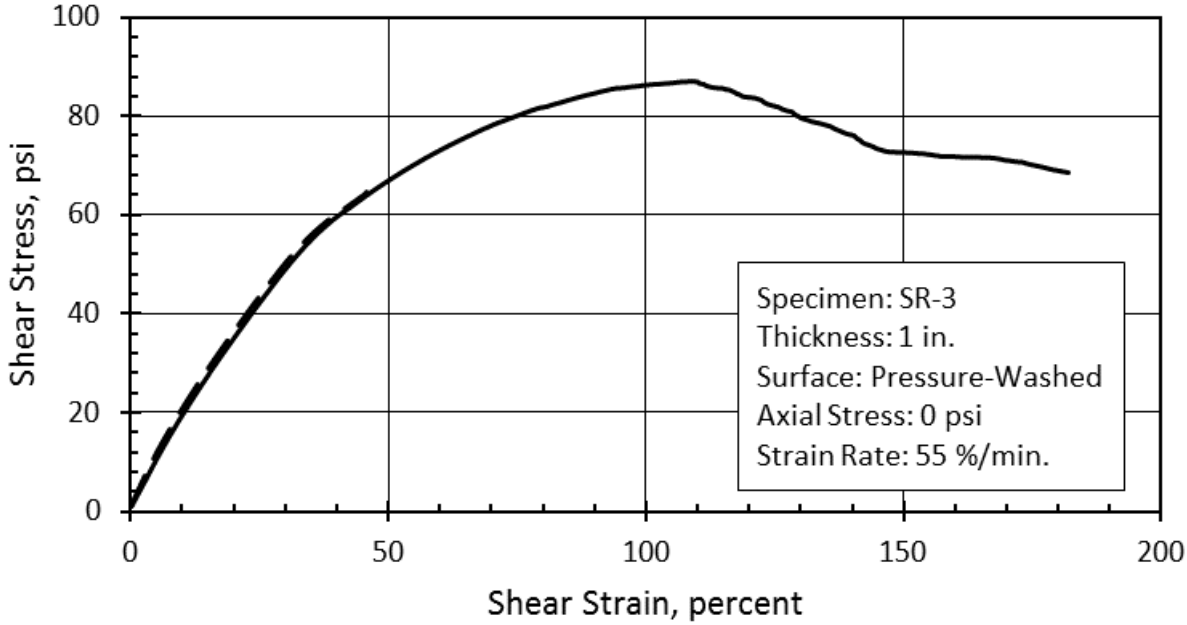


**Figure D-35.** Shear Response of Specimen SR-3

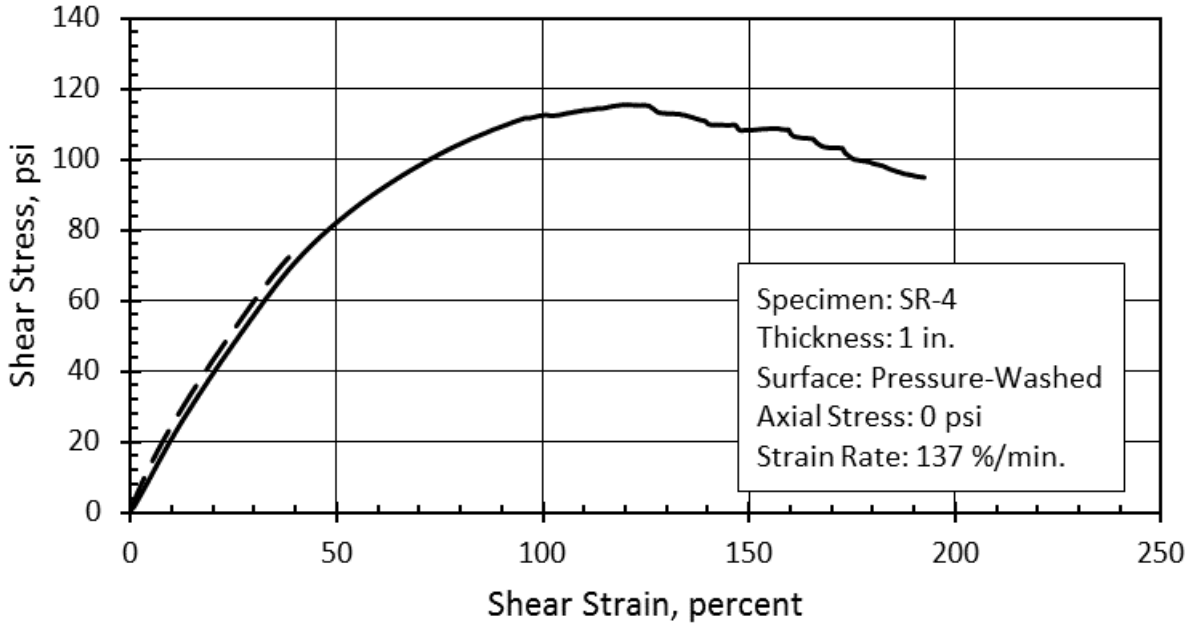


**Figure D-36.** Shear Response of Specimen SR-4

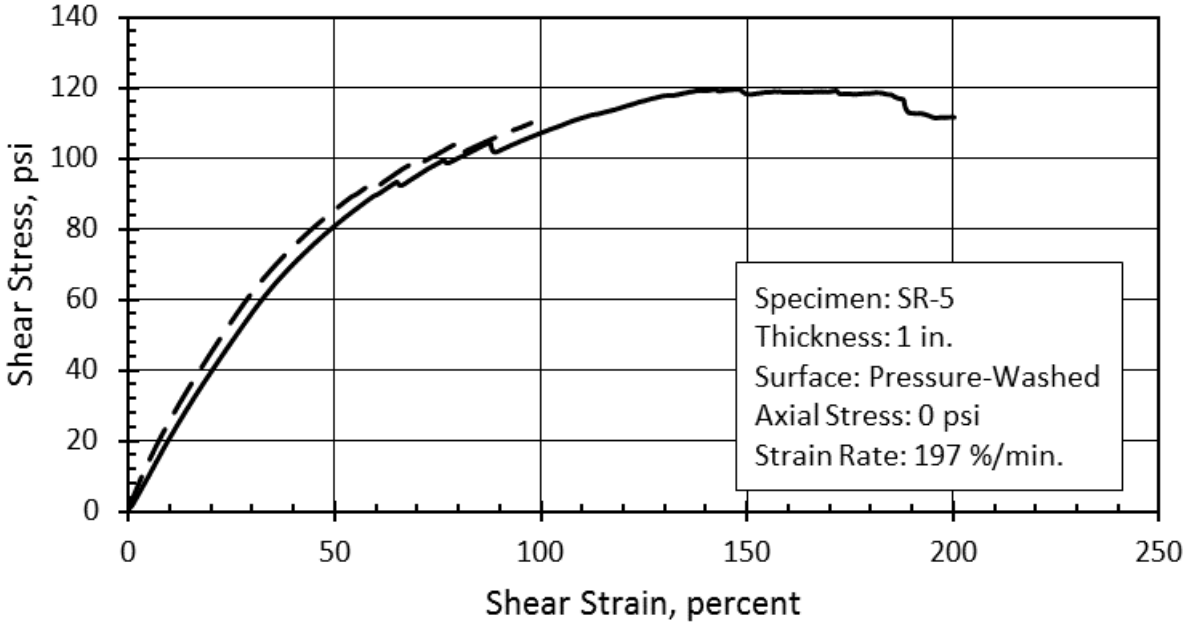


**Figure D-37.** Shear Response of Specimen SR-5

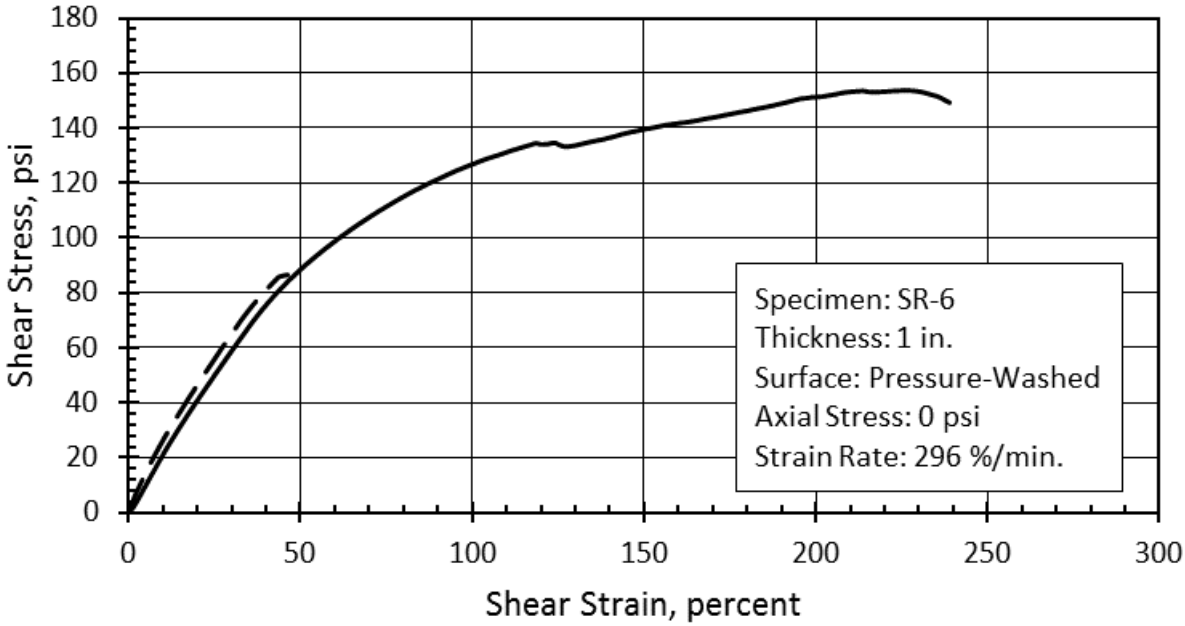


**Figure D-38.** Shear Response of Specimen SR-6

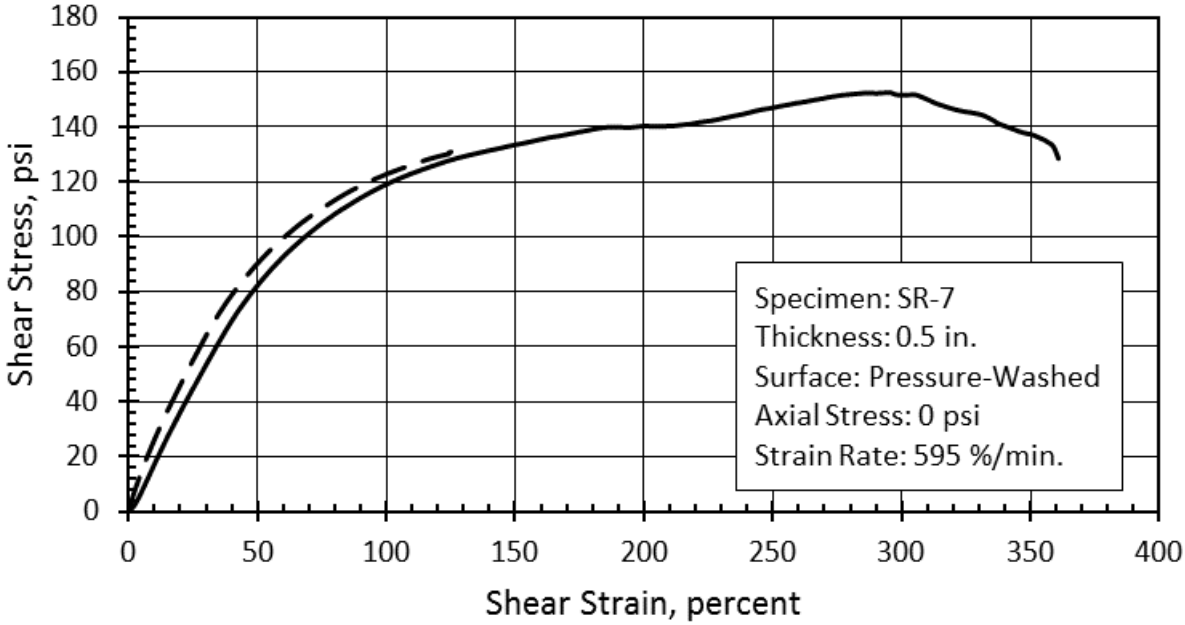


**Figure D-39.** Shear Response of Specimen SR-7

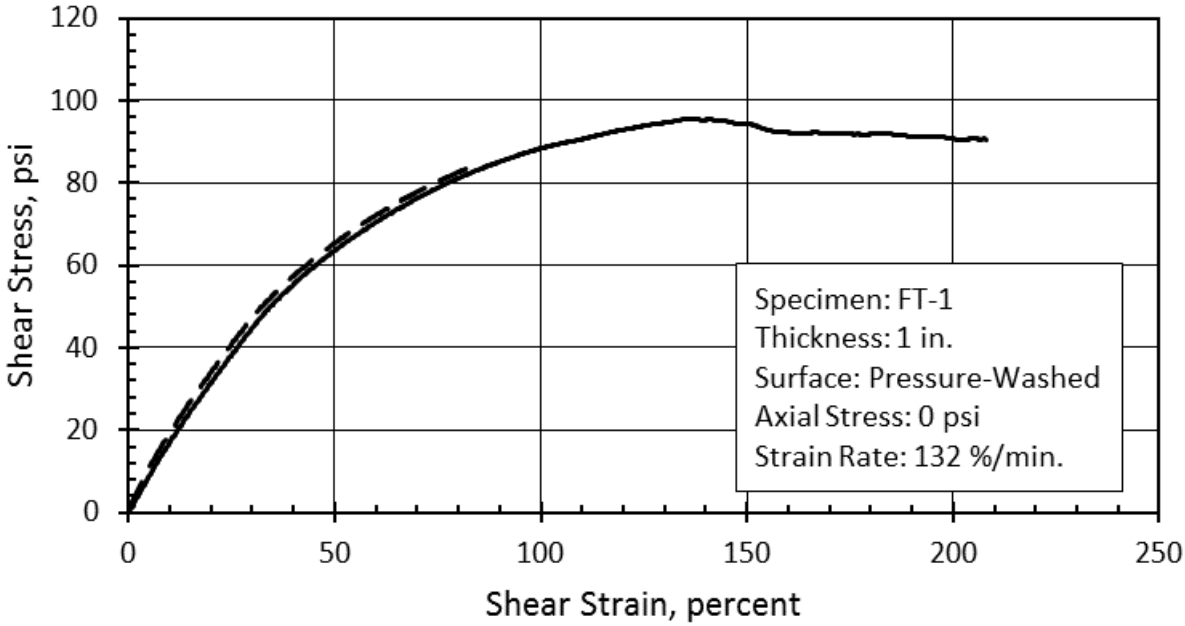


**Figure D-40.** Shear Response of Specimen FT-1

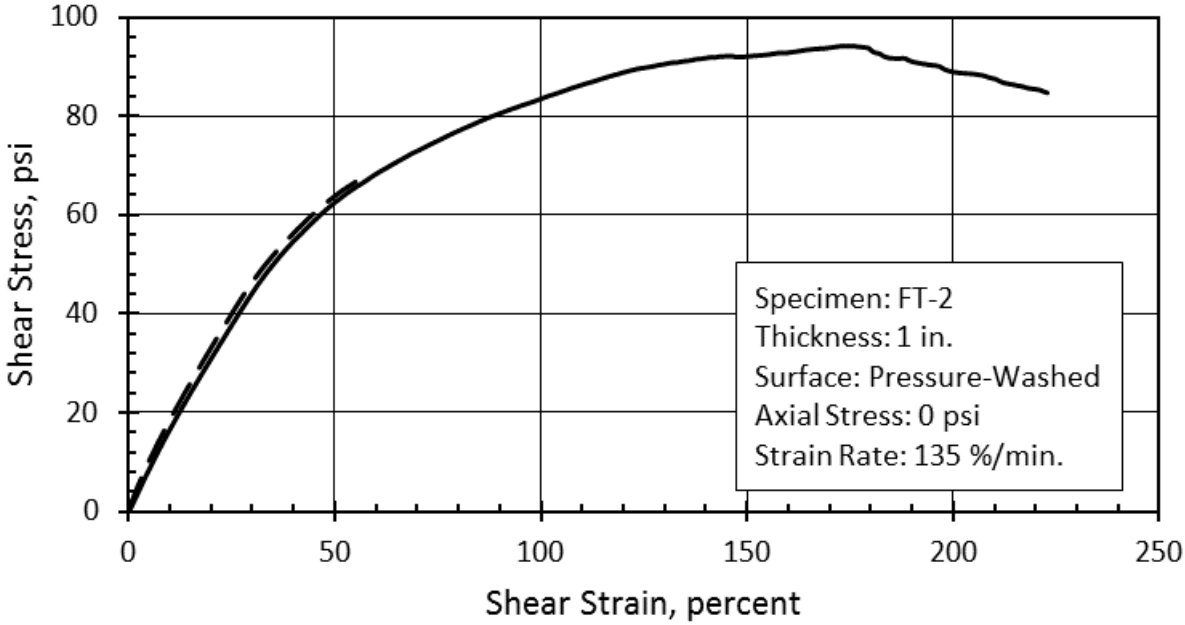


**Figure D-41.** Shear Response of Specimen FT-2

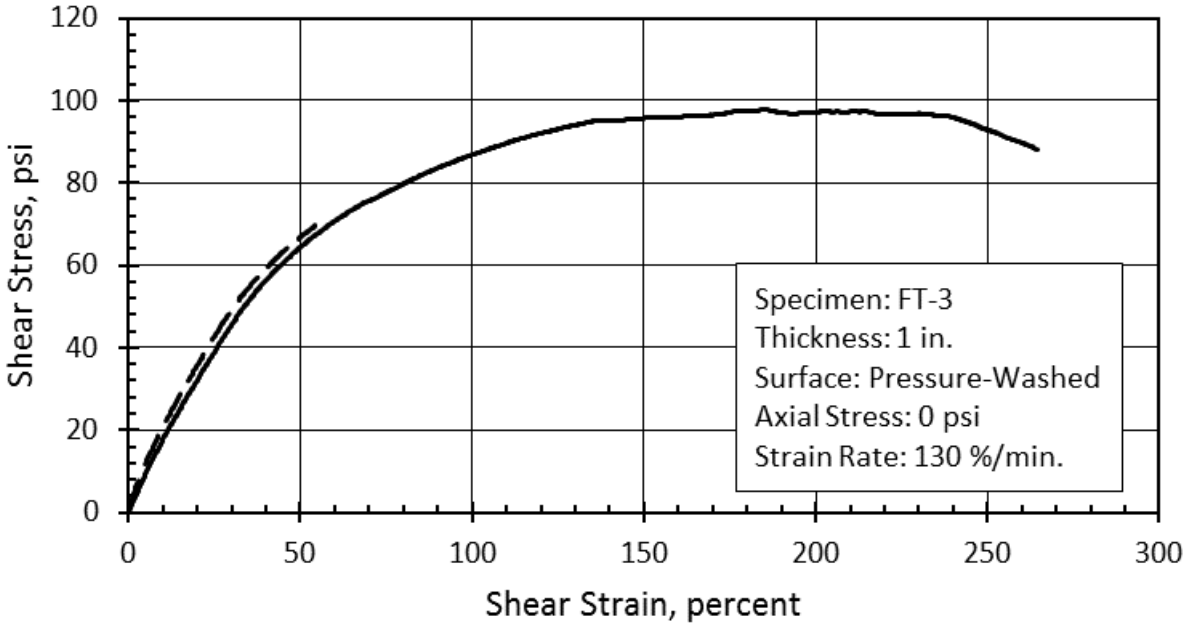


**Figure D-42.** Shear Response of Specimen FT-3

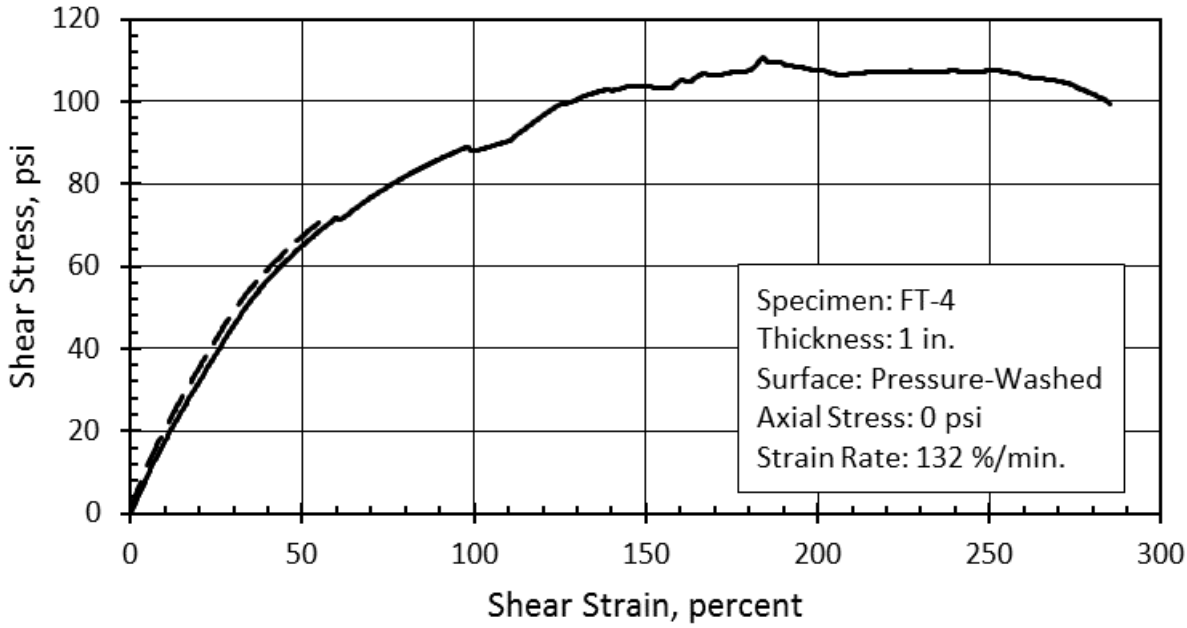


**Figure D-43.** Shear Response of Specimen FT-4

# Appendix E | EdilonSedra Product Data and Safety Sheets

# E.1 Corkelast VA-60 Product Data Sheet

## 1 DESCRIPTION

**edilon)(sedra Corkelast VA-60** is a two-component polyurethane elastomer material for in-situ pouring applications in rail constructions.

The visco-elastic properties of **edilon)(sedra Corkelast VA-60** are designed for the absorption of dynamic loads. Over time the product maintains these properties even under intensive cyclic loads under various climatic conditions.

**edilon)(sedra Corkelast VA-60** also accommodates the insulation of electric currents in the rail. This is an effective prevention against stray currents.

## 2 INTENDED USE

**edilon)(sedra Corkelast VA-60** is developed for use in rail fastening systems for heavy rail (freight and passenger trains, including high speed trains) and is part of the **edilon)(sedra Embedded Rail System (ERS)** and the **edilon)(sedra Embedded Block System (EBS).**

edilon)(sedra Corkelast VA-60 provides both elastic support and fixation of the rail, combining these properties with a significant reduction of both noise and vibration of the total rail construction.

The application of **edilon)(sedra Corkelast VA-60** in combination with an **edilon)(sedra Resilient ERS Strip** results in a further optimized support stiffness for an excellent damping of noise and vibrations.

## 3 FEATURES & BENEFITS

| Features | Benefits |
|---|---|
| • Excellent electrical insulation | + Effective prevention against stray current |
| • Both components are not subjected to transport regulation | + No additional costs during transportation<br>+ No additional requirements for storage as instructed for dangerous products according to ADR transport legislation |
| • No R40 labelling<br>• No carcinogenic suspected ingredients<br>• No plasticizers | + Safe in use |
| • Excellent processing characteristics<br>• Self-levelling during application | + Simplifies edilon)(sedra ERS installation<br>+ Saves time |
| • Quick cure and rapid mechanical strength development | + Short installation times<br>+ Short track possession time |

## 4 POINTS OF ATTENTION

| Point of attention | Explanation |
|---|---|
| • None | • Not applicable |

## 5 COMPOSITION

**edilon)(sedra Corkelast VA-60** is a solvent and plasticizer free, two component, self-levelling casting elastomer system based on state-of-the-art polyurethane resins with cork granulate and mineral fillers. The curing process is characterized by a low exothermic reaction and therefore volume shrinkage is minimized.

Please see the **edilon)(sedra Corkelast VA-60 Safety Data Sheet** for more detailed information.

## 6 PRODUCT APPROVAL

**edilon)(sedra Corkelast** is officially approved by many national and international infrastructure providers.

## 7 PACKAGING

**edilon)(sedra Corkelast VA-60** is supplied in two separate components: component 1 (resin) and component 2 (hardener). **edilon)(sedra Corkelast VA-60** is available in a unit size of **26.5 lb** (12 kg) end product. Both components are individually packed in the correct mixing proportions.

## 8 STORAGE AND SHELF LIFE

Store **edilon)(sedra Corkelast VA-60** either in the depot or at the place of work under dry conditions and away from direct sunlight. The prescribed storage temperature lies between **+50 °F and +86 °F** (+5 °C and +30 °C).

In its original, well-sealed packaging and under the above-mentioned conditions **edilon)(sedra Corkelast VA-60** has a shelf life of **18** months maximum.

## 9 CHEMICAL & PHYSICAL PROPERTIES

| Property | Standard | Value | Additional information |
|---|---|---|---|
| Density cured product | ISO 1183-1-A | **65.5 ± 3.1 lb/ft³** (1.05 ± 0.05 g/cm³) | |
| Color mixed product | | **Dark grey** | |
| Color component 1 | | **Dark grey** | |
| Color component 2 | | **Clear / yellow** | |
| Viscosity mixed product at **+73.4 °F** (+23 °C) | ISO 3219 | **300,000 cP** (30 Pa·s) | Measured after 2 minutes |
| Mixing ratio by weight component 1 : component 2 | | **100 : 50** | |
| Mixing ratio by volume component 1 : component 2 | | **100 : 50** | |
| Reactivity at **+77 °F** (+25 °C) (viscosity **200,000 cP** (200 Pa·s)) | ISO 10364 | **17 minutes** | |
| Volume resistivity | DIN VDE 0100-610<br>IEC 60093<br>(VDE 0303-30) | **> 11062 MΩ·in** (> 281 MΩ·m)<br>**> 6496 MΩ·in** (> 165 MΩ·m) | Dry<br>Wet (0.1 N NaCl) |
| Water absorption after 7 days at **+73.4 °F** (+23 °C) | ISO 62 | **< 5 %** | By weight |
| UV resistance on surface of cured product (1000 hours QUV exposure) | ASTM G 154 | **Color change** | Visual |
| | ISO 37 | **< 10 %** | Changes in mechanical properties |
| Operational use | | **-22 °F up to 158 °F** (-30 °C up to +70 °C) | |

- Test samples are prepared by mixing both components thoroughly for 75 seconds with an Edimix 14 mobile mixing machine.
- Test results are determined with cured material after 7 days at **+73.4 °F** (+23 °C), unless specified otherwise.
- The applied test samples and test methods are subject to change without prior notice.

## 10 CHEMICAL RESISTANCE

| Tested chemical | Standard | Value | Additional information |
|---|---|---|---|
| Demineralized water | ISO-2812-1 method 2 | **1** | Visually determined<br>0 = No stain visible<br>1 = Stain slightly visible<br>2 = Stain clearly visible / temporary swelling<br>Only visual effects |
| Fresh rain water | | **2** | |
| Sodium hydroxide solution (5 %) | | **1** | |
| Sodium chloride solution (10 %) | | **0** | |
| Oxalic acid solution (5 %) | | **2** | |
| Lime mixture with pH 13 | | **2** | |
| Sulphuric acid solution (2 %) | | **2** | |
| Diesel | | **2** | |
| Petrol (Euro 95) | | **1** | |
| Motor oil SAE 30 | | **1** | |

## 11 MECHANICAL PROPERTIES

| Property | Standard | Value | Additional information |
|---|---|---|---|
| Tensile strength | ISO 527 | **> 145 psi** (> 1.0 MPa) | |
| Modulus of elasticity | ISO 527 | **508 psi** (3.5 MPa) | |
| Tensile strain at break | ISO 527 | **> 140 %** | |
| Static compressive modulus | ISO 604 | **856 psi** (5.9 MPa) | Test sample size:<br>**1.97" × 1.97" × 0.985"**<br>(50 × 50 × 25 mm) |
| Tear strength | ISO 34 | **> 62.8 lb/in** (> 11 N/mm) | |
| Rubber hardness after 24 hours | ISO 7619-1 | **50 ± 5 Shore A** | |
| Rubber hardness after 7 days | ISO 7619-1 | **55 ± 5 Shore A** | |
| Rubber hardness after 30 days | ISO 7619-1 | **55 ± 5 Shore A** | |
| Surface wear resistance (TWA) | ISO 9352 | **< 400 µl / 1000 rotations** | |
| Adhesive properties on primed steel<br>(tested on Primer 21 and Primer U90WB) | Based on ISO 4624 | **> 116 psi** (> 0.8 MPa) | Cohesive Corkelast failure |
| Adhesive properties on concrete<br>(tested on Primer 21 and Primer U90WB) | Based on ISO 4624 | **> 116 psi** (> 0.8 MPa) | Cohesive Corkelast failure |
| Compression set after 7 days at **+73.4 °F** (+23 °C) | ISO 815- Part 1 | **< 50 %** | |
| Linear shrinkage | edilon M012 | **< 0.5 %** | After curing |

- Test samples are prepared by mixing both components thoroughly for 75 seconds with an Edimix 14 mobile mixing machine.
- Test results are determined with cured material after 7 days at of **+73.4 °F** (+23 °C), unless specified otherwise.
- The applied test samples and test methods are subject to change without prior notice.

**Static compression stress-strain curve**

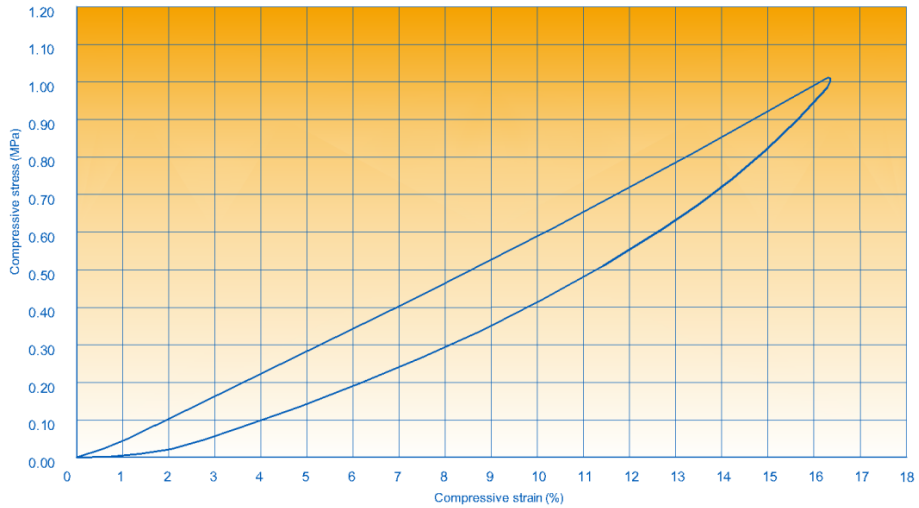


| | |
|---|---|
| Test sample size (l × w × h) | **1.97" × 1.97" × 0.98"** (50 × 50 × 25 mm) |
| Shape factor | **0.5** |
| Loading speed | **0.984 in/min**. (25 mm/min.) |
| Test sample temperature | **68 ± 6 °F** (20 ± 3 °C) |
| No. of Preloading cycles | **5** |
| Compressive modulus | **856 psi, between 29 – 72.5 psi** (5.9 MPa, between 0.2 – 0.5 MPa) |

## 12 SURFACE CONDITIONS

The durability of the rail system, in which **edilon)(sedra Corkelast VA-60** is applied, is directly dependent on the quality of the surface pre-treatment prior to pouring.

Before pouring **edilon)(sedra Corkelast VA-60**, the surface must be pre-treated and it is necessary to use a pre-treatment primer and a bonding primer.

The following primers are suitable for **edilon)(sedra Corkelast VA-60**:

- **Concrete and steel pre-treatment primer:** edilon)(sedra Primer U90WB

  ***NOTE***
  edilon)(sedra Primer U90WB can also be used as a bonding primer if:
  1) the time between application of Primer U90WB and pouring has not exceeded three days;
  2) the surface of Primer U90WB has not been in contact with water;
  3) the pre-treated surfaces are completely clean.

- **Bonding primer:** edilon)(sedra Primer 21 or
  edilon)(sedra Primer 21 2K
  edilon)(sedra Primer 24

Make sure before the pouring of **edilon)(sedra Corkelast VA-60,** that the primered surfaces are completely clean: all contaminations like dust, release agents, curing compounds, hydrophobic agents etc. must be removed from the surfaces. The primered surfaces must be dry and edilon)(sedra Corkelast VA-60 must be applied within the working window of the bonding primer.

Please see the **edilon)(sedra Primer U90WB** and **edilon)(sedra Primer 21 / edilon)(sedra Primer 21 2K / edilon)(sedra Primer 24 Product information sheet** for more information about surface pre-treatment and primer application.

## 13 USER INSTRUCTIONS

Please see the **edilon)(sedra Corkelast VA-60 User instruction sheet** and the applicable **edilon)(sedra Installation Instructions** for detailed application instructions.

## 14 APPLICATION CONDITIONS

| Conditions | Value | Additional information |
|---|---|---|
| Surface | **Dry and clean** | Only apply the product on pre-treated surfaces (see section 12). To determine visually. |
| Environment | **Dry** | Or in a conditioned environment to avoid contact with (rain)water. |
| Relative humidity air | **< 75 %** | Based on Primer 21 |
| | **< 85 %** | Based on Primer 21 2k |
| | **< 90 %** | Based on Primer 24 |
| Surface temperature[1)] | **+41 °F to +77 °F** (+5 °C to +25 °C) | Based on Primer 21 |
| | **+41 °F to +95 °F** (+5 °C to +35 °C) | Based on Primer 21 2k |
| | **+41 °F to +113 °** (+5 °C to +45 °C) | Based on Primer 24 |
| Safety margin in relation to dew point (ΔT) | **> 6 °F** (> 3 °C) | In order to ensure a safety margin, the surface temperature must be **6 °F** (3 °C) above the dew point. |
| Product temperature | **+59 °F to +86 °F** (+15 °C to +30 °C) | |

- Recommended measuring device: TQC DewCheck or Elcometer 319s
- Direct contact with (rain)water must be avoided.

1) Applies to any surface on which the product is poured. At light cloudy and sunny weather, the surface temperature is always higher than the air temperature due to radiation heat from the sun.

## 15 SAFETY RECOMMENDATIONS

During application of **edilon)(sedra Corkelast VA-60**, it is imperative that protective clothing, rubber gloves and safety goggles are worn.

Before using **edilon)(sedra Corkelast VA-60**, please read the packing label and the **edilon)(sedra Corkelast VA-60 Safety Data Sheet** for more detailed safety recommendations.

**edilon)(sedra Corkelast VA-60** must be stored in the original well-sealed packaging.

**edilon)(sedra Corkelast VA-60** is not for internal consumption, but for industrial use only.

## 16 MIXING

Prior to mixing of **edilon)(sedra Corkelast VA-60**, pour all of component 2 into the packaging of component 1. Mix both components thoroughly with an **edilon)(sedra Edimix 14 mobile mixing machine** to achieve a homogeneously mixed compound.

To ensure proper mixing and to protect the edilon)(sedra Edimix 14 mobile mixing machine from damage (overload), edilon)(sedra advises to mix both components at product temperatures between **+59 °F and +86 °F** (+15 °C and +30 °C).

Please see the **edilon)(sedra Edimix 14 User Instruction** for more detailed information.

The pot life of **edilon)(sedra Corkelast VA-60** depends on the product temperature and the mixed volume. The table below gives an indication of the pot life of the product at different product temperatures.

| Product temperature | | Pot life (minutes) |
|---|---|---|
| **°F** | (°C) | |
| **59** | (15) | 19 |
| **68** | (20) | 18 |
| **77** | (25) | 17 |
| **86** | (30) | 16 |

## 17 CURING

The minimum curing time of **edilon)(sedra Corkelast VA-60** is related to the surface temperature. The product is capable of carrying dynamic loads after the minimum curing time. After 24 hours the material can be fully loaded.

| Surface temperature | | Minimal curing period after mixing (hours) |
|---|---|---|
| **°F** | (°C) | |
| **41** | (5) | 5 |
| **50** | (10) | 3 |
| **59** | (15) | 2.5 |
| **68 – 77** | (20 – 25) | 2 |
| **86 – 95** | (30 – 35) | 1.5 |

## 18 CLEANING

Clean used tools immediately after use with **edilon)(sedra Toolcleaner**. Please see the **edilon)(sedra Toolcleaner Safety Data Sheet** before use.

## 19 DISPOSAL CONSIDERATIONS

The following waste products can arise at the application of **edilon)(sedra Corkelast VA-60:**

| Description | Type of waste |
|---|---|
| Cured product | Non-hazardous waste |
| Packaging with cured product | Non-hazardous waste |
| Packaging with component 1 or component 2 | Hazardous waste |
| Packaging with uncured product | Hazardous waste |

The waste products should be incinerated in a suitable installation according to federal, tribal, state or local regulations or disposed of according to U.S. regulations regarding proper management of hazardous and non-hazardous waste.

## 20 COLOR TINT

The color tint of **edilon)(sedra Corkelast VA-60** may change due to environmental influences (such as chemicals, high temperature, and UV radiation) that affect the material. These color changes on the surface have small influences on the mechanical properties of the product surface.



**2000-0202** **Date of issue: 01-07-2014**

**Issue based on edilon)(sedra original document (EN) 100706 rev 05**

**edilon)(sedra inc.**
**511 W. 195th Street**
**Glenwood, IL 60425, USA**

**T +1 708 790 0626**
**F +1 708 754 4058**

**mail@edilonsedra.com**
**www.edilonsedra.com**

# E.2 Editaan 70U Product Data Sheet

**1 DESCRIPTION**

**edilon)(sedra Editaan 70U** is a two component self-levelling undergrouting material based on special polyurethane resins and filler material.

The visco-elastic properties of edilon)(sedra Editaan 70U are designed for the absorption of dynamic loads. Over time the product maintains these properties even under intensive cyclic loads.

edilon)(sedra Editaan 70U is developed with the objective of optimally combining the required stiffness and stability with a significant reduction of environmental inconvenience, such as noise and vibration. edilon)(sedra Editaan 70U provides excellent electrical insulation properties.

edilon)(sedra Editaan 70U combines a low viscosity with excellent pouring characteristics.

**2 INTENDED USE**

**edilon)(sedra Editaan 70U** is especially developed for undergrouting machine fundaments, railway track structures, light poles etc.

**3 FEATURES & BENEFITS**

| Features | Benefits |
|---|---|
| • Sophisticated product composition for undergrouting<br>• Developed for the application with easy-to-handle packaging | + Trouble-free application without weighing<br>+ Accurate and fast processing<br>+ Always correct mixing ratios<br>+ Clean and environmental friendly processing |
| • Excellent processing characteristics<br>• Self-levelling during application | + Simple processing<br>+ Saves time |
| • Quick cure and rapid mechanical strength development | + Short installation time<br>+ Short possession time |
| • Minimum shrinkage | + Clean finish |
| • Absorbs vibration energy<br>• Long lasting resistance against dynamic loads | + Optimal damping of noise and vibration<br>+ Very durable |
| • In combination with edilon)(sedra primers, edilon)(sedra Editaan 70U has excellent adhesion properties | + Durable support and fixation<br>+ Saves maintenance cost |
| • Excellent electrical insulation | + Effectively prevents stray current leakage |
| • Resistant against deterioration in aggressive environments<br>• Weatherproof under harsh conditions | + Guarantees a durable elastic support and fixation |
| • Easy to remove mechanically and re-applicable | + Short out of service time |

**4 POINTS OF ATTENTION**

| Point of attentions | Explanation |
|---|---|
| • The application of a primer is necessary to obtain a good bonding to the surface | • Application without primer will lead to insufficient bonding to the surface |

**5 COMPOSITION**

**edilon)(sedra Editaan 70U** is a solvent-free, two component, self-levelling casting elastomer material based on special polyurethanes and filler materials.

Please see the **edilon)(sedra Editaan 70U Safety Data Sheet** for more information.

**6 PRODUCT APPROVAL**

**edilon)(sedra Editaan 70U** is officially approved by many national and international infra providers.

**7 PACKAGING**

**edilon)(sedra Editaan 70U** is supplied in two separate components, and available in a unit size of **35 lbs** (16 kg) product. Both components are individually packed in the correct mixing ratio. The product is also available in packaging for use with an automated two component mixing and pouring machine.

## 8 STORAGE AND SHELF LIFE

Store **edilon)(sedra Editaan 70U** either in the depot or at the place of work under dry conditions and away from direct sunlight. The prescribed storage temperature lies between **+41 °F and +86 °F** (+5 °C and +30 °C).
In its original, well-sealed packaging and under the above-mentioned conditions edilon)(sedra Editaan 70U has a shelf life of **18** months maximum.

## 9 CHEMICAL & PHYSICAL PROPERTIES

| Property | Standard | Value | Additional information |
|---|---|---|---|
| Density cured product | ISO 1183-1-A | **56.81 ± 3.12 lb/ft³** (0.91 ± 0.05 g/cm³) | |
| Color mixed product | | **Grey** | |
| Color component 1 | | **Grey** | |
| Color component 2 | | **Brown** | |
| Viscosity component 1 at **+68 °F** (+20°C) | ISO 3219 | **10,000 cP** (10 Pa·s) | |
| Mixing ratio by weight component 1 : component 2 | | **100 : 15** | |
| Mixing ratio by volume Component 1 : component 2 | | **100 : 10.9** | |
| Reactivity at **+77 °F** (+25 °C) (viscosity **20,000 cP** (200 Pa·s)) | ISO 10364 | **10 minutes** | |
| Specific electrical break through resistance (volume resistivity) | DIN VDE 0100-610 IEC 60093 (VDE 0303-30) | **> 2598 GΩ·in** (> 66 GΩ·m) **> 1378 GΩ·in** (>35 GΩ·m) | Dry: VDV 6201 specs **> 7.9 MΩ·in** (> 0.2 MΩ·n Wet (0.1% N NaCl) |
| Water absorption after 7 days at **+73.4 °F** (+23 °C) | ISO 62 | **< 2 %** | |
| UV-light effect on the surface of cured product (1000 hours UV exposure) | ASTM G 154 | **Color change** | Visual |
| | ISO 37 | **< 20 %** | Changes in mechanical properties |
| Temperature stability | | **-40 °F to +176 °F** (-40 °C to +80 °C) | Temporary up to **+302 °F** (+150 °C) |

- Test samples are prepared by mixing both components thoroughly with the power assisted hand mixer.
- Test results are determined with cured material after 7 days at a temperature of **+68 °F** (+20 °C), unless specified otherwise.
- The applied samples and test methods are subject to change without prior notice.

## 10 CHEMICAL RESISTANCE

| Tested chemical | Standard | Value | Additional information |
|---|---|---|---|
| Fresh rain water | ISO-2812-1 method 2 | **0** | Visually determined<br>0 = No stain visible<br>1 = Stain slightly visible<br>2 = Stain clearly visible / temporary swelling<br>Only visual effects |
| Sodium hydroxide solution (5 %) | | **1** | |
| Sodium chloride solution (10 %) | | **0** | |
| Oxalic acid solution (5 %) | | **2** | |
| Lime mixture with pH 13 | | **1** | |
| Sulphuric acid solution (2 %) | | **1** | |
| Diesel | | **2** | |
| Petrol (Euro 95) | | **2** | |
| Motor oil SAE 30 | | **0** | |

## 11 MECHANICAL PROPERTIES

| Property | Standard | Value | Additional information |
|---|---|---|---|
| Tensile strength | ISO 527 | **> 290 psi** (> 2 MPa) | VDV 6201 specification **> 217.6 psi** (> 1.5 N/mm$^2$) |
| Modulus of elasticity | ISO 527 | **1160 psi** (8 MPa) | |
| Tensile strain at break | ISO 527 | **> 100 %** | VDV 6201 specification > 100 % |
| Static bedding modulus | VDV method 6201 | **> 1841.86 lb/in$^3$** (> 0.5 N/mm$^3$) | VDV 6201 specification **> 1473.49 lb/in$^3$** (> 0.4 N/mm$^3$) |
| Static Stiffness | VDV method 6201 | **> 565305 lb/in per inch** (> 99 kN/mm per meter) | VDV 6201 specification > **457 lb/in per i** (> 80 kN/mm per meter) |
| Tear strength | ISO 34 | **> 69 lb/in** (> 12 N/mm) | VDV 6201 specification > **34 lb/in** (> 6 N/ |
| Rubber hardness after 24 hours | ISO 7619-1 | **50 ± 5 Shore A** | |
| Rubber hardness after 7 days | ISO 7619-1 | **60 ± 5 Shore A** | |
| Rubber hardness after 30 days | ISO 7619-1 | **65 ± 5 Shore A** | VDV 6201 specification 60-70 Shore A |
| Surface wear resistance | ISO 9352 | **< 800 µl / 1000 rotations** | |
| Adhesive properties on primed steel (tested on edilon)(sedra primers with Editaan 70U) | Based on ISO 4624 | **> 217.6 psi** (> 1.5 MPa) | Cohesive Editaan 70U failure |
| Adhesive properties on concrete (tested on edilon)(sedra primers with Editaan 70U) | Based on ISO 4624 | **> 217.6 psi** (> 1.5 MPa) | Cohesive Editaan 70U failure |

- Test samples are prepared by mixing both components thoroughly with the power assisted hand mixer.
- Test results are determined with cured material after 7 days at a temperature of **+68 °F** (+20 °C), unless specified otherwise.
- The applied samples and test methods are subject to change without prior notice.

**Static stiffness characteristic**

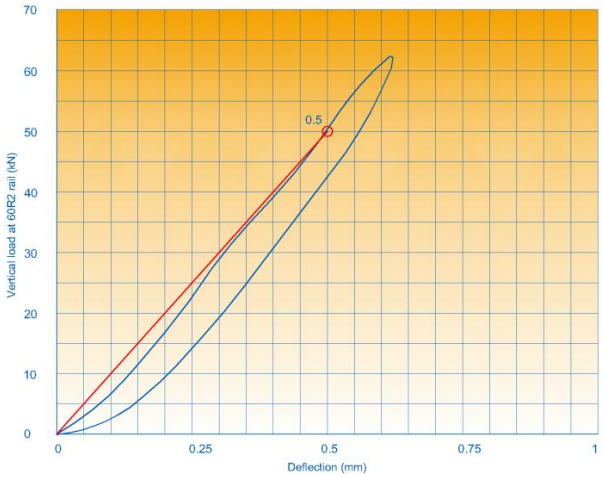


| | |
|---|---|
| Test sample size (L × W × H) | **39" × 7" × 0.98"** (1000 × 180 × 25 mm) |
| Loading speed | **450 lb/s** (2 kN/s) |
| Test sample temperature | **+68 ± 6 °F** (+20 ± 3 °C) |
| No. of preloading cycles | **3** |
| Static stiffness | **565,305 lb/in per inch** (99 kN/mm per meter) |
| Tested by | Technical University of Munich – Test report nr. 2281 |
| Specs datasheet VDV 6201 | **> 456812 lb/in per inch** (> 80 kN/mm per meter) as issued by the German Association of Transportation Companies |

## 12 SURFACE CONDITIONS

The durability of the rail system, in which **edilon)(sedra Editaan 70U** is applied, is directly dependent on the quality of the surface preparation prior to the application.

Before using edilon)(sedra Editaan 70U**,** the surface needs to be prepared and it is necessary to use a pre-treatment primer and a bonding primer.

The following primer types are suitable for edilon)(sedra Editaan 70U:

- **Concrete and steel pre-treatment primer:** edilon)(sedra Primer U90WB

  ***NOTE***
  edilon)(sedra Primer U90WB can also be used as a bonding primer if:
  1) the time between application of Primer U90WB and pouring has not exceeded three days;
  2) the surface of Primer U90WB has not been in contact with water;
  3) the pre-treated surfaces are completely clean.

- **Bonding primer:** edilon)(sedra Primer 21 or
  edilon)(sedra Primer 21 2K or
  edilon)(sedra Primer 24

Make sure before the pouring of **edilon)(sedra Editaan 70U,** that the primered surfaces are completely clean: all contaminations such as sand or dust must be removed from the surfaces. The primered surfaces must be dry and edilon)(sedra Editaan 70U must be applied within the working window of the bonding primer.
Please see the **edilon)(sedra Primer U90WB** and **edilon)(sedra Primer 21 / edilon)(sedra Primer 21 2K / edilon)(sedra Primer 24 Product Data Sheet** for more information about surface preparation and primer application.

## 13 USER INSTRUCTIONS

Please see the **edilon)(sedra Editaan 70U User Data Sheet** for detailed instructions.

## 14 APPLICATION CONDITIONS

| Conditions | Value | Additional information |
|---|---|---|
| Surface | **Dry** | Only apply the product on pre-treated surfaces (see section 12 |
| Environment | **Dry** | Or in a conditioned environment |
| Relative humidity air | **< 75 %** | Based on Primer 21 |
| | **< 85 %** | Based on Primer 21 2k |
| | **< 90 %** | Based on Primer 24 |
| Surface temperature[1)] | **+41 °F to +77 °F** (+5 °C to +25 °C) | Based on Primer 21 |
| | **+41 °F to +95 °F** (+5 °C to +35 °C) | Based on Primer 21 2k |
| | **+41 °F to +113 °** (+5 °C to +45 °C) | Based on Primer 24 |
| Safety margin in relation to dew point (ΔT) | **> 6 °F** (> 3 °C) | In order to ensure a safety margin, the surface temperature mu be **6 °F** (3 °C) above the dew point. |
| Product temperature | **+59 °F to +77 °F** (+15 °C to +30 °C) | |

- Recommended measuring device: TQC DewCheck or Elcometer 319s.
- Direct contact with (rain)water must be avoided.

1) Applies to any surface on which the product is poured. At light cloudy and sunny weather, the surface temperature is always higher than the air temperature due to radiation heat from the sun.

## 15 SAFETY RECOMMENDATIONS

During application of **edilon)(sedra Editaan 70U**, it is imperative that protective clothing, rubber gloves and safety goggles are worn.

Before using edilon)(sedra Editaan 70U, please read the packing label and the **edilon)(sedra Editaan 70U Safety Data Sheet** for more detailed safety recommendations.

edilon)(sedra Editaan 70U must be stored in the original well-sealed packaging.

## 16 MIXING

Prior to mixing pour all of the content of the component 2 packaging into the bucket with component 1. Mix both components thoroughly with the power assisted hand mixer to achieve a homogeneous mixture.

To ensure proper mixing and to protect the power assisted hand mixer from damage (overload), edilon)(sedra advises to mix both components at product temperatures between **+59 °F and +86 °F** (+15 °C and +30 °C).

The pot life of **edilon)(sedra Editaan 70U** depends on the product temperature and the mixed volume. The table below gives an indication of the pot life of the product at different product temperatures.

| Product temperature | | Pot life (minutes) |
|---|---|---|
| **°F** | (°C) | |
| **41** | (5) | 17 |
| **50** | (10) | 13 |
| **59** | (15) | 11 |
| **68** | (20) | 10 |
| **77** | (25) | 8 |
| **86** | (30) | 7 |

## 17 CURING

The minimum curing time of **edilon)(sedra Editaan 70U** is related to the surface temperature. The product is capable of carrying dynamic loads after the minimum curing time. After 24 hours the material can be fully loaded.

| Surface temperature | | Minimal curing period after mixing (hours) |
|---|---|---|
| **°F** | (°C) | |
| **41** | (5) | 7 |
| **50** | (10) | 6 |
| **59** | (15) | 5 |
| **68 – 86** | (20 – 30) | 4.5 |
| **95 – 113** | (35 – 45) | 4 |

## 18 CLEANING

Clean used tools immediately after use with **edilon)(sedra Toolcleaner**. Please read the **edilon)(sedra Toolcleaner Safety Data Sheet** before use.

## 19 DISPOSAL CONSIDERATIONS

The following waste products can arise at the application of **edilon)(sedra Editaan 70U:**

| Description | Type of waste |
|---|---|
| Cured product | Non-hazardous waste |
| Packaging with cured product | Non-hazardous waste |
| Packaging with component 1 or component 2 | Hazardous waste |
| Packaging with uncured product | Hazardous waste |

The waste products should be incinerated in a suitable installation according to federal, tribal, state or local regulations or disposed of according to U.S. regulations regarding proper management of hazardous and non-hazardous waste.

## 20 COLOR TINT

The color tint of **edilon)(sedra Editaan 70U** may change due to environmental influences (such as chemicals, high temperature, and UV radiation) which affect the material. These color changes have small influences on the mechanical properties of the product surface.



**2005-0104-31** **Date of issue: 01-07-2014**

**Issue based on edilon)(sedra original document (EN) 070908 rev 06**

**edilon)(sedra inc.**
**511 W. 195th Street**
**Glenwood, IL 60425, USA**
**T +1 708 790 0626**
**F +1 708 754 4058**
**mail@edilonsedra.com**
**www.edilonsedra.com**

# E.3 DexG Product Data Sheet

## 1 DESCRIPTION

**edilon)(sedra Dex-G** is a high performance grout system for durably undergrouting machines and engineering structures under heavy, dynamic load conditions. Its good adherence to damp, humid or wet surfaces and its high initial compression strength make edilon)(sedra Dex-G exceptionally suitable for difficult applications where working time is limited. edilon)(sedra Dex-G is available in three types (standard grades) with carefully selected and tuned components.

| Dex-G type | Number of components | Recommended for pouring heights |
|---|---|---|
| **Dex-G 20** | **2** | **0 – 0.79 in** (0 – 20 mm) |
| **Dex-G 40** | **3** | **0.79 – 1.58 in** (20 – 40 mm) |
| **Dex-G 80** | **3** | **1.58 – 3.2 in** (40 – 80 mm) |

On request:
**edilon)(sedra Dex-G Fast** can be delivered by adding our Catalyst package **edilon)(sedra Catalyst for Dex-G Component 4**.

## 2 INTENDED USE

**edilon)(sedra Dex-G** is specially developed for undergrouting machine fundaments, railway track structures, **edilon)(sedra EDF** baseplates, light poles etc. Other edilon)(sedra Dex-G applications are for stress free anchoring of anchor bolts, threaded rods, splice and reinforcement bars, bolt heads and armature hubs in concrete and / or the repair of concrete structures. edilon)(sedra Dex-G is also used for gluing steel plates and strips onto concrete as well as **edilon)(sedra Resilient ERS Strips** as part of the **edilon)(sedra Embedded Rail System.**

## 3 FEATURES & BENEFITS

| Features | Benefits |
|---|---|
| • Excellent adhesion to damp, humid or wet surfaces | + Application conditions are generally not restrictive<br>+ Applicable in rain weather conditions<br>+ Submerged applications possible |
| • High performance mechanical properties<br>• Excellent electrical insulation | + Guarantees a perfect alignment of machines, structures and rails under severe static and dynamic loads<br>+ Good fatigue resistance |
| • Minimal shrinkage | + Thick layers can be applied in one pouring cycle<br>+ Guarantees perfect alignment |
| • Packed in individual balanced units | + Accurate and fast processing<br>+ Always the correct mixing ratios |
| • Low viscosity (Dex-G type 20) | + Well applicable in tight spaces<br>+ Saves money |
| • Resistant to oil and most other chemical substances | + Guarantees a durable support and fixation |
| • Offers long term resistance to vibrations and dynamic loads | + Extremely useful for under grouting edilon)(sedra DFS baseplates and machines |

## 4 POINTS OF ATTENTION

| Point of attention | Explanation |
|---|---|
| • Preparation of the surfaces required for optimum adhesion | • Concrete surfaces might have reduced adhesion due to release agents and curing compounds |
| • The standard curing time of Dex-G is 24 hours | • Dex-G Fast has a quicker curing time and is recommended for use at temperatures between **+50 °F and +77 °F** (+10 and +25 °C) |

## 5 COMPOSITION

**edilon)(sedra Dex-G** is a solvent free, self-levelling grout system based on special epoxy resins and high quality mineral filler materials.

Please see the **edilon)(sedra Dex-G Safety Data Sheet** for more detailed information.

## 6 PACKAGING

Depending on the product type, **edilon)(sedra Dex-G** is packed in two or three individually packed components in the correct mixing proportions; component 1 (resin), component 2 (hardener) and – if applicable – component 3 (balanced quantity of mineral filler material).

The **edilon)(sedra Catalyst for Dex-G Component 4** is available in additional bottles.

The standard unit sizes for Dex-G are:

| Dex-G type | Standard unit size |
|---|---|
| **Dex-G 20** | **5.5 or 22 lb** (2.5 or 10 kg) |
| **Dex-G 40** | **33 lb** (15 kg) |
| **Dex-G 80** | **44 lb** (20 kg) |

## 7 STORAGE AND SHELF LIFE

Store **edilon)(sedra Dex-G** either in the depot or at the place of work under dry conditions and away from direct sunlight. The prescribed storage temperature is between **+41 °F and +86 °F** (+5 °C and +30 °C).

In its original, well-sealed packaging and under the above-mentioned conditions **edilon)(sedra Dex-G** has a shelf life of **24** months maximum.

## 8 CHEMICAL & PHYSICAL PROPERTIES

| **Dex-G type** | | **Dex-G 20** | **Dex-G 40** | **Dex-G 80** |
|---|---|---|---|---|
| **Property** | **Standard** | **Value** | **Value** | **Value** |
| Density cured product | ISO 1183-1-A | **100 ± 3 lb/ft³** (1.61± 0.05 g/cm³) | **109 ± 3 lb/ft³** (1.75 ± 0.05 g/cm³) | **119 ± 3 lb/ft³** (1.90 ± 0.05 g/cm³) |
| Color mixed product | | **Grey** | **Grey** | **Grey** |
| Color component 1 | | **Beige** | **Beige** | **Beige** |
| Color component 2 | | **Black** | **Black** | **Black** |
| Color component 3 | | **–** | **Beige** | **Beige** |
| Viscosity component 3 at **+77 °F** (+25 °C) | ISO 3219 | **– cP** (– Pa·s) | **–** | **–** |
| Viscosity mixed product (1+2) at **+77 °F** (+25 °C) | ISO 3219 | **11,000 cP** (11 Pa·s) | **11,000 cP** (11 Pa·s) | **11,000 cP** (11 Pa·s) |
| Mixing ratio by weight component 1 : component 2 | | **100 : 20.05** | **100 : 20.05** | **100 : 20.05** |
| Mixing ratio by weight mixed product (1+2) : component 3 | | **–** | **100 : 50** | **100 : 100** |
| Reactivity at **+77 °F** (+25 °C) (viscosity **20,000 cP** (200 Pa·s)) | ISO 10364 | **30 min** | **30 min** | **35 min** |
| Thermal conductivity λ50 – λ104 between **+50 °F and +104 °F** (λ10 – λ40 between +10 °C and +40 °C) | EN 12667 | **2.98 Btu in/h·ft²·°F** (0.430 W/m.K) | **–** | **–** |
| Volume resistivity | DIN VDE 0100-610<br>IEC 60093 (VDE 0303-30) | **Dry: > 39370 MΩ·in** (> 1000 MΩ·m)<br>**Wet, 0.1 N NaCl: > 39370 MΩ·in** (> 1000 MΩ·m) | | |

- Test samples are prepared by mixing both components thoroughly for 2 minutes.
- Test results, are determined with cured material after 7 days at a temperature of **+73.4 °F** (+23 °C), unless specified otherwise.
- The applied test samples and test methods are subject to change without prior notice.

## 9 MECHANICAL PROPERTIES

| Dex-G type | | Dex-G 20 | Dex-G 40 | Dex-G 80 |
|---|---|---|---|---|
| **Property** | **Standard** | **Value** | **Value** | **Value** |
| Flexural-tensile strength<br>Test samples dimensions: 1.6" × 1.6" × 6.3"<br>(40 × 40 × 160 mm) | EN 196-1 | **8224 psi**<br>(56.7 MPa) | **4467 psi**<br>(30.8 MPa) | **4743 psi**<br>(32.7 MPa) |
| Compression strength<br>Test samples dimensions: 3.9" × 3.9" × 1.6"<br>(100 × 100 × 40 mm) | Based on EN 196-1 | **> 13054 psi**<br>(> 90 MPa) | **> 18275 psi**<br>(> 126 MPa) | **> 20305 psi**<br>(> 140 MPa) |
| Modulus of elasticity | ISO 178 | **> 652680 psi** (> 4500 MPa) | | |
| Shear strength | ASTM D1002 | **> 2176 psi** (> 15 MPa) | | |
| Flexural strength | ISO 178 | **> 5656 psi** (> 39 MPa) | | |
| Rubber hardness after 24 hours | ISO 7619-1 | **75 ± 5 Shore D** | | |
| Rubber hardness after 7 days | ISO 7619-1 | **80 ± 5 Shore D** | | |
| Surface wear resistance (TWA) | ISO 9352 | **< 440 µl / 1000 rotations** | | |
| Adhesive strength on steel (S235 JR, Sa 2½) | ISO 4624 | **> 5076 psi** (> 35 MPa) | | |
| Adhesive strength on concrete (dry) | EN 1542 | **218 psi (Concrete failure)** (1.5 MPa (Concrete failure)) | | |
| Adhesive strength on concrete (humidity 6%) | | | | |
| Adhesive strength on concrete (submerged) | | | | |

- Test samples are prepared by mixing both components thoroughly for 2 minutes.
- Test results, are determined with cured material after 7 days at a temperature of **+73.4 °F** (+23 °C), unless specified otherwise.
- The applied test samples and test methods are subject to change without prior notice.

## 10 SURFACE PREPARATION

The durability of the system, in which **edilon)(sedra Dex-G** is applied, is directly dependent on the preparation of the surface prior to the application. For optimum adhesion performance the prepared surface should be clean.

**edilon)(sedra Dex-G** is applied directly after surface preparation.

**Concrete surfaces:**
In case of concrete surfaces, the following conditions apply:

- Minimum concrete quality C20/25 according to EN 206
- At least 7 days old
- Adhesive strength on concrete surface > **218 psi** (1.5 MPa ) according to EN 1542

In order to obtain optimal adhesion on concrete surfaces, surface preparation must be carried out at all times. All concrete surfaces must be sound and free of laitance, curing compounds, release agents and contaminations such as oil, dirt and grease. Appropriate methods to carry out concrete surface preparation are blast cleaning (dry or wet) and grinding.

After surface preparation, the concrete surface must be thoroughly cleaned from all loose parts and dust.

**IMPORTANT NOTE: Use of either curing compounds or release agents could have drastic effects on the adhesion properties of edilon)(sedra Dex-G.**

**Repair mortar:**
In order to obtain the optimal adhesion to repair mortar surfaces, the same requirements and surface preparation apply as for concrete surfaces.

**Steel surfaces:**
In order to obtain optimal adhesion on steel surfaces, surface preparation must be carried out at all times. Loose parts, dust and dirt, mill scale, rust and other contaminants must be removed from the steel surface. In case of galvanized steel the surface must be free of zinc salts as well.

**IMPORTANT NOTE: edilon)(sedra Dex-G must be applied as quickly as possible after preparing the steel surfaces. Steel surfaces must be completely dry prior to application. In order to avoid that rust develops in the time between preparation and application, steel surfaces could only be stored in dry conditions.**

- **Untreated steel:**
  Blast cleaning to meet the demands of Sa 2½ according to EN ISO 8501-1. The surface roughness Rz should be **1968.50 – 2755.91 µinch** (50 – 70 µm).
- **Galvanized steel:**
  Sweep blast cleaning with a non-metallic type of abrasive according to NEN 5254.

## 11 USER INSTRUCTIONS

Please see the **edilon)(sedra Dex-G User Data Sheet** and the applicable **edilon)(sedra Installation Instructions** for detailed application instructions.

## 12 APPLICATION CONDITIONS

| Conditions | Value | Additional information |
|---|---|---|
| Surface | **Dry to wet, clean** | Only apply the product on prepared surfaces (see section 10). To determine visually. |
| Environment[1)] | **Dry to wet** | |
| Relative humidity air | **No restrictions** | |
| Surface temperature | **+41 °F to +113 °F** (+5 °C to +45 °C) | Applies to any surface on which the product is applied. At light cloudy and sunny weather, the surface temperature is always higher than the air temperature due to radiation heat from the sun. |
| Product temperature | **+59 °F to +86 °F** (+15 °C to +30 °C) | |

- Recommended measuring device: TQC DewCheck or Elcometer 319s

1) **Exception: Bonding of the Resilient Strip in the ERS channel should be done under dry conditions.**

## 13 SAFETY MEASURES

During application of **edilon)(sedra Dex-G**, it is imperative that protective clothing, rubber gloves and safety goggles are worn.

Provide sufficient ventilation when working with **edilon)(sedra Dex-G**.

Before using **edilon)(sedra Dex-G**, please read the packing label and the **edilon)(sedra Dex-G Safety Data Sheet** for more detailed safety recommendations.

**edilon)(sedra Dex-G** must be stored in the original well-sealed packaging.

## 14 MIXING

Prior to mixing, shake component 2 thoroughly for **1** minute and slowly pour the content entirely into component 1. If **edilon)(sedra Catalyst for Dex-G Component 4** is used, then pour the content of one bottle into component 1 prior to mixing with component 2.

For **edilon)(sedra Dex-G 20/40** the **edilon)(sedra Edimix 14 mobile mixing machine** can be used. Mix the product 2 times.

Alternatively for **edilon)(sedra Dex-G type 20/40/80,** mix both components thoroughly with a power assisted hand mixer for **2** minutes while moving the mixer through the packaging, to achieve a homogeneous grey colored mixture.

For **edilon)(sedra Dex-G 40/80** components 1 and 2 should be mixed first as described above. Then one should slowly add the balanced quantity of component 3 to the mixture. Finally mix for another 1 minute with the Edimix 14 mobile mixing machine (Dex-G 40) or with the power assisted hand mixer (Dex-G 80) to achieve a homogeneous mixture.

To protect the edilon)(sedra Edimix 14 mobile mixing machine from damage (overload) and to improve the pouring properties of the mixed product, edilon)(sedra advises to mix the components at product temperatures between **+59 °F and +86 °F** (+15 $^{0}$C and +30 $^{0}$C).

Please see the **edilon)(sedra Edimix 14 User Data Sheet** for more detailed information.

| **Specifications** | **Hand mixer** |
|---|---|
| Type | Hand drill or similar |
| Mixing propeller set | edilon)(sedra WK 90 |
| Power | **0.54 hp** (400 W) |
| Speed | 400-500 rpm |
| **Suitable for:** | |
| **Dex-G type** | **20, 40, 80** |

## 15 POT LIFE

The pot life of **edilon)(sedra Dex-G** depends on the product temperature and the mixed volume.

In the table below the pot life with and without the addition of **edilon)(sedra Catalyst for Dex-G Component 4** (**Dex-G 20 Fast**) is given.

| **Product temperature** | | **Pot life Dex-G 20 (minutes)** | **Pot life Dex-G 20 Fast (minutes)** |
|---|---|---|---|
| **°F** | (°C) | | |
| **59** | (15) | 40 | 26 |
| **68** | (20) | 30 | 18 |
| **77** | (25) | 22 | - |
| **86** | (30) | 17 | - |

## 16 CURING

The minimum curing time **edilon)(sedra Dex-G** is related to the surface temperature.

In the table below the curing time with and without the addition of **edilon)(sedra Catalyst for Dex-G Component 4** (**Dex-G 20 Fast**) is given.

| **Product temperature** | | **Curing time Dex-G 20 (hours)** | **Curing time Dex-G 20 Fast (hours)** |
|---|---|---|---|
| **°F** | (°C) | | |
| **50** | (10) | 24 | 10 |
| **59** | (15) | 16 | 7 |
| **68** | (20) | 12 | 3 |
| **77** | (25) | 9 | 2 |
| **86 – 113** | (30 – 45) | 5 | 2 |

## 17 CLEANING

Clean used tools immediately after use with **edilon)(sedra Toolcleaner**. Please see the **edilon)(sedra Toolcleaner Safety Data Sheet** before use.

## 18 DISPOSAL CONSIDERATIONS

The following waste products can arise at the application of **edilon)(sedra Dex-G:**

| Description | Type of waste |
|---|---|
| Cured product | Non-hazardous waste |
| Packaging with cured product | Non-hazardous waste |
| Packaging with component 1 or component 2 | Hazardous waste |
| Packaging with component 3 | Non-hazardous waste |
| Packaging with component 4 | Hazardous waste |
| Packaging with uncured product | Hazardous waste |

The waste products should be incinerated in a suitable installation according to federal, tribal, state or local regulations or disposed of according to U.S. regulations regarding proper management of hazardous and non-hazardous waste.

## 19 COLOR TINT

The color tint of **edilon)(sedra Dex-G** may change due to environmental influences (such as chemicals, high temperature, and UV radiation) which affect the material. These color changes on the surface have small influences on the mechanical properties of the product surface.



**T2011-0503** **Date of issue: 17-07-2014**

**Issue based on edilon)(sedra original document (EN) 070704 rev 09**

**edilon)(sedra inc.**
**511 W. 195th Street**
**Glenwood, IL 60425, USA**
**T +1 708 790 0626**
**F +1 708 754 4058**
**mail@edilonsedra.com**
**www.edilonsedra.com**

# E.4 Primer U90WB Product Data Sheet

## 1 DESCRIPTION

**edilon)(sedra Primer U90WB** is a two-component pre-treatment primer based on epoxy resins, which can be directly applied on pre-treated steel and concrete surfaces.

edilon)(sedra Primer U90WB is applied by means of a brush / roller or with airless spray equipment.

## 2 INTENDED USE

**edilon)(sedra Primer U90WB** is developed for the pre-treatment of concrete and steel surfaces. The primer increases the adhesive strength of concrete and steel surfaces. edilon)(sedra Primer U90WB can be used on earlier applied and cured layers of edilon)(sedra Primer U90WB.

edilon)(sedra Primer U90WB is part of the **edilon)(sedra Embedded Rail System (ERS)** and **edilon)(sedra Embedded Block System (EBS)**.

Optimal bonding is ensured when using edilon)(sedra Primer U90WB in combination with **edilon)(sedra Primer 21 / edilon)(sedra Primer 21 2K / edilon)(sedra Primer 24.**
edilon)(sedra Primer U90WB can either be applied in one layer or in two layers.
For corrosion protection it is necessary to apply 2 layers with a dry film thickness of **5.91 mils** (150 µm) of edilon)(sedra Primer U90WB on steel.

## 3 FEATURES & BENEFITS

| Features | Benefits |
|---|---|
| • Water based system | + No solvents, no Volatile Organic Compounds |
| • Not sensitive to moist concrete surfaces | + No extensive drying needed |
| • Grey color | + Clearly visible coverage |

## 4 POINTS OF ATTENTION

| Point of attention | Explanation |
|---|---|
| • Avoid application in thick layers | • Curing will take longer than indicated<br>• A thick layer will lead to curtains |
| • Curing at temperatures lower than **+50 °F** (+10 °C) will increase curing times | • Curing times are temperature related |
| • When primer has been applied more than one month ago at the time of ERS installation, cleaning of surfaces and reapplication of primer will be necessary | • Removal of deposit caused by contamination |

## 5 COMPOSITION

**edilon)(sedra Primer U90WB** is a two-component, water-based primer based on special epoxy resins and mineral fillers.

Please see the **edilon)(sedra Primer U90WB Safety Data Sheet** for more information.

## 6 PRODUCT APPROVAL

**edilon)(sedra Primer U90WB** is officially approved by many national and international infrastructure providers.

## 7 PACKAGING

**edilon)(sedra Primer U90WB** is supplied in two-component packaging in a standard unit size of **6.6 lbs** (3 kg) product. Both components are individually packed in the correct mixing proportions.
On request an **11 lb** (5 kg) unit is available for spraying applications.

## 8 STORAGE AND SHELF LIFE

Store **edilon)(sedra Primer U90WB** either in the depot or at the place of work under dry conditions and away from direct sunlight. The prescribed storage temperature is between **+50 °F and +86 °F** (+15 °C and +30 °C).
In its original, well-sealed packaging and under the above-mentioned conditions edilon)(sedra Primer U90WB has a shelf life of **18** months maximum.

## 9 CHEMICAL & PHYSICAL PROPERTIES

| Property | Standard | Value | Additional information |
|---|---|---|---|
| Density cured product | ISO 2811 | **87.4 ± 6.2 lb/ft$^3$** (1.40 ± 0.1 g/cm$^3$) | |
| Color mixed product | | **Grey** | |
| Color component 1 | | **Dark grey** | |
| Color component 2 | | **Beige** | |
| Viscosity mixed product at **+73 °F** (+23 °C) | ISO 3219 | **3000 cP** (3 Pa·s) | |
| Mixing ratio by weight<br>component 1 : component 2 | | **25 : 100** | |
| Reactivity | | **60 minutes** | |

- The applied test samples and test methods are subject to change without prior notice.
- Test samples are prepared by mixing both components thoroughly for 1 minute.

## 10 MECHANICAL PROPERTIES

| Property | Standard | Value | Additional information |
|---|---|---|---|
| Adhesive strength of Primer U90WB on steel<br>(after 7 days at **+68 °F** (+20 °C)) | ISO 4624 | **> 1450 psi** (> 10 MPa) | Based on all failure mechanisms |
| Adhesive strength of Primer U90WB on concrete<br>(after 7 days at **+68 °F** (+20 °C)) | ISO 4624 | **> 218 psi** (> 1.5 MPa) | Based on cohesive concrete failure |

- The applied test samples and test methods are subject to change without prior notice.

## 11 NOMINAL USE

| Use | Value | Additional information |
|---|---|---|
| Dry film thickness steel according ISO 2808<br>(application of one layer) | **2 – 4 mils** (50 – 100 µm) | |
| Nominal use[1)] on steel surface with a dry film thickness of **3 mils** (75 µm) per layer – brush or roller | **0.05 lb/ft$^2$** (0.25 kg/m$^2$) | One layer on blasted steel[2)] |
| | **0.08 lb/ft$^2$** (0.40 kg/m$^2$) | Two layers on blasted steel[2)] |
| Nominal use[1)] on concrete surface with a dry film thickness of **3 mils** (75 µm) per layer – brush or roller | **0.08 lb/ft$^2$** (0.40 kg/m$^2$) | Pre-treated concrete |
| Nominal use[1)] on steel surface with a dry film thickness of **3 mils** (75 µm) per layer – airless spray | **0.06 lb/ft$^2$** (0.30 kg/m$^2$) | One layer on blasted steel[2)] |
| | **0.10 lb/ft$^2$** (0.50 kg/m$^2$) | Two layers on blasted steel[2)] |
| Nominal use[1)] on concrete surface with a dry film thickness of **3 mils** (75 µm) per layer – airless spray | **0.10 lb/ft$^2$** (0.50 kg/m$^2$) | Pre-treated concrete |

[1)] Nominal use depends on surface structure, application viscosity and layer thickness. Therefore always check actual consumption on test surface.

[2)] See section 12

| NOMINAL USE IN edilon)(sedra ERS BRUSH AND ROLLER | | | |
|---|---|---|---|
| **ERS Design** | **Treatment** | **Value** | **Additional information** |
| Standard ERS channel with rail type 60E1 / 54E1 / 49E1 / 35G etc. | one layer concrete channel + one layer rail | **0.47 lb/ft track** (0.7 kg/m track) | Channel: pre-treated concrete<br>Rail: blasted steel[1)] |
| | one layer steel channel + one layer rail | **0.40 lb/ft track** (0.6 kg/m track) | Channel: blasted steel[1)]<br>Rail: blasted steel |
| | two layers steel channel + one layer rail | **0.47 lb/ft track** (0.7 kg/m track) | |
| Large ERS channel with rail type Ri60(N) / Ri59(N) / NP4AM / PH37A etc. | one layer concrete channel + one layer rail | **0.60 lb/ft track** (0.9 kg/m track) | Channel: pre-treated concrete<br>Rail: blasted steel[1)] |
| | one layer steel channel + one layer rail | **0.47 lb/ft track** (0.7 kg/m track) | Channel: blasted steel[1)]<br>Rail: blasted steel |
| | two layers steel channel + one layer rail | **0.60 lb/ft track** (0.9 kg/m track) | |
| [1)] See section 12 | | | |

| NOMINAL USE IN edilon)(sedra ERS AIRLESS SPRAY | | | |
|---|---|---|---|
| **ERS Design** | **Treatment** | **Value** | **Additional information** |
| Standard ERS channel with rail type 60E1 / 54E1 / 49E1 / 35G etc. | one layer concrete channel + one layer rail | **0.60 lb/ft track** (0.9 kg/m track) | Channel: pre-treated concrete<br>Rail: blasted steel |
| | one layer steel channel + one layer rail | **0.47 lb/ft track** (0.7 kg/m track) | Channel: blasted steel*<br>Rail: blasted steel |
| | two layers steel channel + one layer rail | **0.60 lb/ft track** (0.9 kg/m track) | |
| Large ERS channel with rail type Ri60(N) / Ri59(N) / NP4AM / PH37A etc. | one layer concrete channel + one layer rail | **0.67 lb/ft track** (1.0 kg/m track) | Channel: pre-treated concrete<br>Rail: blasted steel |
| | one layer steel channel + one layer rail | **0.54 lb/ft track** (0.8 kg/m track) | Channel: blasted steel*<br>Rail: blasted steel |
| | two layers steel channel + one layer rail | **0.74 lb/ft track** (1.1 kg/m track) | |
| • Nominal use depends on surface structure, application viscosity and layer thickness. Therefore always check the actual consumption on a test surface.<br>• Airless spray: nominal use is 20% more due to overspray<br>* = See section 12 | | | |

## 12 SURFACE PREPARATION

The durability of the rail system, in which **edilon)(sedra Primer U90WB** is applied, is directly dependent on the pre-treatment of the surface prior to the application. For optimum adhesion performance the pre-treated surfaces must be clean.

edilon)(sedra Primer U90WB is applied directly after surface pre-treatment.

**Concrete surfaces**
The following conditions apply:

- Minimum concrete quality C20/25 according to EN 206
- The adhesive strength of Primer U90WB on the concrete surface must be in accordance with the property as mentioned in section 10, provided that cohesive failure of concrete occurs

In case the adhesive strength on the concrete surface is lower than the mentioned value due to laitance, curing compounds, release agents or contaminations, then the laitance has to be removed by means of blast-cleaning, grinding or water jetting.

**Use of either curing compounds or release agents could have drastic effects on the adhesion properties of edilon)(sedra Primer U90WB.**

In order to obtain optimal adhesion on concrete surfaces, surface pre-treatment must be carried out at all times. All concrete surfaces must be sound and free of curing compounds, release agents and contaminations such as oil, dirt and grease. Appropriate methods to carry out concrete surface pre-treatment are blast cleaning (dry or wet) and grinding.

After surface pre-treatment, the concrete surface must be washed down thoroughly by means of high pressure cleaning to remove all loose parts and dust.

**Repair mortar**
In order to obtain the optimal adhesion to repair mortar surfaces, the same requirements and surface pre-treatment apply as for concrete surfaces.

**Steel surfaces**
In order to obtain optimal adhesion on steel surfaces, surface pre-treatment must be carried out at all times. Loose parts, dust and dirt, mill scale, rust and other contaminants must be removed from the steel surface. In case of galvanized steel the surface must be free of zinc salts as well.

- **Untreated steel:**
  - Blast cleaning to surface preparation grade Sa 2 according to ISO 8501-1. The surface roughness Rz should be **1.18 ─ 2.76 mils** (30 ─ 70 µm).
  - Brushing with hand or power tools to surface preparation grade St 3 according to ISO 8501-1. Please ensure that the surface is degreased after brushing it with hand or power tools.
- **Galvanized steel:**
  - Sweep blast cleaning with a non-metallic type of abrasive according to NEN 5254.

**edilon)(sedra Primer U90WB must be applied as quickly as possible after the pre-treatment of the steel surfaces. Steel surfaces must be completely dry prior to application. In order to avoid that rust develops in the time between pre-treatment and application, steel surfaces should only be stored in dry conditions.**

- **Rails**
  - Blast cleaning to meet the demands of Sa 2 according to ISO 8501-1. The surface roughness Rz should be **3.15 ─ 3.94 mils** (80 ─ 100 µm).

## 13 USER INSTRUCTIONS

Please see the **edilon)(sedra Primer U90WB User Data Sheet** and the applicable **edilon)(sedra Installation Instructions** for detailed application instructions.

## 14 APPLICATION CONDITIONS

| Conditions | Value | Additional information |
|---|---|---|
| Application of the product | **As quickly as possible after preparation of the surface** | To prevent further contamination and corrosion of the surface. |
| Steel surface | **Dry and clean** | Also during the time between pre-treatment and application of the primer. |
| Concrete surface moisture content | **< 6 %** | Only apply the product on pre-treated surfaces (see section 12).<br>Moist on surfaces is no problem; the surfaces should be free from layers of water. |
| Environment | **Dry** | Or in a conditioned environment. |
| Relative air humidity | **< 90 %** | |
| Safety margin in relation to dew point (ΔT) | **> 6 °F** (>3 °C) | In order to ensure a safety margin, the surface temperature must be **6 °F** (3 °C) above the dew point. |
| Surface temperature | **+41 °F to +113 °F** (+5 °C to +45 °C) | Applies to any surface on which the product is applied. At light cloudy and sunny weather, the surface temperature is always higher than the air temperature due to radiation heat from the sun. |
| Product temperature | **+59 °F to +86 °F** (+15 °C to +30 °C) | During application. |
| • Recommended measuring device: TQC DewCheck or Elcometer 319s and Tramex Concrete Moisture Encounter (CME4), scale 0-6%.<br>• During application and curing direct contact with (rain)water must be avoided | | |

## 15 SAFETY MEASURES

During application of **edilon)(sedra Primer U90WB** it is imperative that protective clothing, rubber gloves and safety goggles are worn.

Before using edilon)(sedra Primer U90WB, please refer to the packing label and the **edilon)(sedra Primer U90WB Safety Data Sheet** for more detailed safety recommendations.

edilon)(sedra Primer U90WB should be stored in the original well-sealed packaging, and is not for internal consumption, but for industrial use only.

## 16 MIXING AND APPLICATION

Prior to mixing, shake component 1 thoroughly for **20** seconds and slowly pour the content entirely into component 2. Mix both components thoroughly with a power assisted hand mixer for **1** minute to achieve a homogeneous grey colored mixture.

| Specifications | Hand mixer |
|---|---|
| Type | Hand drill or similar |
| Mixing propeller set | WK 70 |
| Power | **0.54 hp** (400 W) |
| Speed | 400-500 rpm |

Move the mixing propeller during mixing up, down and around in the packaging to ensure a correct mixing of both components.

After mixing the product can be used for **60** minutes (pot-life). After these **60** minutes, the mixed product cannot be used, and should be disposed of.

Apply **edilon)(sedra Primer U90WB** onto the surface in a solid grey colored coating with an even layer thickness by using a brush, roller or airless spray equipment. To prevent sagging do not apply thick layers.

If the first layer has insufficient coverage, a second layer can be applied, at least **2** hours after the first layer (at **+73.4 °F** (+23 °C) surface temperature).

On prefabricated steel channels it is necessary to apply two layers with a dry film thickness of **3.94 ─ 7.87 mils** (100 ─ 200 µm) of edilon)(sedra Primer U90WB.

edilon)(sedra recommends the use of Wagner high pressure airless spray equipment. Please see the User instructions of the **Wagner SuperFinish 27-31.**

| Specifications high pressure airless spray equipment | | |
|---|---|---|
| Type | | Wagner SuperFinish 31 |
| Max. operating pressure | | **3626 psi** (250 bar) |
| Product supply | | Hopper or stainless steel suction tube |
| Accessories | - Hose | **24.6 ft** (7.5 m) Wagner NW10 high pressure hose with M16x1.5 couplings |
| | - Spray tips | Wagner Tips 209, 111, 211 |
| Voltage | | 110 V AC |
| Power | | **2.28 hp** (1.7 kW) |

## 17 CURING

**edilon)(sedra Primer U90WB** applied on concrete or steel surfaces, should cure in dry conditions and at temperatures between **+41 °F and +95 °F** (+5 °C and +35 °C).

If there was any contact between primer and (rain)water within the curing period, a new application of the primer is required on a clean and dry surface (see section 12).

The open time window of edilon)(sedra Primer U90WB is related to the surface temperature:

| Surface temperature | | Open time window after application (hours) |
|---|---|---|
| °F | (°C) | |
| **+41 — +50** | (+5 — +10) | 48 |
| **+50 — +95** | (+10 — +35) | 24 |

After curing, the applied layer of edilon)(sedra Primer U90WB is ready for the application of bonding primer **edilon)(sedra Primer 21 / edilon)(sedra Primer 21 2K / edilon)(sedra Primer 24**.

When 72 hours have passed after the application of Primer U90WB at the time of ERS installation, it will be necessary to clean the coated surfaces in order to remove the deposit of contamination.

When one month has passed after the application of Primer U90WB at the time of ERS installation, both cleaning of the coated surfaces and reapplication of the primer will be necessary.

Cleaning can be done with **edilon)(sedra Cleaner S** or a low pressure dry steam cleaner.

Not all applications require the use of an additional bonding primer. In a protected and dry environment edilon)(sedra Primer U90WB has bonding primer properties for a limited time after application (max. 72h). Strict protected and dry environment conditions apply. edilon)(sedra Corkelast VA-40 N and VA-60 N are excluded for this single primer option. Please contact edilon)(sedra for additional information.

## 18 CLEANING

Clean used tools immediately after use with clean water. If high pressure airless spray equipment has been used clean immediately after use met clean water to prevent the curing of product in the pump of the machine.

## 19 DISPOSAL CONSIDERATIONS

The following waste products can arise at the application of **edilon)(sedra Primer U90WB**:

| Description | Type of waste |
|---|---|
| Cured product | Non-hazardous waste |
| Packaging with cured product | Non-hazardous waste |
| Packaging with component 1 or component 2 | Hazardous waste |
| Packaging with uncured product | Hazardous waste |

The waste products should be incinerated in a suitable installation and according to the local authority regulations or disposed according to the prescriptions of the European list of waste products.

## 20 COLOR TINT

The color tint of **edilon)(sedra Primer U90WB** may change due to environmental influences (such as chemicals, high temperature, and UV radiation) which affect the material.

The information and recommendations provided either verbally or in writing regarding the technical implementation of products supplied by edilon)(sedra have been provided by edilon)(sedra to the best of its knowledge. This information and the recommendations made are simply informal indications and it is the responsibility of the user to ensure that he/she does not infringe the rights of third parties. Such information or recommendations do not release the user from his/her obligation to inspect the products supplied by edilon)(sedra with regard to their suitability for carrying out the processes intended and achieving their objectives, nor do they release the user from his/her obligation to take the necessary precautions. The application, use and processing of edilon)(sedra products takes place beyond the control of edilon)(sedra. The user shall therefore bear sole responsibility in that regard. edilon)(sedra shall, of course, be responsible for the applicability and quality of its products. We also refer to the General Terms and Conditions of edilon)(sedra in this regard.



**2005-1002-4** **Date of issue: 17-07-2014**

**Issue based on edilon)(sedra original document (EN) 090906 rev 07**

**edilon)(sedra inc.**
**511 W. 195th Street**
**Glenwood, IL 60425 USA**
**T +1 708 790 0626**
**F +1 708 754 4058**
**mail@edilonsedra.com**
**www.edilonsedra.com**

# E.5 Primer 21-2K Product Data Sheet

## 1 DESCRIPTION

**EDILON Primer 21 2K** is a fast curing two component bonding primer with a long working window. Specially formulated for use with EDILON Corkelast or EDILON Editaan to ensure an optimal bonding with steel or concrete.

## 2 INTENDED USE

**EDILON Primer 21 2K** is part of the **EDILON Corkelast Embedded Rail System (ERS)** and the **EDILON Corkelast Embedded Block System (EBS)**.

To achieve an optimal bonding and corrosion inhibition use a combination of **EDILON Primer 21 2K** and **EDILON Primer U90WB.**

**EDILON Primer 21 2K** is specially developed to ensure a durable bonding on surfaces which have been prepared with **EDILON Primer U90WB.** After the preparation and the application of EDILON Primer 21 2K bonding primer an optimal bonding is achieved with EDILON Corkelast and EDILON Editaan systems.

**EDILON Primer 21 2K c**an also be applied on cured surfaces of EDILON Corkelast and EDILON Editaan, or on earlier applied and cured layers of EDILON Primer 21 2K.

## 3 FEATURES & BENEFITS

| Features | Benefits |
|---|---|
| • Promotes the bonding between EDILON Corkelast and EDILON Editaan on the prepared surface | + Durable bonding of EDILON Corkelast and EDILON Editaan on the surface |
| • White colour | + Visible covered layer after application |
| • Applicable in two layers | + Good corrosion inhibition because of film thickness |
| • Low viscosity | + Excellent application with brush or EDILON Spray Unit |
| • Excellent adhesion on prepared steel, concrete and existing EDILON Corkelast surfaces | + Suitable within EDILON Corkelast Embedded Rail System and EDILON Corkelast Embedded Block System |
| • Short drying time after application | + Shortens the installation time |
| • Long working window | + Up to 12 hours after application extended installation time |
| • Two component system | + Less dependant on air humidity |
| • No rust of blisters according ASTM criteria in neutral saltwater spray tests | + No rust formation when the combination of primers is used<br>+ Passes the Dutch ProRail criteria for rust prevention in combination with EDILON Primer U90WB. |

## 4 POINTS OF ATTENTION

| Point of attention | Explanation |
|---|---|
| • Only apply on dry surfaces at dry weather conditions | • To prevent the influences of water on the properties of the primer |
| • Prevent the application of thick coats of the primer | • Thick coats may lead to foam generation<br>• Pay special attention at horizontal surfaces |
| • Apply an maximum of 2 layers | • More than 2 layers lead to a reduced bonding strength |
| • Apply the product direct after mixing | • Use EDILON Primer 21 2K within the 45 minutes pot life |

## 5 COMPOSITION

**EDILON Primer 21 2K** is a two component primer based on special polyurethane resins and solvents.

Refer to the **EDILON Primer 21 2K Material Safety Data Sheet** for more detailed information.

## 6 PRODUCT APPROVAL

**EDILON Primer 21 2K** is officially approved by many national and international Infra providers.

## 7 PACKAGING

**EDILON Primer 21 2K** is supplied in two separate components. EDILON Primer 21 2K is packed in a unit size of 2 kg product. Both components are individually packed in the correct mixing proportions.

## 8 STORAGE AND SHELF LIFE

Store **EDILON Primer 21 2K** either in the depot or at the place of work under dry conditions and away from direct sunlight. The prescribed storage temperature lies between **50 °F and 86 °F** (+ 10 °C and + 30 °C).

In its original, well-sealed packaging and under the above-mentioned conditions the **EDILON Primer 21 2K** has a shelf life of **12** months maximum.

## 9 CHEMICAL & PHYSICAL PROPERTIES

| Property | Standard | Value | Units | Additional information |
|---|---|---|---|---|
| Density mixed product | ISO 2811 | **77.4 ± 6.2**<br>1.24 ± 0.02 | lb/ft$^3$<br>g/cm³ | Direct after mixing |
| Colour mixed product | | **White** | | |
| Colour component 1 | | **White** | | |
| Colour component 2 | | **Clear yellow** | | |
| Viscosity component 1 at 77 °F (+ 25 °C) | | **300**<br>300 | cps<br>mPas | |
| Viscosity component 2 at 77 °F (+ 25 °C) | | **150**<br>150 | cps<br>mPas | |
| Viscosity mixed product. at 77 °F (+ 25 °C) | ISO 3219 | **10** | sec | DIN cup 4 |
| Mixing ratio by weight<br>component 1 : component 2 | | **25 : 100** | | |
| Reactivity at 77 °F (viscosity 2000 poise)<br>Reactivity at +25 °C (viscosity 200 Pas) | ISO 10364 | **45** | minutes | |
| Nominal use with a dry film thickness of 1.97 mil (50 µm) per layer [1)] | | **0.02 - 0.04**<br>0.1 – 0.2 | lb/ft$^2$<br>kg/m$^2$ | |
| Neutral saltwater spray test on zinc plated steel<br>Zinc plated steel – 1x Primer U90WB –<br>1x Primer 21 2K | ASTM D714 | **No blisters** | | |
| | ASTM D610 | **10** | Rust scale | No rust |
| Neutral saltwater spray test on blasted steel steel – 2x Primer U90WB –<br>1x Primer 21 2K | ASTM D714 | **No blisters** | | |
| | ASTM D610 | **10** | Rust scale | No rust |

- [1)] Nominal use depends on surface structure, application viscosity and layer thickness.
- Test samples are prepared by mixing both components thoroughly for 1 minute.
- Test results, are determined with cured material after 7 days at 73.4 °F (+ 23 °C), unless specified otherwise.
- The applied test samples and test methods can be changed without further notice.
- In the neutral saltwater spray test the spray time was 1000 hours at 95 °F (+ 35 °C), spray is an 5% salt solution.

## 10 NOMINAL USE IN EDILON CORKELAST ERS

| ERS Design | Treatment | Value | Unit | Additional information |
|---|---|---|---|---|
| Standard ERS channel with rail type 60E1 / 54E1 / 49E1 / 35G etc. | one layer concrete channel + one layer rail pre-treated with Primer U90WB | **0.20**<br>0.3 | lb/ft track<br>kg/m track | Channel +rail: pre-treated with Primer U90WB |
| Large ERS channel with rail type Ri60(N) / Ri59(N) / NP4AM / PH37A etc. | one layer concrete channel + one layer rail pre-treated with Primer U90WB | **0.27**<br>0.4 | lb/ft track<br>kg/m track | Channel +rail: pre-treated with Primer U90WB |
| • Nominal use depends on surface structure, application viscosity and layer thickness. | | | | |

## 11 MECHANICAL PROPERTIES

| Property | Standard | Value | Unit | Additional information |
|---|---|---|---|---|
| Dry film thickness on steel (1 coat application) | ISO 2808 | **1.97**<br>50 | mils<br>µm | |
| Adhesion strength 1 coat on steel | EN 4624 | **4351**<br>30 | psi<br>MPa | |
| Adhesion strength 2 coats on steel | EN 4624 | **2901**<br>20 | psi<br>MPa | |
| Bonding properties Steel – Primer 21 2K – Corkelast | ISO 8339 | – | – | Cohesive Corkelast failure |
| Bonding properties Steel – Primer U90WB – Primer 21 2K – Corkelast | ISO 8339 | – | – | Cohesive Corkelast failure |
| • The applied test samples and test methods can be changed without further notice.<br>• Test results, are determined with cured material after 7 days at 73.4 °F (+ 23 °C),, unless specified otherwise. | | | | |

## 12 SURFACE PREPARATION AND PRIMER APPLICATION

The durability of any system, in which **EDILON Primer 21 2K** as bonding primer is applied, is directly dependent on the condition of the surface prior to the application of EDILON Primer 21 2K.

The conditions for an optimal adhesion of **EDILON Primer 21 2K** to a surface are:

- Completely clean surface, so all contaminations like dust, mould release agents, curing compounds, hydrophobic agents etc. must be removed from the surface
- Absolutely dry surface

**Surface pre-treated with EDILON Primer U90WB:**
On steel and concrete surfaces a coat of the pre-treatment primer **EDILON Primer U90WB** should have been applied according the user instructions of the product.

Before **EDILON Primer 21 2K** can be applied it must be checked whether the following conditions are met:

- The layer **EDILON Primer U90WB** must be fully cured (see Product Information Sheet EDILON Primer U90WB)
- The layer EDILON Primer U90WB must not feel sticky anymore
- The layer EDILON Primer U90WB must be free from all contaminations( see above)
- The layer EDILON Primer U90WB must be absolutely dry

If after the check, it appears that the layer EDILON Primer U90WB is contaminated, than this layer must be cleaned with **EDILON Cleaner S**.

Refer to the **EDILON Cleaner S Product Information Sheet** for detailed information.

**Surfaces existing of EDILON Corkelast of EDILON Editaan:**
Before **EDILON Primer 21 2K** can be applied it must be checked whether the following conditions are met:

- EDILON Corkelast or EDILON Editaan must be fully cured (see Product Information Sheet EDILON Corkelast or EDILON Editaan)
- EDILON Corkelast or EDILON Editaan must not feel sticky anymore
- EDILON Corkelast or EDILON Editaan must be free from all contaminations( see above)
- EDILON Corkelast or EDILON Editaan must be absolutely dry

If after the check, it appears that EDILON Corkelast or EDILON Editaan is contaminated, than the surface must be cleaned with **EDILON Cleaner S**.

Refer to the **EDILON Cleaner S Product Information Sheet** for detailed information.

## 13l USER INSTRUCTIONS

Refer to the **EDILON Primer 21 2K User instruction sheet** and the applicable **edilon)(sedra Installation Instructions** for detailed application instructions.

## 14 APPLICATION CONDITIONS

| Conditions | Value | Additional information |
|---|---|---|
| Surface | **As soon as possible after the application of the pre-treatment primer** | To prevent further contamination of the pre-treated surface. |
| Weather conditions | **Dry** | Or in a conditioned environment. |
| Relative humidity air | **< 90%** | |
| Air temperature | **41 °F till 95 °F**<br>+ 5 °C till + 35 °C | |
| Surface temperature | **41 °F till 95 °F**<br>+ 5 °C till + 35 °C | Required for all surfaces on which the primer is applied. At light cloudy or sunny weather, the surface temperature is always higher than the air temperature due to radiation heat from the sun. |
| Safety margin in relation to dew point (ΔT) | **> 3 °C** | In order to ensure a safety margin, the surface temperature must be 3 °C above the dew point. |
| Product temperature | **59 °F till 86 °F**<br>+ 15 °C till + 30 °C | During application. |
| • Recommended measuring device: TQC Dew Check or elcometer 319s<br>• Direct contact with (rain) water must be avoided. | | |

## 15 SAFETY RECOMMENDATIONS

During application of **EDILON Primer 21 2K**, it is imperative that protective clothing, rubber gloves and safety goggles are worn. Provide sufficient ventilation when working with EDILON Primer 21 2K.

In confined spaces with insufficient ventilation or if an **EDILON Spray Unit** is used, wear an approved half face mask with filter type AX.

Before using **EDILON Primer 21 2K**, please refer to the packing label and the **EDILON Primer 21 2K Material Safety Data Sheet** for more detailed safety recommendations.

**EDILON Primer 21 2K** must be stored in the original well-sealed packaging.

## 16 MIXING

Both components of **Edilon Primer 21 2K** should be mixed before use. Shake component 1 approximately 10 seconds and pour the content into the **EDILON Spray Unit.** Now pour component 2 in the EDILON Spray Unit**.** Shake the EDILON Spray Unit with content for **1** minute. The mixture is ready for use.

**Do not add additional solvent into the mixed components to dilute the product.**

The pot life for the product is 45 minutes and it is advised that the mixed product is used without interruptions. Application can be done with a brush or if large quantities have to be applied with the **EDILON Spray Unit**. Use only the EDILON Spray Unit, as this piece of equipment has special selected parts which are chosen for user's safety.

Refer to the **EDILON Spray Unit User instruction sheet** for detailed application instructions.

The covering rate of **EDILON Primer 21 2K** on the surface is done visually. Never apply more than 2 coats of EDILON Primer 21 2K. When more coats are applied the bonding strength cannot be guaranteed.

## 17 WORKING WINDOW

**EDILON Primer 21 2K** applied on pre-treated surfaces (see 12.) should cure at dry weather conditions at a temperature between **41 °F till 95 °F** (+ 5 °C and + 35 °C).

When the primer comes into contact with (rain) water within its curing time, apply the primer again on a dry and clean surface.

After curing time a working window starts. Within the working window, **EDILON Primer 21 2K** has the function of a bonding primer. EDILON Corkelast or EDILON Editaan can be applied within the working window. The surface temperature should be kept within the conditions as pre-scribed at the applications conditions (see 14.) and the surfaces should be kept clean and dry.

When the working window has elapsed, a new layer of **EDILON Primer 21 2K** can be applied.
In case of contaminated surfaces, clean these surfaces with **EDILON Cleaner S**.
The working window of **EDILON Primer 21 2K** is related to the surface temperature.

| Surface temperature | | Working window (hours) | |
|---|---|---|---|
| °F | °C | minimum | maximum |
| 41 - 50 | +5 – +10 | 1 | 12 |
| 50 - 95 | +10 – +35 | ½ | 12 |

**ATTENTION: Curing of the EDILON Primer 21 2K ends when the minimum working window has passed or when the applied layer does not feel sticky anymore.**

**ATTENTION: Do not apply more than two layers of EDILON Primer 21 2K**.

## 18 CLEANING

Clean used tools immediately after use with **EDILON Toolcleaner,** except for the **EDILON Spray Unit**. This should be cleaned with **odourless mineral spirit**.

## 19 DISPOSAL CONSIDERATIONS

The following waste products can arise at the application of **EDILON Primer 21 2K:**

| Description | Type of waste | Waste code |
|---|---|---|
| Cured product | Non-hazardous waste | – |
| Packaging with cured product | Non-hazardous waste | – |
| Packaging with component 1 or component 2 | Hazardous waste | 15 01 10 |
| Packaging with uncured product | Hazardous waste | 15 01 10 |

Used packaging of **EDILON Primer 21 2K** should be emptied as much as possible. Leave the packaging open to cure the remaining. The waste products should be incinerated in a suitable installation and according to the local authority regulations or disposed according to the prescriptions of the European list of waste products.

## 20 COLOUR TINT

The colour tint of **EDILON Primer 21 2K** can be changed by environmental influences (chemicals, high temperature, UV radiation) that affect the material.



| = CHANGES COMPARED TO THE PREVIOUS VERSION, ALWAYS CHECK THAT YOU HAVE THE MOST RECENT REVISION.

**121108 rev 01/2005-0902-12/0113** **Date of issue: 10-01-2013**

**Translation based on edilon)(sedra original document (EN) 080716 rev 03**

**edilon)(sedra inc.**
**511 W. 195th Street**
**Glenwood, IL 60425, USA**

**T +1 708 790 0626**
**F +1 708 754 4058**

**mail@edilonsedra.com**
**www.edilonsedra.com**